Combining multi-step biocatalysis with process intensification – Enzymatic synthesis and downstream processing of chiral amino alcohols from renewables

Von der Fakultät für Mathematik, Informatik und Naturwissenschaften der RWTH Aachen University zur Erlangung des akademischen Grades einer Doktorin der Ingenieurwissenschaften genehmigte Dissertation

vorgelegt von

M. Sc. Molekulare und Angewandte Biotechnologie
Laura Katharina Grabowski

aus
Rheine, Nordrhein-Westfalen, Deutschland

Berichter:
Univ.-Prof. Dr. rer. nat. Dörte Rother
Univ.-Prof. Dr.-Ing. Lars M. Blank

Tag der mündlichen Prüfung: 17.11.2023

Diese Dissertation ist auf den Internetseiten der Universitätsbibliothek verfügbar.

Eidesstattliche Erklärung

Ich, Laura Katharina Grabowski, erkläre hiermit, dass diese Dissertation und die darin dargelegten Inhalte die eigenen sind und selbstständig, als Ergebnis der eigenen originären Forschung, generiert wurden.

Hiermit erkläre ich an Eides statt

1. Diese Arbeit wurde vollständig oder größtenteils in der Phase als Doktorand dieser Fakultät und Universität angefertigt;
2. Sofern irgendein Bestandteil dieser Dissertation zuvor für einen akademischen Abschluss oder eine andere Qualifikation an dieser oder einer anderen Institution verwendet wurde, wurde dies klar angezeigt;
3. Wenn immer andere eigene oder Veröffentlichungen Dritter herangezogen wurden, wurden diese klar benannt;
4. Wenn aus anderen eigenen oder Veröffentlichungen Dritter zitiert wurde, wurde stets die Quelle hierfür angegeben. Diese Dissertation ist vollständig meine eigene Arbeit, mit der Ausnahme solcher Zitate;
5. Alle wesentlichen Quellen von Unterstützung wurden benannt;
6. Wenn immer ein Teil dieser Dissertation auf der Zusammenarbeit mit anderen basiert, wurde von mir klar gekennzeichnet, was von anderen und was von mir selbst erarbeitet wurde;
7. Ein Teil oder Teile dieser Arbeit wurden zuvor veröffentlicht, und zwar in:

Mohamed Labib, Laura Grabowski, Christian Brüsseler, Nicolai Kallscheuer, Luisa Wachtendonk, Thomas Fuchs, Andreas Jupke, Wolfgang Wiechert, Jan Marienhagen, Dörte Rother and Stephan Noack. Towards the sustainable production of the active pharmaceutical ingredient metaraminol. *ACS Sustain. Chem. Eng*., 2022, 10, 5117-5128.

Moritz Doeker, Laura Grabowski, Dörte Rother and Andreas Jupke. *In situ* reactive extraction with oleic acid for process intensification in amine transaminase catalyzed reactions. *Green Chem.*, 2022, 24, 295-304.

Kevin Mack, Moritz Doeker, Laura Grabowski, Andreas Jupke and Dörte Rother. Extractive *in situ* product removal for the application of L-alanine as amine donor in enzymatic metaraminol production. *Green Chem.*, 2021, 23, 4892-4901.

Aachen, März 2024

Laura Grabowski

Funding

Part of this work was realized with the financial support of the Bioeconomy Science Center as part of the project HyImPAct ("Hybrid processes for Important Precursor and Active pharmaceutical ingredients"). The scientific activities of the Bioeconomy Science Center were financially supported by the Ministry of Innovation, Science and Research within the framework of the NRW Strategieprojekt BioSC (no. 313/323-400-002 13).

Contributions

Biotechnology is a highly interdisciplinary research field, in which the successful integration of hybrid processes such as pursued in the HyImPAct project are dependent on extensive collaborations across scientific disciplines towards a common goal. Hence, some results presented in this thesis have been acquired in close collaboration with others or with the support of supervised students. Each contribution is fully disclosed at the beginning of each chapter. This thesis is further based on gathered knowledge and experience at the Biosensors and Biocatalysis Group at the Institute of Bio- and Geosciences – Biotechnology (IBG-1) at the Research Center Jülich, which is acknowledged with deep gratitude.

Danksagung

Zum Gelingen dieser Arbeit haben eine Vielzahl von Menschen auf direkte und indirekte Weise beigetragen, die ich an dieser Stelle ganz besonders herausstellen möchte. Zuallererst möchte mich bei Prof. Dr. Dörte Rother für die herausragende Betreuung bedanken. Dörte, vielen Dank für deine fachliche Leitung, große Unterstützung und grenzenlosen Optimismus. Für alle Erfahrungen, die mir während meiner Doktorandenzeit ermöglicht wurden, sowie für die empathische Führung unserer Gruppe während einer Pandemie bin ich dir sehr dankbar. Außerdem möchte ich mich bei Prof. Dr.-Ing. Lars M. Blank für die Übernahme des Zweitgutachtens bedanken. Mein Dank gilt außerdem Prof. Dr. Wolfgang Wiechert für die Möglichkeit, meine Doktorarbeit unter den hervorragenden Arbeitsbedingungen des IBG-1 anzufertigen.

Ein großer Dank gilt an dieser Stelle der gesamten Biokatalyse („*Biocats*“) -Gruppe. Danke an Prof. Dr. Martina Pohl für die herausragende Co-Führung, Organisation und fachliche Kompetenz. Deine wissenschaftlichen Impulse und Direktheit habe ich während meiner Zeit bei euch sehr geschätzt. Darüber hinaus möchte ich mich von ganzem Herzen bei Heike Offermann, Lilia Arnold, Doris Hahn und Ilona Frindi-Wosch für die moralische Unterstützung in Büro 123 und die große Hilfe im Labor bedanken. Danke, dass ihr für jedes Problem noch eine Lösung gefunden habt. Besonderer Dank gilt Lilia, für deine unfassbare Arbeitspower, deine Kreativität und Herzlichkeit. Ich habe sehr gerne mit euch allen zusammengearbeitet. Außerdem gilt mein Dank Dr. Torsten Sehl für die geduldige Beantwortung meiner zahlreichen Fragen und die gute Zusammenarbeit. Danke an Stephan Malzacher, Jan-Dirk Spöring, Matthias Rieb, Selina Seide, Maria Allahham, Berit Rothkranz, Douglas Weber und Lisa Seibt. Ihr habt mir stets weitergeholfen und wart unverzichtbar für Kaffeepausen, Kuchen und Krisenmomente. Ohne euren Zuspruch und die schönen gemeinsamen Aktivitäten wäre es nicht dasselbe gewesen.

Mein außerordentlicher Dank gilt meinen Projektpartnern im Projekt „HyImPAct“. Ich möchte mich bei Dr. Stephan Noack für die großartige Projektkoordination sowie für die Unterstützung und zielgerichtete Zusammenarbeit an Experimenten und Veröffentlichungen bedanken. Mein Dank gilt dabei auch ganz besonders Dr. Mohamed Labib. Vielen Dank an Kevin Mack und allen Kooperationspartnern in der Fluidverfahrenstechnik der RWTH Aachen University, Moritz Doeker, Thomas Fuchs und Prof. Dr.-Ing. Andreas Jupke, für die äußerst erfolgreiche Kooperation, bei der ich sehr viel lernen konnte. Für die Konstruktion der *Bacillus subtilis* Stämme und fachlichen Austausch in einer spannenden Kooperation bedanke ich mich bei Dr. Marianna Karava und Prof. Dr. Johannes Kabisch.

Insbesondere meinen Studentinnen Sarah Schmitz, Anneke Strumpel und Nina Klos möchte ich danken, da sie einen großen Beitrag zum Gelingen dieser Arbeit geleistet haben. Vielen Dank für euren großen Einsatz. Die Zusammenarbeit mit euch hat mir immer sehr viel Spaß bereitet. Des

Weiteren möchte ich mich bei Dr. Christiane Claaßen und Rainer Goldbaum für die Unterstützung bei NMR-Analysen bedanken. Ich bedanke mich außerdem ausdrücklich bei Jochem Gätgens für die Messung von GC-ToF und die angeregten Diskussionen.

Meine tiefe Dankbarkeit gilt an dieser Stelle meiner Familie und meinen Freunden. Danke für die unvergessliche Zeit in Aachen, viele von euch sind seit der ersten Woche dabei und ich bin ein Glückspilz, so viele Erlebnisse, „Hochzeiten“ wie auch Lockdowns, mit euch an meiner Seite durchlebt zu haben. Am IBG-1 möchte ich mich besonders bei Katja Rohr, Laura Helleckes, Valentin Steier und Tobias Schwanemann bedanken. Ihr seid unabhängig von eurer Arbeit einfach fantastische Menschen, dass ihr mir dazu aber auch mit allerlei Biotechnologie-Wissen weiterhelfen könnt, ist ziemlich cool.

Mein größter Dank gilt meiner Familie. Ihr habt mich in allen meinen bisherigen Unterfangen unterstützt. Danke für euer Verständnis, eure Unterstützung und Seelsorge sowie euer Interesse, welche mich während meines Studiums und dieser Arbeit stützten. Philipp, dir danke ich für deine Geduld, deine Ratschläge und allwährende Unterstützung, die zum Gelingen dieser Arbeit unverzichtbar waren.

Dissemination

Peer-reviewed journal articles

Laura Grabowski, Lilia Arnold, Nina Klos and Dörte Rother. 2023 (*in preparation).*

Mohamed Labib[§], Laura Grabowski[§], Christian Brüsseler, Nicolai Kallscheuer, Luisa Wachtendonk, Thomas Fuchs, Andreas Jupke, Wolfgang Wiechert, Jan Marienhagen, Dörte Rother and Stephan Noack. Toward the sustainable production of the active pharmaceutical ingredient metaraminol. *ACS Sustain. Chem. Eng*., 2022, 10, 5117 - 5128.

Moritz Doeker[§], Laura Grabowski[§], Dörte Rother and Andreas Jupke. *In situ* reactive extraction with oleic acid for process intensification in amine transaminase catalyzed reactions. *Green Chem.*, 2022, 24, 295 - 304.

Kevin Mack[§], Moritz Doeker[§], Laura Grabowski, Andreas Jupke and Dörte Rother. Extractive *in situ* product removal for the application of L-alanine as amine donor in enzymatic metaraminol production. *Green Chem.*, 2021, 23, 4892 - 4901.

Oral presentations

Laura Grabowski, Mohamed Labib, Moritz Doeker, Christian Brüsseler, Nicolai Kallscheuer, Thomas Fuchs, Andreas Jupke, Jan Marienhagen, Stephan Noack and Dörte Rother. Bio-based synthesis of metaraminol using microbially produced precursors and reactive *in situ* product removal. *Biocatalysis Gordon Research Seminar, Manchester, NH, USA (10.07.2022).*

Laura Grabowski, Mohamed Labib, Moritz Doeker, Christian Brüsseler, Nicolai Kallscheuer, Thomas Fuchs, Andreas Jupke, Jan Marienhagen, Stephan Noack and Dörte Rother. Bio-based production of metaraminol with integration of reactive *in situ* product removal. *IBPRO2022 Intensifying Biocatalytic Processes, Bielefeld, Germany (29.03.2022).*

[§] These authors contributed equally to the publication.

Laura Grabowski, Moritz Doeker, Andreas Jupke and Dörte Rother. Process intensification of the enzymatic cascade to metaraminol by integration of *in situ* liquid-liquid extraction. *13th European Congress of Chemical Engineering and 6th European Congress of Applied Biotechnology (online, 23.09.2021).*

Laura Grabowski, Moritz Doeker, Andreas Jupke and Dörte Rother. Approaching sustainable biocatalytic processes – reaction intensification of the enzymatic metaraminol production by *in situ* liquid-liquid extraction. *Himmelfahrtstagung on Bioprocess Engineering (online, 12.05.2021).*

Kevin Mack, Laura Grabowski, Moritz Doeker, Andreas Jupke and Dörte Rother. *In situ* liquid-liquid extraction as means for shifting the equilibrium during the chemo-enzymatic production of metaraminol. *Amine Biocatalysis 4.0, Stuttgart, Germany (18.02.2020).*

Poster presentations

Laura Grabowski, Mohamed Labib, Moritz Doeker, Thomas Fuchs, Christian Brüsseler, Nicolai Kallscheuer, Jan Marienhagen, Stephan Noack, Andreas Jupke and Dörte Rother. Bio-based synthesis of metaraminol in an enzyme cascade integrating microbially produced precursors and reactive *in situ* product removal**.** *Biocat, Hamburg, Germany (28.08.2022 - 01.09.2022)*

Laura Grabowski, Mohamed Labib, Moritz Doeker, Thomas Fuchs, Christian Brüsseler, Nicolai Kallscheuer, Jan Marienhagen, Stephan Noack, Andreas Jupke and Dörte Rother. Combining microbial cell factories and an enzyme cascade to produce metaraminol from renewable feedstocks. *Biocatalysis Gordon Research Conference, Manchester, NH, USA (10.07.2022 - 15.07.2022).*

Laura Grabowski, Moritz Doeker, Andreas Jupke and Dörte Rother. Towards a sustainable enzymatic production of metaraminol with integrated *in situ* reactive extraction. *Himmelfahrtstagung on Bioprocess Engineering, Mainz, Germany (23.05.2022 - 25.05.2022).*

Laura Grabowski, Mohamed Labib, Moritz Doeker, Thomas Fuchs, Christian Brüsseler, Jan Marienhagen, Stephan Noack, Andreas Jupke and Dörte Rother. A multi-disciplinary approach for bio-based production of metaraminol in a synthetic enzyme cascade from renewable feedstocks. *5th Multistep Enzyme Catalyzed Processes Congress (online, 13.09.2021 - 16.09.2021).*

Laura Grabowski, Mohamed Labib, Moritz Doeker, Thomas Fuchs, Christian Brüsseler, Jan Marienhagen, Stephan Noack, Andreas Jupke and Dörte Rother. Bio-based synthesis of metaraminol in an enzymatic cascade using microbially produced precursors from renewable feedstocks. *Biotrans (online, 19.07.2021 - 22.07.2021).*

Laura Grabowski, Kevin Mack, Moritz Doeker, Andreas Jupke and Dörte Rother. Process intensification of the enzymatic cascade to metaraminol with integrated *in situ* liquid-liquid product removal. *34. DECHEMA-Jahrestagung der Biotechnologen (online, 21.09.2020 - 24.09.2020).*

Oral presentations (consortium meetings and institute seminars)

Laura Grabowski. Process intensification of the biocatalytic production of chiral amino alcohols from bio-based precursors. *2nd doctoral seminar (14.06.2022)*

Laura Grabowski. Process intensification of the biocatalytic production of chiral amines with integration of bio-based precursors. *1st doctoral seminar (07.10.2020)*

Moritz Doeker, Kevin Mack, Laura Grabowski. *In situ* product removal of metaraminol from enzymatic reactions. *4th HyImPAct project meeting, Aachen, Germany (29.11.2019).*

Laura Grabowski, Wieland Freyer. Efficient synthesis of chiral amino alcohol building blocks using 2-step enzyme cascades in repetitive batch mode. *3rd HyImPAct project meeting, Jülich, Germany (10.04.2019).*

Supervised Student Theses

Nina Klos (2023). Investigation of factors influencing the enzymatic transamination towards chiral amino alcohols and resulting reaction engineering concepts. *Master thesis, RWTH Aachen University.*

Anneke Strumpel (2022). Efficiency increase of the synthesis of metaraminol by catalyst recycling using immobilized carboligase and amine transaminase. *Bachelor thesis, Darmstadt University of Applied Sciences.*

Supervised Student Theses (continued)

Sarah Schmitz (2021). Charakterisierung der *in-vivo* Immobilisierung einer Carboligase und einer Amintransaminase über die Sporenoberfläche von *Bacillus subtilis. Bachelor thesis, FH Aachen University of Applied Sciences.*

Contents

Abstract ---------- V
Zusammenfassung ---------- VII
Nomenclature ---------- IX
1 General Introduction ---------- - 3 -
1.1 Sustainable synthesis of (chiral) products ---------- - 3 -
1.1.1 Goals of green chemistry principles ---------- - 3 -
1.1.2 Biocatalysis as a sustainable synthesis approach ---------- - 3 -
1.1.3 Asymmetric synthesis ---------- - 4 -
1.2 Chiral amino alcohols – synthesis and application ---------- - 5 -
1.2.1 Chemical synthesis of chiral amino alcohols ---------- - 5 -
1.2.2 (Chemo-)enzymatic synthesis of chiral amino alcohols ---------- - 7 -
1.2.3 Applications of chiral amino alcohols as fine chemicals and active pharmaceutical ingredients ---------- - 10 -
1.3 Enzymatic synthesis of metaraminol ---------- - 11 -
1.3.1 Multi-step enzymatic synthesis of metaraminol using a carboligase and an amine transaminase ---------- - 11 -
1.3.2 Carboligases ---------- - 12 -
1.3.3 Amine transaminases ---------- - 14 -
1.4 Challenges in amine transaminase catalyzed reactions and resulting (process) engineering concepts ---------- - 15 -
1.5 HyImPAct project ---------- - 18 -
1.6 Scope of the thesis ---------- - 20 -
2 Materials & Methods ---------- - 25 -
2.1 Materials ---------- - 25 -
2.1.1 Chemicals ---------- - 25 -
2.1.2 Devices ---------- - 26 -
2.1.3 Bacterial strains, plasmids and enzymes ---------- - 28 -
2.2 Methods ---------- - 29 -
2.2.1 Biocatalyst production ---------- - 29 -
2.2.2 Enzyme immobilization ---------- - 33 -
2.2.3 Enzyme activity assays ---------- - 36 -

2.2.4 Biotransformations ---- - 37 -
2.2.5 Stability of amine transaminases under relevant process conditions ---- - 41 -
2.2.6 Production and utilization of bio-based precursors from fermentation supernatants ---- - 43 -
2.2.7 Determination of pK_a values *via* titration ---- - 45 -
2.2.8 Pure substance extraction studies without enzyme ---- - 45 -
2.2.9 *In situ* product removal experiments within transamination with L-alanine as amine donor ---- - 47 -
2.2.10 Instrumental analytics ---- - 52 -
2.2.11 Formula and statistical information ---- - 57 -
3 Results ---- - 61 -
3.1 Combining microbial cell factories and multi-step enzymatic synthesis to produce metaraminol from bio-based precursors ---- - 65 -
3.1.1 Abstract ---- - 65 -
3.1.2 Introduction ---- - 65 -
3.1.3 Results & Discussion ---- - 66 -
3.1.4 Conclusion ---- - 78 -
3.2 Process intensification by *in situ* liquid-liquid product extraction ---- - 81 -
3.2.1 Abstract ---- - 81 -
3.2.2 Introduction ---- - 81 -
3.2.3 Results & Discussion ---- - 83 -
3.2.4 Conclusion ---- - 95 -
3.3 Process intensification by *in situ* reactive product extraction ---- - 99 -
3.3.1 Abstract ---- - 99 -
3.3.2 Introduction ---- - 99 -
3.3.3 Results & Discussion ---- 101 -
3.3.4 Conclusion ---- 116 -
3.4 Enzyme immobilization as a tool in biocatalytic process intensification ---- 119 -
3.4.1 Abstract ---- 119 -
3.4.2 Introduction ---- 119 -
3.4.3 Results & Discussion ---- 122 -
3.4.4 Conclusion ---- 133 -

3.5 Process intensification by further reaction parameter optimization ---------- - 137 -

3.5.1 Abstract ---------- - 137 -

3.5.2 Introduction ---------- - 137 -

3.5.3 Results & Discussion ---------- - 138 -

3.5.4 Conclusion---------- - 146 -

3.6 Enlarging the product spectrum to 4-hydroxylated amino alcohols ---------- - 149 -

3.6.1 Abstract ---------- - 149 -

3.6.2 Introduction ---------- - 149 -

3.6.3 Results & Discussion ---------- - 150 -

3.6.4 Conclusion---------- - 157 -

4 General Discussion & Outlook ---------- - 161 -

4.1 Opportunities of hybrid processes for bio-based syntheses of chiral products - 161 -

4.2 Evaluation of process intensification methods presented in this thesis -------- - 163 -

4.3 Challenges and prospects of ISPR strategies---------- - 166 -

4.4 Transfer of reactive extraction for (*in situ*) recovery of other amine products - 167 -

4.5 Outlook ---------- - 169 -

References ---------- - 171 -

Appendix---------- - 191 -

Curriculum Vitae ---------- - 225 -

Abstract

Chiral amine compounds such as amino alcohols are industrially important precursors to produce pharmaceuticals and other fine chemicals. The development of multi-step biocatalysis has enabled the enzymatic production of chiral amino alcohols, which is characterized by high selectivity and step efficiency. A sustainable synthesis of high-value chiral products can be achieved through the efficient integration of microbiological, enzymatic and chemical steps with direct product recovery in hybrid processes. In the presented work, this approach is demonstrated for the enzymatic synthesis of metaraminol ((1*R*,2*S*)-2-amino-1-(3-hydroxyphenyl)propan-1-ol), an active pharmaceutical ingredient for treating hypotension. As a novel strategy, microbial cell factories and an enzyme cascade are combined to produce the necessary precursors L-alanine and pyruvate from sugars as renewable resources by engineered *Corynebacterium glutamicum* and utilize them in the two-step metaraminol synthesis using a carboligase and an amine transaminase. Since the transamination step with L-alanine as amine donor was thermodynamically limited, two complementary *in situ* product extraction concepts were developed. The operational window was defined by physicochemical characterization of the reaction system, screening of suitable extraction solvents and compatibility tests with the amine transaminase from *Chromobacterium violaceum Cv*2025. The integration of *in situ* product extraction with the transaminase reaction enabled to shift the reaction equilibrium. The physical extraction of metaraminol was characterized by a narrow operational window concerning the applicable pH, which was revealed as a central bottleneck of this approach. In contrast, the reactive extraction concept made use of a bio-based solvent system, consisting of 1-octanol and oleic acid as the reactive extractant. Upon integration of the reactive extraction with the transamination reaction, higher extraction efficiencies, higher total product yields and improved product selectivity were achieved. The *in situ* reactive extraction was shown to be effective through repeated extractions or in a semi-continuous process setup. The enzymatic metaraminol synthesis was further limited by inhibitory effects of substrate and product on *Cv*2025, which was only observed for the 3-hydroxylated substrate system.

To deal with emulsification in biphasic reaction systems and allow for high specific biocatalyst yields, two enzyme immobilization methods for the recycling of carboligases and amine transaminases were investigated as novel tools for biocatalytic process intensification, namely His-tag-mediated affinity adsorption on EziG™ carriers and spore display by using *Bacillus subtilis*. Finally, enlarging the product spectrum towards 4-hydroxylated amino alcohols was achieved by identifying an efficient and stereoselective enzyme combination, laying the foundation for the

enzymatic production of further bioactive compounds. This thesis thereby additionally demonstrates the efficient enzymatic synthesis of the substituted, aromatic chiral amino alcohols ((1*R*,2*S*)- und (1*R*,2*R*)-2-amino-1-(4-hydroxyphenyl)propan-1-ol), leveraging the application of bio-based precursors through reaction- and process engineering strategies.

Zusammenfassung

Chirale Amine und Aminoalkohole sind industriell wichtige Ausgangsstoffe für die Herstellung von Arzneimitteln und anderen Feinchemikalien. Die Entwicklung der mehrstufigen Biokatalyse ermöglicht die enzymatische Herstellung chiraler Aminoalkohole, die sich durch eine hohe Selektivität und Stufeneffizienz auszeichnet. Eine nachhaltige Synthese hochwertiger, chiraler Produkte kann durch die effiziente Kombination aus mikrobiellen, enzymatischen und chemischen Reaktionsschritten sowie durch die direkte Integration von Produktaufarbeitung in Hybridprozessen erreicht werden. Dies wurde in dieser Arbeit anhand der enzymatischen Synthese von Metaraminol ((1*R*,2*S*)-2-amino-1-(3-hydroxyphenyl)propan-1-ol), einem pharmazeutischen Wirkstoff zur Behandlung von Hypotonie, demonstriert. Durch die neuartige Kombination von mikrobiellen Zellfabriken und einer Enzymkaskade wurden die Co-Substrate L-Alanin und Pyruvat zunächst in rekombinanten *Corynebacterium glutamicum* aus nachwachsenden Rohstoffen produziert und in der zweistufigen Metaraminol-Synthese unter Verwendung einer Carboligase und einer Amin-Transaminase eingesetzt. Da der Transaminierungsschritt mit L-Alanin als Amin-Donor ein ungünstiges thermodynamisches Gleichgewicht aufweist, wurden zwei komplementäre Strategien zur *in situ* Produktextraktion entwickelt. Das Betriebsfenster wurde durch die physiochemische Charakterisierung des Reaktionssystems, das Screening geeigneter Extraktionslösungsmittel und Kompatibilitätstests mit der Amin-Transaminase aus *Chromobacterium violaceum Cv*2025 definiert. Die Integration der *in situ* Produktextraktion mit der Transaminase-Reaktion ermöglichte eine Verschiebung des Reaktionsgleichgewichtes. Hierbei war die physikalische Extraktion von Metaraminol durch ein eingeschränktes Betriebsfenster definiert, da der alkalische pH-Bereich zwar Voraussetzung für den Extraktionsprozess war, jedoch die Enzymaktivität und Produktstabilität herabsetzte. Als alternative Strategie wurde die Reaktivextraktion im neutralen pH-Bereich unter Verwendung von Ölsäure als reaktives Extraktionsmittel entwickelt. Hierbei konnten hohe Extraktionseffizienzen, gesteigerte Produktausbeuten und eine verbesserte Produktselektivität erreicht werden. Die Reaktivextraktion wurde in wiederholten Extraktionsschritten oder in einem semi-kontinuierlichen Prozessaufbau gezeigt. Die enzymatische Metaraminol-Synthese wurde außerdem durch inhibitorische Effekte von Substrat und Produkt auf *Cv*2025 eingeschränkt, die nur für das 3-hydroxylierte Substratsystem beobachtet wurden. Um der Emulsionsbildung in zweiphasigen Reaktionssystemen entgegenzuwirken und hohe spezifische Ausbeuten zu ermöglichen, wurden zwei Methoden zur Enzymimmobilisierung (His-Tag-vermittelte

Affinitätsadsorption an EziG™-Trägern und das Sporendisplay durch *Bacillus subtilis*) für das Recycling von Carboligasen und Amintransaminasen untersucht. Zur Erweiterung des Produktspektrums wurde die Synthese 4-hydroxylierter Aminoalkohole, (1*R*,2*S*)- und (1*R*,2*R*)-2-amino-1-(4-hydroxyphenyl)propan-1-ol, entwickelt, wodurch die Grundlage für die enzymatische Produktion weiterer bioaktiver Substanzen gelegt wurde. Diese Arbeit demonstriert die effiziente enzymatische Synthese chiraler, aromatischer Aminoalkohole, wobei die Nutzung biobasierter Ausgangsstoffe durch die Integration von reaktions- und verfahrenstechnischen Strategien ermöglicht wurde.

Nomenclature

Abbreviations

Enzyme denotation	Description
*Ac*TA	amine transaminase from *Arthrobacter citreus*
ADH	alcohol dehydrogenase
AlaDH	NADH-dependent alanine dehydrogenase
AlaT	L-glutamate-dependent aminotransferase
AvtA	L-valine-dependent aminotransferase
*Ap*PDC E469G	pyruvate decarboxylase variant from *Acetobacter pasteurianus*
*Ap*PDC var	pyruvate decarboxylase variant from *Acetobacter pasteurianus*
*As*TA	amine transaminase from *Arthrobacter spec.*
*Bm*TA	amine transaminase from *Bacillus megaterium*
*Cv*2025	amine transaminase from *Chromobacterium violaceum*
LDH	lactate dehydrogenase
FDH	formate dehydrogenase
*Ll*KdcA	branched-chain keto acid decarboxylase from *Lactococcus lactis*
*No*CAR	carboxylate reductase from *Nocardia otitidiscaviarum*
PDHC	pyruvate dehydrogenase complex
PQO	pyruvate:quinone oxidoreductase
PEPC	phosphoenolpyruvate carboxylase
*Sc*PDC	pyruvate decarboxylase from *Saccharomyces cerevisiae*
*Zm*PDC	pyruvate decarboxylase from *Zymomonas mobilis*

Abbreviation	Description
2D-UHPLC	two-dimensional high-performance liquid chromatography
3-AHP	2-amino-1-(3-hydroxyphenyl)propan-1-ol
4-AHP	2-amino-1-(4-hydroxyphenyl)propan-1-ol
3-OH-BA	3-hydroxybenzaldehyde
3-OH-PAC	3-hydroxy-phenylacetylcarbinol;1-hydroxy-1-(3-hydroxyphenyl)propan-2-one)
4-OH-PAC	1-hydroxy-1-(4-hydroxyphenyl)propan-2-one)
3-OH-BZ	3-hydroxybenzoate

Abbreviation	Description
4-OH-BOH	4-hydroxybenzyl alcohol
ACN	acetonitrile
AI	autoinduction (medium)
ALA	alanine
AP	acetophenone
API	active pharmaceutical ingredient
APP	1-amino-1-phenylpropan-2-one
APPO	2-amino-1-phenyl-propan-1-one
ATP	adenosine triphosphate
Aq	aqueous
BE	back extraction (phase)
BCA	bicinchoninic acid assay
BHI	brain heart infusion (medium)
BioSC	Bioeconomy Science Center
BSA	bovine serum albumin
CCE	crude cell extract
CDW	cell dry weight
CPG	controlled porosity glass
DAD	diode array detector
DEA	diethylamine
De	diastereomeric excess
DMSO	dimethyl sulfoxide
DO	dissolved oxygen
DSP	downstream processing
E.C.	enzyme commission
Ee	enantiomeric excess
EDTA	ethylenediaminetetraacetic acid
FAD	flavin adenine dinucleotide
FLD	fluorescence detector
GC	gas chromatography
GC-ToF-MS	gas chromatography time-of-flight mass spectrometry
HEPES	4-(2-hydroxyethyl)-1-piperazineethanesulfonic acid
His-tag (His6)	hexahistidine tag
HPLC	high-performance liquid chromatography

Abbreviation	Description
HPP	1-hydroxy-1-phenylpropan-2-one
HyImPAct	hybrid processes for important precursors and active pharmaceutical ingredients
Ic	isomeric content
IMAC	immobilized metal affinity chromatography
IPA	isopropylamine
IPTG	isopropyl-β-D-thiogalactoside
ISPR	*in situ* product removal
KDa	kilo dalton
Kpi	potassium phosphate (buffer)
LB	lyogeny broth (medium)
LLE	liquid-liquid extraction
LWC	lyophilized whole cells (of *Escherichia coli*)
Lyo	lyophilizate
Metaraminol	(1*R*,2*S*)-2-amino-1-(3-hydroxyphenyl)propan-1-ol
MBA	methylbenzylamine (1-phenylethan-1-amine)
MTBE	methyl tertiary-butyl ether
NADH	(reduced) nicotinamide adenine dinucleotide
NCS	norcoclaurine synthase
NE	norephedrine
Ni-NTA	nickel-nitrilotriacetic acid
NPE	norpseudoephedrine
OA	oleic acid
Org	organic
OD_{600}	optical density at 600 nm wavelength
PE	purified lyophilized enzyme
PI	process intensification
pK_a	acid dissociation value
PLP	pyridoxal-5'-phosphate
PMP	pyridoxamine-5'-phosphate
PPDO	1-phenylpropane-1,2-dione
PYR	pyruvate
RI	refractive index detector

Abbreviation	Description
Rpm	rounds per minute
SDS-PAGE	sodium dodecyl sulfate-polyacrylamide gel electrophoresis
SEC	size-exclusion chromatography
2xSG	2x Schaefer's glucose (medium)
SN	supernatant
STY	space-time yield
SOC	super optimal broth with catabolite repression (medium)
TA	amine transaminase
TB	terrific broth (medium)
THIQ	tetrahydroisoquinoline
TAE	tris-acetate EDTA buffer
TU	technical university
ThDP	thiamine diphosphate
THIQ	tetrahydroisoquinoline
TFA	trifluoracetic acid
TRIS	tris(hydroxymethyl)aminomethane
v/v	volume concentration (volume per volume)
w/w	mass fraction (weight per weight)
w/v	mass concentration (weight per volume)

Symbols

Symbol	Description	Unit
E	extraction efficiency	-
log*P*	logarithmic partitioning coefficient in 1-octanol/water	-
μ	growth rate	h^{-1}
pK_a	negative logarithm of acid dissociation constant	-
STY	space-time yield	$g\ L^{-1}\ d^{-1}$
t	time	h
T	temperature	°C
U	enzymatic unit	$\mu mol\ min^{-1}$

Chapter 1

General Introduction

Contributions:

This chapter was written by Laura Grabowski and revised by Dörte Rother.

1 General Introduction

1.1 Sustainable synthesis of (chiral) products

1.1.1 Goals of green chemistry principles

With the industrial revolution and vast expansion of the chemical industry, commodity chemicals and pharmaceuticals became readily available, providing social and health welfare in predominantly developed countries. These social advances, however, emerged to the detriment of depleting natural resources and increasing environmental pollution [1]. In fact, the manufacturing of pharmaceuticals is resource- and emission-intensive, thereby contributing tremendously to a polluting fine chemical industry [2]. To counteract climate change and environmental pollution and ensure long-term resilient industries, a more ecological comprehension in the chemical industry gained in importance. In 1998, the 12 green chemistry principles were developed by Paul T. Anastas and John C. Warner to define sustainable chemical processes [3]. The central principles comprise the prevention of waste and pollution and the application of safer chemicals, solvents and auxiliaries. In addition, organic syntheses should be designed for high atom economy, high energy efficiency and should make use of renewable feedstocks. Complementarily, green engineering principles have been proposed, stressing for example for product purification to be designed for minimized consumption of energy and materials [4]. In an effort to improve the characterization of a given process in terms of its environmental impact, the environmental factor (E-factor, the total amount of waste per kilogram product) was introduced as a quantitative metric already in 1992 [5]. The imperative to design and characterize more sustainable manufacturing practices in the (fine) chemical and pharmaceutical sector persists with the ultimate goal to establish a circular bioeconomy. In 2016, the United Nations implemented the Sustainable Development Goals to promote social, ecological, and economic development. In that regard, innovative technologies und industries are needed to advance global social well-being and fight climate change.

1.1.2 Biocatalysis as a sustainable synthesis approach

Catalysts that inherently meet many of the criteria proposed in the green chemistry principles are enzymes. In nature, enzymes have evolved to catalyze reactions under ambient temperatures and pressures, except for extremophilic species. Since the early enzyme discovery and first targeted applications in the 1930s [6], biocatalysis has found its way into various industrial sectors for the manufacturing of polymers, fine chemicals, fragrances and flavors, (bio)pharmaceuticals and food [7]. Nowadays, biocatalytic transformations utilize isolated enzymes, cell free extracts or non-

viable whole cell formulations containing a large mass percentage of the target enzyme [8]. Here, instead of rewiring the hosts metabolism for *de novo* synthesis of the desired product (usually referred to as *in vivo* microbial transformations or fermentation), the *in vitro* application of whole cell catalysts in diverse reaction media allows for suitable microenvironments [9]. With the rapid technological progress in microbial cultivations, molecular gene editing techniques and strain screenings, not only the sphere of known enzymes increased but also the ability to engineer, isolate and adapt enzymes as biocatalysts for novel transformations or selectivities [10]. In this way, the advantages of enzymes were recognized by the well-established chemical industry for specifically challenging or polluting synthesis steps, leading to chemoenzymatic routes, in which a former chemical synthesis step was replaced by a biocatalytic reaction step. For instance, in the synthesis of the diabetes drug sitagliptin, an engineered (*R*)-selective amine transaminase (ATA-117-Rd) facilitated a 13% yield increase and 19% reduction in waste, outcompeting the original chemical synthesis step at industrial scale [11]. This example illustrates how biocatalysis can offer efficient alternative synthetic solutions by making use of renewable, biodegradable biocatalysts that facilitate reactions under mild reaction conditions. Especially high stereo-, regio- and chemoselectivity make biocatalysts an interesting asset to drug synthesis [12]. In combination with other disciplines, completely novel synthetic routes based on renewable resources instead of fossil-based starting materials can be generated according to the aforementioned principles of green chemistry, which will be a central motif in this thesis.

1.1.3 Asymmetric synthesis

One area of chemical catalysis that has caught particular interest in enzymes as alternative catalysts is asymmetric synthesis. Here, the reaction introduces one or more chiral centers to the molecule with high selectivity for one predominant stereoisomer (enantiomer or diastereomer). Thereby, asymmetric synthesis starts with pro- or achiral substrates. In contrast to kinetic resolution, in which a racemic mixture is resolved, resulting in a maximal theoretic yield of 50%, asymmetric synthesis can achieve 100% theoretical yield (Figure 1).

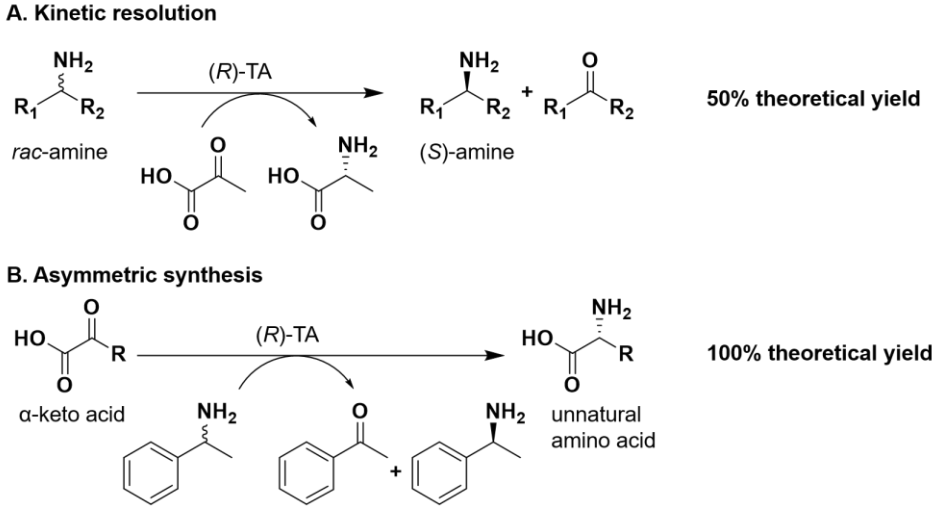

Figure 1 Kinetic resolution and asymmetric synthesis as fundamental catalytic principles applying amine transaminases. The kinetic resolution shows the separation of a racemic mixture applying pyruvic acid as the amine acceptor in this example. In asymmetric synthesis, the optically pure synthesis of D-amino acid is achieved. In this example, racemic *alpha*-methylbenzylamine (α-MBA) is used as the amine donor. Figure was adapted from [13].

As chirality largely affects the biological activity of a compound, the stereoselective synthesis is especially important in the pharmaceutical industry to ensure drug safety and effectiveness [14]. Classical chemical syntheses often depend on transition metal catalysts, chiral auxiliaries, or protection chemistry to achieve stereo- and regioselectivity [15, 16]. In organochemistry, non-metal containing catalytic compounds, such as chiral amines or amino acids, are used for asymmetric synthesis and offer a more environmentally friendly synthesis [17]. The high selectivity of enzymes has been recognized to allow asymmetric synthesis in fewer reaction steps, based on the three-dimensional structure of the protein comprising its highly specific active site. The catalytic function is often dependent on cofactors (metals, inorganic ions) or coenzymes (vitamins or other more complex organic molecules). This molecular environment promotes selective substrate binding and stabilization of transition states towards a favored stereoselective product formation. The active site is therefore a common target in genetic engineering to enlarge the substrate spectrum, promote higher enzymatic activity or alter the stereoselectivity in asymmetric syntheses [18]. As such, enzyme engineering efforts to increase substrate acceptance and conversion are often accompanied by an increase in stereoselectivity.

1.2 Chiral amino alcohols – synthesis and application

1.2.1 Chemical synthesis of chiral amino alcohols

Amino alcohols contain hydroxyl groups and primary ($-NH_2$), secondary (-NHR) or tertiary ($-NR_2$) amino moieties. The carbon atom position of the amino group adjacent to the hydroxyl group further differentiates *alpha*- and *beta*- amino alcohols, the latter is also referred to as vicinal or 1,2-amino alcohols. Many natural, bioactive products such as the hormones adrenaline and

noradrenaline (dopamine derivatives) belong to this group of compounds (Figure 2). Therefore, substantial interest lays in the synthetic production of similar compounds such as norephedrine for fine chemical and pharmaceutical use. Different chemical methods can be applied for the synthesis of vicinal amino alcohols, such as functional groups manipulation, single heteroatom addition, ring opening of epoxides, aminohydroxylation or coupling reactions [19]. The chemical preparation of phenylpropanolamine stereoisomers ((1*R*,2*S*)- and (1*S*,2*R*)-norephedrine, (1*S*,2*S*)- and (1*R*,2*R*)-norpseudoephedrine) was published by Lee *et al.* in 2012, demonstrating an asymmetric transfer hydrogenation reaction from the prochiral cyclic sulfamidate imine of racemic phenylacetylcarbinol (PAC) [20]. Similarly, (1*R*,2*S*)-norephedrine was synthesized from (*R*)-PAC *via* a two-step hydrogenation with benzylamine using a palladium and platinum catalyst with *N*-benzyl-l-norephedrine as intermediate or direct hydrogenation reaction with palladium catalyst, as shown in Figure 3 [21]. Further, nitroaldol (Henry) reaction of aromatic aldehydes with nitroalkanes and subsequent hydrogenation of the 2-nitroalcohol give rise to substituted amino alcohols like metaraminol (refer to section 1.2.3) [22, 23].

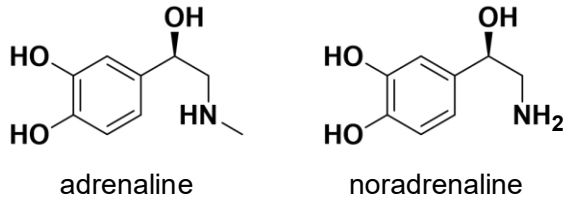

Figure 2 Adrenaline (epinephrine, secondary 1,2-amino alcohol) and noradrenaline (norepinephrine, primary 1,2-amino alcohol) are central hormones of the sympathetic nervous system, acting as α,β-adrenergic receptor agonists and vasoconstrictors.

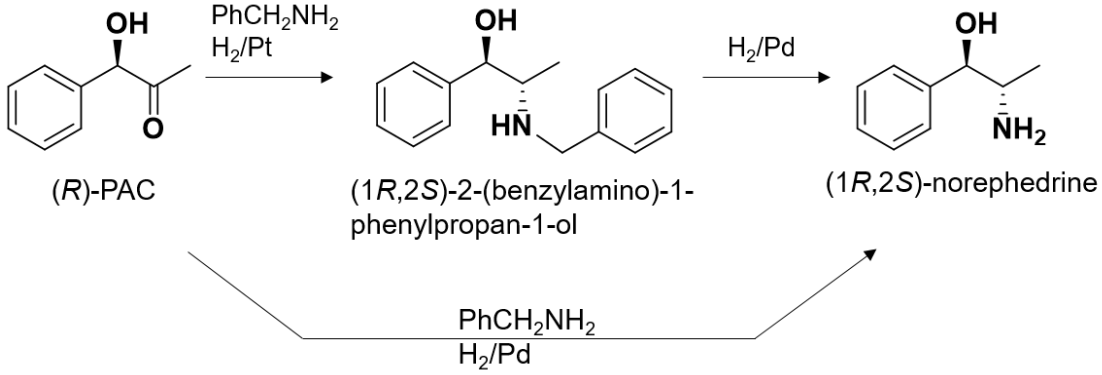

Figure 3 Chemical synthesis of (1*R*,2*S*)- norephedrine from (*R*)-PAC and benzylamine using platinum and palladium catalysts in two separate reaction steps or one combined synthesis. The two-stage process was favorable regarding optical and diastereometric purity but less cost-effective as it required two different metal catalysts and associated recovery methods [21].

PAC can also be derived enzymatically from 3-hydroxybenzaldehyde and pyruvate as shown in Figure 4 in the next section [24]. Instead of using fossil-based starting materials, a common

strategy towards chiral amino alcohols is the hydrogenation of amino acid mixtures to amino alcohols [25, 26]. Recently, a completely green adaption of this strategy was presented by recycling the by-products (inorganic salts) in the subsequent reaction batch, thereby enhancing the overall atom economy [27]. As the demand for chiral compounds rises [28], the efficient production of chiral amino alcohols is a relevant and current research topic in both, academia and industry, promoting the development of novel synthetic routes, such as photocatalysis. Thereby, various 1,2-amino alcohols were obtained by Cr/photoredox dual-catalyzed alkylation from carbonyl compounds and *α*-silyl amines [29], or *via* photoredox-catalyzed decarboxylative radical coupling of aldehydes or ketones with *N*-aryl amino acids [30]. The latter technology utilizes eco-friendly solvents, mild reaction conditions and no harmful additives. However, a major downside to classical chemical syntheses of chiral amino alcohols are non-renewable catalysts. Therefore, the integration of enzymatic steps with organic synthesis was explored as a novel interface [31, 32].

1.2.2 (Chemo-)enzymatic synthesis of chiral amino alcohols

The combination of chemo- and biocatalysis has been studied for multi-step synthesis to exploit the performance-, cost- and environmental benefits of orthogonal catalysts for challenging syntheses. Several reaction engineering aspects thereby enable a suitable combination of multiple catalytic steps, often with the premise to provide precursors with biocatalysts, which are further converted with classical catalysts or *vice versa* [33]. For example, the chemoenzymatic production of ephedrine was shown by first producing the intermediate (*R*)-PAC with yeast pyruvate decarboxylase from benzaldehyde and pyruvate, coupled to a hydrogen and platinum-catalyzed amination step as shown in Figure 4 [24].

Biocatalytic amination reactions towards chiral amino alcohols have initially focused heavily on transaminases using prochiral ketones or aldehydes [34]. Eventually, to further expand the range of products and utilization of various starting materials, the combination of several enzymatic steps was investigated. This resulted in the development of synthetic enzyme cascades, which can vary in cascade mode depending on the temporal or simultaneous addition of enzymes and reactants (simultaneous, sequential or multi-step) and cascade type, describing how the cascade steps are organized and interconnected (linear, divergent, orthogonal, or cyclic among others), allowing for various alternative routes towards amino alcohols [35-38]. If the reaction steps are spatially and temporally separated, for example by integration of intermediate purification or due to incompatible reaction conditions between chemo- and biocatalysts, multi-step enzymatic synthesis is a more appropriate term. The fully enzymatic synthesis of nor(pseudo)ephedrine (N(P)E) was demonstrated in a two-step one-pot sequential mode, as shown in Figure 5 [39, 40]. Here,

Sehl *et al.* achieve the stereo- and regioselective synthesis with two alternative strategies from either benzaldehyde and pyruvate or 1-phenylpropane-1,2-dione, by combining (*R*)- and (*S*)-selective amine transaminases with either carboligases or alcohol dehydrogenases, respectively. Recently, Corrado *et al.* make use of petroleum-based β-methylstyrene as substrate to produce N(P)E stereoisomers in a multi-enzyme approach [41].

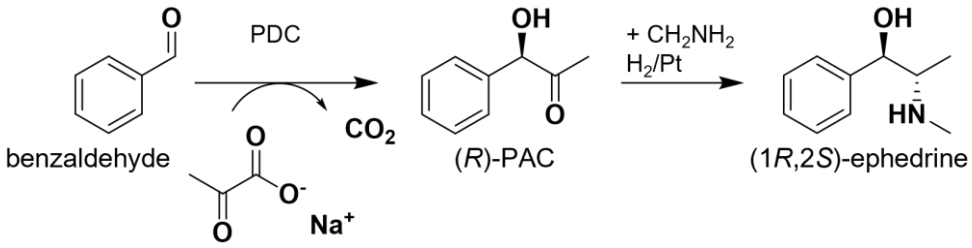

Figure 4 Chemoenzymatic synthesis of (1*R*,2*S*)-ephedrine involving the carboligation of benzaldehyde and pyruvate by a pyruvate decarboxylase (PDC) from yeast and the subsequent hydrogenation of the intermediate (*R*)-PAC with methylamine radicals and platinum catalyst.

Further combinatorial approaches involving the use of amine transaminases as important workhorses in biocatalytic chiral amine syntheses are noteworthy. The enzymatic synthesis of the chiral amino alcohol 2-amino-1,3,4-butanetriol (ABT), a precursor for antiviral inhibitors such as Nelfinavir, was shown in various ways by the combination of a transketolase and an amine transaminase (Figure 6) [42, 43]. In this example, a one-pot recycling cascade facilitated an efficient and cost-effective synthesis approach from natural substrates [37]. Recently, Corrado *et al.* presented several linear and divergent enzyme cascades to produce 1,2-amino alcohols (2-phenylglycinol, phenylethanolamine) from renewable L-phenylalanine with high yield and optical purity [44]. Starting from racemic 1,3-hydroxy ketones or prochiral 1,3-diketones, the production of all four diastereomers of 4-amino-1-phenylpentane-1-ol was established by using a (*S*)-selective keto reductase and enantiocomplementary amine transaminases [45]. While transaminases are applicable to obtain primary amines, other enzymes were explored for the synthesis of secondary and tertiary chiral amines, specifically also amino alcohols [46]. For example, amine dehydrogenases catalyze the reductive amination of α-hydroxy ketones and ammonia to vicinal amino alcohols [47], which allowed the high-yield and stereoselective production of the key intermediate for an antituberculosis drug [48]. Secondary amine products can be generated by an imine reductase (IRED) [49, 50]. A one-pot two-step enzymatic cascade towards chiral *N*-substituted 1,2-amino alcohols and tetrahydroisoquinoline (THIQ) alkaloids was established by combining benzaldehyde-lyase catalyzed hydroxymethylation and IRED-catalyzed reductive amination [51].

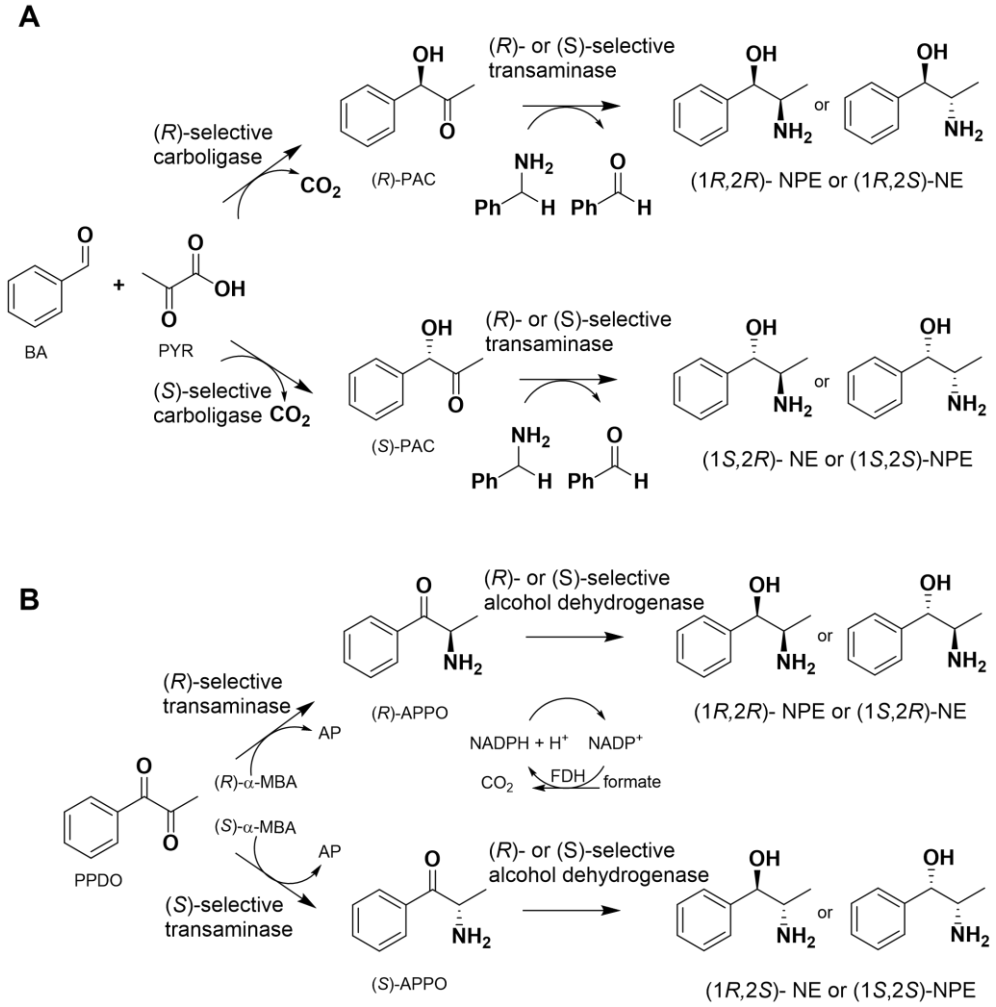

Figure 5 Different enzymatic synthesis strategies towards all stereoisomers of nor(pseudo)ephedrine. The one-pot two-step synthesis strategies make use of complementary amine transaminases in combination with carboligases (A) or alcohol dehydrogenases (B). In A, the reaction substrates are 3-OH-benzaldehyde with PAC as intermediate. In B, 1-phenylpropane-1,2-dione (PPDO) is aminated to 2-amino-1-phenyl-propan-1-one (APPO), which is further reduced by alcohol dehydrogenases. MBA= methylbenzylamine, AP = acetophenone, NE = norephedrine, NPE = norpseudoephedrine, FDH = formate dehydrogenase. Figure adapted from Sehl *et al.* [39].

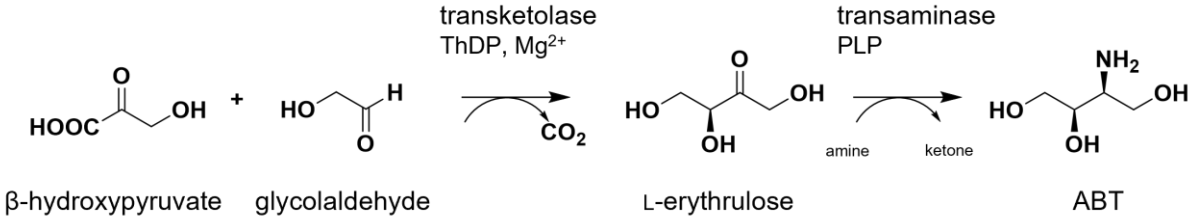

Figure 6 Synthesis of (2*S*,3*R*)-2-amino-1,3,4-butanetriol (ABT) from hydroxypyruvate and glycolaldehyde in a two-step enzymatic synthesis by a transketolase and an amine transamination. The transketolase catalyzes the carbon-carbon bond formation followed by the transamination of the intermediate L-erythrulose to ABT.

Usually, the development of synthetic enzyme cascades is initially conducted in low concentrations ranges (up to 10 mM). During the later stages of reaction optimization, the conversion of higher substrate concentrations towards preparative and industrially relevant scales should be proven. To achieve this, different engineered enzymes, alternative biocatalyst

formulations and alternative (aqueous or organic) reaction media can be potent optimization methods, depending on the targeted synthesis [52]. The preparative, optically pure synthesis (> 99% *ee*) of both enantiomers of valinol, an important precursor of various active pharmaceutical ingredients (APIs) [53], was developed with the amine transaminase from *Bacillus megaterium* (*Bm*TA) and the (*R*)-selective amine transaminase from *Arthrobacter spec.* in crude enzyme formulations, both in organic solvent (with adjusted water activity) and phosphate buffer (Figure 7) [54].

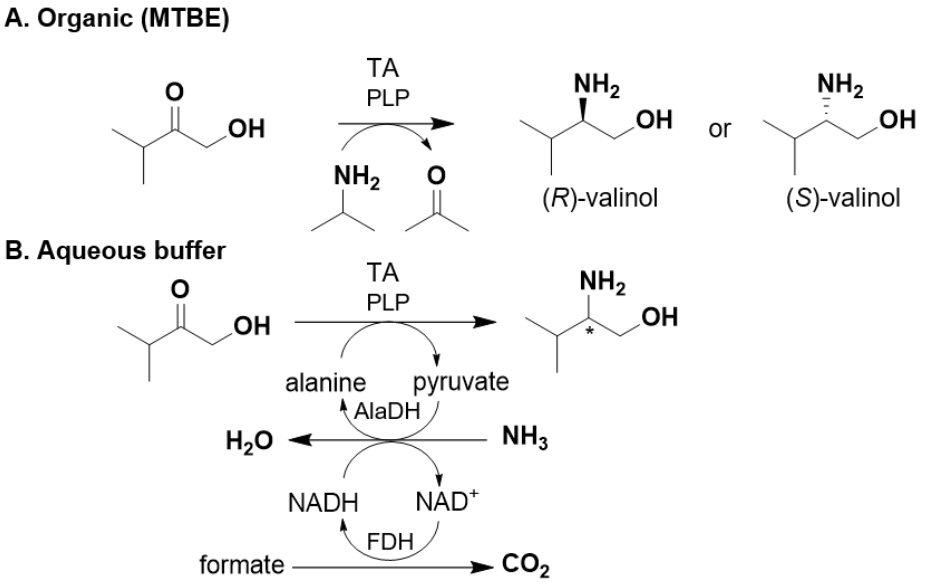

Figure 7 Synthesis of (*R*)- or (*S*)-valinol by an amine transaminase in organic solvent (A) or phosphate buffer (B). In methyl tertiary-butyl ether (MTBE), isopropylamine was applied as amine donor. In the aqueous system, alanine served as amine donor and was recovered by pyruvate recycling using an alanine dehydrogenase (AlaDH) and formate dehydrogenase (FDH) to shift the reaction equilibrium. Figure adapted from Fuchs *et al.* [54].

1.2.3 Applications of chiral amino alcohols as fine chemicals and active pharmaceutical ingredients

The structural motif of chiral amino alcohols can be found in a wide range of natural products or synthetic fine chemicals, including sphingolipids, or pharmaceuticals such as antibiotics or antiviral agents [55]. The structural diversity of molecules containing vicinal amino alcohols moieties is shown in Figure 8. Some of the examples exhibit bioactive properties, others can serve as synthons and chiral auxiliaries in chemical syntheses [56], or as precursor to produce bioactive compounds. Many chiral amino alcohol that are directly used as an API belong to the group of sympathomimetics. For examples, norephedrine and norpseudoephedrine, shown in Figure 8, have multiple applications as cardiovascular stimulant (as influenza medication) or as appetite suppressant [57, 58]. Similarly, ritodrine is an API for controlling premature labor [59] and structurally similar to ritobegron, which is used as treatment against overactive bladder [60]. Metaraminol ((1*R*,2*S*)-2-amino-1-(3-hydroxyphenyl)propan-1-ol, (1*R*,2*S*)-AHP) is a vicinal

amino alcohol and an active pharmaceutical ingredient for the treatment of hypotension [61, 62]. It acts as adrenoceptor agonist predominantly on the α_1-adrenergic receptor causing vasoconstriction.

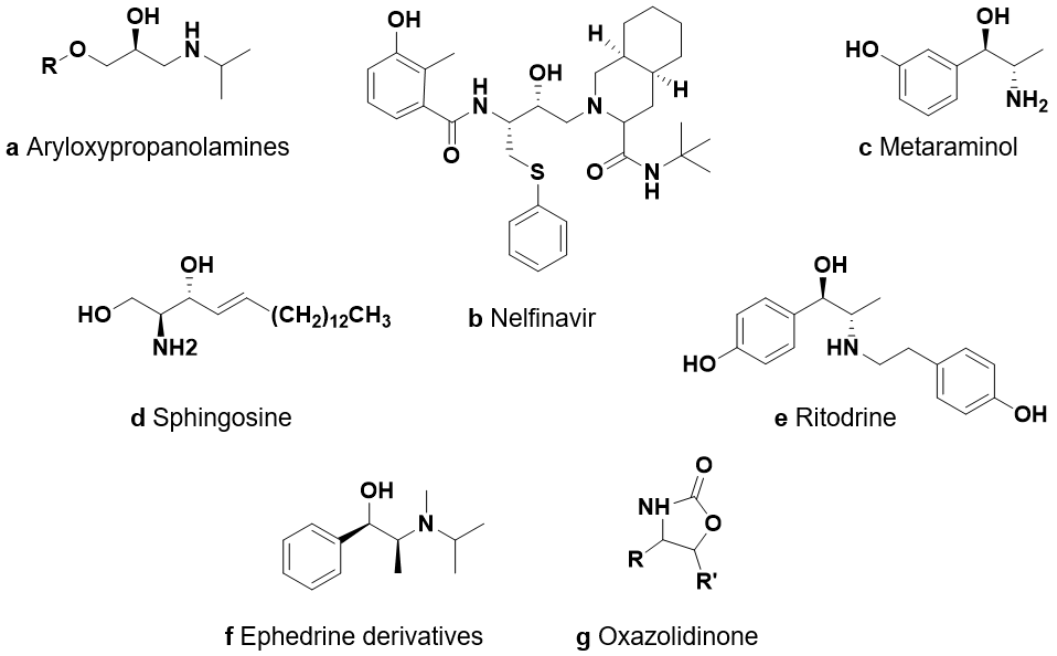

Figure 8 Molecules containing 1,2-amino alcohol moieties. **a**, Aryloxypropanolamines is the common structure of various drug molecules (β-adrenergic receptor agonist, also known as β-blockers) applied in the treatment of heart diseases and hypertension (for example propanolol for R = aryl) **b**, Nelfinavir is an HIV-protease inhibitior [63] **c**, Metaraminol is an active pharmaceutical for the treatment of hypotension [61, 62], **d,** Sphingosine are component of glycosphingolipids, which are involved in cellular signal transduction [64], **e**, Ritodrine is a potential active pharmaceutical ingredient for the control of premature labor [59], **f**, Ephedrine is a sympathomimetic drug [65], **f-g,** Oxazolidinone and ephedrine derivatives can serve as chiral auxiliaries in organic synthesis [66].

1.3 Enzymatic synthesis of metaraminol

The bio-based production of metaraminol by the combinatorial utilization of appropriate biocatalysts and process engineering was a central goal within the BioSC- funded focus lab project "HyImPAct", which is introduced in chapter 1.5. The state of the art of enzymatic metaraminol synthesis and the enzymes involved are explained in the following sections.

1.3.1 Multi-step enzymatic synthesis of metaraminol using a carboligase and an amine transaminase

The enzymatic synthesis of metaraminol was first demonstrated by Erdmann *et al.* in an enzymatic cascade starting from 3-hydroxybenzaldehyde and pyruvate (Figure 9). By combining a carboligation step with a transamination reaction using isopropylamine as the amine donor, the synthesis was achieved with high conversion and stereoselectivity, starting from 10 mM aldehyde concentration [67]. The further conversion of metaraminol in a chemically or enzymatically catalyzed Pictet-Spengler reaction towards tetrahydroisoquinoline (THIQ) derivatives was

established. Depending on the substitutions, THIQs are compounds of interest for the development of anti-tumor and anti-cancer drugs [68, 69]. In the initial ligation step of 3-hydroxybenzaldehyde and pyruvate, Erdmann *et al*. applied the ThDP-dependent acetohydroxyacid synthase I from *Escherichia coli* (*Ec*AHAS-I). This enzyme first catalyzes the decarboxylation of pyruvate to acetaldehyde and the subsequent ligation with the aldehyde moiety in the same active site. The release of carbon dioxide pushes the reaction equilibrium and renders the reaction practically irreversible. The subsequent transamination step makes use of the amine donor isopropylamine, achieving an equilibrium shift *via* the evaporation of the co-product acetone (93% conversion, 97% isomeric content (*ic*)). The final cyclization step gave 99% conversion of the amino alcohol, reaching a total conversion of 88% and 97% *ic*. Likewise, this cascade was shown with an alternative phosphate-catalyzed cyclization reaction giving rise to (1*S*,3*S*,4*R*)-1-(2-bromophenyl)-1,2,3,4-tetrahydroisoquinoline-4,6-diol (77% total conversion, 97% total *ic*). By incorporating an initial enzymatic reduction step of (microbially produced) 3-hydroxybenzoate, the cascade can be established based on renewables [70].

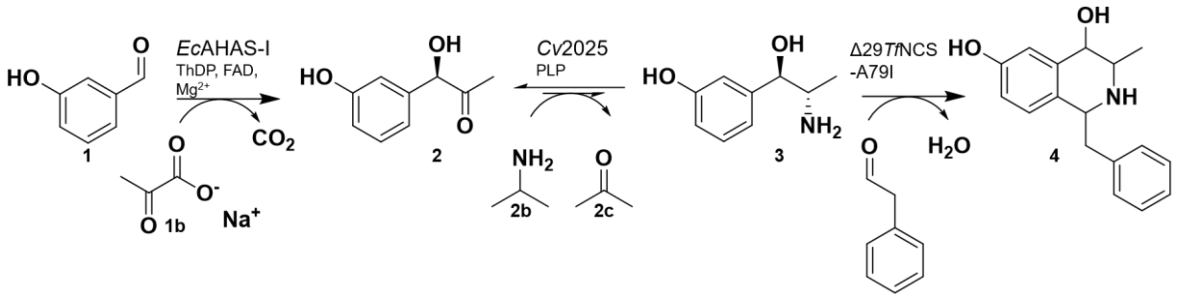

Figure 9 Three-step enzymatic cascade towards 1,3,4-trisubstituted tetrahydroisoquinoline (**4**). The first step of the cascade involves a carboligation reaction starting from 3-hydroxybenzaldehyde (**1**) and pyruvate (**1b**) catalyzed by the acetohydroxy acid synthase I from *Escherichia coli* (*Ec*AHAS-I). The ligase enzyme first decarboxylates pyruvate to acetaldehyde and subsequently catalyzes the ligation with the aldehyde gaining 3-hydroxyphenylacetylcarbinol ((*R*)-3-OH-PAC, **2**). The amine transaminase from *Chromobacterium violaceum* (*Cv*2025) performs the transamination towards (1*R*,2*S*)-AHP (metaraminol, **3**) using isopropylamine (IPA, **2b**) as the amine donor and releasing acetone (2c) as by-product. The third step is catalyzed by a Pictet-Spenglerase variant Δ29*Tf*NCS-A79I (norcoclaurine synthase variant from *Thalictrum flavum*) using phenylacetaldehyde as cosubstrate obtaining (1*S*,3*S*,4*R*)-1-benzyl-3-methyl-1,2,3,4-tetrahydroisoquinoline-4,6-diol (**4**). ThDP = thiamine diphosphate, PLP = pyridoxal-5'-phosphate, FAD = flavin adenine dinucleotide.

1.3.2 Carboligases

Pyruvate decarboxylases (PDC, EC 4.1.1.1) are lyases (EC 4), more specifically carbon-carbon lyases (EC 4.1), which include the carboxy lyases (EC 4.1.1). *In vivo*, the enzyme catalyzes the non-oxidative decarboxylation of pyruvate to acetaldehyde as the key step in alcoholic fermentation. PDCs from *Zymomonas mobilis* and *Saccharomyces cerevisiae* have been applied in various synthetic transformations [71]. The PDC from *Acetobacter pasteurianus* was first described as key enzyme for growth of *A. pasteurianus* on lactic acid, forming acetaldehyde, which was finally oxidized to acetic acid [72]. The enzyme is dependent on thiamine diphosphate

(ThDP) and bivalent cations like Mg^{2+} or Ca^{2+} to exhibit full catalytic activity. The catalytic activity of ThDP originates from the C2 atom of the thiazolium ring, which is one of the three structural units along with a 4'-aminopyrimidine and a diphosphate anchor. The cofactor-mediated decarboxylation and carboligation reactions of PDC are shown in Figure 10. ThDP is bound in the active site of the enzyme with magnesium ions *via* the diphosphate residue. Deprotonation at C2-H converts the ThDP into the catalytically active nucleophilic ylide form. The cations themselves are bound *via* the preserved binding motif Gly-Asp-Gly. The resulting proximity of the 4'-aminopyrimidine and the thiazolium ring enables a proton transfer from C2 to N4'. The negative partial charge on the C2 atom enables a nucleophilic attack on the carboxyl group of pyruvate, forming the intermediate. In case of carboligation, the aldehyde group of the acceptor molecule is attacked by the carbanionic intermediate, resulting in a C-C bond formation. Thus, both decarboxylation and ligation can occur sequentially in the same active site of the enzyme [73, 74]. The pyruvate decarboxylase from *Acetobacter pasteurianus* (*Ap*PDC) was previously evolved by site-directed mutagenesis obtaining several variants of complementary stereoselectivity [75]. In this work, a (*R*)-selective variant (in the following referred to as *Ap*PDC var) with high activity and stereoselectivity towards the synthesis of (*R*)-3-OH-PAC was used, which is the intermediate for metaraminol synthesis. Complementary, the (*S*)-selective carboligase *Ap*PDC E469G was used to synthesize (*S*)-3-OH-PAC. The gene sequences are shown in section A.3.2 in the appendix.

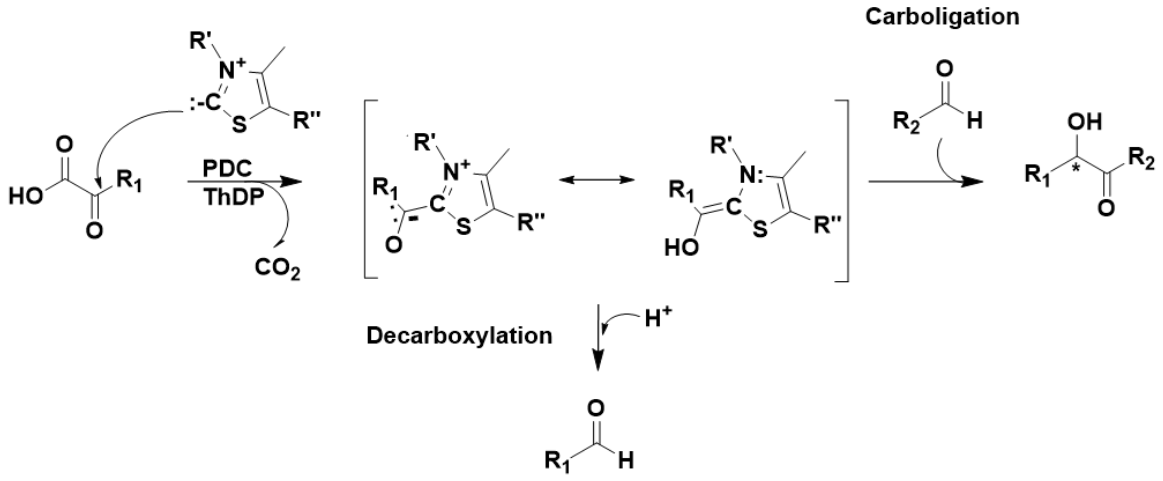

Figure 10 General ThDP-mediated catalysis of PDC showing the non-oxidative decarboxylation step and carboligation reaction with an acceptor aldehyde. With the innate substrate pyruvate (R_1 = Me) as donor, the enzyme produces acetaldehyde and carbon dioxide. The carbanionic intermediate can also nucleophilically attack an acceptor molecule to produce a chiral 2-hydroxy ketone (for example (*R*)-PAC for R_1 = Me and R_2 = Ph). R' = aminopyrimidine, R'' = $(CH_2)_2OP_2O_6$ [76].

1.3.3 Amine transaminases

Transaminases (EC 2.6.1.-) catalyze the reversible, enantioselective transfer of a primary amino group from an amine to an α-ketone or aldehyde. Transaminases require pyridoxal-5'-phosphate (PLP) as cofactor. PLP-dependent enzymes are classified into seven folding classes, with amine transaminase belonging to folding class I and IV [31, 77]. In their physiological role, amine transaminases play a major role in the nitrogen metabolism, exhibiting a wide substrate spectrum for amino acids [78]. Based on their substrate spectrum, transaminases are further classified into α-, ω-, and amine transaminases. Enzymes classified as *α*-transaminases only convert substrates with carboxyl functions in the α-position to the amino group, whereas ω-transaminases accept one to a maximum of twelve carbon atoms between the carboxyl function and the amino group. Within this group, amine transaminases do not require a carboxyl function [79, 80].

Transaminases exhibit a "ping-pong bi-bi" reaction mechanism consisting of two parts depicted for the transamination of 3-OH-PAC with isopropylamine (IPA) in Figure 11. The cofactor PLP is bound to the Lys288 in the phosphate binding coup of the enzyme by a covalent Schiff base linkage to the ε-amino group as an internal aldimine [81]. PLP is stabilized with amino acids of both subunits by eight hydrogen bindings, such as the hydrogen bond between the Asp259 and the nitrogen of PLP. In the first reaction step, which is the oxidative deamination, the amino donor IPA reacts to the corresponding ketone acetone, and PLP converts to pyridoxamine-5′-phosphate (PMP). In the second step, the receptor binds in the active site and the carbonyl group of the receptor is exchanged by the primary amine of the amino acid, forming the reaction product [82]. PMP is regenerated to PLP and (*R*)-3-OH-PAC reacts to the desired product metaraminol. The majority of investigated amine transaminases exhibited (*S*)-selectivity and a substantially smaller number of (*R*)-selective variants are known [83]. An (*R*)-selective variant from *Arthrobacter spec.* KNK168 was found in enrichment screenings from soil isolates and was later applied for the synthesis of various chiral amines [84]. A well characterized (*S*)-selective amine transaminase from *Chromobacterium violaceum* ATCC 12472 (DSM30191) (*Cv*2025, EC 2.6.1.18) was discovered in 2007 and belongs to the transaminase subgroup II and folding class I. It exhibits a dimeric structure and was shown to accept various aldehydes and substituted hydroxy ketones as substrates [39, 85, 86]. Especially its activity on bulky aromatic substrates such as 1,3-dihydroxy-1-phenylpropane-2-one and lignin model substrates makes *Cv*2025 a promising catalyst for synthetic applications [87, 88]. It was used in this thesis for the transamination toward (1*R*,2*S*)-3-AHP (metaraminol). Another (*S*)-selective amine transaminase from *Bacillus megaterium* SC6394 (*Bm*TA) is a tetrameric enzyme (dimer of dimer crystal structure), that was previously characterized in the kinetic resolution of *sec*-butylamine and cyclopropylethylamine with excellent

enantiomeric excess [89] for the (*S*)-enantiomer and therefore also used in the synthesis of (1*S*,2*S*)-methoxamine [90]. In this thesis, *Bm*TA was used in the synthesis of (1*S*,2*S*)-3-AHP in chapter 3.3 and 3.4, as it showed preference for (*S*)-configurated substrates [91].

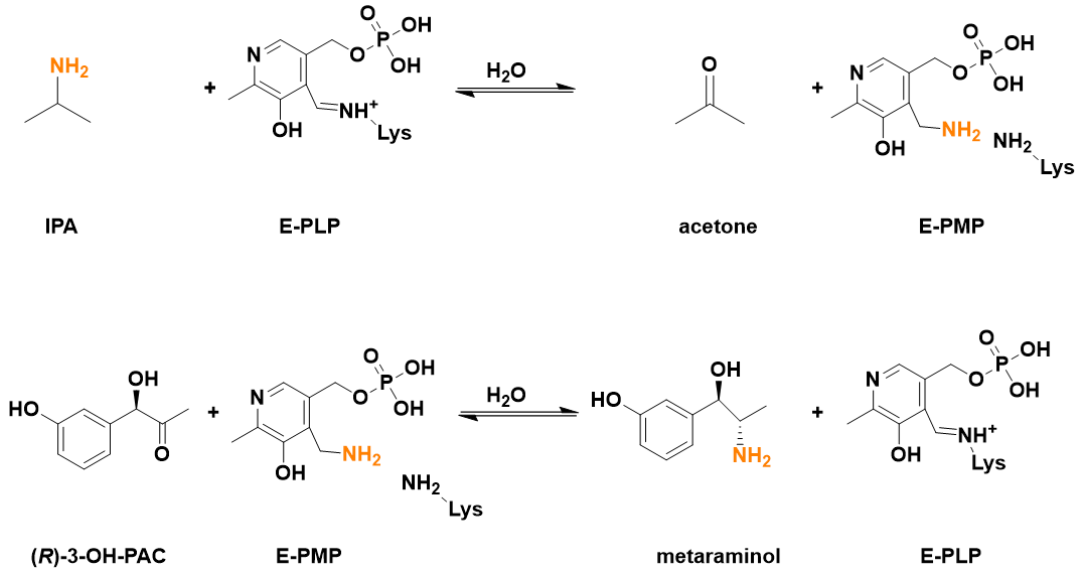

Figure 11 Schematic representation of the reaction mechanism of amine transaminases comprising two half reactions, which are shown with isopropylamine (IPA) as amine donor and 3-OH-PAC as the acceptor molecule. PLP = pyridoxal-5'-phosphate, PMP = pyridoxamine-5'-phosphate.

1.4 Challenges in amine transaminase catalyzed reactions and resulting (process) engineering concepts

As the field of amine transaminase catalyzed reactions emerged and more variants were identified and characterized, unique enzymatic aminations were enabled. Nevertheless, some challenges became apparent. In early amine transaminase research, understanding the substrate spectrum of these enzymes to define the sphere of accessible products was the primary focus. Many applications were limited by a substrate inhibition, product inhibition or limited substrate acceptance [92, 93]. More recently, especially challenging bulky substrates could be made accessible by enzyme engineering [94]. Likewise, reaction and enzyme engineering efforts enabled the acceptance of industrially favorable amine donors such as IPA [95].

A further aspect that currently often limits the applicability of amine transaminases is a lack of operational stability in the presence of high substrate loadings and the resulting low specific productivity [96, 97]. The instability of some transaminases has been associated to the binding capacity and affinity of the enzyme towards the cofactor PLP [93, 97], which encouraged the site-directed enzyme engineering to enhance PLP capacity of a range of class III amine transaminases [98]. Specifically, efforts in enzyme engineering have also been shown to promote stabilization through point mutating distinct surface and interfacial areas of the homodimeric PLP fold type I amine transaminase from *Pseudomonas jessenii* [99]. For stabilization of *Cv*2025, proline

substitutions in flexible protein areas generated enzyme variants with increased half-life at 60 °C or increased melting temperatures. In addition, enzyme immobilization could stabilize the amine transaminase from *Pseudomonas fluorescens*, which facilitated biocatalyst reusability as additional benefit [100].

Thermodynamic limitations are a drastic challenge in asymmetric synthesis with amine transaminases. A reaction is classified as thermodynamically hindered if the Gibbs free energy change ΔG is positive, meaning that substrates are favored over products in equilibrium, as reflected by the equilibrium constant K_{eq}. In this regard, the choice of amine donor has a significant influence on the thermodynamic equilibrium [101]. According to *le Chatelier* [102], the equilibrium of the reaction can be shifted by either an excess of (co-) substrate or removal of (co-) products. Strategies to displace the unfavorable reaction equilibrium in asymmetric transamination reactions are depicted in Figure 12. Using α-MBA as amine donor usually results in the highest K_{eq}, allowing for high conversions with an already moderate molar excess of amine donor as shown in the previous example of N(P)E synthesis. Its applicability and actual K_{eq} for phenolic ketones however depend heavily on the substitution of the aromatic ring and its accommodation in the active site [103, 104]. Further disadvantages of α-MBA are its high price (more severe for the optically pure compound than for racemic α-MBA) as well as a complicated product purification in the presence of MBA and acetophenone [104]. The petroleum-based, cheap amine donor isopropylamine (IPA) is often used as amine donor because the equilibrium can be shifted by acetone evaporation, which can be technically enhanced by reduced pressure, higher temperature, gas stripping or pervaporation [95, 105, 106]. As it is more favorable to consider the downstream processing (DSP) of the product directly with its synthesis, in the last decades several *in situ* product removal (ISPR) strategies were developed to remove the amine product from the reaction into a separate phase. Therefore, *in situ* product crystallization [107] or liquid-liquid product extraction [108, 109] were developed to displace the reaction equilibrium and facilitate product recovery with IPA as amine donor. Lastly, the α-amino acid alanine is a chiral, bio-based amine donor and a natural substrate of many amine transaminases [93]. However, transamination reactions with L-alanine are limited to conversions below 20% due to a very low equilibrium constant (in the range of 4×10^{-5} to 8.81×10^{-4} for MBA production from acetophenone and L-alanine [104, 110] and 2.31×10^{-3} for transamination of PAC with L-alanine [40]) [111, 112]. Possible methods to achieve an equilibrium shift have been either enzymatic co-product recycling or removal [40, 113, 114], ISPR of the amine product [112] or a combination of both [115, 116]. However, the added complexity and costs of auxiliary enzymes and expensive cofactors is often not viable at industrial scales. It is obvious, that process engineering methods and combinatorial solutions to achieve equilibrium shifts in TA reactions are a crucial research objective to leverage

the application of TA for preparative and industrially relevant synthesis of chiral amino alcohols. Ideally, this is realized by utilizing the bio-based, sustainable amine donor L-alanine.

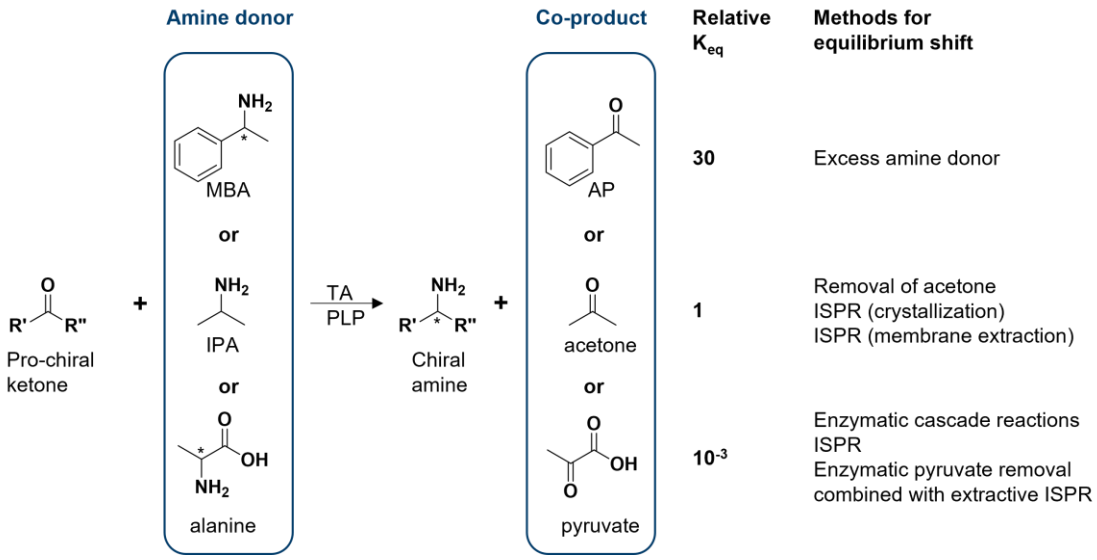

Figure 12 Overview of common amine donors in amine transaminase (TA) -catalyzed asymmetric synthesis and possible methods to shift the reaction equilibrium. Asymmetric carbon atoms are marked. The equilibrium constant K_{eq} is given in relation to isopropylamine (IPA). MBA = methylbenzylamine, ISPR = *in situ* product removal. Figure was adapted from Tufvesson *et al.* [104].

Hybrid approaches and ISPR are integral in process intensification (PI), which describes each innovative principle that contributes to improving a process in terms of productivity, product quality, cost and energy savings among other goals [117-119]. In a narrower sense, PI is often defined as the consolidation of process unit operations to achieve economical and ecological improvements. The consolidation of unit operations also requires a definition of a common operational window for a successful integration as all unit operations must be functional at common reaction conditions. This is illustrated for extraction-based ISPR with transamination reactions in Figure 13. As reflected by the extend of challenges, biotransformations with amine transaminases can benefit from process intensification approaches to push the applicability of these promising enzyme catalysts, some of which were subject of the "HyImPAct" project and are presented in this thesis.

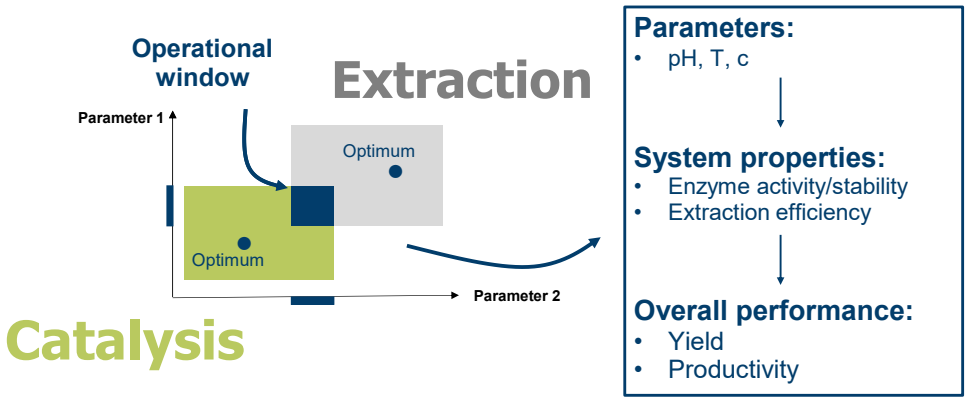

Figure 13 Depiction of the operational window for *in situ* product removal, which is determined by the optimal process conditions for enzymatic catalysis and *in situ* product extraction. Both, the catalysis and extraction process, are dependent on different parameters such as the pH, temperature (T) and concentrations (c) of reaction components.

1.5 HyImPAct project

The transition from a fossil-based industry to a circular bioeconomy represents one of the most pressing challenges of the global society to date [120]. In that regard, more sustainable production chains in the commodity or fine chemical and pharmaceutical sector are required to supply high-value compounds as well as bulk chemicals based on renewable resources. Especially for pharmaceutical applications, established production chains are often complex and have been optimized towards high competitiveness and efficiency. To transfer an existing production route to be based on renewables even increases the complexity and requires the adaptation of synthesis design, manufacturing infrastructure and downstream operations. Therefore, interdisciplinary approaches are needed covering the overall process, from the access to renewables raw materials and their utilization to the valorization of waste streams *via* efficient process routes. It becomes obvious that, while biotechnological advances in the last decades provided crucial tools (*e.g.* molecular biology, high-throughput screening methods, automation), the success heavily relies on the interconnection of these disciplines to establish an efficient production process and meanwhile fully exploit renewables.

The HyImPAct project ("Hybrid processes for important precursors and active pharmaceutical ingredients") was a consortium project funded by the Bioeconomy Science Center in the years 2018 - 2021, aiming at the combinatorial valorization of renewable resources to produce chiral fine chemicals (Figure 14). Ideally, the process chain should be based on second generation feedstocks or lignocellulosic waste materials such as bagasse, a fibrous residual material from sugarcane or sorghum. This is realized in a modular approach, starting by growing microbial cell factories on renewable carbon and energy sources such as D-xylose, which can eventually be obtained from biomass hydrolysates. Upon fermentation optimization, the engineered cells produce fine and bulk chemicals (amino acids, organic or aromatic acids) that can either be used

directly or that serve as precursors for further (chemo-) enzymatic conversions. The appropriate catalysts are chosen depending on their applicability for the respective target synthesis. Certain process steps are leveraged by the integration of ISPR to initiate the first DSP step and facilitate equilibrium shifts in thermodynamically unfavorable reactions. Specifically, the enzymatic, bio-based synthesis of metaraminol with integrated *in situ* product recovery was targeted (Figure 15, following section).

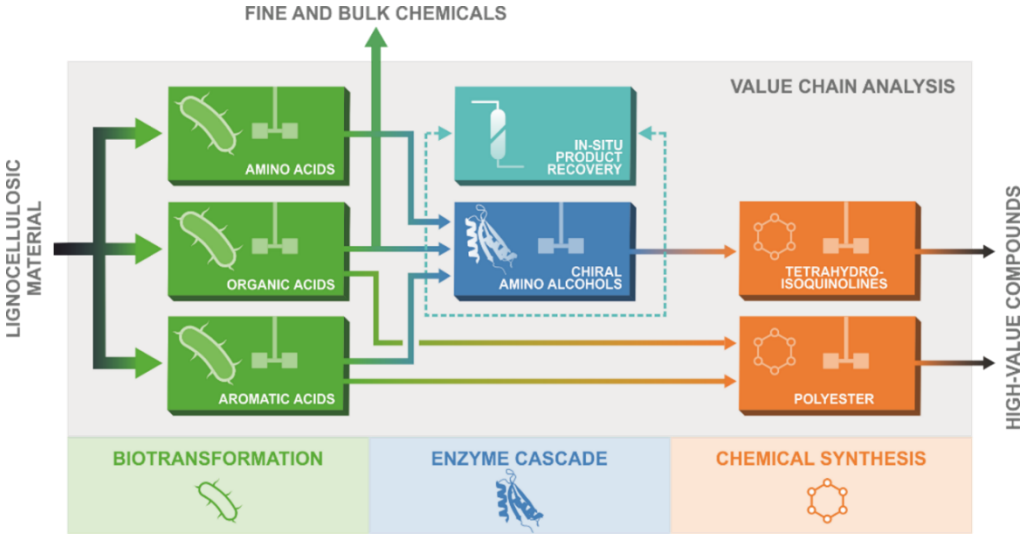

Figure 14 Schematic overview of the HyImPAct project. The production of high-value compounds (chiral amino alcohols THIQ derivatives and polyesters) from renewable resources is achieved by the synergystic integration of microbial biotransformations for the production of fine and bulk chemicals and precursors (green), enzymatic multi-step synthesis (blue) and chemical synthesis (orange), supported by *in situ* product recovery technology (turquoise). The image was acquired from the Bioeconomy Science Center [121].

The HyImPAct hybrid process thus targeted the challenging combination of green and profitable synthesis. Metrics describing the sustainability aspect are the carbon footprint, step and atom efficiency and recyclability or utilization of reaction components, which can be achieved by smart cascade design and efficient downstream strategies. On the other hand, economic feasibility is characterized by high catalyst-specific productivity, high product yield and concentration [122].

1.6 Scope of the thesis

In this thesis, the main objective was the enzymatic metaraminol synthesis in preparative relevant concentration ranges while utilizing bio-based precursors. Different from existing small-scale cascade approaches (developed by Vanessa Erdmann and Douglas Weber in the group of Prof. Dr. Dörte Rother), several reaction and process engineering approaches were used to first, establish the use of microbially produced, renewable precursors and second, improve the performance of the two-step synthesis. As previously introduced, amine transaminase-catalyzed asymmetric synthesis of chiral amines can suffer from different limitations. Several challenges for the enzymatic metaraminol production based on renewables are addressed in this work (Figure 15).

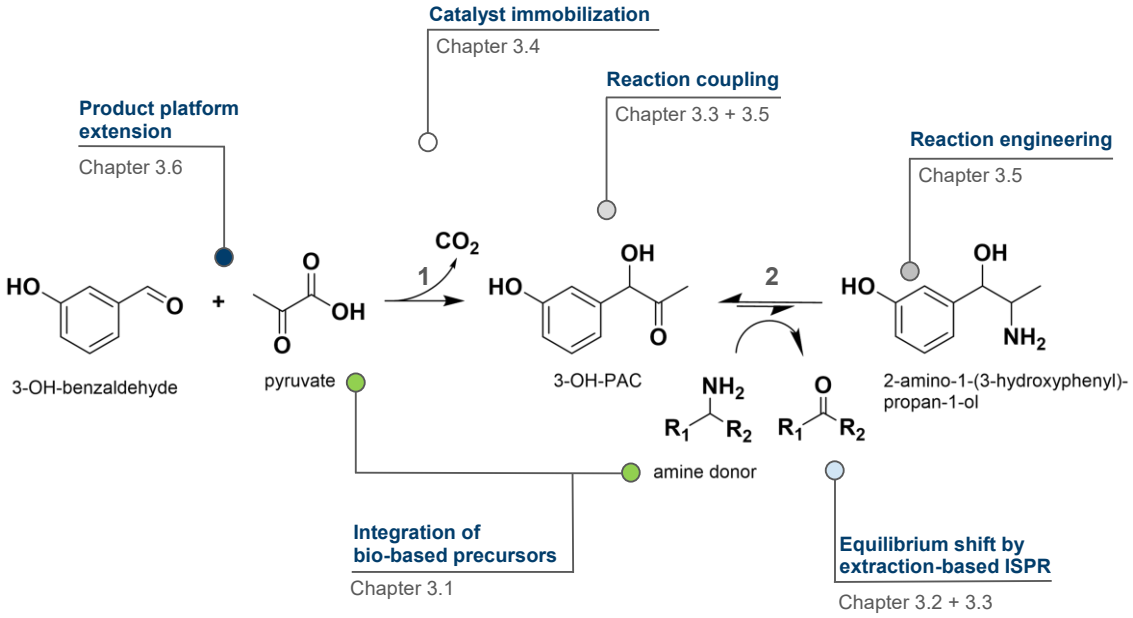

Figure 15 Graphical representation of the two-step enzymatic synthesis of 3-AHP with the respective engineering objectives presented in this thesis. 1 = carboligase, 2 = amine transaminase, PAC = phenylacetylcarbinol, ISPR = *in situ* product removal.

The first aim was the microbial production of the aliphatic precursor molecules pyruvate and L-alanine from renewable resources by engineering *Corynebacterium glutamicum.* The resulting fermentation supernatant was to be optimized for high concentration and reduced side-product formation and subsequently directly applied as substrate reservoir in the enzymatic synthesis of metaraminol (shown in chapter 3.1). Using bio-based L-alanine as amine donor requires measures to shift the thermodynamically unfavorable reaction equilibrium towards higher conversion. For this purpose, two complementary ISPR strategies based on liquid-liquid extraction was targeted for *in situ* metaraminol removal to displace the reaction equilibrium (chapters 3.2 and 3.3). Resulting consequences for the connection of the carboligation and transamination reaction steps are discussed in chapters 3.3 and 3.5. Further, the choice of biocatalyst formulation was

investigated. In this regard, potential advantageous properties of immobilized enzymes were tested for the carboligase and transaminase enzymes used in this thesis, namely a novel *in vivo* immobilization strategy *via* spore display and the commercial immobilization strategy on a solid (carrier) support (EziG™, EnginZyme), both described in chapter 3.4. Further, reaction engineering strategies were pursued to elucidate crucial bottlenecks within the enzymatic metaraminol synthesis towards preparative substrate concentrations, which are presented in chapter 3.5. Finally, to enable further hybrid processes based on bio-based benzoic acid, the transfer to another product platform should be unclosed by identifying suitable enzyme combinations as the missing link between bio-based 4-hydroxylated benzaldehydes and 4-hydroxylated phenolic 1,2-amino alcohols (chapter 3.6). Ultimately, these different integrated engineering approaches should be discussed with respect to their applicability in enzymatic multi-step syntheses of chiral amino alcohols and the resulting implications for biocatalytic hybrid processes.

Chapter 2

Materials & Methods

Partially published in:

[123] Labib M, Grabowski L, Brüsseler C, Kallscheuer N, Wachtendonk L, Fuchs T, Jupke A, Wiechert W, Marienhagen J, Rother D, Noack S. 2022. Toward the sustainable production of the active pharmaceutical ingredient metaraminol. *ACS Sustain. Chem. Eng*. DOI: 10.1021/acssuschemeng.1c08275
[Reproduced (adapted) with permission from ACS Publications. © American Chemical Society 2022]

[124] Doeker M, Grabowski L, Rother D, Jupke A. 2022. *In situ* reactive extraction with oleic acid for process intensification in amine transaminase catalyzed reactions. *Green Chem.* DOI: 10.1039/d1gc03289e
[Reproduced (adapted) with permission from Green Chemistry. © The Royal Society of Chemistry]

[125] Mack K, Doeker M, Grabowski L, Jupke A, Rother D. 2021. Extractive *in situ* product removal for the application of L-alanine as amine donor in enzymatic metaraminol production. *Green Chem.* DOI: 10.1039/d1gc00852h
[Reproduced (adapted) with permission from Green Chemistry. © The Royal Society of Chemistry]

Contributions:

Moritz Doeker is the original author of the Material & Methods subsection 2.6 of the published article [124]. These sections have been adapted and included in this thesis. Mohamed Labib and Stephan Noack are the original authors of the Material & Methods sections “Plasmid and strain construction” and “Lab-scale bioreactor cultivations” of the published article [123], which were adapted and included in this thesis in full or compendious form. Jochem Gätgens provided all technical method information on the GC-ToF-MS analysis which were described in this chapter in a condensed form. Thomas Fuchs performed the L-alanine purification from spiked fermentation supernatant and provided the according method information. Marianna Karava provided the protocols for cultivation of *B. subtilis* KO7 and spore purification, which were adapted and previously described in the Bachelor thesis of Sarah Schmitz [126]. This thesis chapter was written by Laura Grabowski and revised by Dörte Rother.

2 Materials & Methods

2.1 Materials

2.1.1 Chemicals

Chemical	Manufacturer
L-Alanine, > 99%	- Merck, Darmstadt, Germany
Ampicillin sodium salt	- Carl Roth, Karlsruhe, Germany
Benzoase® Nuclease	- Sigma-Aldrich, St. Louis, USA
Boric acid	- AppliChem, Darmstadt, Germany
Calcium nitrate tetrahydrate	- Merck, Darmstadt, Germany
1-Decanol, > 99%	- Merck, Darmstadt, Germany
D-(+)-glucose monohydrate	- Carl Roth, Karlsruhe, Germany
Diethylamine, > 99.5%	- Sigma-Aldrich, St. Louis, USA
Di-Potassium hydrogen phosphate, 98%	- Merck, Darmstadt, Germany
EziG™	- EnginZyme, Sweden, Solna
Ferrous sulfate heptahydrate, 99%	- Carl Roth, Karlsruhe, Germany
Glycerin, > 99.7%	- Carl Roth, Karlsruhe, Germany
HEPES	- Carl Roth, Karlsruhe, Germany
Imidazole	- Carl Roth, Karlsruhe, Germany
Isopropylamine, > 99.5%	- Sigma-Aldrich, St. Louis, USA
Kanamycin sulfate	- Carl Roth, Karlsruhe, Germany
α-Lactose monohydrate	- Carl Roth, Karlsruhe, Germany
LDS Sample buffer 4x	- Novex, Carlsbad, USA
Lysozyme from chicken egg white powder	- Sigma-Aldrich, St. Louis, USA
Magnesium sulfate	- Sigma-Aldrich, St. Louis, USA
Manganese (II) chloride tetrahydrate, 99%	- Sigma-Aldrich, St. Louis, USA
(*S*)-α-Methylbenzylamine, 98%	- Sigma-Aldrich, St. Louis, USA
Metaraminol bitartrate, > 99%	- Trc, North York, Canada
MES SDS Running buffer 20x	- Novex, Carlsbad, USA
Nutrient Broth No. 4	- Sigma-Aldrich, St. Louis, USA
NuPAGE™ 4-12 % Bis-Tris Gel	- Invitrogen, Waltham, USA
3-OH-Benzylaldehyde, 99% or 97%	- Sigma-Aldrich, St. Louis, USA

4-OH-Benzaldehyde, 98%	- AlfaAesar, Haverhill, USA
(*R*)-3-OH-PAC	- IBG-1, Forschungszentrum Jülich, Jülich, Germany
Oleic acid, natural FCC grade	- Sigma-Aldrich, St. Louis, USA
1-Octanol, >99%	- Merck, Darmstadt, Germany
PageRuler^{TM} Plus Prestained Protein Ladder	- Thermo Fisher Scientific, Carlsbad, USA
Peptone ex casein	- Carl Roth, Karlsruhe, Germany
Potassium dihydrogen phosphate, 99%	- Carl Roth, Karlsruhe, Germany
Protein quantification kit BC Assays	- Interchim, Monlucon, France
Pyridoxal-5-phosphate, 98%	- Sigma-Aldrich, St. Louis, USA
Pyruvic acid, 98%	- Thermo Fisher Scientific, Carlsbad, USA
Pyruvic acid sodium salt, > 99%	- Carl Roth, Karlsruhe, Germany
Sample reducing agent 10x	- Novex, Carlsbad, USA
Sodium chloride	- Carl Roth, Karlsruhe, Germany
Sodium hydroxide	- Carl Roth, Karlsruhe, Germany
L-(+)-Tartaric acid, > 99.5%	- Merck, Darmstadt, Germany
Thiamine pyrophosphate	- AppliChem, Darmstadt, Germany
Trifluoroacetic acid, ≥ 99%	- Carl Roth, Karlsruhe, Germany
Urea	- Sigma-Aldrich, St. Louis, USA
Yeast extract	- Carl Roth, Karlsruhe, Germany

2.1.2 Devices

Device	**Manufacturer**
Infinity II 1290 UHPLC	- Agilent, Santa Clara, USA
Infinity 1260 HPLC	- Agilent, Santa Clara, USA
Autoclave	- Systec, Linden, Germany
Äkta™ pure protein purification system	- GE Healthcare, Chicago, USA
Avanti™ J-20 XP centrifuge	- Beckmann Coulter, Brea, USA
Asia syringe pump	- Syrris, Royston, England
Bench-top centrifuge 5424	- Eppendorf, Hamburg, Germany
Centrifuge Universal 32 R	- Hettich, Tuttlingen, Germany
Clean bench	- BDK, Sonnenbühl-Genkingen, Germany
DASGIP® parallel bioreactor systems	- Eppendorf, Hamburg, Germany
Electrophoresis power supply E831	- Consort, Turnhout, Belgium
EasyMax 402	- Mettler Toledo, Columbus, USA

EasySampler 1210	- Mettler Toledo, Columbus, USA
Gas chromatography	- Thermo Fisher Scientific, Waltham, USA
Incubator Certomat® BS-1	- Sartorius, Göttingen, Germany
Incubator HERAtherm	- Themo Fisher Scientific, Waltham, USA
Incubator shaker Ampere chart Multitron II	- Infors HT, Bottmingen, Switzerland
Lyophilizer Cube Alpha 2-4 LSCplus	- Christ, Osterode, Germany
Lyophilizer Alpha 1-4 LDplus	- Christ, Osterode, Germany
Microplate reader infinite M1000	- Tecan, Männedorf, Switzerland
Photometer UV 1800	- Shimadzu, Kyoto, Japan
pH meter 691	- Metrohm, Herisau, Switzerland
Rotary evaporator	- Büchi, Essen, Germany
Rotator Enviro Genie	- Scientific Industries Inc., New York, USA
Thermomixer Comfort	- Eppendorf, Hamburg, Germany
HPLC pump	- ThalesNano, Budapest, Hungary
Titroline 7000	- SI Analytics, Mainz, Germany
Ultimate 3000 HPLC	- ThermoFisher Scientific, Waltham, USA

2.1.3 Bacterial strains, plasmids and enzymes

All strains, plasmids and enzymes, which were used in this thesis, are listed in Table 1. Genes for the heterologous enzyme production in *Escherichia coli* BL21 (DE3) were fused to a C- or N-terminal hexahistidine-tag (His6) as shown in the gene sequences in the appendix. The His-tag allows for protein purification *via* Ni-NTA affinity chromatography.

Table 1 Bacterial strains and plasmids used in this thesis.

Name	Relevant characteristics	Source
***Escherichia coli* strains**		
DH5α	F– Φ80*lacZ*ΔM15 Δ(*lacZYA-argF*)U169 *recA1 endA1 hsdR17* (rK–, mK +) *phoA supE44* λ– *thi-1 gyrA96 relA1*	Invitrogen, Karlsruhe, Germany
BL21 (DE3)	F- *ompT hsdS$_B$* (r_B^-, m_B^-) *gal dcm* (DE3)	Invitrogen, Karlsruhe, Germany
K-12 MG1655 RARE	Δ*dkgB,* Δ*yeaE,* Δ*dkgA,* Δ*yqhC,* Δ*yqhD,* Δ*yjgB,* Δ*yahK*	Invitrogen, Karlsruhe, Germany [127]
***Bacillus subtilis* strains**		
B. subtilis KO7	Δ*cwlD* Δ*sleB* ::lox72	*Bacillus* Genetic Stock Center ID 1A1133
Bs02043	Δ*cwlD* Δ*sleB* ::lox72 + p02043	Marianna Karava, Johannes Kabisch, TU Darmstadt, Germany
Bs02042	Δ*cwlD* Δ*sleB* ::lox72 + p02042	Marianna Karava, Johannes Kabisch, TU Darmstadt, Germany
***Corynebacterium glutamicum* strains**		
MB001 (DE3)	prophage-free derivate of ATCC 13032 with chromosomal expression of the T7 RNA polymerase gene under control of P_{lacUV5} (IPTG-inducible)	[128]
DelAro^5 P_{O6}-*iolT1*	MB001 (DE3) derivative with in-frame deletions of cg0344-cg0347, cg2625-cg2640, cg1226, cg0502, cg3349-cg3354 and two point mutations in the promoter/operator region of the inositol transporter gene *iolT1,* which abolish repression of *iolT1* by IolR	[129]
PYR_ALA_1	DelAro^5 P_{O6}-*iolT1* derivative with an in-frame deletion of the lactate dehydrogenase gene *ldhA* (cg3219)	[123]
PYR_ALA_5	PYR_ALA_1 derivative with an exchange of the native promoter of the pyruvate dehydrogenase gene *aceE* by the *dapA* promotor variant A16 and an in-frame deletion of the alanine transaminase gene *alaT* (cg3149)	[123]
PYR_ALA_7	PYR_ALA_5 derivative with an in-frame deletion of the pyruvate:quinone oxidoreductase gene *pqo* (cg2891)	[123]
PYR_ALA_8	PYR_ALA_7 derivative harboring the plasmid pMKEx2_*alaD*	[123]
Plasmids for heterologous expression in *E. coli* BL21 (DE3)		
pET29a-*Cv*2025-His6	gene from *Chromobacterium violaceum* ATCC 12472	John Ward, UCL London
pET21a-*Bm*TA-His6	gene from *Bacillus megaterium*	Wolfgang Kroutil, TU Graz
pET21a -*As*TA-His6	gene from *Arthrobacter spec.*	Wolfgang Kroutil, TU Graz
pET21a-*Ac*TA-His6	gene from *Arthrobacter citreus*	Wolfgang Kroutil, TU Graz
pET28-*Ll*Kdca-His6	gene from *Lactococcus lactis* subsp. *cremoris* B1157	IBG-1, Research center, Jülich [130]
pET22b-*Ap*PDC var-His6	gene from *Acetobacter pasteurianus* (variant by site directed mutagenesis)	IBG-1, Research center, Jülich
pET22b-*Ap*PDC E469G-His6	gene from *Acetobacter pasteurianus* (variant by site directed mutagenesis)	IBG-1, Research center, Jülich

Name	Relevant characteristics	Source
pETDuet_1_ECPPTase_His-*No*CAR	gene from *Nocardia otitidiscaviarum,* phosphopantetheinyl transferase gene from *Escherichia coli*	Margit Winkler, TU Graz, Austria
Plasmids for heterologous expression in *B. subtilis* KO7		
p02043	pCASCADEv1.0 (pMSE4) ORI: coIE1 (*E. coli, Ec*), repE (*B. subtilis, Bs*), KanR, Resolvase beta; PcotYZ, cotY, *Ap*PDC var (codon optimized for *B. subtilis*)	Marianna Karava, Johannes Kabisch, TU Darmstadt, Germany
p02042	pCASCADEv1.0 (pMSE4) ORI: coIE1 (*Ec*), repE (*Bs*), KanR, Resolvase beta; PcotYZ, cotY, *Bm*TA (codon optimized for *B. subtilis*)	Marianna Karava, Johannes Kabisch, TU Darmstadt, Germany
Plasmids for genetic engineering of *C. glutamicum* MB001 (DE3)		
pMKEx2	*kan*^{r}; *E. coli-C. glutamicum* shuttle vector (*lacI*, P_{T7}, lacO1, pHM1519 ori$_{Cg}$; pACYC177 ori$_{Ec}$)	[128]
pMKEx2_*alaD*	pMKEx2 derivative for the heterologous expression of the alanine dehydrogenase-encoding gene *alaD* from *Lysinibacillus sphaericus* (codon-optimized for *C. glutamicum* ATCC 13032)	[113]
pk19*mobsacB*	*kan*^{r}; vector for allelic exchange in *C. glutamicum* (pK18 oriV_{Ec} *sacB, lacZ* α)	[131]
pk19*mobsacB* A16-*aceE*	pk19*mobsacB* derivative for the exchange of the native promoter of the pyruvate dehydrogenase gene *aceE* by the *dapA* promotor variant A16	[132]
pk19*mobsacB* Δ*alaT*	pk19*mobsacB* derivative for in-frame deletion of *alaT* (cg3149)	[133]
pk19*mobsacB* Δ*ldhA*	pk19*mobsacB* derivative for in-frame deletion of *ldhA* (cg3219)	[134]
pk19*mobsacB* Δ*ppc*	pk19*mobsacB* derivative for in-frame deletion of *ppc* (cg1787)	[134]
pk19*mobsacB* Δ*pqo*	pk19*mobsacB* derivative for in-frame deletion of *pqo* (cg2891)	[134]

2.2 Methods

2.2.1 Biocatalyst production

2.2.1.1 Cultivation procedures

Transformation, cell propagation and shake flask cultivation

For enzyme production, plasmids (Table 1) were used for the transformation of chemically competent *E. coli* BL21 (DE3) cells using a standard heat-shock protocol. Initially, 1 µL of plasmid DNA was transferred to 50 µL thawed competent cells. The mixture was incubated on ice for 30 minutes. To initiate the transformation, the mixture was heated for 90 seconds at 42 °C. After the heat-shock, the cells were cooled on ice for 5 minutes and 500 µL super optimal broth medium (SOC, 20 mM glucose, 2.5 mM KCl, 10 mM $MgCl_2$, 10 mM NaCl, 20 g L^{-1} peptone, 5 g L^{-1} yeast extract) were added. The transformed cells were incubated at 37 °C and 300 rpm. After 1 hour incubation, 50 µL of the transformation mixture were plated on LB agar plates (LB, 10 g L^{-1} NaCl, 10 g L^{-1} peptone, 5 g L^{-1} yeast extract, 15 g L^{-1} agar) containing 50 µg mL^{-1} of the required antibiotic and incubated at 37 °C overnight. For cell propagation, 50 mL LB medium were inoculated with a single transformed colony and incubated at 37 °C and 120 rpm in 250 mL

shake flask with baffles. The next day, 1 L autoinduction medium (AI, 12 g L^{-1} peptone, 24 g L^{-1} yeast extract, 91 mM potassium phosphate buffer pH 7, 2 g L^{-1} lactose, 6.3 g L^{-1} glycerol, 0.5 g L^{-1} glucose, 50 mg L^{-1} respective antibiotic) was inoculated in 5 L shake flasks with baffles 1:200 from the pre-culture. The main culture was incubated at 37 °C and 80 rpm for 3 h before proceeding with the cultivation at 20 °C and 80 rpm for 48 h.

Deviating from this, for lyophilized, whole cell formulations of the branched-chain keto decarboxylase from *Lactococcus lactis* (*Ll*KdcA) the enzyme was produced in *E. coli* BL21 (DE3) in LB medium. For this, the main culture (1 L LB-Kan in a 5 L shake flask) was inoculated with 10 mL from an LB preculture (60 mL LB-Kan in 250 mL shake flask, 37 °C, 150 rpm, 16 h) to an initial OD_{600} of 0.06 and incubated at 37 °C and 150 rpm (80 rpm for shake flask with baffles). At OD_{600} = 0.48 the gene expression was induced by addition of 1 mM IPTG. The incubation was resumed at 20 °C and 150 rpm for a total cultivation time of 24 h. All cells were harvested by centrifugation at 7000 rpm and 4 °C for 30 min. The heterologous production of the target protein was verified *via* SDS-PAGE as described in section 2.2.1.6.

2.2.1.2 Immobilized-metal affinity chromatography (IMAC)

All enzymes used for *in vitro* biotransformations were produced as His-tagged variants allowing for immobilized-metal affinity chromatography (IMAC) as described here, as well as for affinity-based immobilization, which is described in section 2.2.2. For purification of *Ap*PDC var *via* IMAC, the frozen cells were resuspended to a 10% (w/v) suspension in 50 mM potassium phosphate buffer (Kpi) containing 0.1 mM thiamine pyrophosphate (ThDP) and 2.5 mM $MgSO_4$, pH 6.5 and disrupted by ultrasonification in a flow cell on ice (S14D sonotrode, amplitude 40%, cycle time 0.5). The cell debris was removed by centrifugation at 20,000 rpm and 4 °C for 30 min. Afterwards, the supernatant was applied to the ÄKTA pure protein purification system (GE Healthcare, Chicago, USA) with Ni-NTA superflow column material (Qiagen, Hilden, Germany) at a flow rate of 3 mL min^{-1}. Afterwards, the wash buffer (50 mM Kpi, 0.1 mM ThDP, 2.5 mM $MgSO_4$, 50 mM imidazole, pH 7.5) and elution buffer (50 mM Kpi, 0.1 mM ThDP, 2.5 mM $MgSO_4$, 250 mM imidazole, pH 7.5) were applied at a flow rate of 5 mL min^{-1}. The elution fractions were combined and desalted by size-exclusion chromatography (1 L silica-filled column, flow rate 10 mL min^{-1}, 10 mM Kpi pH 6.5, 2.5 mM $MgSO_4$, 0.1 mM ThDP). For protein determination, the Bradford method was used with bovine serum albumin (BSA) as the standard (refer to section 2.2.1.5). The enzyme fractions were combined, lyophilized at circa 0.2 mbar (LyoCube 0.6 mbar) and -80 °C (Lyophilizer Alpha 1-4 LD plus; Martin Christ Gefriertrocknungsanlagen GmbH, Osterode, Germany) and stored at -20 °C.

For purification of amine transaminases (*Cv*2025 or *Bm*TA), the same procedure was applied with either Tris buffers (equilibration buffer: 100 mM Tris pH 7.5, 0.2 mM PLP, 300 mM NaCl, wash buffer: 100 mM Tris pH 7.5, 0.2 mM PLP, 300 mM NaCl, 25 mM imidazole, elution buffer: 100 mM Tris pH 7.5, 0.2 mM PLP, 300 mM NaCl, 300 mM imidazole, desalting buffer: 10 mM Tris pH 7.5, 0.2 mM PLP) or Kpi buffers (equilibration buffer: 50 mM Kpi pH 7.5, 0.2 mM PLP, wash buffer: 50 mM Kpi pH 7.5, 0.2 mM PLP, 50 mM imidazole, elution buffer: 50 mM Kpi pH 7.5, 0.2 mM PLP, 250 mM imidazole, desalting buffer: 10 mM Kpi pH 7.5, 0.2 mM PLP). The purification success was verified *via* SDS-PAGE with > 90% purity for all enzymes applied. The target protein content in the cells was between 10 - 34% of the total protein content for all cultivations. The protein content of the lyophilizate was determined between 25 - 33% (*Ap*PDC var), 29 - 50% (*Cv*2025) and 36 - 41% (*Bm*TA) (w/w).

2.2.1.3 Preparation of crude cell extract and lyophilized whole cells

The frozen cell sediment was resuspended in 50 mM Kpi buffer pH 6.5 for the *Ap*PDC *var* or in 50 mM Kpi buffer pH 7.5 for *Cv*2025 to a 10% (w/v) cell suspension, which was sonicated in a continuous flow cell on ice (S14D sonotrode head, 70% amplitude, 0.5 cycle time, 30 minutes). The suspension was centrifuged at 23000 *x g*, 4 °C for 35 minutes to remove the cell debris. The supernatant was frozen at -20 °C in a lyophilization dish with a temperature sensor and lyophilized as stated before. For lyophilized whole cells (LWC), the frozen cell sediment was directly lyophilized and ground to a fine powder.

2.2.1.4 Biocatalyst storage

All biocatalyst formulations (purified enzyme, crude cell extract or lyophilized whole cells) were stored as lyophilizates at -20 °C. Upon use, the container was thawed in a desiccator and directly frozen afterwards.

2.2.1.5 Protein quantification

Bradford assay

The Bradford assay was used to determine the protein concentration of purified enzyme solutions [135]. The enzyme solution was diluted with the reaction buffer until the extinction values after sample preparation and incubation were in the linear range of the calibration (between 0.1 to 0.45 AU, referring to 0.02 to 0.1 mg mL^{-1} protein). 100 µL of the dilution were mixed with 900 µL Bradford reagent (100 mg mL^{-1} Coomassie Brilliant Blue G-250, 5% (v/v) ethanol, 8.5% (v/w) phosphoric acid) containing Coomassie Brilliant BlueG-250 in a plastic cuvette and mixed with a plastic stick. The mixture was incubated for 5 minutes at 25 °C and the extinction was measured at 595 nm in a photometer. A blank measurement with buffer prepared in the same way was

measured prior to all samples. The protein concentration was determined in triplicates in relation to a calibration curve with bovine serum albumin (BSA).

Bicinchoninic acid assay (BCA)

The BCA assay was used for protein quantification during EziG™ immobilization experiments (section 2.2.2.1). For every BCA assay, a new calibration curve of BSA was measured in a concentration range of 0 to 2 mg mL^{-1} BSA. 25 µL of the sample were mixed with 196 µL reagent A (containing bicinchoninic acid) and 4 µL reagent B (containing Cu^{2+}, Protein Quantification Kit, Interchim, Mannheim, Germany) in a 1.5 mL reaction tube and incubated for 30 minutes at 37 °C in a thermomixer at 1000 rpm. Afterwards, the samples were centrifuged for 3 minutes at 14000 *x g*. 150 µL of the supernatant were transferred into a 96-well plate and measured at 562 nm (Microplate reader infinite M1000, Tecan, Männedorf, Switzerland). To determine the amount of immobilized protein on EziG™ beads, 25 µL of the bead suspension after the immobilization procedure was used for the described BCA sample preparation.

2.2.1.6 Sodium dodecyl sulfate polyacrylamide gel electrophoresis (SDS-PAGE)

For verification of the target protein *via* SDS-PAGE, 5 mL of the cell culture was centrifuged for 15 minutes at 4000 *x g* and the cell sediment was stored at -20 °C overnight. The sediment was resuspended in 300 µL 100 mM Kpi buffer pH 7.5 containing lysozyme (1:1000) and benzoase (1:5000). The sample was incubated for 20 minutes on ice and subsequently centrifuged for 25 minutes at 4 °C and 14000 *x g*. From this supernatant, 1 µL was mixed with 9 µL of SDS-solution (140 µL SDS-solution contain 100 µL sample buffer and 40 µL reducing agent, NuPAGE™ Bis-Tris SDS buffer kit, ThermoFisher Scientific, Waltham, USA). The resulting fraction represented the soluble fraction. The remaining buffer was discarded. The insoluble fraction was obtained by adding 300 µL 7 M urea in 100 mM Kpi buffer pH 7.5 to the sediment and centrifugation for 40 minutes at 4 °C and 14000 *x g*. The sample was prepared by mixing 1 µL of the supernatant with 9 µL SDS-solution. All samples were incubated at 95 °C for 5 minutes in a thermomixer without agitation. For each sample, 5 - 10 µL were loaded on NuPAGE™ 4 - 12% Bis-Tris gel. The electrophoresis was performed with MES SDS running buffer (Invitrogen, Thermo Scientific) at 200 V and 60 mA for 45 - 60 minutes. The gel was stained with SimplyBlue SafeStain for approximately 1 hour and subsequently destained by replacing the staining solution with water multiple times. Likewise, SDS-PAGE samples were prepared for the enzyme purification (2.2.1.4) to analyze the purification procedure. The samples after the purification were diluted to a protein concentration of 1 mg mL^{-1} and 19.5 µL sample were mixed with 7.5 µL

sample buffer and 3 µL reducing agent from the NuPAGE™ Bis-Tris SDS buffer kit. Exemplary SDS-gels are shown in the appendix, Figure A1.1.

2.2.2 Enzyme immobilization

2.2.2.1 *In vitro* enzyme immobilization *via* EziG™

For enzyme immobilization on EziG™ carriers (EnginZyme, Solna, Sweden), 30 mg of the respective bead type (Coral, Amber or Opal) were provided in 1.5 mL glass vials. The lyophilized crude cell extract or purified enzyme lyophilizate was thawed and resuspended in 20 mM HEPES buffer pH 7.5 containing 500 mM NaCl, 0.1 mM ThDP and 2.5 mM $MgSO_4$ for *Ap*PDC var or 500 mM NaCl and 0.1 mM PLP for *Cv*2025. A concentration of 20 $mg_{lyo}\,mL^{-1}$ (crude cell extract *Ap*PDC var), 14 $mg_{lyo}\ mL^{-1}$ (purified *Cv*2025 lyophilizate in 10 mM Kpi buffer pH 7.5, 0.2 mM PLP) and 40 $mg_{lyo}\ mL^{-1}$ (crude cell extract *Cv*2025) was targeted. A volume of 1.1 mL from the enzyme solution were added to the EziG™ beads and incubated rotating for 30 minutes at 30 °C. To remove excess of adsorbed target enzyme or non-specifically bound enzymes, the beads were washed twice with 20 mM HEPES buffer pH 7.5 containing 500 mM NaCl and the respective cofactors and once with 100 mM HEPES pH 7.5 and the respective cofactors in glass vials with intermediate centrifugation steps (3 minutes at 4000 *x g*). The concentration of the enzyme stock solution and the immobilized enzyme was determined *via* BCA (section 2.2.1.5).

2.2.2.2 *In vivo* immobilization with *Bacillus subtilis* spores

Cultivation procedures for sporulation of recombinant *Bacillus subtilis* strains

Plasmid construction and transformation of *B. subtilis* KO7 with natural competence was performed by Dr. Marianna Karava at TU Darmstadt [136]. The cultivation procedures were adapted for the purpose of this work from Karava *et al*. [137, 138]. The cultivation media components are listed in Table 2.

Table 2 Components of cultivation media for *Bacillus subtilis.*

Compound	Concentration
Lysogeny broth (LB[5])	
Peptone	10 g L^{-1}
NaCl	5 g L^{-1}
Yeast extract	5 g L^{-1}
Glucose solution	
D-glucose	50% (w/v)
2x Schaefer's glucose (2xSG) sporulation medium	
Base medium	
Nutrient Broth No. 4 (Sigma-Aldrich)	16.0 g L^{-1}
KCl	2.0 g L^{-1}
$MgSO_4$ x 7 H_2O	0.5 g L^{-1}
Calcium nitrate stock solution (1 M)	
$Ca(NO_3)_2$	0.33 g mL^{-1}
Ferrous sulfate stock solution (1 M)	
$FeSO_4$	0.30 mg mL^{-1}
Manganese chloride stock solution (0.1 M)	
$MnCl_2$	24.58 mg mL^{-1}
Kanamycin stock solution (1000x)	50.00 mg mL^{-1}

The base medium was prepared in deionized water and autoclaved. The salt stock solutions were sterile filtrated. After cooling of the autoclaved base medium, 2 mL of glucose solution were added. While stirring, 1 mL of the remaining stock salt stock solutions were added.

The strains were stored as 20% glycerol stocks at - 80 °C. For cell propagation, 10 µL of the glycerol stock were transferred onto LB agar plates containing kanamycin (wildtype without antibiotic) and incubated at 37 °C overnight. In a 50 mL Erlenmeyer flask without baffles, 10 mL of LB-glucose medium containing 1% (v/v) D-glucose and 0.01 mL of Kanamycin were inoculated with a single colony and incubated at 37 °C and 150 rpm overnight. The preculture was centrifuged at 3.488 *x g* for 15 min and the cell sediment was resuspended in 2 mL of Schäfer's sporulation

(2xSG) medium. The 2xSG medium (100 mL in 500 mL cultivation shake flask without baffles) was prewarmed and supplemented with the respective antibiotic before inoculating with 1 mL of the resuspended cell sediment obtained from the preculture. Depending on the cultivation temperature (20 °C, 30 °C or 37 °C), the main culture was cultivated for 48 h to 72 h at 150 rpm in biological duplicates. For each culture, the optical density at 600 nm (OD_{600}) was measured in technical duplicates to monitor cell growth. The sporulation progress was additionally examined microscopically, aiming for a high ratio of spores to vegetative cells (transmitted-light microscope DM LB, Leica, Wetzlar, Germany or phase contrast microscope Eclipse Ti2, Nikon, Tokyo, Japan).

Spore purification and application in biotransformations

To harvest the spores, the culture broth was centrifuged for 30 min at 3,488 *x g* and 4 °C. The cell sediment was resuspended in 20 mL of lysozyme solution (75 µg mL^{-1}, prepared fresh and stored on ice until use) and incubated for 45 min in an overhead shaker at the previously used cultivation temperature. The obtained lysate was centrifuged for 15 min at 3,488 *x g* and 4 °C. To separate the spores from the cell fragments, the sediment was washed twice by resuspension in 20 mL of the ice-cold washing buffer (100 mM Kpi pH 6.5, 1 mM ThDP, 2.5 mM $MgSO_4$ pH 6.5 for spores displaying *Ap*PDC var or 100 mM HEPES pH 7.5, 0.2 mM PLP for spores displaying *Bm*TA) followed by repeated centrifugation. Finally, the spore sediment was resuspended in 5 mL of the wash buffer and the spore suspension was analyzed by microscopy (phase contrast microscope Eclipse Ti2, 1000x fold, phase contrast setting Ph 3).

Instead of enzyme concentration, the optical density was used to adjust spore amount in the biotransformation. Therefore, the optical density of the resulting spore suspension was measured in plastic cuvettes at dilutions of 1:1, 1:10 or 1:100 at a wavelength of 600 nm in triplicates, using the respective wash buffer for dilution and blank measurement. The usual target OD_{600} of spores in the reaction was between 40 and 60, corresponding to circa 3 mg spore dry weight. If the spore yield was too low, the applied OD_{600} was reduced accordingly as specified in the results section. In general, the reaction solution was incubated with the catalytically active spores at 25 °C (*Ap*PDC var) or 30 °C (*Bm*TA) in 1.5 mL glass reaction vials in a thermomixer at 1000 rpm for 24 h. The respective reaction conditions are indicated in the results section. For spore recycling in a repeated batch approach, the first reaction batch was centrifuged for 5 min at 13000 rpm in 1.5 mL reaction tubes. The spore pellet was washed twice with the respective washing buffer and finally resuspended in a new reaction solution for another 24 h incubation as described above.

2.2.3 Enzyme activity assays

2.2.3.1 Carboligation activity determination

In the reaction buffer (50 mM Kpi buffer pH 6.5, 1 mM ThDP, 2.5 mM $MgSO_4$), separate stock solutions of 3-hydroxybenzaldehyde (3-OH-BA, 20 mM), sodium pyruvate (500 mM) and the catalyst (purified lyophilized enzyme, 10 mg mL^{-1} determined by Bradford assay) were prepared. All components except for sodium pyruvate were combined in a 1.5 mL glass vial to final concentrations of 50 mM Kpi buffer, 1 mM ThDP, 2.5 mM $MgSO_4$, 10 mM 3-OH-BA, and the desired enzyme concentration (usual final concentrations: 1 mg mL^{-1} purified enzyme according to Bradford assay, 0.1 mg mL^{-1} LWC). Upon sodium pyruvate addition (final concentration 50 mM pyruvate), the reaction was incubated open at 700 rpm and 25 °C and samples for HPLC analysis (20 µL volume) were taken in the first 15 minutes (min) of the reaction progress (0, 1, 2, 3, 5, 10, 15 min) and quenched immediately with 50% (v/v) acetonitrile (ACN) in water to further process as described in section 2.2.9. The specific activity was determined in the linear range < 10% conversion. The enzyme activity was measured as mmol of produced (*R*)-3-OH-PAC per minute and liter under the applied conditions. The specific activity of purified *Ap*PDC var was 0.3 - 0.4 U $mg_{protein}^{-1}$ directly after purification and lyophilization. The specific activity of *Ap*PDC var as lyophilized, whole cell formulation was 0.8 - 1.0 U mg_{cells}^{-1}.

2.2.3.2 Transamination activity determination

Photometer-based activity assay for purified amine transaminases

The herein described activity assay for amine transaminases was first published by Schätzle *et al.* [139]. For initial activity assays of purified and lyophilized amine transaminase (*Bm*TA or *Cv*2025), an enzyme stock solution was prepared in 50 mM HEPES buffer pH 7.5 and the concentration was determined *via* the Bradford assay (typical protein concentrations of 5 mg mL^{-1}). The reaction buffer and pH were varied according to the experimental purpose. Stock solutions of 25 mM (*S*)-α-MBA, 50 mM sodium pyruvate and 1 mM PLP were prepared individually in the appropriate buffer and the pH was adjusted if necessary. The initial activity was measured in a quartz glass cuvette (d = 1 cm) at 25 °C *via* the acetophenone production at 300 nm using a UV-Vis spectrophotometer (final concentrations in the assay: 50 mM HEPES buffer pH 7.5, 0.1 mM PLP, 2.5 mM (*S*)-α-MBA, 5 mM pyruvate, 0.1 mg mL^{-1} enzyme). Under the stated conditions, one Unit (U) is defined as the amount of catalyst producing one µmol acetophenone per minute. The calculation of the specific activity is described in section 2.2.9.

HPLC-based activity assay for lyophilized whole cells and crude cell extract containing amine transaminases

In 100 mM HEPES buffer pH 7.5, stock solutions of PLP (2 mM), sodium pyruvate (100 mM), (*S*)-α-methylbenzylamine ((*S*)-α-MBA) (100 mM) were prepared. To prepare the substrate solution, 1 mL of PLP stock solution, 2 mL of sodium pyruvate stock solution and 2 mL (*S*)-α-MBA stock solution were combined, the pH was adjusted to pH 7.5 and the total volume was adjusted to 10 mL with buffer. A cell solution of 0.5 - 4 mg mL^{-1} lyophilized whole cells (LWC) (or 0.25 mg mL^{-1} crude cell extract, CCE) was prepared in the reaction buffer. 500 µL of the substrate solution was incubated in a 1.5 mL glass reaction vial in a thermomixer at 37 °C and 500 rpm. To the substrate solution, 500 µL of the cell solution was added (final concentrations: 10 mM (*S*)-α-MBA, 10 mM pyruvate, 0.1 mM PLP, 2 mg mL^{-1} LWC). Deviating from this, where indicated, racemic α-MBA was used, and the reaction vials was incubated without a lid. Within the first 20 min (0, 1, 2, 3, 5, 10, 15, 20 min), samples each containing 100 µL of the reaction mixture were quenched with 100 µL of 100% ACN and centrifuged at 13,000 rpm for 3 min. The samples were analyzed with HPLC method V (section 2.2.9, Table 5). The linear increase of acetophenone concentration (in mM) as a function of time (in min) below 10% conversion was the volumetric activity in U mL^{-1}. The specific activity was calculated with the final catalyst concentration (for lyophilized whole cells containing *Cv*2025 and *Bm*TA the specific activity was 0.3 - 0.8 U mg_{cells}^{-1}).

$$specific\ activity\ [U\ mg^{-1}] = \frac{volumetric\ activity\ [U\ mL^{-1}]}{concentration\ [mg\ mL^{-1}]}$$

2.2.4 Biotransformations

2.2.4.1 Carboligation reaction setup on an analytical scale

Analytical scale carboligation reactions of 3-OH-BA and pyruvate were typically performed by preparing a substrate solution in 100 mM Kpi buffer pH 6 - 6.5 containing 20 - 40 mM 3-OH-BA, 3 to 5-fold molar excess of sodium pyruvate, 0.1 - 1 mM ThDP and 2.5 mM $MgSO_4$. Lyophilized whole cells containing the desired carboligase were weighed out in 1.5 mL glass reaction vials (10 mg) and 1 mL of the substrate solution was added, followed by incubation at 750 rpm and 25 °C for 24 h. To measure the exact initial concentration of 3-OH-BA a sample was taken directly upon substrate addition to the cells (20 µL in 380 µL 50% (v/v) ACN in water, section 2.2.9, method II).

2.2.4.2 Carboligation reaction setup on a preparative scale and product work up of 2-hydroxy ketone ((*R*)-3-OH-PAC or (*S*)-3-OH-PAC)

In 400 mL total volume, 60 mM 3-OH-BA (99%, 122.12 g moL^{-1}) and 180 mM sodium pyruvate (> 99%, 110.04 g mol^{-1}) were dissolved in 100 mM Kpi buffer pH 6.5 containing 1 mM ThDP and 2.5 mM $MgSO_4$. Upon dissolving the reaction components, the pH was adjusted to pH 6.5. Lyophilized whole cells containing *Ap*PDC var were added to the reaction mixture (10 mg mL^{-1}) and the reaction was stirred at 350 rpm in a 500 mL glass reactor with a 4-pitched blade stirrer (38 mm diameter, 45° angle) at 25 °C for 24 h (EasyMax 402, Mettler Toledo, Columbus, USA). For purification of the 2-hydroxy ketone, the cells were removed by centrifugation (6500 rpm, 20 min, 10 °C). The supernatant was acidified to pH 2 with 20% HCl to precipitate dissolved proteins and subsequently centrifuged again. The supernatant was filtered twice. To extract the target compound from the aqueous phase, three extraction steps with 100 mL ethyl acetate each were performed. Afterwards, the aqueous phase was adjusted to pH 7 and two more extraction step were performed. The organic phase was washed with a saturated $NaHCO_3$ solution and dried over $MgSO_4$. The drying agent was removed by filtration and the organic solvent was evaporated at 40 °C and 100 mbar, obtaining isolated yields in the range of 61 - 74%.

For (*S*)-3-OH-PAC synthesis, the same setup and reaction conditions were used. The reaction was catalyzed by lyophilized whole cells containing *Ap*PDC E469G (10 mg mL^{-1}) to selectively produce the (*S*)-isomer. The synthesis was complete after 2.5 h and followed by immediate product workup as described above because longer incubation caused the reverse reaction. If the *ee* of the obtained product was < 95% for the (*S*)-isomer, the initially obtained crystalline product was re-crystallized by dissolving the product mixture in ethyl acetate at 60 °C (lowest amount needed for solubilization), which was slowly cooled and subsequently stored overnight at -20 °C. The crystals were separated by filtration and further dried at 40 °C and < 50 mbar in a rotary evaporator (53 - 72% isolated yield, *ee* > 98% after recrystallization). In all syntheses, the isolated yield, purity and enantiomeric excess were determined by HPLC measurements (section 2.2.8, Table 5, methods I and II).

2.2.4.3 Multi-step enzymatic transamination reactions to 3-hydroxylated amino alcohols

Transamination of 3-OH-PAC with L-alanine as amine donor

If not stated otherwise, analytical scale transaminations with L-alanine were performed in 1.5 mL glass reaction vials with a sealed screw cap. The substrate solution was prepared by combining all reaction components in 100 mM HEPES or Kpi buffer at pH 7.5. Typical final concentrations were 20 - 40 mM 3-OH-PAC (166.18 g mol^{-1}), 100 - 250 mM L-alanine (99%, 89.09 g mol^{-1}), 0.1 - 1 mM PLP (98%, 247.14 g mol^{-1}) and 1 - 2 mg mL^{-1} purified and lyophilized enzyme or

10 mg mL^{-1} lyophilized whole cells containing the desired amine transaminase. The reactions were performed in triplicates and incubated at 30 °C and 700 - 850 rpm for 24 h as specified in the results.

Transaminations of 3-OH-PAC with isopropylamine as amine donor

The transamination of 3-OH-PAC with isopropylamine (IPA) as amine donor was performed for the immobilization studies in chapter 3.4 and the reaction engineering concepts in chapter 3.5.

A 1 M IPA stock solution was prepared by adding 4.296 mL IPA (> 99.5%, 59.112 g mol^{-1}, 688 mg mL^{-1}) to 15 mL 100 mM KPi buffer pH 7.5 while stirring. The pH was adjusted to pH 7.5 with 37% HCl and the final volume was adjusted to 100 mL with buffer.

The standard transaminase reaction is performed in a reaction solution containing 100 mM Kpi buffer pH 7.5, 1 mM PLP (98%, 247.14 g mol^{-1}), 20 mM (*R*)-3-OH-PAC, 125 mM IPA (from a 1 M stock solution, referring to a 6.25-fold molar excess) and 10 mg mL^{-1} lyophilized whole cells containing *Cv*2025. Where indicated, the buffer, substrate concentration, cofactor concentration, enzyme loading, reaction volume and mixing were varied for reaction engineering purposes as specified in the results sections.

Transamination of 3-OH-PAC with IPA in the presence of different organic solvents and oleic acid concentration

For solvent screening in chapter 3.2, transamination reactions using IPA as an amine donor were performed with 10% (v/v) of organic solvents in a total reaction volume of 200 µL (20 mM (*R*)-3-OH-PAC, 0.2 mM PLP, 100 mM IPA in 100 mM HEPES buffer pH 7.5 containing 0.1 mM ThDP and 2.5 mM $MgCl_2$). The reaction was started by the addition of 5 mg mL^{-1} purified *Cv*2025 from a 57 mg mL^{-1} enzyme stock solution in the reaction buffer. The enzyme concentration of the stock solution was determined *via* the Bradford assay. The reactions were incubated in 1.5 mL glass vials with sealed screw caps at 30 °C and 700 rpm.

In chapter 3.3, the effect of different oleic acid concentrations was investigated in the target reaction to metaraminol using IPA as the amine donor (20 mM (*R*)-3-OH-PAC, 100 mM IPA, 100 mM HEPES buffer pH 7.5, 0.2 mM PLP, 10 mg mL^{-1} lyophilized whole cells *Cv*2025 or 1 mg mL^{-1} purified *Cv*2025, 10% 1-octanol with 0.1 M, 0.25 M and 0.5 M oleic acid (282.47 g mol^{-1}, 0.89 g mL^{-1}), 1 mL reaction volume in 1.5 mL glass reaction with sealed screw cap). The reaction was incubated at 30 °C and 750 rpm and the conversion was determined *via* endpoint measurements after 24 h in technical triplicates.

2.2.4.4 Multi-step enzymatic synthesis towards 4-hydroxylated amino alcohols

The following methods were used to generate the results presented in chapter 3.6.

Carboligation reaction setup in analytical scale

Possible enzyme variants to catalyze the carboligation of 4-hydroxybenzaldehyde (4-OH-BA, 98%, 122.12 g mol^{-1}) and pyruvate were screened in 1 mL reaction volume with 100 mM Kpi buffer pH 6.5 containing 0.1 mM ThDP and 2.5 mM $MgSO_4$, 20 mM 4-OH-BA and 60 mM sodium pyruvate. Upon dissolving the reaction components, the pH of the substrate solution was adjusted to pH 6.5. The enzymes were added at 5 mg mL^{-1} lyophilizate or glycerol stock concentration (corresponding to 0.1 - 1 mg mL^{-1} final enzyme concentration in the reaction as specified in the results section 3.6.3) or 10 mg mL^{-1} LWC and the reaction was incubated in an open 1.5 mL glass vial at 25 °C and 750 rpm in a thermomixer. Samples were diluted 1:20 in ACN, centrifuged as described before and the supernatant was measured *via* GC-MS or HPLC (section 2.2.10.2, method VI or section 2.2.10.3).

Preparative-scale production of 4-OH-PAC and product work up

Preparative-scale reactions were performed in stirred glass reactor vessels with temperature and pH control (EasyMax402, Mettler Toledo) using 60 mM 4-OH-BA, 300 mM sodium pyruvate, 0.1 mM ThDP, 2.5 mM $MgSO_4$ in potassium phosphate buffer pH 6.5 and 10 mg mL^{-1} of *E. coli* BL21 (DE3) cells (lyophilized whole cells) containing *Ll*KdcA. For product work-up, the cells were removed by centrifugation (20000 rpm, 30 min, 15 °C) and remaining soluble protein was precipitated by acidification with 37% HCl until pH 2. After repeated centrifugation, the reaction supernatant was extracted three times with 100 mL ethyl acetate, respectively. The combined organic phase was filtered, washed with saturated $NaHCO_3$ and dried over anhydrous $MgSO_4$. The solvent was evaporated at 40 °C and 100 mbar. Recrystallization was performed by dissolving the product mixture in 5 mL of ethyl acetate at 60 °C, which was cooled stepwise and subsequently stored overnight at -20 °C. The crystals were obtained by filtration and remaining solvent was evaporated at 40 °C and < 50 mbar in a rotary evaporator.

Transamination of 4-OH-PAC

The obtained 2-hydroxy ketone product from the previous step was further converted by testing four different amine transaminases with this substrate. The substrate solution was prepared from stock solutions. The reaction conditions were 100 mM HEPES pH 7.5, 1 mM PLP, 20 - 40 mM 4-OH-PAC, 12.5-fold molar excess of IPA (from a 1 M stock solution in 100 mM HEPES containing 1 mM PLP and adjusted to pH 7.5). To start the reaction, 10 mg mL^{-1} lyophilized whole

cells containing the desired amine transaminase were added to 1 mL substrate solution. The reactions were performed in duplicates and incubated in open 1.5 mL glass reaction vials at 30 °C and 850 rpm for 24 h.

2.2.5 Stability of amine transaminases under relevant process conditions

2.2.5.1 Storage stability in the presence of an organic overlay containing oleic acid

For the long-term initial activity assays, purified and lyophilized *Cv*2025 was incubated in 50 mM HEPES buffer pH 7.5, which was pre-saturated with the respective organic solvents (chapter 3.2). Pre-saturation was accomplished by mixing the respective solvent with the buffer and incubating this mixture for 24 h. After that, the organic solvent was discarded and only a monophasic buffer, with trace amounts of soluble organic solvent, remained and was applied subsequently. The enzyme concentration was determined *via* the Bradford assay. After distinct incubation times, the enzyme initial activity was measured photometrically as described in section 2.2.3.2. For each activity assay after a certain incubation time, a constant volume from the incubated enzyme stock solution was added to a fresh substrate solution in the cuvette.

Likewise in chapter 3.3, the stability in the presence of oleic acid was determined after the addition of 10% (v/v) 1-octanol or 1-decanol containing 0.1 M, 0.25 M or 0.5 M oleic acid (282.47 g mol^{-1}, 0.89 g mL^{-1}) to the enzyme stock solution to create an aqueous-organic interface. The solutions were incubated rotating at 20 °C under exclusion of light. The enzyme activity was measured as describe above after 0, 1, 3 and 7 days of incubation. The activity measurements for *Cv*2025 were performed in technical triplicates from two individual enzyme incubation batches per condition. For *Bm*TA, one enzyme incubation batch per condition was prepared and activity measurements were performed in triplicates.

2.2.5.2 Stability assay of *Cv*2025 in the presence of (substituted) PAC and IPA

A stability assay was developed to investigate inhibitory effects of reaction components on *Cv*2025. In technical duplicates, 10 mg mL^{-1} lyophilized whole cells were incubated in 1 mL incubation solution (Tables 3 and 4) for 10 min or 3 h at 30 °C and 850 rpm in an open glass reaction vial.

Table 3 Composition incubation solutions for the stability assay in the presence of (*R*)-3-OH-PAC or IPA for 10 min incubation. Compounds were dissolved in 100 mM Kpi buffer pH 7.5.

Condition	IPA [mM]	(*R*)-3-OH-PAC [mM]	PLP [mM]
reference	-	-	1
125 mM IPA	125	-	1
500 mM IPA	500	-	1
40 mM (*R*)-3-OH-PAC	-	40	1
100 mM (*R*)-3-OH-PAC	-	100	1
160 mM (*R*)-3-OH-PAC	-	160	1

Table 4 Composition of incubation solutions for the stability assay in the presence of (*R*)-3-OH-PAC or IPA for 3 h incubation. Compounds were dissolved in 100 mM Kpi buffer pH 7.5.

Condition	IPA [mM]	(*R*)-3-OH-PAC [mM]	PLP [mM]
reference	-	-	1
125 mM IPA	125	-	1
250 mM IPA	250	-	1
500 mM IPA	500	-	1
40 mM (*R*)-3-OH-PAC	-	40	1
100 mM (*R*)-3-OH-PAC	-	100	1
100 mM (*R*)-3-OH-PAC	-	100	10
160 mM (*R*)-3-OH-PAC	-	160	1

After incubation, the suspension was pipetted into a 1.5 mL reaction tube and centrifuged at 14,680 rpm for 3 min. The supernatant was discarded and 1 mL reaction solution, containing 20 mM (*R*)-3-OH-PAC, 125 mM IPA, 1 mM PLP and 100 mM Kpi buffer (pH 7.5), was added to resuspend the cell pellet. The reaction was incubated for 24 h at 30 °C and 850 rpm in an open glass reaction vial. 20 µL samples were taken after 0 h, 40 min, 1 h, 1.3 h, 1.6 h, 2 h, 2.5 h, 3 h, 3.5 h, 4 h, 5 h, 22 h, 24 h and diluted 1:20 in 50% (v/v) acetonitrile in water. The metaraminol concentration in the samples was measured by HPLC (section 2.2.10, Table 5, method VII).

The stability assay was also performed with 160 mM (*R*)-PAC or (*R*)-4-OH-PAC, respectively for 10 min and the initial product formation rate was determined with 20 mM (*R*)-PAC or 20 mM (*R*)-4-OH-PAC, 125 mM IPA, 1 mM PLP and 100 mM Kpi buffer pH 7.5. The samples were diluted 1:20 in 50% (v/v) acetonitrile in water for (*R*)-4-OH-PAC and in 100% acetonitrile containing 0.1% TFA for the reactions with (*R*)-PAC. The samples of the experiment with (*R*)-4-OH-PAC were measured with HPLC method VIII (section 2.2.10, Table 5). The (*R*)-PAC samples were

measured with HPLC method VII (section 2.2.10, Table 5, retention times: (*R*)-PAC 15.2 min, (1*S*,2*R*)-norephedrine 12.2 min). The evaluation of the stability test with (*R*)-4-OH-PAC was based on the measured peak areas, as standards of the synthesized amine product were not available. The linear part of the time-dependent course was determined by plotting the product concentration [mM] against the time [min] in the linear range between 0 - 180 min. A linear regression was performed to obtain a linear equation. The slope of the equations for the different conditions was set in relation to the slope of the reference to obtain the initial relative product formation rate.

2.2.6 Production and utilization of bio-based precursors from fermentation supernatants

2.2.6.1 Fermentation of recombinant *C. glutamicum* strains for the production of pyruvate and L-alanine

Lab-scale cultivations were performed using a parallel bioreactor system (DASGIP, Eppendorf, Jülich, Germany) with an initial working volume of 1.2 L. During the cultivation, the pH was measured using a pH electrode (405-DPAS-SC-K80/225, Mettler Toledo, Columbus, USA), and the pH was maintained at pH 7.0 by the addition of 5 M H_3PO_4 and 5 M NH_4OH at 30 °C. To achieve aerobic process conditions with a dissolved oxygen concentration (DO) of at least 30% (DO electrode, VisifermDO 225, Hamilton, Reno, USA), the airflow was set to 0.5 vvm while stirring at 400 - 1200 rpm. Exhaust gas composition (GA4, DASGIP AG) was additionally used for online measurements. All cultivations were started with 40 g L^{-1} D-glucose and an initial OD_{600} of 0.5 from an exponentially growing pre-culture in defined CGXII medium [140], which contained 40 g L^{-1} D-glucose. When acetate was necessary for growth, the cultivation was started with 20 g L^{-1} sodium acetate. This was followed by the injection of acetate pulses in the total form of either 45 mL of 80% (v/v) acetate or 172 mL of 368 g L^{-1} sodium acetate.

After D-glucose (and acetate) were consumed (indicated by a sudden increase in the DO signal) D-glucose pulse-feeding and microaerobic process conditions were initiated. The D-glucose feed contained a solution of 600 g L^{-1} D-glucose in deionized water and the total feeding volume of 440 mL D-glucose solution was distributed into pulses to maintain D-glucose concentrations above 15 mM until the end of cultivation. The first D-glucose pulse of 165 mL was injected upon the start of the microaerobic phase and was followed by three pulses of 155 mL, 60 mL and 60 mL after 23 h, 46 h and 67 h of the microaerobic phase start, respectively. Unless otherwise indicated, the microaerobic cultivation conditions were maintained by setting the stirrer speed, airflow and percentage of oxygen in gas flow to 900 rpm, 0.1 vvm and 8%, respectively. For cultivations using acetate auxotrophic strains, the total feeding volume of 380 mL of D-glucose solution was distributed into pulses of 165 mL, 155 mL and 60 mL after 0 h, 23 h and 46 h of microaerobic phase start. In the modified process condition, the total feeding volume of 460 mL of D-glucose

solution (550 g L^{-1} stock solution) was injected as pulses of 130 mL, 180 mL and 150 mL after the start of the microaerobic phase. Cell dry weight (CDW) was determined gravimetrically as follows. In a weighted reaction tube, 2 mL cultivation broth was collected and centrifuged at 13,000 rpm for 10 min. The cell sediment was resuspended in 0.9% (w/v) NaCl. After repeated centrifugation, the supernatant was removed by decantation and the cell sediment was dried at 80 °C for 24 h followed by gravimetric CDW determination.

2.2.6.2 Recovery and purification of L-alanine from fermentation supernatant

To purify L-alanine from the fermentation supernatant, commercial L-alanine was added to the cell-free fermentation supernatant to reach a final concentration of 100 g L^{-1}. The L-alanine concentration was determined with an Agilent 1200 HPLC system and a Nucleodur C18ec column as described before [141]. Sulfuric acid was added to adjust the broth to pH 2. For all ion-exchange process steps, the chromatography unit Azura® LC system with two P6.1L pump heads (Knauer Wissenschaftliche Geräte GmbH, Berlin, Germany) was used. The cation exchange resin Dowex® Monosphere® 99Ca/320 (Sigma-Aldrich, St. Louis, USA) was packed into a glass column with 16 mm inner diameter to a final bed volume of 60 mL. The column was equilibrated with 5 column volumes (CVs) of 0.5 M ammonium sulfate solution and washed with 2 CVs of purified water with a flow rate of 5 mL min^{-1}. The prepared fermentation supernatant was then pumped through the cation exchange column for 1.25 CVs. After a washing step with 2 CVs of purified water, the elution buffer containing 0.5 M ammonium sulfate adjusted to pH 9 with ammonia was applied to the column for 3 CVs. The fraction eluting from 0.58 to 1.5 CVs of elution buffer was pooled and used as product fraction for further purification. The product fraction was transferred to a round bottom flask and heated to 75 °C in a rotary evaporator (Stuart® RE300 rotary evaporator; Keison Products, Chelmsford, UK), reducing the volume by 80% at reduced pressure below 350 mbar. The concentrated solution was cooled to 4 °C in the EasyMax 102 system (Mettler Toledo, Columbus, USA), while adjusting the pH value to pH 6.15 by adding sodium hydroxide (20 min, 150 rpm). The resulting slurry was filtered (Whatman® grade 50 filter papers; GE Healthcare, Chicago, USA) and the crystals were dried in a vacuum oven at 40 °C.

2.2.6.3 Biotransformation using precursors from fermentation supernatant

The fermentation broth (section 2.2.6.1) was centrifuged at 13,000 rpm for 10 min and filtered through a 0.2 µm cellulose-acetate syringe filter (DIA-Nielsen, Düren, Germany). The supernatant was frozen in 50 mL aliquots at -20 °C until further use. The fermentation supernatant was thawed and supplemented with 10% (v/v) 1 M Kpi buffer pH 6. For the carboligation step, 20 - 40 mM 3-OH-BA, 1 mM ThDP, 2.5 mM $MgCl_2$ were added, and the pH of the substrate solution was

adjusted to pH 6.5. Upon addition of *Ap*PDC var (1 mg mL^{-1} purified enzyme according to the Bradford assay or 10 mg mL^{-1} lyophilized whole cells) the reactions were incubated shaking for 24 h (1 mL reaction volume, 1.5 mL glass reaction vial closed with sealed screw cap, 750 rpm, 25 °C). Samples for HPLC analysis were prepared and analyzed as described in section 2.2.10. If indicated, the fermentation supernatant was heated at 90 °C for 15 min and subsequently cooled on ice before adding the additional reaction components.

The carboligation reaction was performed similarly in 50 mL glass flasks (40 mL reaction volume, 25 °C, overhead shaker). Directly upon aldehyde depletion, the cells were removed by centrifugation (20,000 rpm, 15 min). The supernatant was adjusted to pH 3 by addition of 20% HCl and centrifuged to precipitate and remove remaining proteins. The carboligation product was extracted twice with ethyl acetate and the organic phase (60 mL) was washed with $NaHCO_3$ (10% of the total organic volume) and dried over anhydrous $MgSO_4$. The organic solvent was filtered and subsequently evaporated in a rotary evaporator at 150 mbar and 40 °C. The obtained 2-hydroxy ketone product was dissolved in 100 mM HEPES buffer pH 7.5 supplemented with 0.2 mM PLP. To the solution, 250 mM L-alanine were added (commercial or purified from fermentation supernatant as described in section 2.2.6.2). The transamination reaction was started by adding 10 mg mL^{-1} lyophilized whole cells containing *Cv*2025. The transamination reaction was performed in triplicates (1 mL) and incubated at 30 °C and 750 rpm for 24 h.

2.2.7 Determination of pK_a values *via* titration

The pK_a values for metaraminol bitartrate and (*R*)-3-OH-PAC were determined in automatic titration experiments with equimolar concentration of NaOH in technical duplicates (Titroline 7000, SI Analytics, Mainz, Germany). The titrant was added in linear steps of 0.0250 mL at 25 °C while stirring with a magnetic stirrer and measuring the pH by a combination pH electrode (InLab Micro, Mettler Toledo, Columbus, USA). The pK_a value was determined with the "half-equivalence" method based on the inflection points [141, 142].

2.2.8 Pure substance extraction studies without enzyme

2.2.8.1 Physical liquid-liquid extraction studies

Solutions of 1 g L^{-1} metaraminol bitartrate were buffered in 12.5 mM sodium tetraborate decahydrate and 50 mM phosphoric acid. The pH of the aqueous phases was adjusted to pH 7.0 - 10.5 in 0.25 increments with NaOH. The organic phase (1-decanol) was saturated with distilled water prior to the extraction. 1 mL of the aqueous solution and 0.5 mL of the saturated organic phase were mixed in a thermomixer for 16 h at 20 °C and subsequently separated *via* centrifugation at 3,000 rpm for 10 minutes. The organic phase was transferred to a vial containing 1 mL of 0.1 M

HCl and was mixed for 16 h for back extraction. Metaraminol concentrations in the aqueous phase before and after extraction as well as after back extraction were determined *via* HPLC (method section A.1 in the appendix, Tables A1.2 and A1.3). Likewise, 0.5 mL solutions of 8 g L^{-1} (*R*)-3-OH-PAC in 50 mM potassium phosphate-borate buffer were adjusted to pH 7.0 - 10.5 in 0.5 increments with 4 M KOH. The organic extraction phase consisting of 0.5 mL of water-saturated 1-decanol was added and the biphasic system was incubated rotating for 24 h. The aqueous concentration of (*R*)-3-OH-PAC was determined by HPLC measurements before and after the extraction experiment (section 2.2.10.2, Table 5, gradient method II). Phase separation was achieved by centrifugation as described above.

2.2.8.2 Reactive extraction studies with metaraminol bitartrate

The initial aqueous solution consisted of 0.02 M (6 g L^{-1}) metaraminol bitartrate in water adjusted to pH 5. The solution was divided into individual samples and mixed with equal volumes of NaOH solution. The NaOH solutions differed in concentrations, which were calculated as a molar proportion of metaraminol between 0 to 200% in steps of 10%. The resulting aqueous phases contained 0.01 M of metaraminol between pH 5.0 - 9.5. A volume of 1 mL of this aqueous phase was mixed with 1 mL of organic extraction phase consisting of 0 M, 0.1 M, 0.25 M and 0.5 M oleic acid (282.47 g mol^{-1}, 0.89 g mL^{-1}) in 1-octanol in a 2 mL micro centrifuge tube and incubated shaking in a thermomixer for 16 h at 20 °C. The organic extraction phase was saturated with water prior to the extraction experiments. All extraction experiments were performed in duplicates and samples for HPLC measurements (Table A1.2 and A1.3, analysis was performed at the Chair of Fluid Process Engineering, RWTH Aachen University) were taken from the aqueous phase after centrifugation at 3,000 rpm for 10 minutes before and after the incubation.

2.2.9 *In situ* product removal experiments within transamination with L-alanine as amine donor

2.2.9.1 *In situ* physical liquid-liquid extraction

Transamination reactions with integrated physical product extraction were performed in a 20 mL scale reaction phase. If not stated otherwise, the aqueous reaction phase contained 50 mM (*R*)-3-OH-PAC, 250 mM L-alanine (purchased) and 1 mM PLP in 50 mM borate buffer (boric acid-sodium hydroxide) at pH 9. The organic phase (1-decanol) was added in a 2 : 1 aqueous : organic ratio, after both phases were pre-saturated with water or organic solvent, respectively. The reaction was started by the addition of 10 mg mL^{-1} *Cv*2025 (lyophilized whole cells) and incubated at 30 °C in an overhead shaker. For repeated batch mode experiments, the organic phase was back extracted after 4 h, 6 h and 24 h and the samples were taken from the aqueous phase. Larger reactions (40 mL) were performed in a 100 mL stirred-tank reactor (EasyMax 402, Mettler Toledo, Columbus, USA) at 30 °C and with the addition of pH control by automatic titration of 1 M NaOH. For product recovery, the organic extraction phase was transferred to an acidic aqueous phase (50 mM L-(+)-tartaric acid, > 99.5%, 150.087 g mol^{-1}) at 25 °C and stirred at 600 rpm for 1 h. The tartaric acid solution was sterile filtered before use. To aid in phase separation, biphasic systems were transferred to Falcon reaction tubes (50 mL) and centrifuged (4,000 rpm, 10 °C, 10 min). Afterwards, the samples were taken from the aqueous reaction and back extraction phases and analyzed separately *via* HPLC analysis. Reference reactions without organic overlay were performed under identical process conditions at pH 7 (40 mL reaction phase, 40 mM (*R*)-3-OH-PAC, 250 mM L-alanine, 1 mM PLP, 100 mM HEPES, 10 mg mL^{-1} lyophilized whole cells *Cv*2025).

2.2.9.2 *In situ* reactive extraction – test scale in buffer (15 mL)

To test various reaction conditions at once, the transamination reaction with reactive product extraction of metaraminol was performed in 15 mL scale buffered reaction systems. The biphasic system consisted of 12 mL aqueous reaction phase and 3 mL organic extraction phase in a 20 mL glass reaction vial with a sealed screw cap. This was the minimal volume needed to allow for reproducible phase separation and back extraction of the organic extraction phase. The aqueous reaction conditions were 40 - 70 mM (*R*)-3-OH-PAC, 6.25-fold molar excess of L-alanine, 0.2 - 1 mM PLP in 100 mM Kpi buffer pH 7.6. Upon dissolving all reaction components, the solution (aqueous reaction phase) was adjusted to pH 7.6. The organic extraction phase consisted of 1-octanol containing 0.25 - 0.35 M oleic acid, which was prepared fresh and pre-saturated with water before use in ISPR experiments. The respective reaction conditions are specified in the results section.

The biphasic reaction system was equilibrated for 1 h (30 °C, horizontally pivoting) to determine the phase distribution of (*R*)-3-OH-PAC. To start the biotransformation, 10 mg mL^{-1} lyophilized whole cells containing *Cv*2025 were added to the aqueous reaction phase. The pH of the aqueous reaction phase was adjusted twice after 3 h and 8 h. The reactions were incubated horizontally pivoting in an overhead shaker under light exclusion at 30 °C for 24 h. Afterwards, the biphasic system was transferred to a 15 mL Falcon tube and centrifuged at 4,000 rpm for 15 min. The organic phase was transferred to a new glass vial containing 3 mL 100 mM L-(+)-tartaric acid and mixed on an orbital shaker at 600 rpm for 1 h for back extraction. After repeated centrifugation, HPLC samples from the aqueous reaction phase and back extraction phase were prepared and analyzed according to section 2.2.10.2.

2.2.9.3 *In situ* reactive extraction – laboratory scale with pH control (50 mL)

To allow for automated pH control, all further *in situ* reactive extraction experiments within the transamination reaction were conducted in a 100 mL stirred glass reactor with a small 4-pitched blade stirrer (25 mm diameter, 45° angle, second deepest position) (EasyMax 402, Mettler Toledo, Columbus, USA). The 40 mL aqueous reaction phase consisted of 40 mM (*R*)-3-OH-PAC, 250 mM L-alanine, 1 mM PLP in purified ("Milli-Q") water. The pH of the aqueous substrate solution was adjusted to pH 7.3 - 7.6 with 0.5 M NaOH. An organic extraction phase, consisting of 1-octanol with different concentrations of oleic acid, was added to the aqueous reaction phase. The aqueous to organic phase ratio was 4 to 1. The organic phase was pre-saturated with water beforehand. The pH in the reaction phase was measured in the aqueous reaction phase with a pH electrode (InLab Semi-Micro L pH electrode, Mettler Toledo, Columbus, USA) and controlled *via* automated titration of 0.5 M NaOH from 10 mL syringe-dosing units. Initially, the biphasic system was equilibrated at 30 °C and 150 rpm for 1 h. Afterwards, the phase distribution of the substrate (*R*)-3-OH-PAC was determined *via* HPLC samples from the aqueous reaction phase before and after the equilibration step. The biotransformation was started by the addition of 10 mg mL^{-1} lyophilized whole cells containing *Cv*2025 to the aqueous reaction phase, which was subsequently stirred at 250 rpm and 30 °C for 24 - 48 h. Afterwards, product recovery was achieved by back extraction as follows. To aid in phase separation, the biphasic reaction system was transferred to a 50 mL Falcon tube and centrifuged at 4,000 rpm and 10 °C for 15 min. The organic extraction phase was transferred to an acidic aqueous phase in 50 mL Falcon tubes (10 or 40 mL of 50 mM L-(+)-tartaric acid) and mixed on an orbital shaker at 600 rpm and 20 °C. Afterwards, samples from the aqueous reaction phase and back extraction phase were analyzed *via* HPLC. Reference reactions without ISPR were performed as described here using the same reactant concentrations and reaction parameters but without *in situ* product extraction (by omitting oleic acid in the organic

phase or without any organic phase) or in 1 mL scale without organic phase as specified in the results sections. Oleic acid (OA) can degrade by oxidation in the presence of air and light (usually visible by yellow coloration) and can contain unspecified byproducts (purity specification is only FCC grade). Therefore, fresh oleic acid was stored under argon in a light-tight container and was only aliquoted to use up quickly. To exclude potential effects of OA purity on the substrate system or misleading HPLC peak allocation, control experiments were performed as described above using lyophilized whole cells without recombinant amine transaminase (empty vector control), showing no substrate conversion and no product peak in the aqueous reaction phase nor the acidic back extraction phase after 24 h.

2.2.9.4 *In situ* reactive extraction with repeated extraction steps

The same setup as specified in section 2.2.9.3 was used. After 24 h, the biphasic reaction system was transferred to a 50 mL Falcon tube and centrifuged (4,000 rpm, 10 °C, 15 min) and the organic extraction phase (10 mL) was transferred to 10 mL 50 mM L-(+)-tartaric acid in another Falcon tube and mixed on an orbital shaker at 600 rpm for 30 minutes at 20 °C to recover the extracted product (represents the first extraction step). Meanwhile, the aqueous reaction phase was transferred to the same reaction vessel to resume the reaction (30 °C, 250 rpm, pH 7.6). Afterwards, the desaturated organic phase was added back to the aqueous reaction phase and the process was resumed for a second and third extraction step, repeating the same back extraction procedure twice more. This setup was also transferred to the reaction system with (*S*)-3-OH-PAC as the amine acceptor and lyophilized whole cells containing *Bm*TA as biocatalyst (presented in the results section 3.3.3.4).

For all ISPR experiments, samples for HPLC analysis (Table 5, method II and III) were taken from the aqueous phases by piercing through the organic phase with the pipette tip. The air was first pressed out of the pipette tip in the reaction solution to displace any organic phase that had penetrated. The HPLC sample preparation was carried out as described in section 2.2.10. The total product yield was calculated from the molar amount of amino alcohol ($C_P \cdot V$) in three back extraction phases (*BE1-3*) and the aqueous reaction phase at the end of the process (*aq,t3*) as shown in the following equation, with n_P as the total molar amount of product (2-amino-1-(3-hydroxyphenyl)propan-1-ol, 3-AHP) and $n_{S,t0}$ the initial molar amount of substrate (3-OH-PAC) in the aqueous reaction phase. Further, *BE* describes the back extraction phase and *aq* the aqueous reaction phase, assuming that back extraction of the amino alcohol product was complete (negligible product remaining in the organic phase).

$$Total\ product\ yield = \frac{\sum n_P}{n_{S,t0}}$$

$$= \frac{C_{P,BE1} \cdot V_{BE1} + C_{P,BE2} \cdot V_{BE2} + C_{P,BE3} \cdot V_{BE3} + C_{P,aq} \cdot V_{aq,t3}}{C_{S,aq} \cdot V_{aq,t0}}$$

To reconstruct the mass balance and calculate the product selectivity (as the ratio of total product yield to substrate depletion, refer to section 2.2.11.), the substrate depletion after three *in situ* product extraction steps was calculated considering the remaining substrate in all phases. Assuming no complete back extraction but a remaining phase distribution of the substrate between the acidic back extraction phase and the organic extraction phase, the remaining substrate in the organic extraction phase was approximated with the substrate distribution, that was determined during the initial equilibration step (equ) of aqueous reaction phase and organic extraction phase:

$$n_{S,org,t3} = \left(\left(\frac{n_{S,org,equ}}{n_{S,aq,equ}}\right) * n_{S,aq,t3}\right) - n_{S,BE3}$$

$$Substrate\ depletion = \frac{\left(n_{S,aq,t0} - n_{S,BE1} - n_{S,BE2} - n_{S,BE3} - n_{S,aq,t3} - n_{S,org,t3}\right)}{n_{S,aq,t0}}$$

2.2.9.5 Semi-continuous extraction-back extraction setup (50 – 100 mL)

Two alternative reaction setups were designed to enable a semi-continuous process in which the organic phase is continuously back extracted instead of the discontinuous, repeated extraction steps described in the previous section. To keep the phase ratio of aqueous reaction and organic extraction phase constant (4 : 1) the reactor dimensions and according volumes had to be chosen carefully to allow for sufficient phase separation and precise pumping of the organic extraction phase. For pumping of the organic extraction phase and the acidic back extraction phase, two pumps (Syrris Asia syringe pump) were connected with Agilent solvent tubing and slightly larger Teflon tubing (TYGON® R-3603). The flow rate was 0.6 mL min^{-1}. The pH in the reaction phase was controlled *via* automated titration of 0.5 M NaOH (Titroline 7000, SI Analytics, Mainz, Germany). The reaction vessel was heated to 30 °C by a water bath (M3, Lauda, Lauda-Königshofen, Germany). A membrane contactor (3M Liqui-Cell MM Series G591.5X1, 3M, Saint Paul, USA) was used to contact organic extraction phase (shell side direction) and aqueous back extraction phase (100 mM L-(+)-tartaric acid, cross flow direction) as shown in Figure 16.

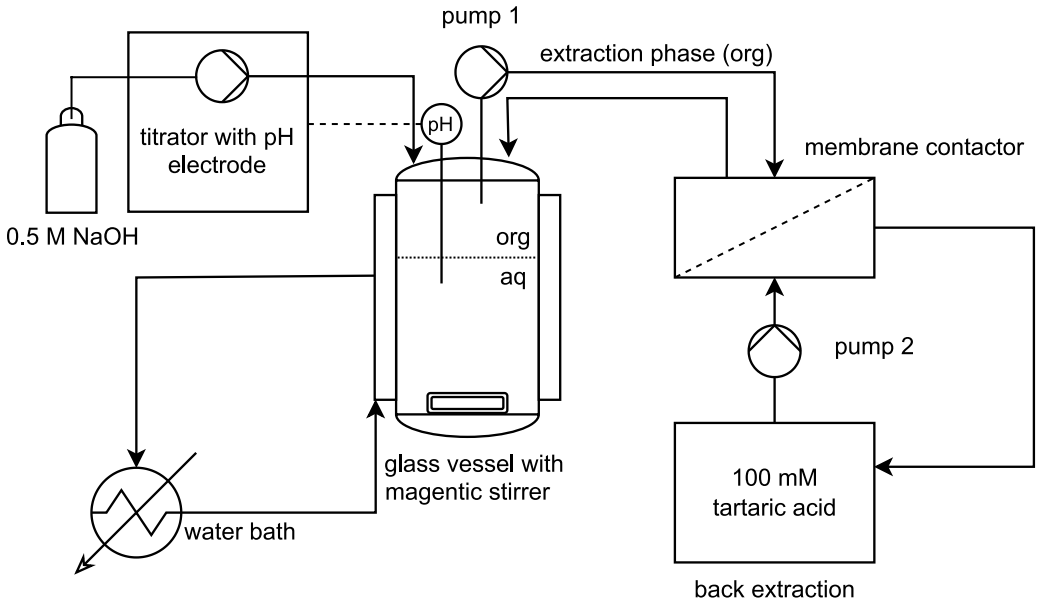

Figure 16 Schematic representation of the reaction setup for semi-continuous *in situ* extraction and back extraction of metaraminol (not true to scale).

2.2.10 Instrumental analytics

2.2.10.1 Sample preparation

Samples (20 µL or 10 µL) from enzyme reactions were diluted 1:20 or 1:40 in 50% (v/v) acetonitrile (ACN)/50% purified water and mixed thoroughly to quench the reaction and precipitate dissolved proteins. The sample was centrifuged at 13,000 rpm for 4 min and the supernatant was used for HPLC analysis (Table 5). For HPLC method VI, the sample was diluted in 100% ACN and for method VII in 100% ACN containing 0.1% trifluoroacetic acid (TFA). For method IV, 100 µL samples were diluted 1:2 in 0.24 M HCl solution (2% w/w in purified water) and centrifuged for 10 minutes at 13,000 rpm.

2.2.10.2 (Ultra-) High-Performance Liquid Chromatography

Quantitative determination of biotransformations

Several HPLC analysis methods were used for qualitative or quantitative determination of reaction components. For quantitative determination, a standard was diluted in 50% (v/v) acetonitrile in purified water and subsequently prepared as described in 2.2.10.1. The external calibration curves are shown in the appendix (Figures A1.3 - A1.14). The HPLC methods are shown in Table 5. The mobile phases of methods IV - VI were premixed to the respective volumetric concentrations. In all cases, purified water (commonly also referred to as Milli-Q water) was used for the preparation of all aqueous mobile phases, which was subsequently filtered *via* a regenerated cellulose membrane filter (Sartorius, Göttingen, Germany). HPLC columns were purchased from Agilent, Machery-Nagel or Diacel Chiral Technologies and are indicated as trade names in Table 5.

Table 5 HPLC methods for the analysis of biotransformations. TFA = trifluoroacetic acid, DEA = diethylamine, BA = benzaldehyde, BZ = benzoate, BOH = benzyl alcohol, PAC = phenylacetylcarbinol, AHP = 2-amino-1-(3-hydroxyphenyl)propan-1-ol ((1*R*,2*S*)-3-AHP is metaraminol), MBA = methylbenzylamine.

No.	HPLC	Method	Retention times [min]	Application
I	Agilent Infinity 1260	Chiralpak IE (4.6 x 250 mm, 5 µm) 20 °C, 5 µL injection volume, **isocratic**, 25% ACN/ 75% H_2O, 0.9 mL min^{-1} (0.7 mL min^{-1} for 4-hydroxylated compounds), 10 min total, DAD 220 nm	(*R*)-3-OH-PAC: 5.6 (*S*)-3-OH-PAC: 4.9 3-OH-BA: 6.7 (*R*)-4-OH-PAC: 6.2 (*S*)-4-OH-PAC: 5.9 4-OH-BA: 6.8	chiral detection 2-hydroxy ketones, carboligations
II	Agilent Infinity 1290 II	Zorbax Eclipse plus C18 (2 x 100 mm, 1.8 µm), 20 °C, 5 µL injection volume, DAD 220 nm **gradient method:** 10% ACN and 90% H_2O + 0.1% DEA + 0.075% TFA, up to 90% ACN in 5 minutes, 6 min total, 0.5 mL min^{-1}	3-OH-PAC: 1.9 3-OH-BA: 2.5 3-AHP: 0.5 3-OH-BZ: 2.1	carboligations, detection of 3-OH-PAC in ISPR reaction phase and back extraction phase
III	Agilent Infinity 1290 II	Zorbax Eclipse plus C18 (2 x 100 mm, 1.8 µm), 20 °C, 5 µL injection volume, DAD 220 nm **isocratic method:** 85% H_2O + 0.1% DEA + 0.075% TFA and 15% ACN, 0.3 mL min^{-1}, 10 min total	3-AHP: 0.91 3-OH-PAC: 2.75	transaminations, detection of metaraminol in ISPR reaction and back extraction phase
IV	Agilent Infinity 1260	Crownpak CR-I (+) (3 x 150 mm, 5 µm), 15 °C, 5 µL injection volume, **isocratic**, 80% 0.1 M $HClO_4$ /20% ACN, 0.3 mL min^{-1}, 20 min total, DAD 210 nm	(1*R*,2*S*)-3-AHP: 7.5 (1*S*,2*S*)-3-AHP: 6.7 3-OH-PAC: 5.6 (1*R*,2*S*)-4-AHP: 6.5 (1*R*,2*R*)-4-AHP: 5.5 4-OH-PAC: 5.1	chiral detection of amino alcohols
V	Thermo Scientific UltiMate 3000	LiChrospher 100 RP-18 (25 cm x 4 mm, 5 µm), 25 °C, 10 µL injection volume, **isocratic**, 45% ACN/ 55% H_2O, 1.5 mL min^{-1}, 10 min, UV-VIS, detection at 254 nm (acetophenone) and 213 nm (α-MBA)	acetophenone: 4.1 (*S*)-α-MBA: 1.8	transaminase activity assay (or model reaction)
VI	Thermo Scientific UltiMate 3000	LiChrospher 100 RP-18 (25 cm x 4 mm, 5 µm), 25 °C, 10 µL injection volume, **isocratic**, 20% ACN/80% H_2O, 1.5 mL min^{-1}, 10 min total, UV-VIS 200 nm	4-OH-BA: 5.28 4-OH-PAC: 3.19 4-OH-BZ: 2.24	carboligation of 4-OH-BA and pyruvate
VII	Thermo Scientific Ultimate 3000	LiChrospher 100 RP-18 (25 cm x 4 mm, 5 µm), 25 °C, 10 µL injection volume, **gradient** solvent A (ACN + 0.1% TFA, 3 - 97%) and solvent B (H_2O + 0.1% TFA), 0.5 mL min^{-1}, 25 min total, UV-VIS 220 nm (3-OH-BZ at 254 nm)	4-OH-BA: 14.10 4-OH-PAC: 11.98 3-OH-PAC: 12.60 3-AHP: 10.7 4-OH-BZ: 12.77 4-OH-BOH: 11.32 PAC: 15.22 norephedrine: 12.20	carboligation of 4-OH-BA and pyruvate, transaminations in chapter 3.3.3.5
VIII	Agilent Infinity 1290 II	Poroshell 120 (EC-C18, 2.1 x 100 mm, 1.9 µm), 20 °C, 5 µL injection volume, DAD 220 nm **isocratic method** from III for AHP, **gradient method** for 3-OH-PAC**:** 5% ACN, 95% H_2O + 0.1% DEA + 0.075% TFA up to 95% ACN in 6 min, 6 min total, 0.5 mL min^{-1}	3-OH-PAC: 2.11 3-AHP: 0.81 4-AHP: 0.94	transamination reactions with IPA (chapter 3.3.3.5)

HPLC methods for analysis of pure substance extraction studies without enzyme

The following HPLC method was used for metaraminol quantification in pure substance extraction studies performed by Moritz Doeker (chapter 3.2 and 3.3).

Analysis of extraction samples was performed on an Agilent 1200 HPLC equipped with a Machery-Nagel Nucleodur C18ec-pre-column (2 × 4 mm, 5 µL). The injection volume was 5 µL and the column oven temperature was set to 40 °C. The gradient elution was performed with two solvents, (A) with 2.5 mM acetic acid in water containing 10% methanol at pH 6 and (B) methanol, the gradient profile is specified in the appendix. Detection of components was achieved by a DAD at 334 nm. All standards and samples were diluted with 0.1 M HCl solution to achieve metaraminol concentrations below 0.01 mol L^{-1}. Before measurement pre-column online derivatization of the sample was performed using *ortho*-phthalaldehyde (OPA, Maisch, Ammerbuch, Germany). The derivatization procedure is specified in the appendix (Tables A1.2 and A1.3, Figure A1.2).

HPLC methods for fermentation supernatant analysis

The following HPLC methods were used in the analysis of fermentation supernatant (chapter 3.1, section 3.1.3.1). For the quantification of sugars and acids, a previously described HPLC method was adopted [143]. For quantification of substrate and product, additional culture samples were centrifuged (10,000 *x g*, 4 °C, 10 min) and the resulting supernatants were filtered through a cellulose-acetate syringe filter (0.2 µm, DIA-Nielsen, Düren, Germany). Precolumn sample preparation of L-alanine was achieved by mixing 5 µL sample, 5 µL *ortho*-pthaldialdehyde for derivatization and 5 µL water. Concentrations were determined by applying an external calibration of linear regression of weighted standards.

Table 6 HPLC methods for analysis of microbial fermentation supernatant.

No.	HPLC	Method	Application
1	Agilent 1100 Infinity	Organic Acid Resin HPLC column (5 µm, 300 × 8 mm, CS Chromatography, Düren, Germany), 40 °C, 20 µL injection volume, **isocratic method** with 0.1 M H_2SO_4, 0.6 mL min^{-1}, DAD 215 nm, RI detection (only glucose) at 35 °C	quantification of D-glucose, pyruvate, lactate, succinate, and acetate in fermentation supernatant
2	Agilent 1100 Infinity	Kinetex C18 reverse phase column (5 µm, 150 x 4.6 mm, Phenomenex, Aschaffenburg, Germany), 40 °C, 15 µL injection volume, buffer A (26 mM $NaH_2PO_4 \cdot 2\ H_2O$, 14.8 mM $Na_2HPO_4 \cdot 2\ H_2O$, and 5 mL L^{-1} tetrahydrofuran) and buffer B (15% acetonitrile, 35% methanol, and 50% buffer A without tetrahydrofuran), 0.9 mL min^{-1}, fluorescence detector, excitation at 230 nm/ emission at 460 nm **Gradient** increase of buffer B: minute 0 - 7: 20 - 80%, minute 7 - 14: 80 - 80%, minute 14 - 17: 80 - 100%, minute 17 - 33: 100 - 100%, and minute 33 - 35: 100 - 20%.	quantification of L-alanine in fermentation supernatant

2.2.10.3 Gas chromatography time-of-flight (ToF) mass spectrometry

GC-ToF-MS was used for product verification and characterization of the reaction matrix of carboligation reactions in fermentation supernatant (chapter 3.1). The method was also used for elucidation of chemical background reactions in transamination reaction with L-alanine as amine donor (chapter 3.2).

Sample preparation and derivatization

The reaction mixture was centrifuged at 14,000 *x g* for 10 minutes and the supernatant was adjusted to pH 7. Aliquots of 13 µL and 130 µL from the cell free supernatant were transferred to 1.5 mL reaction tubes and frozen in liquid nitrogen and subsequently stored at -20 °C. The samples were lyophilized overnight in a Christ LT-105 freeze dried (Martin Christ Gefriertrocknungsanlagen, Osterode am Harz, Germany). The freeze-dried samples were derivatized with 50 µL MeOX (20 mg mL^{-1} O-methylhydroxylamine, Sigma-Aldrich, St. Louis, USA in pyridine, Honeywell, Charlotte, USA) for 90 min at 30 °C and 600 rpm in a thermomixer, followed by addition of 80 µL of MSTFA (N-acetyl-N-(trimethylsilyl)-trifuoroacetamide, Sigma-Aldrich, St. Louis, USA) and incubation for 90 min at 40 °C and 600 rpm.

Data acquisition and analysis

For the determination of the derivatized metabolites an Agilent 8890N double SSL gas chromatograph (Agilent, Waldbronn, Germany) equipped with a L-PAL3-S15 liquid autosampler was used, coupled to a LECO GCxGC HRT+ 4D high resolution time of flight mass spectrometer (LECO, Mönchengladbach, Germany). A sample (1 µL) was injected into a split/splitless injector at 280 °C at varying split modes. For 1D GC analysis the Back Injector was equipped with a 30 m Agilent EZ-Guard VF-5ms and 10 m guard column (Agilent, Waldbronn, Germany). For 2D GCxGC analysis the Front Injector was equipped with a 30 m HP 5-ms Ui column (HP) connected to a 2 m Rtxi17 column (Restek) in a secondary oven. Constant Helium flow was adjusted to 1 mL min^{-1} for the active injector and column and to 0.5 mL min^{-1} for the passive injector.

The GC temperature program started at 60 °C with a hold time of 2 min, followed by a temperature ramp of +12 °C min^{-1} up to the final temperature of 300 °C and a hold time of 8 min. The secondary oven temperature offset was set to +15 °C above the first oven temperature with a transferline temperature of 300 °C. The ToF-MS was operated in positive electron impact $[EI]^+$ mode at an electron energy of 70 eV and an ion source temperature of 250 °C.

The MS was tuned and calibrated with the mass fragmentation pattern of PFTBA (heptacosafluoro-tributylamine). During analysis the accurate masses were corrected to a single point lockmass of heptacosa as an external reference at m/z 218,9856. 1D Data acquisition was

performed in stick mode with a scan rate of 12 scans per second. Known metabolites were identified by comparing a baseline noise corrected fragmentation pattern and the actual retention time index (RI value) to the in-house accurate m/z database JuPoD, and to the commercial nominal database NIST20 (National Institute of Standards and Technology, USA). No elucidation of unknown metabolites was performed.

2.2.10.4 Gas chromatography mass spectrometry (GC-MS)

GC-MS analysis was used for carboligation reactions of 4-hydroxybenzaldehyde (4-OH-BA) and pyruvate to 4-OH-PAC presented in chapter 3.6. Samples (20 µL) were diluted 1:20 in 100% acetonitrile, centrifuged and the supernatant was used for GC analysis on a Thermo Scientific Trace 1310 GC system equipped with a single quadrupole MS system (Thermo Scientific ISOLCT), a AS1310 autosampler and a DB-5MS column (30 m x 0.25 mm x 0.25 µm, T_{max} = 300 °C, MS up to 400 m/z, EI 70 eV inlet: 220 °C, split flow 23 mL min^{-1}, 15 split ratio). The temperature profile started at 130 °C increasing to 280 °C after 17 minutes with a temperature ramp of +10 °C per minute. The compounds were detected by a flame ionization detector (FID) (retention time of 4-OH-PAC was 6.8 min, retention time of 4-OH-BA was 4.7 min). The quantification of the substrate 4-OH-BA was achieved by external calibration. The quantification of the product concentration was initially approximated by external calibration with (*R*)-3-OH-PAC as an analogue. Eventually, the calibration with the enzymatically synthesized and purified (*R*)-4-OH-PAC as standard was used.

2.2.10.5 ^{1}H-NMR

^{1}H-NMR data was recorded by Rainer Goldbaum at the Institute of Bioorganic Chemistry, University of Düsseldorf, using a Bruker Advance DRX 600 MHz (Bruker, Billerica, USA). The spectra were analyzed using MNova (Mestrelab Research, Santiago de Compostela, Spain).

2.2.11 Formula and statistical information

Data evaluation

The reaction progress in a biotransformation was analyzed according to equations 1 - 3 with *c* as the compound concentration in the reaction phase and *n* as the molar amount at reaction start t_0 or sampling time point *t*.

$$conversion = \frac{c_{product\ of\ interest,\ t}}{c_{substrate,\ t} + c_{product\ of\ interest,\ t} + c_{\ side-products,\ t}} \cdot 100\% \quad (1)$$

$$substrate\ depletion = \frac{c_{substrate,\ t0} - c_{substrate,\ t}}{c_{substrate,\ t0}} \cdot 100\% \quad (2)$$

$$yield = \frac{n_{product\ of\ interest,\ t}}{n_{substrate,\ t0}} \cdot 100\% \quad (3)$$

The product selectivity assesses the amount of (chemical) side reactions that do not produce the target product (equation 4). If no side reaction occurs, the product selectivity is 1.

$$product\ selectivity = \frac{yield}{substrate\ depletion} \quad (4)$$

The stereoselectivity was defined as enantiomeric excess (*ee*) or isomeric content (*ic*) as shown in equation 5 and 6. I_1 is the concentration of the excessive (target) isomer (or the HPLC peak area, if standards were not available) and I_2 is the concentration of the minor isomer (or the HPLC peak area, if standards were not available; specifically in the case of 4-OH-PAC). The isomeric content *ic* is defined in equation 6 as the ratio of target isomer to the sum of all isomers.

$$ee = \frac{I_1 - I_2}{I_1 + I_2} \cdot 100\% \quad (5)$$

$$ic = \frac{I_1}{\sum I} \cdot 100\% \quad (6)$$

In the pure substance extraction experiments, the extraction efficiency was calculated as shown in equation 7 with *c* as the concentration and *V* as the phase volume.

$$extraction\ efficiency = \frac{c_{metaraminol,org} \cdot V_{org}}{c_{metaraminol,aq} \cdot V_{aq} + c_{metaraminol,org} \cdot V_{org}} \quad (7)$$

The space-time-yield (STY) was calculated according to equation 8.

$$STY\ [g\ L^{-1}\ d^{-1}] = \frac{m,total}{V_{aq} \cdot t} \quad (8)$$

The growth rate μ and doubling time t_d were defined in formula 9 and 10 with x_t and x_0 as the optical density of the culture at sampling time point and inoculation and t as the time in hours.

$$\mu\ [h^{-1}] = \frac{\ln x_t - \ln x_0}{t_x[h] - t_0[h]} \quad (9)$$

$$t_d\ [h] = \frac{\ln 2}{\mu\ [h^{-1}]} \quad (10)$$

Determination of initial rate activity

The evaluation of amine transaminase photometric activity assay (procedure described in section 2.2.3.2) was achieved by plotting the absorbance as a function of time and using the slope in the linear range to calculate the volumetric enzyme activity in U mL^{-1} as follows. One enzymatic Unit (U) is defined as the amount of enzyme which produces 1 μmol acetophenone per minute under the defined conditions.

$$volumetric\ activity\ [\frac{U}{mL}] = \frac{\frac{dA}{min} * V}{\varepsilon * v * d} * f = \frac{dA}{min} * F * f\ [\mu mol\ min^{-1} mL^{-1}] \quad (11)$$

$$F = \frac{V}{\varepsilon * d * v} \quad (12)$$

dA/min: change of absorbance at 300 nm per minute [min^{-1}]

V: total test volume (1000 μL)

ε: molar extinction coefficient (acetophenone) 0.322 $mMol^{-1}$ cm^{-1}

v: enzyme volume (*e.g.* 100 μL)

d: light path (1 cm)

f: dilution factor of enzyme stock solution (if there is no further dilution: f = 1)

Further, the specific activity in U mg_{enzyme}^{-1} was calculated according to equation 13.

$$specific\ activity\ \left[\frac{U}{mg} = \mu mol\ min^{-1}\ mg^{-1}\right] = \frac{Vol.\ activity\ [\mu mol\ min^{-1}\ mg^{-1}]}{enzyme\ stock\ concentration\ [mg\ mL^{-1}]} \quad (13)$$

Definition of replicates and error bars

In this work, all coherent series of experiments were performed with one batch of produced biocatalyst, referring to a single cultivation that was further used for protein purification (purified enzyme, PE) or preparation of other biocatalyst formulations (crude cell extract, CCE or lyophilized whole cells, LWC). While this represents one biological replicate, the experimental setups itself were performed repeatedly in separate experiments corresponding to technical duplicates (n = 2) or technical triplicates (n = 3) as indicated in the results sections [144]. Error bars are defined as the standard deviation from the mean (for n = 3) or as the variance between the mean of technical duplicates (for n = 2). If the error bars are too small to be visualized, this is also indicated in the figure description.

3 Results

Chapter 3.1

Combining microbial cell factories and multi-step enzymatic synthesis to produce metaraminol from bio-based precursors

Partially published in:

[123] Labib M, Grabowski L, Brüsseler C, Kallscheuer N, Wachtendonk L, Fuchs T, Jupke A, Wiechert W, Marienhagen J, Rother D, Noack S. 2022. Toward the sustainable production of the active pharmaceutical ingredient metaraminol. *ACS Sustainable Chemistry & Engineering.*
DOI: 10.1021/acssuschemeng.1c08275
[Reproduced (adapted) with permission from ACS Publications. © American Chemical Society 2022]

Contributions:

Christian Brüsseler and Nikolai Kallscheuer performed the genetic engineering work supervised by Jan Marienhagen. Mohamed Labib performed the fermentations with assistance of Luisa Wachtendonk under supervision of Stephan Noack. Thomas Fuchs purified L-alanine from the fermentation supernatant. Laura Grabowski utilized the fermentation supernatant, performed multi-step enzymatic synthesis, intermediate work up and reaction engineering presented in the original manuscript. The first chapter of the published manuscript was written by Mohamed Labib and Stephan Noack and adapted to be included in this thesis. All other manuscript chapters were written by Laura Grabowski with revision by Stephan Noack and Dörte Rother. Selected sections and figures were adapted and included in this chapter, which was written by Laura Grabowski and reviewed by Dörte Rother.

3.1 Combining microbial cell factories and multi-step enzymatic synthesis to produce metaraminol from bio-based precursors

3.1.1 Abstract

The enzymatic production of metaraminol was shown previously in an enzymatic cascade starting from 3-hydroxybenzaldehyde and pyruvate to form the intermediate (*R*)-3-OH-PAC, which was subsequently aminated using the fossil-based amine donor isopropylamine in excess, thereby releasing large amounts of acetone. As an alternative approach, IPA was replaced by bio-based L-alanine as a more sustainable amine donor. L-Alanine and the second required precursor, pyruvate, were gained by microbial transformations using engineered *Corynebacterium glutamicum* strains. The one-pot microbial production of pyruvate and L-alanine was achieved in microaerobic fed-batch fermentations. The final concentrations were suitable for direct carboligation of 3-hydroxybenzaldehyde and bio-based pyruvate to (*R*)-3-OH-PAC in the fermentation supernatant. By incorporating a heat treatment step of the fermentation supernatant and an intermediate purification step, high conversion (≥ 92%) and stereoselectivity (> 98% *ee*) were achieved. The intermediate (*R*)-3-OH-PAC can be subsequently converted to metaraminol by an amine transaminase using bio-based L-alanine as the amine donor.

3.1.2 Introduction

Chiral amino alcohols offer various applications as pharmaceutically active ingredients, precursors thereof or synthons for the fine chemical industry. Producing chiral molecules in high yields and purity usually requires a chemical multi-step synthesis consisting of protection steps, toxic auxiliaries, and harsh reaction conditions. This procedure is heavily dependent on crude-oil based precursors and produces substantial waste streams. Unlike established chemical catalysis, a biocatalytic production of chiral amines can provide these valuable compounds from renewable resources under environmentally favorable process conditions. The amino alcohol metaraminol is an active pharmaceutical ingredient for hypotension treatment and can serve as precursor for more complex, bioactive compounds. Previously, enzyme cascades consisting of a carboligation and transamination step to produce chiral amino alcohols using selective and biodegradable enzyme catalysts were published [40, 67]. To establish the synthesis of metaraminol upon bio-based precursors, it was adapted in several ways. First, the previously used amine donor isopropylamine (IPA) is a non-renewable compound that must be applied in large excess (8-10-fold molar for > 90% conversion), leaving a toxic residue, and complicating downstream processing [145]. It was thus envisaged to exchange IPA by bio-based L-alanine, as both aliphatic precursors, L-alanine and pyruvate, can be produced microbially from second generation feedstocks. Further, the enzymes

should be applied as lyophilized whole cell formulation to reduce the cost-contribution of the biocatalyst [146].

The central objective of the HyImPAct project (section 1.5) was to establish a hybrid process that would convert renewable resources to platform chemicals *via* microbial transformation and provide high-value, chiral compounds by further enzymatic or chemoenzymatic catalysis. In case of metaraminol synthesis, the microbial production of L-alanine and pyruvate as biobased precursors was targeted. For the bio-based precursor supply, the Gram-positive, non-sporulating bacterium *Corynebacterium glutamicum* was used, which is widely applied in industrial biotechnology for the large-scale production of various amino acids [147, 148]. *C. glutamicum* remains metabolically active under low-oxygen conditions, and several extensively engineered strains are known to allow the exclusive production of pyruvate or L-alanine from D-glucose in separate cultures [149-152]. In this case, however, both precursors should be supplied by a single fermentation broth to be used in further enzymatic synthesis. This strategy was chosen as the complete *in vivo* synthesis would possibly lead to large amounts of undesired by-products because of amine transaminase cross reactivity. Therefore, the microbial cell factory was engineered to provide both precursors L-alanine and pyruvate. In that regard, both the strain and the cultivation parameters have to be optimized towards high concentrations of both precursors and reduce the amount of metabolic by-products in the fermentation supernatant in an iterative manner.

In this chapter, the strain engineering is briefly described, focussing on the variants that were cultivated reproducibly and for which the fermentation supernatant was subsequently used for the enzymatic synthesis of metaraminol. The results of the two-step, enzymatic synthesis towards metaraminol and implications on intermediate work up steps are drawn.

3.1.3 Results & Discussion

3.1.3.1 One-pot production of L-alanine and pyruvate by engineered *C. glutamicum*

In previous publications, high-titer production of pyruvate or L-alanine, respectively, was possible by engineered *C. glutamicum* [150, 151]. To enable the growth-decoupled one-pot production of both precursors in sufficient titers for further enzymatic transformation, an alternative metabolic engineering strategy was pursued. An overview of the metabolic engineering targets is shown in Figure 17. Pyruvate can be lost by conversion into the by-product lactate under oxygen-limited cultivation conditions catalyzed by the NADH-dependent lactate dehydrogenase. Therefore, the corresponding gene *ldhA* was deleted.

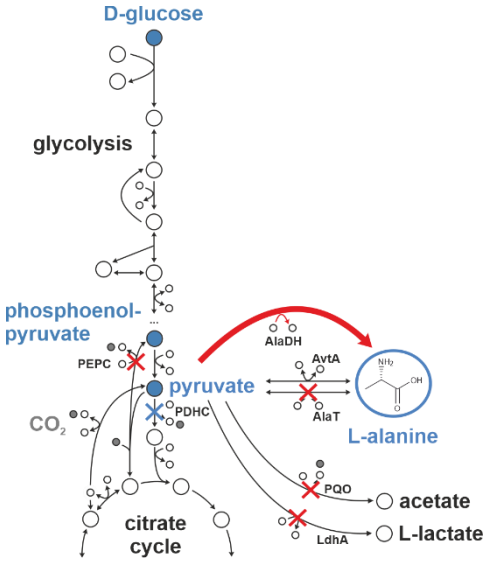

Figure 17 Overview of the metabolic engineering targets for *C. glutamicum* to facilitate the one-pot production of pyruvate and L-alanine. Gene deletions are indicated by red crosses while the blue cross represents a targeted down-regulation of gene expression. The red arrow represents plasmid-based (over)expression. Abbreviations: AlaDH, NADH-dependent alanine dehydrogenase; AlaT, L-glutamate-dependent aminotransferase; AvtA, L-valine-dependent aminotransferase; LdhA, lactate dehydrogenase; PEPC, phosphoenolpyruvate carboxylase; PDHC, pyruvate dehydrogenase complex; PQO, pyruvate:quinone oxidoreductase. This figure was previously published [123] and is reprinted with permission from American Chemical Society.

The strain was further modified by plasmid-based expression of the NADH-dependent alanine dehydrogenase AlaD from *Lysinibacillus sphaericus* to increase L-alanine production (resulting in the strain *C. glutamicum* DelAro^5 P_{O6}-*iolT1* Δ*ldhA* pMKEx2_*alaD*, abbreviated as PYR_ALA_2) as shown previously [151]. The fermentation process consisted of a batch phase followed by a growth-decoupled production phase by switching to microaerobic conditions and repeated pulse-feeding of D-glucose. This dual phase fermentation principle was demonstrated previously to enhance the production of various compounds with engineered *C. glutamicum*, including pyruvate [150, 153, 154]. The strain PYR_ALA_2 accumulated 44 mM pyruvate and 80 mM L-alanine after the fermentation (Table 7), but also produced significant amounts of succinate and acetate and lower amounts of lactate as by-products. While this seems surprising, lactate formation was also reported for a prototrophic pyruvate production *C. glutamicum* strain lacking *ldhA* [155].

To avoid the loss of pyruvate by succinate formation, the strain PYR_ALA_2 was further modified by the inactivation of the phosphoenolpyruvate carboxylase (encoded by *ppc*) as well as the reduction of pyruvate dehydrogenase complex (PDHC) activity. To minimize acetate formation, a deletion of the *pqo* gene, encoding the pyruvate:quinone oxidoreductase, was introduced. The resulting strains *C. glutamicum* DelAro^5 P_{O6}-*iolT1* A16-*aceE* Δ*ldhA* Δ*alaT* Δ*pqo* pMKEx2_*alaD* (abbreviated as PYR_ALA_8), and the plasmid-free variant PYR_ALA_7, required supplementation of acetate to enable unrestricted growth under microaerobic fed-batch conditions because of impaired acetyl-CoA availability with D-glucose as sole carbon and energy source. The

concentration profiles over the process time and final titers are shown in Figure 18 and Table 7, respectively.

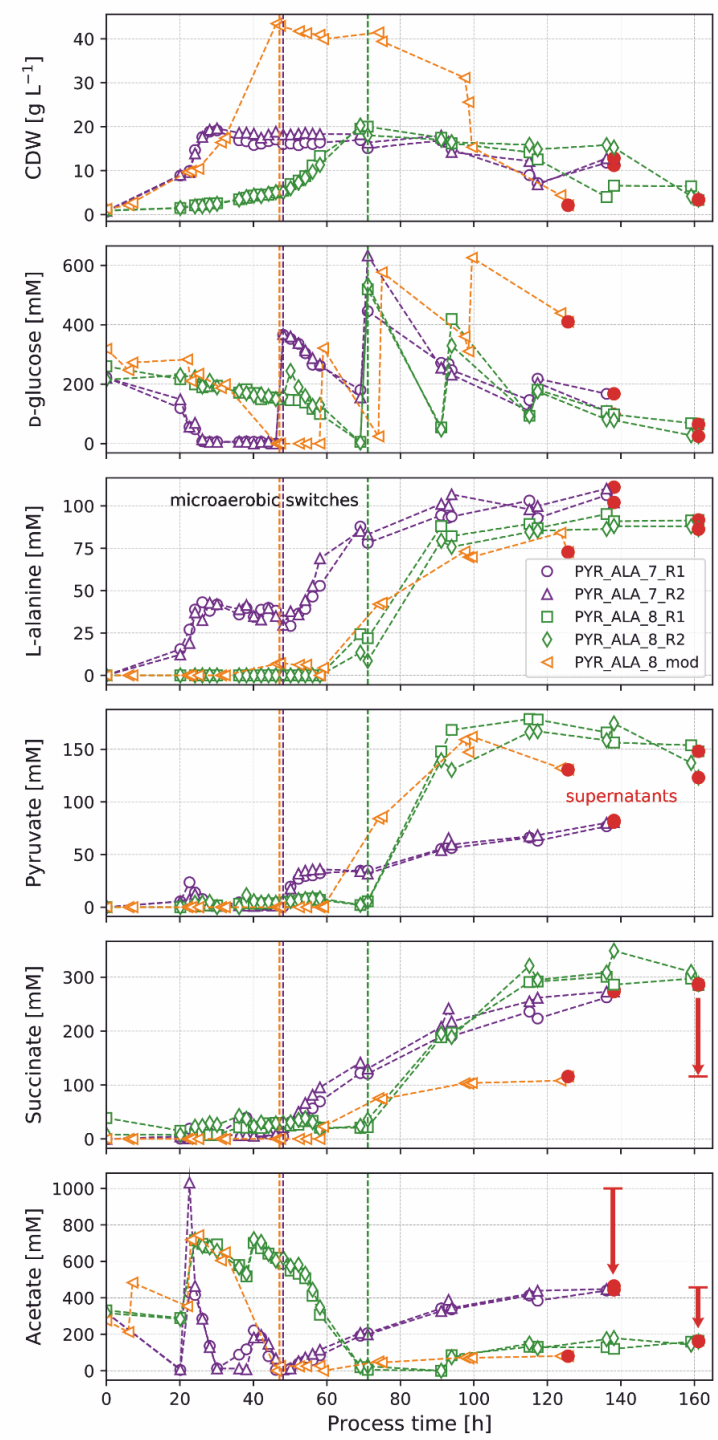

Figure 18 Fed-batch bioreactor cultivations of engineered *C. glutamicum* strains for the co-production of pyruvate and L-alanine. Cultivations of acetate-auxotrophic strains PYR_ALA_7/8 in biological duplicates (R1, R2) in CGXII medium containing 40 g L^{-1} D-glucose and 20 g L^{-1} sodium acetate. A total of 36 g acetate and 228 g D-glucose were fed to the cells during the growth and co-production phases. The strain PYR_ALA_8 was subject to modified process conditions (PYR_ALA_8_mod) by feeding a total of 63 g sodium acetate and 253 g D-glucose during the growth and co-production phases, respectively. The co-production phase was started by switching to microaerobic conditions (dotted vertical lines). The red circles represent the collection of cell-free supernatants for subsequent utilization in the enzyme cascade. The red arrows highlight the successful minimization of by-product formation by rational metabolic engineering. This figure was previously published [123] and is reprinted with permission from the American Chemical Society.

Table 7 Final titers and carbon-specific yields of produced target compounds pyruvate and L-alanine and by-products during microaerobic fed-batch cultivations of the different engineered *C. glutamicum* strains.

Strains	**Target products**				**By-products**		
	Pyruvate		**L-Alanine**		**Succinate**	**Acetate**	**Lactate**
	[mM]	[mol mol^{-1}]	[mM]	[mol mol^{-1}]	[mM]	[mM]	[mM]
PYR_ALA 7_R1	82.3	0.07	111.0	0.10	277.0	465.0	13.1
PYR_ALA 7_R2	80.8	0.07	102.0	0.09	273.0	444.0	n.d.
PYR_ALA 8_R1	148.0	0.12	91.7	0.08	285.0	165.0	33.6
PYR_ALA 8_R2	123.0	0.10	86.3	0.07	288.0	160.0	32.1
PYR_ALA 8_mod	131.0	0.13	72.7	0.07	116.0	79.9	91.8

The plasmid-free strain PYR_ALA_7 reproducibly showed faster growth on D-glucose and acetate as compared to PYR_ALA_8, reaching a biomass titer of 20 g L^{-1} after 30 h of batch cultivation. A very high accumulation of L-alanine (42 mM) in the culture supernatant was observed for PYR_ALA_7 during this phase. With the switch to microaerobic conditions and repeated pulse feeding of D-glucose, the continued accumulation of L-alanine and pyruvate was achieved. The L-alanine concentration reached the highest value (111 mM) across all strains and conditions tested (Table 7), while the pyruvate concentration remained comparatively low (82 mM). This result suggests that the plasmid-based expression of the alanine dehydrogenase (as tested in strain PYR_ALA_8) is not effective for increased L-alanine biosynthesis in this approach, either because the dehydrogenase is produced as an inactive enzyme or because it catalyzes the reverse reaction towards pyruvate, depending on the redox state of the cells. Moreover, the formation of acetate as a by-product was greatly reduced with PYR_ALA_8. Some acetate formation was expected as PDHC activity was merely downregulated and not completely deleted. Finally, an alternative cultivation strategy was tested with strain PYR_ALA_8 (denoted as PYR_ALA_8_mod), feeding increased amounts of D-glucose and sodium acetate (253 g and 63 g). Moreover, the microaerobic conditions were intensified by maintaining the DO at 5% (400 – 750 rpm) with an increased airflow of 0.25 vvm. This resulted in a doubled biomass formation during the batch phase. In addition, the succinate formation was reduced by half while accumulating significantly higher lactate concentrations (Table 7).

Overall, the carbon-specific product yields ($mol_{product}$ $mol_{substrate}^{-1}$) were much lower compared to the best literature data that are based on specifically engineered hosts for either pyruvate or L-alanine production. However, in this case, the high-titer production of both precursors in one fermentation process was targeted. For instance, the currently highest pyruvate yield of 1.9 mol mol^{-1} was reported for an acetate-auxotrophic *Escherichia coli* strain, following a two-stage process and using resting cells for the production phase [156]. There, no secretion of L-alanine was observed. Furthermore, a comparable high yield of 1.49 mol mol^{-1} was reported for the engineered strain *C. glutamicum* Δ*aceE* Δ*pqo* Δ*ldhA* ΔC-T *ilvN* Δ*alaT* Δ*avtA*, which carries two additional modifications to prevent further conversion of pyruvate into L-alanine and L-valine, respectively [150]. The resulting strain required additional supplementation of L-alanine and acetate to establish sufficient cell growth. The currently highest L-alanine titer of 98 g L^{-1} was reported for the strain *C. glutamicum* Δ*ldhA* Δ*ppc* Δ*alr* +*alaD* +*gapA* applying a fermentation process under oxygen deprived conditions [151]. No yields for L-alanine and no secretion of pyruvate are reported in that study. In addition, no beneficial effect of the heterologous expression of the alanine dehydrogenase from *Lysinibacillus sphaericus* could be confirmed here. As product yields and concentration in L-alanine production processes can have contrary trends [157], the herein presented strategy focused on high concentrations over yields for the purpose of direct enzymatic utilization of both precursors.

In conclusion, the presented strategy facilitated the targeted one-pot production of pyruvate and L-alanine. The results demonstrated how strain engineering and adaptions of cultivation parameters enabled the production of high titers of both precursors in one process and partly reduced by-product formation. As a result, not one ideal fermentation supernatant was obtained, but several successful production runs with differing supernatant compositions. PYR_ALA_7_R2 achieved the highest L-alanine concentrations while producing no lactate as by-product. PYR_ALA_8_R1 provided the highest pyruvate concentrations and substantial reduction of acetate formation. PYR_ALA_8_mod facilitated the lowest by-product formation of succinate and acetate while providing high to moderate concentrations of pyruvate and L-alanine. The resulting supernatants from these three mentioned fermentation runs were used as precursor reservoir for the enzymatic multi-step synthesis of metaraminol.

3.1.3.2 Utilization of microbially produced precursors in the enzymatic multi-step synthesis of metaraminol

Reaction optimization of carboligation in the fermentation supernatant

For the carboligation of 3-hydroxybenzaldehyde (3-OH-BA) and pyruvate, instead of the AHAS-I from *Escherichia coli* [67], a single-mutation variant of the pyruvate decarboxylase from

Acetobacter pasteurianus (*Ap*PDC var; sequence is given in the appendix) was used. The enzyme provides high chemo- and stereoselectivity for the (*R*)-isomer of the 2-hydroxy ketone and does not produce acetoin or acetolactate as by-products from releasing acetaldehyde. In general, an excess of co-substrate is favorable in mixed carboligation reactions to facilitate full conversion. Preliminary tests converting 20 mM or 40 mM 3-OH-BA with excess pyruvate in different concentrations in buffer systems showed that a 2- to 3.75-fold molar excess of the co-substrate was sufficient for a rapid conversion. No major increase in reaction rates was obtained with higher initial excess of pyruvate (Figure A2.2, appendix). Therefore, a concentration of 131 mM pyruvate as gained by the microbial production (Table 7) was expected to be suitable for the conversion of 20 - 40 mM 3-OH-BA. The time-dependent reaction progress in the fermentation supernatant from the fermentation process PYR_ALA_8_mod is shown in Figure 19. Within 8 h reaction time, almost complete conversion of 3-OH-BA with solely bio-based pyruvate in the fermentation supernatant (117 mM pyruvate SN) was reached. Here, the indicated pyruvate concentration in the supernatant reflects the final concentration after dilution with buffer. Additionally supplementing the pyruvate concentration to a final concentration of 200 mM pyruvate restored the reaction rate, which was comparable to the control reaction with commercial, purchased pyruvate.

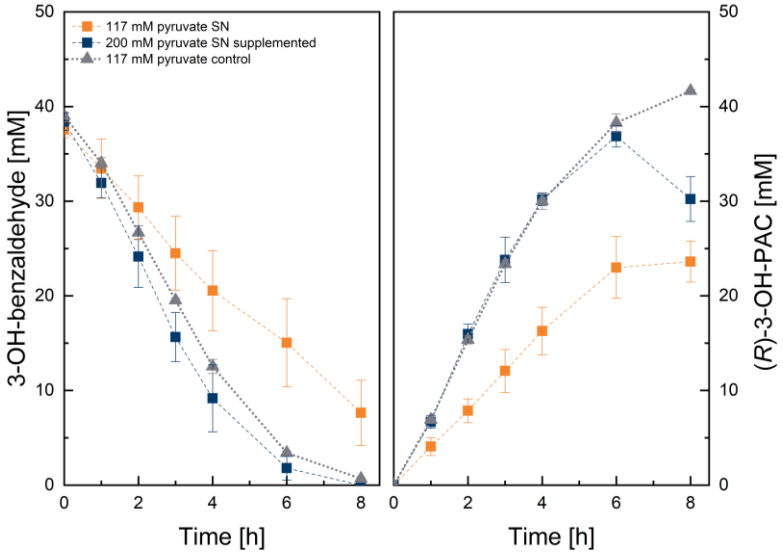

Figure 19 Carboligation of 3-OH-BA and pyruvate in the fermentation supernantant (SN) PYR_ALA_8_mod or buffer supplemented with commercial pyruvate (control). Reaction conditions: 40 mM 3-OH-BA, 117 mM pyruvate after dilution with buffer or supplemented with additional, commercial pyruvate to a final concentration of 200 mM pyruvate, 100 mM Kpi buffer pH 6.5, 1 mM ThDP, 2.5 mM $MgCl_2$, 10 mg mL^{-1} lyophilized whole cells (*Ap*PDC var), 25 °C, 700 rpm, 1 mL reaction volume. The error bars show the standard deviation of technical triplicates. This figure was previously published [123] and is reprinted with permission from American Chemical Society.

Reaction endpoints after 24 h with purified *Ap*PDC var (PE) or lyophilized whole cells (containing *Ap*PDC var; LWC) are shown in Figure 20. Slightly lower conversions for the carboligation in the fermentation supernatant were observed compared to buffered reference reaction with identical, commercial pyruvate concentrations (92% with PE and 94% with LWC compared to > 99%,

respectively). In all reaction batches, the *ee* values for the (*R*)-enantiomer were comparable (94% *ee* with purified enzyme) or only slightly reduced for whole cell-catalyzed reactions (90% *ee*) in the fermentation supernatant. These results imply that the stereoselectivity of the pyruvate decarboxylase was minimally compromised by the complex reaction matrix in the fermentation supernatant. This outcome is remarkable as small adjustments in the reaction conditions can already have a large impact on the stereoselectivity of similar enzyme variants [158, 159]. Strikingly, *ee* values were at > 99% in all reactions after 5 h incubation, indicating that prolonged incubation lowers the *ee* for (*R*)-3-OH-PAC. The fermentation medium further ensured a sufficient supply of magnesium ions necessary for the catalytic function of the pyruvate decarboxylase, as shown by comparable reaction outcomes in the supernatant with and without additional supplementation of magnesium chloride (Figure 20).

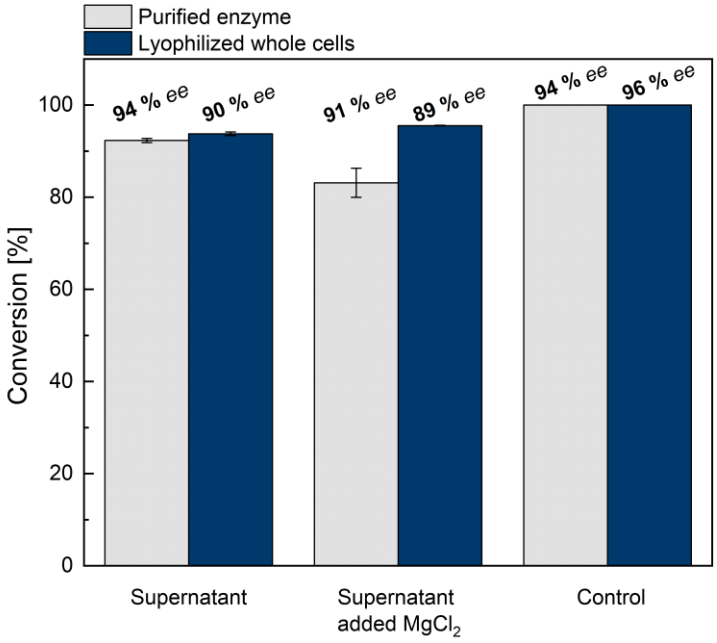

Figure 20 Conversion of 3-OH-BA and bio-based pyruvate and *ee* values for (*R*)-3-OH-PAC in the fermentation supernatant and buffer system (control) after 24 h. The reactions were performed directly in the fermentation supernatant PYR_ALA_8_mod with and without additional magnesium chloride. The control shows a reference reaction performed in buffer. Reaction conditions: 40 mM 3-OH-BA, 117 mM pyruvate after dilution with buffer (from SN PYR_ALA_8_mod or supplemented), 1 mM ThDP, 10 mg mL^{-1} lyophilized whole cells or 1 mg mL^{-1} purified enzyme (*Ap*PDC var), 100 mM Kpi buffer pH 6.5, 2.5 mM $MgCl_2$ (added if indicated and in control), 25 °C, 700 rpm, 1 mL reaction volume, 24 h. The error bars show the standard deviation of technical triplicates (in the control, the error is < 0.01 and thus not visible). This figure was previously published [123] and is reprinted with permission from the American Chemical Society.

In contrast, the carboligation in the fermentation supernatant from PYR_ALA_8_R1 was heavily restricted (Figure 21, B). A similar result was observed for the supernatant from PYR_ALA_7_R2 (plasmid-free strain variant with identical cultivation conditions, Figure 21, A). The cultivation conditions differed from PYR_ALA_8_mod in terms of total amount of acetate and glucose, which was fed throughout the process, and slightly adapted aeration and agitation. This suggests an impact of the process conditions on the resulting supernatant composition and its applicability for

enzymatic carboligations. The reaction progress first shows a formation of the desired carboligation product within the first 5 h, upon which the product concentrations stalls for endpoint determination after 20 and 24 h. In case of the reaction with supernatant from PYR_ALA_8_R1, a reaction pH of 7.5 was slightly more favorable with respect to the overall conversion, nevertheless drastic inconsistencies in the mass balance are evident. Therefore, a heat treatment of the fermentation supernatant prior to substrate addition was performed by heating the thawed supernatant in 2 mL reaction tubes at 90 °C for 15 min before cooling on ice for 10 min. Precipitates were removed by filtration through a 0.45 µm syringe filter before 3-OH-BA, buffer and cofactors were added to prepare the reaction solution. This procedure increased the overall product yields substantially and facilitated complete aldehyde depletion after 3 h and 5 h (Figure 21).

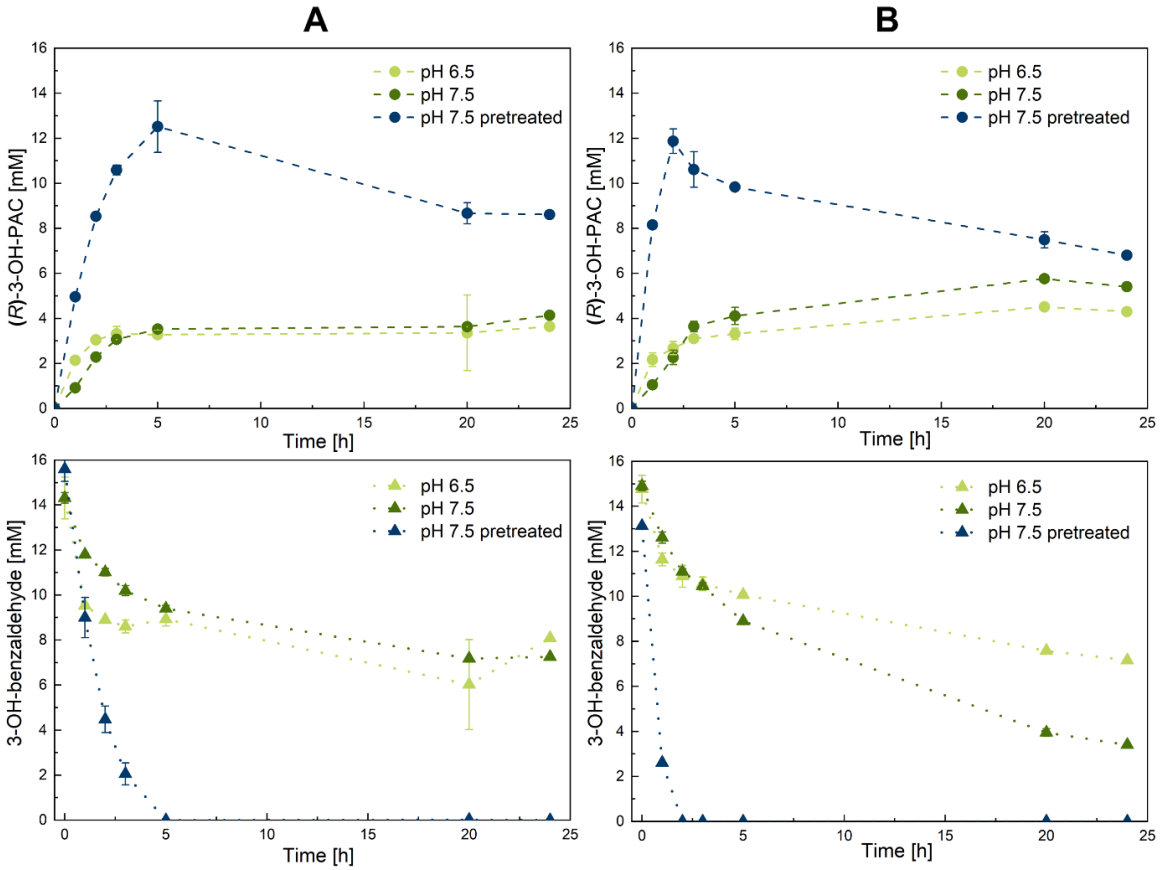

Figure 21 Carboligation reaction in fermentation supernatants PYR_ALA_7_R2 (A) and PYR_ALA_8_R1 (B) with and without heat treatment of the fermentation supernatant. Reaction conditions: 20 mM 3-OH-BA, 2.5 mM $MgSO_4$, 1 mM ThDP, 81 mM or 148 mM pyruvate produced in the fermentation supernatant, 100 mM Kpi buffer pH 6.5 or 7.5 from 1 M Kpi stock solution, 1 mg mL^{-1} *Ap*PDC var (purified enzyme), 1 mL reaction volume, 25 °C, 750 rpm. Heat treatment of the fermentation supernatant in 2 mL reaction tubes (90 °C, 15 min, 10 min cooling on ice) before filtration (0.45 µm) and addition of 3-OH-BA, buffer and cofactors. The error bars show the range between technical duplicates.

Upon longer incubation, however, the formed product was degraded (Figure 21, dashed blue line). This effect was observed for both, purified enzymes and lyophilized whole cells, excluding the

cell background to cause unwanted side reactions in the fermentation supernatant. Several conclusions can be drawn from this data. The apparent degradation of (*R*)-3-OH-PAC can be attributed to unknown chemical side reactions, which would require further thorough investigation to elucidate. Further, the limited conversions in the untreated fermentation supernatant could arise from proteolytic enzyme degradation, as extracellular proteases could be released in the late stages of the fermentation process when cells are not viable anymore. Since the heat treatment led to the formation of a precipitation, which was subsequently removed by filtration, it is likely that soluble proteins were thereby inactivated and removed. Other unidentified, heat-sensitive inhibitors could bind in the active site of the carboligase, preventing further conversion of 3-OH-BA.

In summary, varying performance of the carboligation reaction in fermentation supernatants from PYR_ALA_7/8_R2/R1 and PYR_ALA_8_mod was observed. Therefore, the most promising strategy consisted of a heat treatment step of the supernatant to facilitate high conversions and the direct isolation of the product to prevent product degradation. In that regard, complete aldehyde depletion was a crucial achievement, as remaining substrate would interfere with product isolation by extraction, drastically complicating the subsequent purification and transamination of (*R*)-3-OH-PAC. Moreover, while this strategy was applicable for an intermediate concentration range between 20 - 40 mM 3-OH-BA, further intensification of the process would require feeding of the aldehyde to overcome substrate solubility limits. However, higher substrate concentrations would in turn require enhanced pyruvate supply in the fermentation supernatants.

Elucidation of possible matrix effects from supernatant components on the enzymatic carboligation

Investigating the carboligation activity in different fermentation supernatants implied varying performances depending on the applied supernatant. Even though a heat treatment of the supernatant prior to catalysis was found to be an efficient strategy to enhance conversions, a deeper understanding of potential underlying effects was desired. As the fermentation supernatant contained additional organic acids as by-products from the metabolism of the production strains, a putative influence of these components on the carboligase activity was tested. The experiments were performed in buffer systems with individual addition of commercial lactate, succinate or acetate, respectively. The supplemented concentrations were chosen in a higher range than actual concentrations in the final fermentation broth (Table 7). The specific activity of purified *Ap*PDC var in the presence of 200 mM lactate or 200 mM acetate reflected the control reaction without addition of other components, while the supplementation with 150 mM succinate resulted in a slight decrease of the specific activity (0.29 µmol min^{-1} mg^{-1} compared to 0.37 µmol min^{-1} mg^{-1}, Figure 22, A). Further, complex fermentation broth can exhibit higher ionic

strengths depending on the media composition and cultivation conditions. The effect of increased ionic strength was assessed by addition of 200 mM NaCl to the reaction mixture of the activity assay (section 2.2.3.1), which led to a decrease in initial enzyme activity by 18% (Figure 22, B). Previously, activity losses of a phosphoenolpyruvate carboxylase in the presence of high ionic strength (200 - 400 mM NaCl) were attributed to dissociation of the homotetrameric enzyme over time [160]. However, *Ap*PDC var catalyzed full conversion of 10 mM 3-OH-BA within 1 h in the presence of 200 mM NaCl (data not shown). Further time-resolved conversion curves over 8 h reaction time showed a comparable reaction progress in presence of either 150 mM succinate, 100 mM or 200 mM acetate compared to a reference reaction (Figure A2.3, appendix). Based on these results, it is unlikely that the previously shown reduced reaction rates (Figure 19) or loss in performance (Figure 21) can be attributed due to any of the quantified side components or enhanced ionic strengths in the fermentation supernatants.

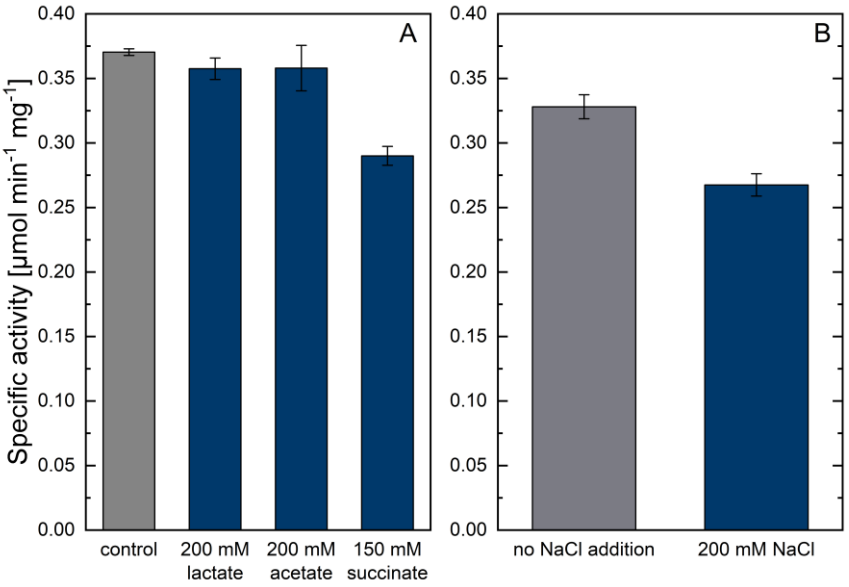

Figure 22 Specific activity of *Ap*PDC var under initial rate conditions with and without supplementation of by-products (lactate, acetate or succinate) or 200 mM NaCl in comparison to reference reactions without supplementation (control). Reaction conditions: 10 mM 3-OH-BA, 50 mM pyruvate, 50 mM Kpi buffer pH 6.5, 1 mM ThDP, 2.5 mM $MgCl_2$, 1 mg mL^{-1} *Ap*PDC var, 22 °C, 700 rpm, 1 mL reaction volumes. The error bars indicate the standard deviation of technical triplicates.

Two-step synthesis of metaraminol using microbially produced pyruvate and L-alanine

Finally, the enzymatic synthesis of metaraminol in a two-step synthesis using bio-based precursors was envisaged. Several experiments showed that a two-step one-pot cascade for metaraminol production in the supernatant was not possible as the amino alcohol product was not detectable. This result can be explained by several reasons. The supernatant contained remaining pyruvate and insufficient L-alanine concentrations after the carboligation step. Consequently, the unfavorable reaction equilibrium for the transamination reaction was reinforced, remaining heavily on the substrate side. In addition, instability of the carboligation product (*R*)-3-OH-PAC was observed for longer incubation in the supernatant, making a sequential mode with intermediate purification more favorable. Here, the carboligation product (*R*)-3-OH-PAC was purified from the fermentation supernatant directly upon aldehyde depletion and the subsequent transamination step was performed in buffered systems with a molar excess of purified L-alanine. The preparative-scale carboligation reaction was conducted in 40 mL reaction volume in the fermentation supernatants providing 82 mM (PYR_ALA_7_R2, Figure 23, A) and 148 mM pyruvate (PYR_ALA_8_R1, Figure 23 B), respectively. In both cases, complete aldehyde depletion was measured after 6 h, corresponding to > 99% and 92% conversion from 20 mM (Figure 23, A) and 30 mM (Figure 23, B) 3-OH-BA, respectively. Subsequently, the intermediate was isolated by extraction and the solvent-free product was identified as the (*R*)-enantiomer by chiral HPLC, which confirmed a high stereoselectivity for the desired configuration. Conclusively, the optimized reaction conditions facilitated the carboligation reaction towards (*R*)-3-OH-PAC in the fermentation supernatant with excellent stereoselectivity and full conversion. The purified product (40% isolated yield, 63% HPLC purity) was subsequently aminated using lyophilized whole cells containing *Cv*2025. The transamination reaction reached 21% and 23% conversion with purified and with commercial L-alanine, respectively (Figure 23 C). In reference reactions for the transamination with L-alanine, solely the product peak corresponding to the (1*R*,2*S*)-stereoisomer was detected *via* chiral HPLC, suggesting that the previously described excellent stereoselectivity of the amine transaminase *Cv*2025 was also verified in this setup [39, 67].

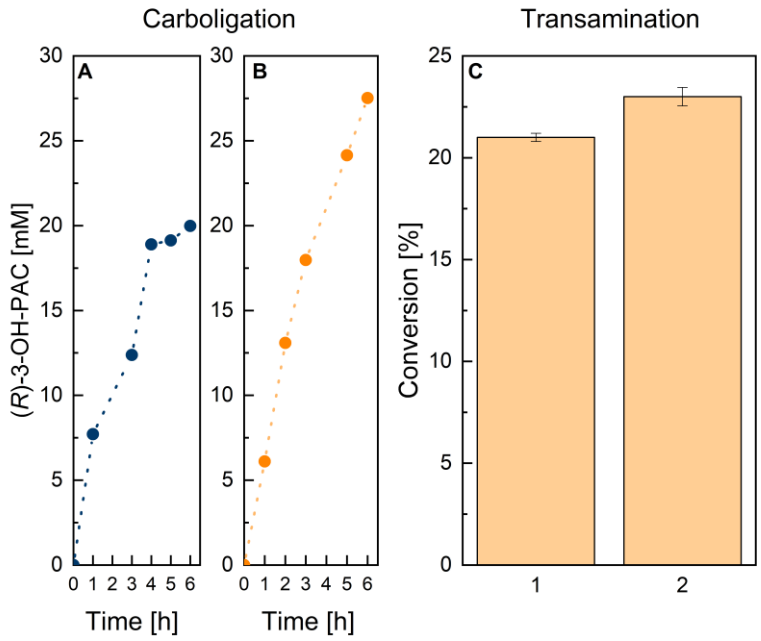

Figure 23 Two-step synthesis of metaraminol using bio-based pyruvate and L-alanine. Two separate preparative carboligation reactions in different fermentation supernatants are shown in A and B. The purified intermediate from B was used in the transamination reaction shown in C. Reaction conditions: **A**, 20 mM 3-OH-BA, 1 mM ThDP, 2.5 mM $MgSO_4$, 100 mM potassium phosphate buffer, pH 6.5 in fermentation supernatant PYR_ALA_7_R2 containing 82 mM pyruvate, 25 °C, overhead shaker, 40 mL, 10 mg mL^{-1} *Ap*PDC var lyophilized whole cells. **B**, 30 mM 3-OH-BA, 1 mM ThDP, 2.5 mM $MgSO_4$, 100 mM potassium phosphate buffer pH 6.5 in fermentation supernatant PYR_ALA_8_R1 containing 148 mM pyruvate, 25 °C, overhead shaker, 40 mL, 10 mg mL^{-1} *Ap*PDC var lyophilized whole cells. **C**, 18 mM (*R*)-3-OH-PAC (purified from B), 0.2 mM PLP, 250 mM L-alanine (1, purified from PYR_ALA_ 7_R2; 2, commercial), 100 mM HEPES pH 7.5, 30 °C, 750 rpm, 1 mL, 10 mg mL^{-1} *Cv*2025 lyophilized whole cells. Error bars indicate the standard deviation of technical triplicates. This figure was previously published [123] and is reprinted with permission from the American Chemical Society.

The slightly diverging conversions in the transamination step could be explained by the higher purity of the commercial L-alanine product (> 99%). As conversion and product yield were congruent, no instability of (*R*)-3-OH-PAC was determined in the buffered reaction system. It can be concluded that the intermediate purification prevented degradation due to instabilities of the 2-hydroxy ketone. Furthermore, the intermediate purification step enabled the conversion of (*R*)-3-OH-PAC to metaraminol, partly circumventing the unfavorable reaction equilibrium by using L-alanine in a higher molar excess and removal of residual pyruvate from the reaction mixture. Nevertheless, the transamination with L-alanine as amine donor resulted in very low conversions, requiring further process intensification strategies to reach higher product yields. This objective was pursued by two complementary extractive ISPR concepts described in chapter 3.2 and 3.3 of this thesis.

In future, the starting aromatic aldehyde can also be obtained from bio-based resources. A current research focus is the integration of bio-based 3-hydroxybenzoate *via* a preceding enzymatic reduction step to afford the starting 3-OH-BA [161]. The application of a set of carboxylic acid reductases was recently published by Weber *et al.* to produce benzaldehyde and substituted benzaldehydes enzymatically from carboxylates, which are optimally gained from renewable

resources *via* microbial transformation [162]. Here, overoxidation or the dependence on toxic reaction compounds as known from classical chemical transformations could be avoided. In this way, the entire cascade can be based on microbially produced precursors from renewable resources.

3.1.4 Conclusion

The two-step enzymatic synthesis of metaraminol was realized using bio-based pyruvate and L-alanine. Both aliphatic precursors were provided in the supernatant allowing for further transformations directly or indirectly. For the carboligation step, the pyruvate concentration in the supernatant was sufficient for direct enzymatic catalysis in the fermentation supernatant. Here, retaining high conversion and stereoselectivity was challenging due to the complex and poorly characterized reaction matrix imposing an inhibiting effect on the carboligation. Eventually, a heat inactivation step of the supernatant prior to catalysis facilitated excellent conversion and stereoselectivity. By further elucidating possible inhibitions from common fermentation side products and GC-Tof-MS characterization of the fermentation supernatant matrix, valuable information for linking microbial cell factories to biocatalytic syntheses will be provided. While the herein presented results indicated a good compatibility of enzymatic carboligation reactions with bio-based pyruvate from fermentation supernatant, the robustness of the overall process is heavily dependent on the reproducibility of the fermentative process. Further, the intermediate work-up and spatial separation of carboligation and transamination reaction was required to enable metaraminol synthesis. The purification of (*R*)-3-OH-PAC prevented intermediate degradation and partly overcame the unfavorable reaction equilibrium. Nevertheless, the low yield demonstrates how the transamination reaction remains thermodynamically inhibited, demanding further process intensification to shift the equilibrium.

Chapter 3.2

Process intensification by *in situ* liquid-liquid product extraction

Partially published in:

[125] Mack K, Doeker M, Grabowski L, Jupke A, Rother D. 2021. Extractive *in situ* product removal for the application of L-alanine as amine donor in enzymatic metaraminol production. *Green Chemistry.*

DOI: 10.1039/d1gc00852h

[Reproduced (adapted) with permission from Green Chemistry. © The Royal Society of Chemistry]

Contributions:

Kevin Mack (KM) performed the initial solvent screening. Laura Grabowski (LG) performed enzyme stability determination as part of her master thesis together with support by KM. The physical extraction studies in pure substance systems were performed by Moritz Doeker (MD) with support by LG. Titration experiments were performed by LG. The ISPR experiments in the enzymatic system were performed by LG with support by KM. The original manuscript was written by KM, MD, and LG. All parts that were not originally written by LG were paraphrased and adapted for the scope of this thesis. Figures of the original manuscript were adapted and included in this chapter. This chapter was written by Laura Grabowski and reviewed by Dörte Rother.

3.2 Process intensification by *in situ* liquid-liquid product extraction

3.2.1 Abstract

The transamination reaction towards metaraminol is heavily limited by an unfavorable reaction equilibrium, limiting the conversion with a 6.25-fold molar excess of L-alanine as the amine donor to around 20% as shown in the previous chapter. For this reason, *in situ* product removal based on liquid-liquid extraction was investigated as a strategy to increase conversion and thereby leverage a potential synthesis route with a bio-based amine donor. To design extraction concepts, the pK_a values of the reaction components (*R*)-3-OH-PAC and metaraminol were experimentally determined, deducing two possible *in situ* extraction techniques for metaraminol: physical liquid-liquid extraction and reactive liquid-liquid extraction, the former being the focus of this chapter. The operational window for physical product extraction in the enzymatic transamination reaction was defined regarding the requirements for simultaneous extraction and high enzyme activity. In an initial solvent screening, 12 organic solvents were tested for retained transaminase activity, which revealed substantial enzyme activity and storage stability in the presence of 1-decanol and 1-octanol. Pure substance extraction studies with 1-decanol (without enzyme) of (*R*)-3-OH-PAC and metaraminol showed a reciprocal pH dependent extraction behavior, in which (*R*)-3-OH-PAC showed a high distribution towards the organic phase at low and neutral pH while alkaline pH values above the first pK_a value favored distribution of metaraminol to the organic phase. The enzyme activity was suboptimal at alkaline pH values, emphasizing a necessary tradeoff between high extraction efficiency and product formation rate. While the integration of physical product extraction with the enzymatic synthesis enabled a conversion increase, the alkaline operating pH caused a chemical reaction of metaraminol with the co-product pyruvate, reducing the final product concentration and overall process performance.

3.2.2 Introduction

The transformation to a circular bioeconomy requires the transfer of classical petrochemical processes towards greener synthesis routes from renewable (bio-based) starting materials. As described in chapter 1.5, part of the HyImPAct project aimed at the green production of metaraminol from bio-based, microbially produced precursors as presented in the previous chapter. Several conclusions for the setup of the two-step synthesis of metaraminol were drawn from the therein presented results. The sequential separation of carboligation and transamination reaction is necessary due to cross reactivity of the transaminase on the aldehyde substrate. In addition, a two-step one-pot regime was not successful as excess pyruvate and insufficient

L-alanine concentrations prevented any conversion in the transamination step due to the thermodynamical coupling and transaminase activity on pyruvate. As a results, the separation of the reaction steps was favored, decoupling carboligation from transamination. Due to the sequential reaction steps, pyruvate cannot be simultaneously depleted in the carboligation reaction to shift the reaction equilibrium of the transamination. Alternative enzymatic removal of the co-product pyruvate has been shown before in the transamination of PAC to norephedrine as an effective way to shift the equilibrium [40]. However, this entails lowering the overall atom economy of the process and complicating the setup by additionally required auxiliary enzymes, which represent a major cost factor at scale. Likewise, shifting the equilibrium by a higher excess of amine donor is not applicable due to solubility limitations and possible inhibition of the catalyst. For instance, Tufvesson *et al.* illustrated the theoretically required excess of amine donor as a function of equilibrium constant to achieve a certain conversion window, which was as large as a 10,000-fold excess for $K_{eq} = 10^{-3}$ for 90% conversion [163]. From an economical point of view, the substantial cost contribution of pure precursors and decreasing atom efficiency from using high stochiometric excess of co-substrates limit the feasibility of this approach. As an alternative, *in situ* product removal (ISPR) can be favorable for several reasons. In holistic process development, the consideration of downstream concepts at an early stage is advised [164]. In this regard, integrating ISPR was shown to accomplish multiple purposes for process intensification, *i.e.,* initializing product recovery as a first step in downstream processing [165], prevention of inhibitory effects of substrates or products [166-169], maintenance of process performance in case of excessively foaming products [164] and for equilibrium shift of thermodynamically challenging transformations [109, 170]. The latter is the focus of this chapter and the following chapter 3.3 in this thesis.

In literature, several methods for *in situ* product removal within amine transamination reactions are published [107, 109]. Focusing on *in situ* extraction, the physical extraction of an amine product was accomplished at alkaline reaction conditions *via* extraction into an organic dodecane phase. The product recovery was achieved by another pH-shift into an acidic phase. In this example, the reaction phase, organic extraction phase and back extraction phase were separated by a membrane, resulting in a supported liquid membrane (SLM) setup [108, 112]. For ISPR by extraction, the product synthesis and extraction run simultaneously. Therefore, it is inevitable to define an operational window of reaction conditions suitable for both unit operations. Notably, the development of a suitable extraction strategy is highly dependent on physicochemical properties of the reaction system as well as the biocatalyst chosen for the specific catalysis. In this chapter, the fundamental exploration of reaction conditions for amine transaminase catalyzed production of metaraminol from (*R*)-3-OH-PAC and *in situ* extraction are shown. First, the pH dependent

dissociation of both reaction components is described to deduce possible extraction strategies. Based on this, suitable organic solvents are determined by enzyme compatibility tests and further characterized regarding maximal extraction efficiencies for metaraminol extraction from an aqueous stream. The optimal conditions are taken for integrating physical ISPR with the enzymatic metaraminol synthesis.

3.2.3 Results & Discussion

3.2.3.1 Physicochemical system characterization for downstream processing of metaraminol

Liquid-liquid extraction of a target compound from an aqueous to an organic liquid phase is dependent on solubility of the target compound in the organic extraction phase compared to the aqueous phase. For the herein described application, the aqueous phase corresponds to the enzymatic reaction phase in which the transformation of (*R*)-3-OH-PAC to metaraminol is performed. Protonation or dissociation of functional groups affects the compound's hydrophobicity and affinity towards an organic phase. Therefore, dissociation behavior of metaraminol and (*R*)-3-OH-PAC was characterized by titration experiments as shown in Figure 24. From the titration with commercial metaraminol bitartrate, the pK_a values for the amino group (pK_a 8.9) and hydroxyl group (pK_a 10.2) were derived. The pK_a values of tartaric acid at 3.3 and 4.4 are also visible. The determined pK_a values of metaraminol were assigned to the functional groups in comparison to structurally similar compounds such as norephedrine (pK_a 9.05, determined by hybrid pH-metric/UV method), having only the amino group and no hydroxyl functionality at the aromatic ring [171]. In this way, the determined values lie in the expected range but differ slightly from a previously published value of 8.6 [172]. However, in that publication, there was no methodology for the experimental pK_a determination provided, which might explain the slight variation. Based on the determined pK_a values, three dissociation states are possible, depicted in Figure 24 A. Below pK_{a1}, the amine group is protonated, and the molecule has a positive charge. Between pK_{a1} and pK_{a2} a neutral species prevails with an isoelectric point (IEP) of 9.55. Above pK_{a2} the hydroxyl group dissociates, causing an overall negative charge. Likewise, one pK_a value of 9.6 for the hydroxyl functionality at the aromatic ring of the substrate (*R*)-3-OH-PAC was determined, resulting in a distribution between a neutral or anionic species, depending on the pH (Figure 24 B, D).

The presented dissociation behavior of metaraminol defines two strategies for the *in situ* extraction of metaraminol: physical liquid-liquid extraction and reactive liquid-liquid extraction. While physical extraction is only possible for a neutral target molecule, the reactive extraction of metaraminol involves a cation exchange mechanism, which is subject of chapter 3.3. The

negatively charged species was not further regarded for extraction-based ISPR, as particularly the required alkaline range above pH 11 was not considered a suitable operating range for the amine transaminase *Cv*2025 [173]. Conclusively, the results suggest that an alkaline pH value, ideally around the IEP of metaraminol at pH 9.6, was necessary for physical *in situ* product extraction. The detailed determination of suitable organic extraction phases and reaction parameters regarding extraction efficiencies and enzyme compatibility is shown in the subsequent section.

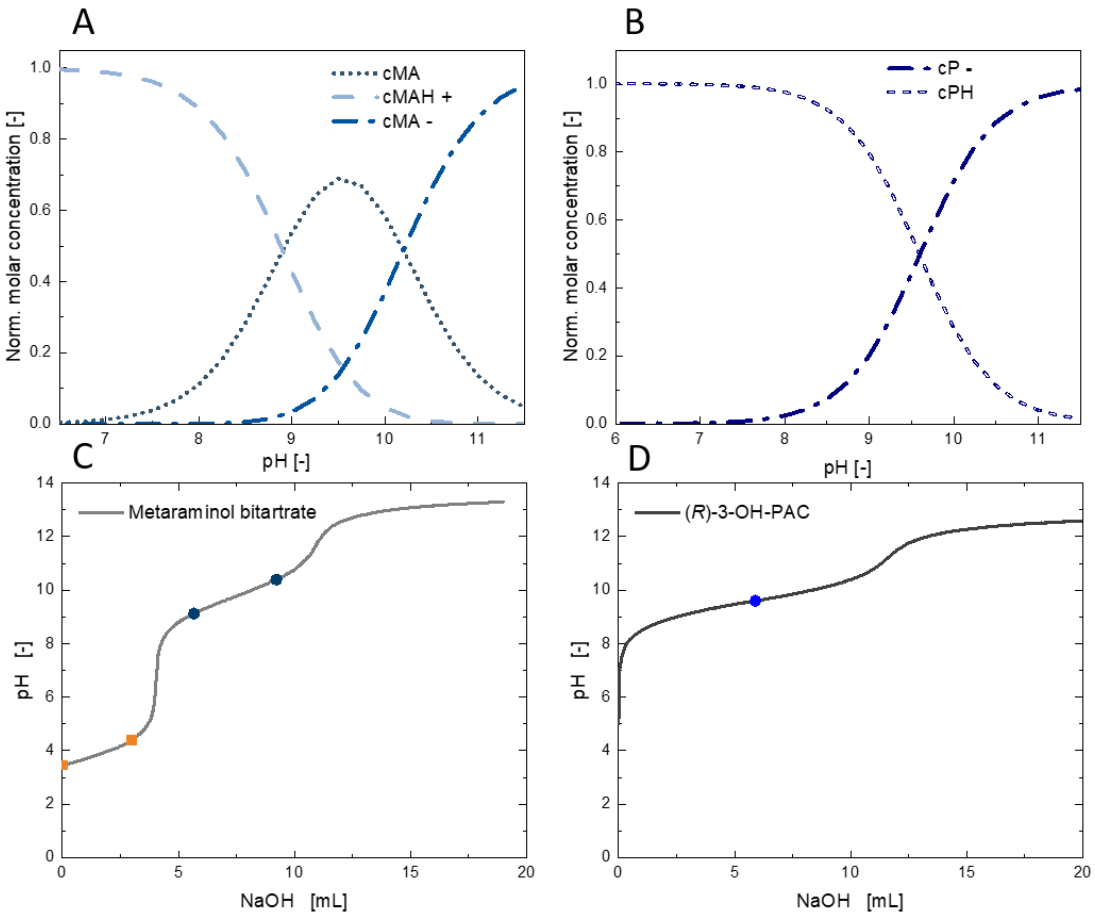

Figure 24 Titrations curves of metaraminol bitartrate (C) and (*R*)-3-OH-PAC (D) with NaOH and corresponding depiction of the pH dependent dissociation behavior (A and B). The pK_a values for metaraminol are indicated in blue (pK_{a1} = 8.9 and pK_{a2} = 10.2). The pK_a values of the tartaric acid are marked in orange (pK_{a1} = 3.3 and pK_{a2} = 4.4). The pK_a value of (*R*)-3-OH-PAC is marked in green (pK_a = 9.6). The figure parts C and D were previously published and reprinted with permission from Green Chemistry [125]. MA indicates the protonation states of metaraminol (neutral, anionic or cationic) and P indicates protonation states of (*R*)-3-OH-PAC (neutral or anionic).

3.2.3.2 Defining an operational window for *in situ* liquid-liquid product extraction and enzyme catalysis

Solvent selection regarding transaminase activity and stability

In designing an efficient (*in situ*) product recovery by extraction, the selection of an appropriate extraction solvent is a crucial step. Factors influencing the solvent selection are high solubility of the target product and ideally selective extraction of said compound. For an efficient and ecological process, recyclability and minor cross solubility of the solvent are desired [174]. In biological

reaction systems, the solvent must exhibit high biocompatibility. In the following, the experimental screening of suitable reaction conditions for *in situ* liquid-liquid extraction of the product metaraminol is described. The approach comprised both the extraction (determination of pH dependent extraction and maximal distribution coefficients) for the substrate and the product of the reaction system, as well as the enzymatic process (compatibility of enzyme activity and stability with different organic solvents). As a first step, ten organic solvents were tested for compatibility with the amine transaminase *Cv*2025 as a purified enzyme formulation. This was achieved by assessing the conversion in a model reaction, in which 20 mM 3-OH-PAC was aminated using isopropylamine (IPA) as the amine donor. The use of IPA allowed for higher conversions (in the control reaction without organic solvent), partly circumventing the limiting reaction equilibrium by acetone evaporation. In this way, absolute evaluation of potential effects of the organic solvent on the conversions were more assessable. As the cross solubility of the tested solvents differ, any effect on conversion could result from denaturation and agglomeration of the enzyme at an aqueous-organic interface [175, 176], or from co-dissolved solvent affecting enzyme activity. The conversion after 3.5 h is shown in Figure 25. Solvents with high cross solubility (with a log*P* below 1: 2-propanol, 1-propanol, *tert*-butanol and 1-butanol) caused catalyst inactivation and thereby drastically reduced the conversion in comparison to a control without solvent addition. The remaining solvents led to comparable or higher conversions, indicating that no inactivation at the aqueous-organic interface occurred under the tested conditions.

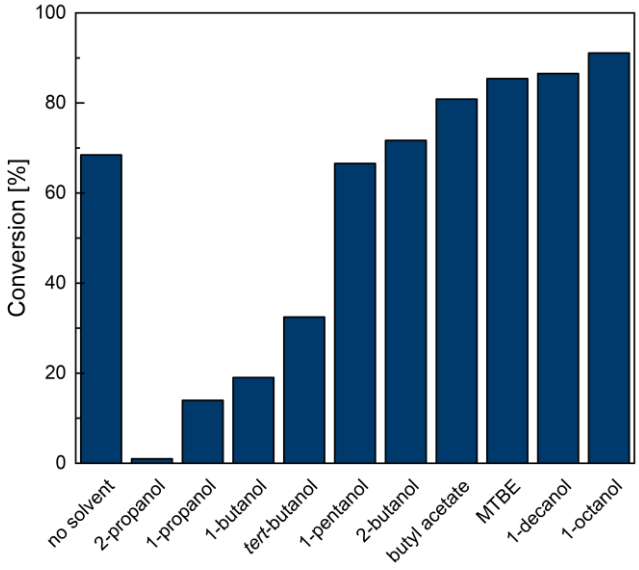

Figure 25 Conversion of (*R*)-3-OH-PAC with IPA as amine donor in the presence of 10% (v/v) organic solvents. Reaction conditions: 20 mM (*R*)-3-OH-PAC, 100 mM IPA, 100 mM HEPES pH 7.5, 0.2 mM PLP, 5 mg mL^{-1} *Cv*2025, 30 °C, 700 rpm, 3.5 h. The organic solvents exhibit differing cross solubility with the aqueous reaction phase. This data was previously published [125] and is reprinted with permission from Green Chemistry.

The best performing conditions were observed with 1-decanol and 1-octanol, both solvents with low cross solubility. The low distribution to water is not only beneficial for enzyme activity but also preferable for efficient extraction processes. In addition, efforts are made to produce these solvents microbially from renewable resources [177, 178]. Consequently, 1-decanol and 1-octanol were considered as suitable extraction solvents to retain high activity of *Cv*2025 and were chosen for further experiments. To obtain a complete picture, initial enzyme activity and long-term stability analysis was used as a complementary parameter to assess enzyme compatibility. Repeated initial rate measurements were conducted after enzyme incubation in buffer, which were pre-saturated with the respective organic solvent to reflect enzyme activity at maximal organic cross solubility. For 1-octanol and 1-decanol, almost full initial activity was retained for 13 days of incubation in contrast to a control without organic solvent saturation (Figure 26). The results suggest that substantial enzyme longevity is present and that no detrimental effects of co-dissolved organic solvent were observed. Based on the slightly higher absolute enzyme activity, 1-decanol was selected as a promising solvent candidate and subsequently tested for its applicability as (*in situ*) extraction solvent for metaraminol.

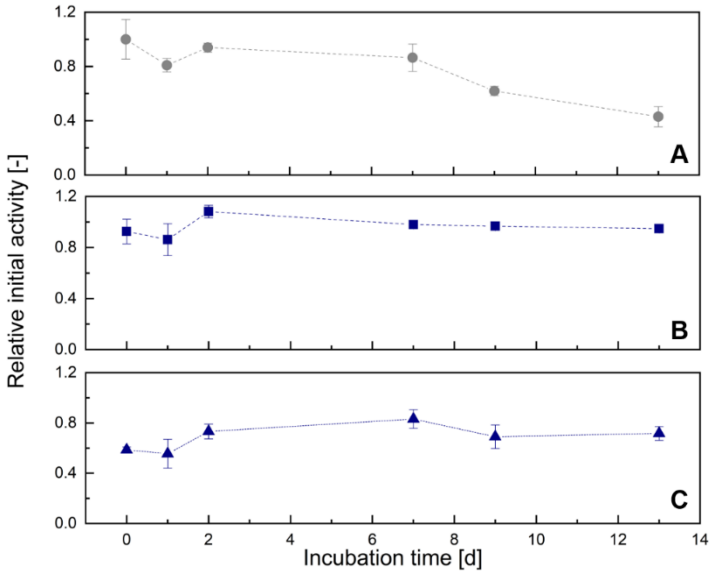

Figure 26 Storage stability of *Cv*2025 upon incubation in buffer without organic solvent (A) and in a monophasic buffer phase pre-saturated with 1-decanol (B) or 1-octanol (C). Error bars show the standard deviation of technical triplicates. This figure was originally designed by Kevin Mack and the data was previously published [125, 179]. The figure was adapted and included for the overall context of this thesis.

Characterization of liquid-liquid extraction in pure substance systems without enzyme

A central metric for an extraction process is the solubility of the target product in the organic extraction phase. As described in section 3.2.3.1, this solubility is highly dependent on protonation and dissociation states of the reaction compounds. Having the apparent pK_a values at hand, the next step was to verify the assumed dissociation behavior *via* liquid-liquid extraction experiments

of the pure substances as a function of pH (without enzyme addition). Consistent with previously published data, L-alanine and pyruvate were not extractable due to a negative charge in aqueous solution [112]. In contrast, a pH dependent extraction behavior was observed for metaraminol and (*R*)-3-OH-PAC (Figure 27).

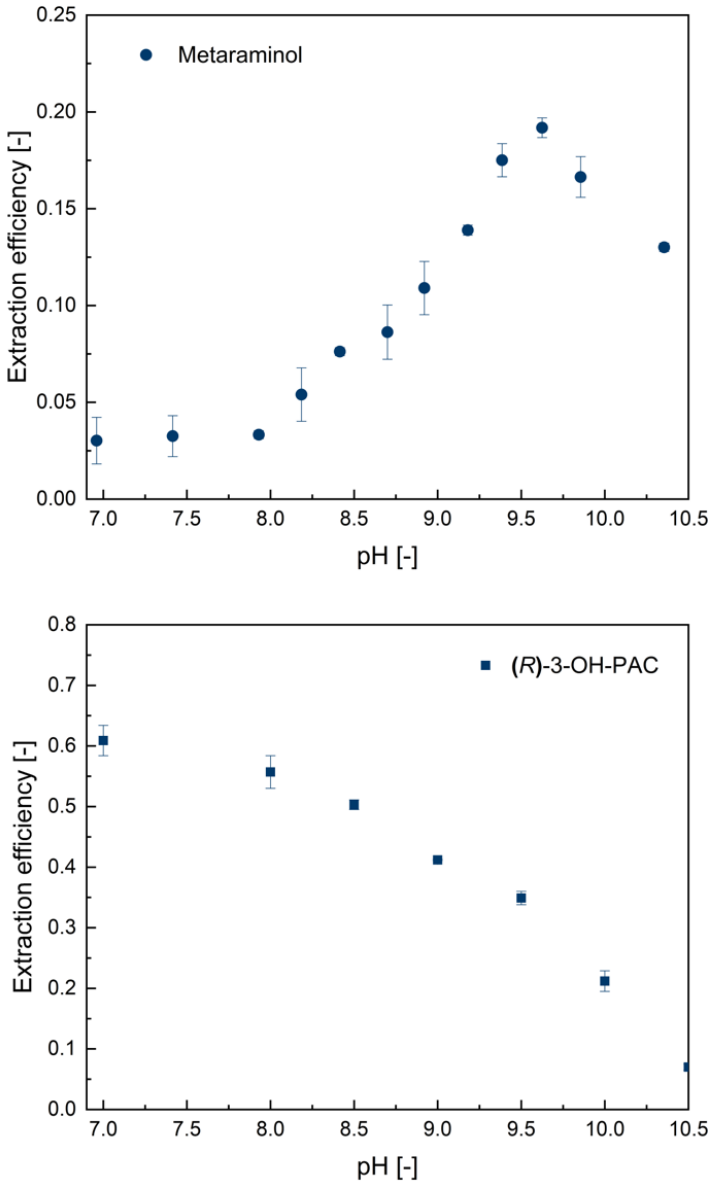

Figure 27 Extraction efficiency of metaraminol (upper) and (*R*)-3-OH-PAC (lower) from aqueous solutions at different pH values using 1-decanol as the extraction solvent. Error bars show the range of technical duplicates. This data was previously published [125] and reprinted in adapted format with permission by Green Chemistry. The data of the lower graph was additionally previously published in [179] and included in an adapted format for the context of this thesis.

For metaraminol, negligible distribution to the organic phase was observed at pH 6.9 - 7.9. With increasing pH, the extraction efficiency increased to a maximal extraction yield of 18% at pH 9.5. The experimental optimal point of extraction thereby coincides with the previously determined

IEP of 9.6 at which metaraminol is mostly present in the neutral and therefore extractable form. Above the IEP, the extraction efficiency decreased again due to a shift towards a prevailing anionic metaraminol species. The recovery of metaraminol was achieved in back extractions by transferring the organic phase to an acidic aqueous phase (*i.e.,* hydrochloric acid or tartaric acid pH < 3). The pH-shift causes the protonation of the amino group and thus facilitates distribution to the back extraction phase. In all cases, back extraction efficiencies were between 80% and 95% allowing almost complete product recovery to be assumed.

The extraction efficiency of (*R*)-3-OH-PAC in the pH range of 7 to 10.5 is shown in Figure 27. A maximal extraction efficiency of 60% was determined at pH 7. With increasing pH, the extraction yield decreased continuously. Close to the optimal pH for metaraminol extraction ($IEP_{metaraminol}$ = 9.55), the extraction efficiency of (*R*)-3-OH-PAC is around 35%. These results thus show a reciprocal, pH dependent extraction behavior for metaraminol and (*R*)-3-OH-PAC, as expected from the previously determined pK_a values. In back extractions, a distribution of 3-OH-PAC between the organic and the acidic back extraction phase is obtained with a preference of 3-OH-PAC for the organic extraction phase.

Concluding, a pH around 9.6 facilitates maximal physical extraction efficiencies for metaraminol, while substantial co-extraction of the substrate is present. The alkaline range is therefore a requirement for metaraminol extraction and was subsequently tested for enzyme compatibility.

Determination of pH dependent enzyme activity of *Cv*2025

The initial activity of *Cv*2025 in the pH range from 6.7 to 9 was determined in an adapted photometric assay by measuring the acetophenone production at 300 nm [139]. The highest initial activity was determined at pH 8.5, whereas the initial activity was reduced substantially at pH 9 (Figure 28).

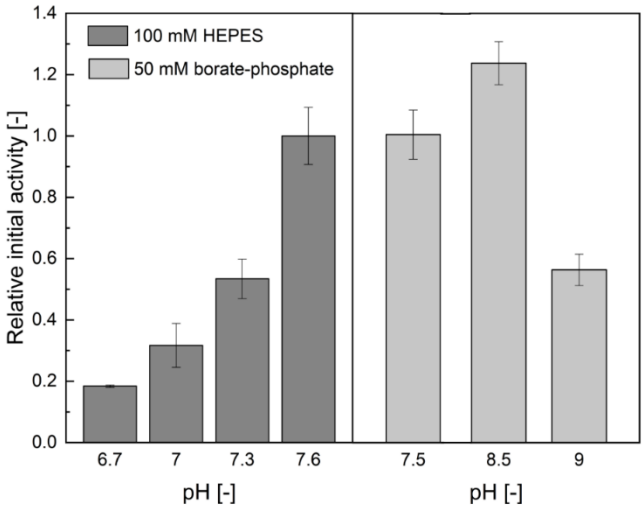

Figure 28 The pH dependent initial activity of purified *Cv*2025 in HEPES buffer or borate-phosphate buffer at pH 6.7 - 9.0. The error bars show the standard deviation of the mean of technical triplicates.

In contrast to initial rates, final conversions reflect the operational activity and stability of the enzyme under given reaction conditions. Therefore, final conversions in the transamination of (*R*)-3-OH-PAC to metaraminol with IPA at different pH values were performed, showing decreased conversions at pH 8.5 and pH 9.0 (Figure 29). The drop in performance at pH 9.0 corresponds with the reduced initial rates at pH 9 in Figure 28 and underlines that alkaline reaction conditions are suboptimal for *Cv*2025 activity. An optimal pH range for *Cv*2025 between pH 7.5 - 8.0 has been shown before in a different reaction system [85]. In these conversion experiments, it was frequently observed that a divergence between conversion and yield became apparent and that the overall mass balance was not closed. This was a common problem at alkaline pH ranges in this reaction system and is discussed more thoroughly in section 3.2.3.3.

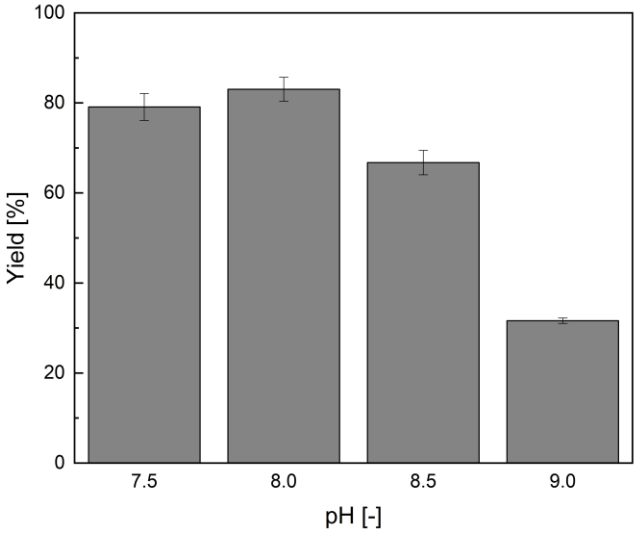

Figure 29 Transamination of (*R*)-3-OH-PAC to metaraminol using isopropylamine (IPA) as amine donor at different pH values as end-point detection after 24 h. Reaction conditions: 50 mM HEPES buffer pH 7.5 or pH 8; 50 mM borate buffer pH 8.5 or pH 9, 20 mM (*R*)-3-OH-PAC, 250 mM IPA, 1 mM PLP, 10 mg mL^{-1} lyophilized whole cells *Cv*2025, 1 mL, 30 °C, 700 rpm, 24 h. The error bars show the standard deviation of the mean of technical triplicates.

In combination with the previously shown pH dependent extraction behavior of metaraminol it becomes obvious that optimal pH conditions for product extraction (pH 9.6) do not completely match the optimal pH conditions for enzymatic product formation (pH ≤ 8.5). Nevertheless, as enzyme activity of *Cv*2025 was not completely abolished in the presented experiments, an operating pH between pH 8.5 and pH 9 was considered an acceptable compromise to realize *in situ* product extraction of metaraminol.

Summary of selected reaction conditions and setup

To summarize, a solvent screening revealed that solvents with high log *P* (1-decanol and 1-octanol) and thus minor cross solubility retain long-term enzyme activity. The high cross solubility is also favorable for extraction processes, as little solvent is lost. Extraction studies showed that 1-decanol efficiently extracts metaraminol in comparison to other non-polar non-protic solvents tested, indicating a general good correlation of enzyme compatibility and extraction behavior. However, an alkaline pH value preferably at the IEP of metaraminol was necessary to achieve a maximal extraction yield of metaraminol and likewise reduce substrate co-extraction. As enzyme activity was hampered in the alkaline pH range, a tradeoff between maximal enzymatic rates and extraction efficiency was necessary. The resulting reaction system is depicted in Figure 30.

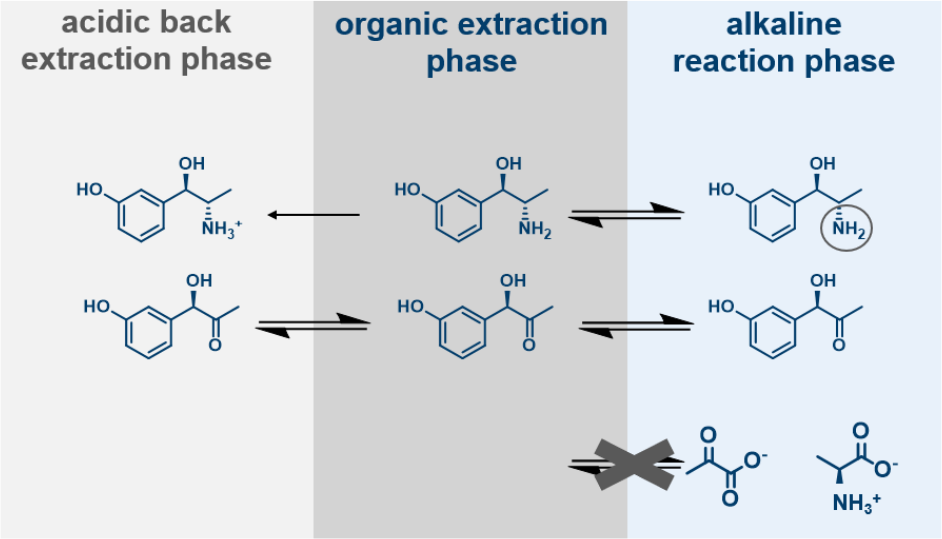

Figure 30 Schematic overview of the physical *in situ* extraction concept for metaraminol. In an alkaline aqueous reaction phase, metaramniol is produced enzymatically at pH 8.5 – 9.0 and remains largely in the neutral form. In that way, metaraminol is extracted into the organic extraction phase (1-decanol) and completely recovered *via* a pH-shift to an acidic back extraction phase (tartaric acid, pH < 3). The substrate (*R*)-3-OH-PAC is partly coextracted and distributes between the phases. The amine donor L-alanine and the co-product pyruvate are not extracted and remain in the aqueous reaction phase.

The conditions summarized in Figure 30 were chosen for ISPR experiments at 25 - 50 mL scale (40 - 50 mM substrate). Notably, a higher organic phase ratio was required for efficient extraction of metaraminol in the integration experiments (section 3.2.3.3) compared to the previously described enzyme compatibility screenings of activity and stability. As the maximal cross solubility of the organic solvent was reached in the herein described experiments and the remaining volume of organic solvent ensured the formation of a biphasic system with an aqueous-organic interface, no influence of the organic phase ratio on the enzyme activity was assumed.

3.2.3.3 Integration of *in situ* liquid-liquid product extraction for an equilibrium shift in the transamination reaction

Based on the results obtained from single characterization steps, the integration of all process parameters for the *in situ* extraction of metaraminol into the enzymatic transamination reaction was targeted to leverage the use of L-alanine as a bio-based amine donor. The experiments were performed with purified (*R*)-3-OH-PAC (refer to section 2.2.4.2 and Figure A2.1 in the appendix) and lyophilized whole cells as a less labor- and cost-intensive biocatalyst formulation compared to purified enzyme. To stabilize the pH in the required alkaline range for product extraction, borate and phosphate buffers were used. First, the transamination reaction was performed without ISPR at pH 7 and pH 9, providing two relevant operational pH values for comparison. For both pH

values, the yields were at 15% after 24 h. As no further conversion was observed for longer incubation times, the yield represented the maximal equilibrium yield (Figure 31). Performing the reaction in a biphasic system comprised of the reaction phase at pH 9 and an organic extraction phase (1-decanol, 2 : 1 aqueous to organic phase ratio), the yield after 24 h was increased to 24%.

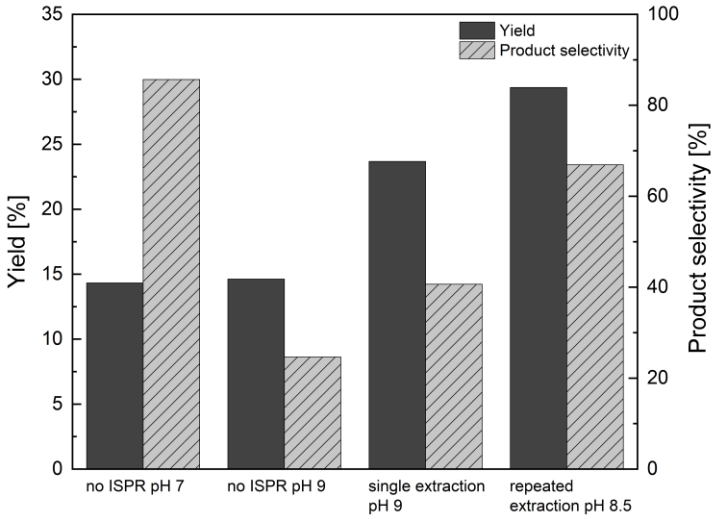

Figure 31 Yield and product selectivity of the enzymatic transamination reaction to metaraminol without ISPR and with integration of single and repeated *in situ* product extraction. For ISPR experiments, the final yield was calculated from the aqueous and organic phase after back extraction after 24 h. The data was previously published [125] and reprinted in an adapted format with permission from Green Chemistry.

This increase in product yield indicates that the reaction equilibrium was shifted slightly to the product side *via in situ* extraction of metaraminol into the organic phase. Here, the yield indicates the total amount of product per initial amount of substrate. Meanwhile, difficulties to completely close the mass balance of the process emerged, which is not reflected by the final yield of a process. Therefore, the product selectivity, referring to the ratio of product yield to substrate depletion was a measure to assess unspecific background reactions and thereby further characterize the process performance. At pH 7, a good product selectivity of above 85% was observed. An increase of pH to 9 without integration of the ISPR resulted in the same yield but with a reduced product selectivity of 25%. One explanation for this sharp drop in product selectivity may be the formation of imines, which is favored in either organic solvents [180] or in alkaline conditions [181]. For the single-stage ISPR extraction, an increase of selectivity from 25% to over 40% was observed. To further improve selective target product formation ("product selectivity", referring to the degree of undesired, spontaneous or enzymatic background reactions) and yield, additional modifications were made. To increase product selectivity, the operating pH was slightly adapted to pH 8.5. At the same time, as known from the previous extraction studies, this reduction of the operating pH causes a lower single-stage extraction efficiency of metaraminol (refer to Figure 27). Therefore, repeated extraction steps into an acidic phase were performed after 4, 6 and 24 hours of the

experiment to provide an overall higher extraction efficiency. After three repeated extraction steps, the product yield was increased to 29%, which corresponds to a doubled equilibrium yield compared to the reaction without ISPR. Furthermore, the repeated batch operation at pH 8.5 allowed for a significant increase in the product selectivity (68%). These results suggest, that by repeated *in situ* product extraction steps both, the yield and product selectivity towards metaraminol, can be increased.

A reduction in product selectivity can arise from instability of the substrate or the product because of spontaneous chemical background reactivity. As an alkaline pH was shown to promote imine formation of an amine and a keto group [181], in principle several undesired background reactions between substrates or products of the reaction system are possible. In fact, incubation of 3-OH-PAC at pH 9.5 resulted in considerable reduction of the HPLC peak area by 60% after 48 h (data not shown). The formation of 3-hydroxybenzoate as degradation product was confirmed in GC-ToF-MS measurements (Figure A2.4 in the appendix). Another possibility was elucidated by incubation experiments of commercial metaraminol bitartrate with equimolar amounts of pyruvate at pH 6.5 - 11 (Figure 32). Upon incubation at alkaline pH values, the initial concentration of metaraminol was reduced drastically. The highest reduction was observed at pH equal to the pK_{a1} of metaraminol, suggesting reactivity of the neutral species with pyruvate. Notably, the observed reactivity was time-dependent, further lowering the final concentration of metaraminol after longer incubation times. While imine formation of metaraminol and pyruvate is likely, no complete structural elucidation by instrumental analytics was pursued. In the ISPR experiments, part of the product was spatially separated from pyruvate by extraction from the aqueous reaction phase to the organic extraction phase. Likewise, the co-extraction of (*R*)-3-OH-PAC separated some of the substrate from L-alanine, which is only present in the aqueous reaction phase, thus reducing another source of undesired imines. The organic extraction phase thus partially prevented the reactivity of product and co-product, explaining the improved product selectivity by integration of ISPR.

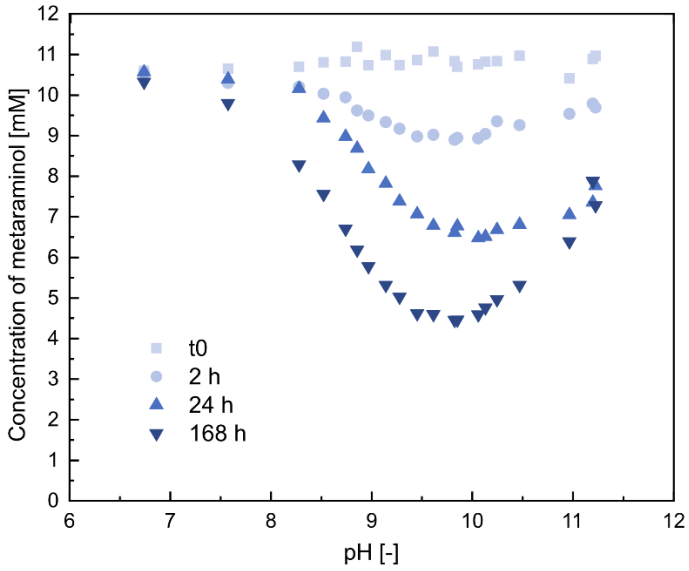

Figure 32 Incubation of metaraminol at different pH values in the presence of equimolar amounts of pyruvate. This figure was originally designed by Moritz Doeker and adapted for this thesis.

Concluding, the integration of extraction-based ISPR served three main purposes in this application. First, the reaction equilibrium was shifted towards the product side and the overall yield was increased. Second, product recovery was implemented, either initiating complete downstream processing of the product or providing metaraminol in an acidic aqueous phase for further chemoenzymatic modifications. Finally, applying a biphasic reaction system enabled *in situ* substrate supply *via* the organic phase, which can be especially beneficial for substrates with low solubility in aqueous reaction phases and which is prone to undesired background reactivity with a co-substrate as shown in this reaction system [182, 183]. Finally, while the repeated extraction mode facilitated further increase of the product yield, distinct optimization potential of the presented ISPR strategy is evident. In literature, several ISPR applications were presented in which a continuous regime was in favor of the overall process performance. While this requires more elaborate technical setups, *e.g.* by incorporation of membrane modules or additional cell retention, these examples suggest that a continuous extraction and back extraction process within metaraminol production could potentially further increase the yield [184-186]. This is mainly achieved by supplying sufficient organic phase to compensate low single-stage extraction efficiencies. However, the comparably high co-extraction of the substrate (as shown in section 3.2.3.2) could be reinforced by continuous extraction, ultimately causing substantially longer conversion times. In addition, the reduced activity of *Cv*2025 at alkaline pH values necessary for metaraminol extraction can further add to high resident times in continuous mode. Both aspects contribute to prolonged process times, which in turn promote background reactivity of the product. This lowers the overall product concentration and entailing mass balance issues to the disfavor of the overall process performance. Altogether, these aspects might limit the

applicability of a continuous extraction regime. A final evaluation of its applicability would only be possible with experimental data, which were not within the scope of this work as another ISPR strategy was preferentially chosen (see chapter 3.3). Nevertheless, the general concept is expected to be transferable to the biocatalytic synthesis of a range of amino alcohols and chiral amines, especially for reaction system with L-alanine as amine donor as neither L-alanine nor the co-product pyruvate are extractable and thus do not contaminate the extraction and back extraction phases. Further, it is likely that the degree of background reactivity and extraction efficiency are highly dependent on the reaction system. Consequently, the operational conditions such as the applicable pH range and the optimal solvent must be determined for each biocatalyst and target transformation individually.

3.2.4 Conclusion

In this chapter, *in situ* product extraction was investigated as a measure to shift the reaction equilibrium of the transamination to metaraminol using the bio-based amine donor L-alanine. A confined operational pH window for enzymatic metaraminol synthesis and simultaneous physical extraction was found, discovering an alkaline operating pH to be necessary for product extraction and identifying 1-decanol and 1-octanol as two suitable extraction solvents. For product recovery, back extraction with an acidic aqueous phase was implemented. By repeated *in situ* extraction steps, both, the yield and product selectivity of the transamination reaction, were increased. The main bottlenecks of this strategy are a limited extraction efficiency for metaraminol and the reduction of the final product concentration by chemical background reactions at alkaline pH values. These disadvantages are most likely system dependent and could differ for another reaction system. Altogether, these aspects limit the applicability of physical product extraction as ISPR strategy for metaraminol synthesis with L-alanine as amine donor. Therefore, reactive *in situ* extraction was investigated as a second extraction-based ISPR strategy, which is presented in the subsequent chapter.

Chapter 3.3

Process intensification by *in situ* reactive product extraction

Partially published in:

[124] Doeker M, Grabowski L, Rother D, Jupke A. 2022. *In situ* reactive extraction with oleic acid for process intensification in amine transaminase catalyzed reactions. *Green Chemistry.*

DOI: 10.1039/d1gc03289e

[Reproduced (adapted) with permission from Green Chemistry. © The Royal Society of Chemistry]

Contributions:

Laura Grabowski conducted the enzyme production, identification of suitable process parameters and performed all ISPR-integrated transaminations experiments. Moritz Doeker designed the reactive extraction-based on other amines and performed the metaraminol extraction experiments (without enzyme). Laura Grabowski and Moritz Doeker equally contributed to writing the original published article, which is integrated in this chapter. Moritz Doeker is the original author of sections 3.1 and 3.3, which have been adapted to include in this thesis. Sections 3.2 and 3.4 were originally written by Laura Grabowski and included in this chapter either in full or in compendious form. Laura Grabowski is the original author of this chapter, which was reviewed by Dörte Rother.

3.3 Process intensification by *in situ* reactive product extraction

3.3.1 Abstract

Liquid-liquid reactive product extraction was investigated as a second ISPR strategy to shift the reaction equilibrium within the transamination reaction towards metaraminol. The strategy makes use of renewable oleic acid as extractant, enabling *in situ* product extraction of metaraminol at neutral pH. An applicable operational window was defined focusing on the oleic acid concentrations and pH range. Pure substance extraction studies showed extraction efficiencies > 90% (without enzyme) for metaraminol with 0.1 - 0.5 M oleic acid in 1-octanol. The suitable oleic acid concentrations for high enzyme activity and stability of *Cv*2025 were 0.1 M or 0.25 M oleic acid in 1-octanol. By integrating reactive product extraction in a 50 mL biphasic pH stat system, single extraction steps facilitated the desired equilibrium shift by substantially increasing final product yields. Repeated extraction further increased the total product yield to 69% after three consecutive extraction and back extraction steps. As alternative process modes, a two-step one-pot regime and a semi-continuous extraction-back extraction regime were established. The presented concepts achieved continuous concentration of metaraminol in the back extraction phase over 72 h, but no further increase in conversion compared to the repeated extraction strategy. Finally, the ISPR strategy was transferred to an alternative substrate system ((*S*)-3-OH-PAC and *Bm*TA as biocatalyst) to produce the complementary product isomer (1*S*,2*S*)-3-AHP. Similarly, the product yield was increased to 56% by repeated extraction steps, demonstrating the general transferability of the ISPR strategy for shifting the reaction equilibrium.

3.3.2 Introduction

In transamination reactions with unfavorable reaction equilibrium, *in situ* product removal (ISPR) can enhance conversions by removing the product from the reaction phase during the production when a high excess of amine donor or removal of the co-product is not suitable to shift the reaction equilibrium. As shown in chapter 3.1 and 3.2, the transamination reaction towards metaraminol with L-alanine as amine donor is thermodynamically limited causing a conversion in equilibrium of 15 - 20% under the applied reaction conditions. For that reason, physical *in situ* product extraction was investigated as a strategy to circumvent the unfavorable reaction equilibrium. A central drawback of the physical extraction approach described in chapter 3.2 was the alkaline reaction conditions required for the physical extraction of metaraminol in its neutral dissociation state. However, the pH range between pH 9 and 10 was not ideal for the biotransformation as it reduced the activity of the amine transaminase *Cv*2025 and caused unwanted side reactions,

lowering the final product concentration substantially. To overcome these constraints, an alternative ISPR strategy was necessary. In the neutral and physiologically most relevant pH range for best activity of most enzymes, amine compounds are protonated and thereby show very little affinity to an organic extraction phase (refer to section 3.2.3.1). As a result, downstream processing from mostly aqueous streams must be designed carefully as the initial recovery step is difficult. In that case, reactive extraction can be an efficient method. Reactive extraction involves the reversible reaction between the target molecule and reactant that is added to the organic solvent, or the prior (reversible) chemical modification of the target compound to another species, that exhibits higher distribution behavior toward the organic solvent phase [187, 188]. For reactive extraction as it is considered here, an additional reactant present in the organic extraction phase forms an ionic complex with the target product, allowing for selective product removal from the aqueous reaction phase into the organic extraction phase. In biotechnological processes, the applicability of reactive extraction has been shown as a recovery method of organic acids produced by fermentation [166, 189, 190]. In biocatalytic amine synthesis, few examples of reactive product extraction have been shown. For example, crown ethers were used as reactant for the chiral separation of amines and amino alcohol. This approach entailed the added benefit of enhancing the overall enantioselectivity by using a stereoselective reactant [191, 192]. However, this example is restricted to downstream operations and is not applicable for ISPR due to inhibitory effects of the reactant on cells or enzymes [193]. For *in situ* product extraction targeting an equilibrium shift, the extraction system is not independent of the enzymatic reaction system, requiring both, biocompatibility of the diluent and reactant and extractability of the target compound [174]. More biocompatible reactants for *in situ* recovery of cationic amines were phosphoric acids, 4-nonylphenol or fatty acids [194-196]. In the herein described approach, oleic acid ((9*Z*)-octadec-9-enoic acid, 18:1 *cis*-9) was used as reactant. The feasibility of the reactive extraction with oleic acid was previously demonstrated for the recovery of model amines from aqueous streams [141] and was recently shown as a biocompatible reactant mitigating product inhibition in fermentative production of 2-phenylethanol by yeast [197].

In this chapter, suitable parameters for maximal extraction efficiencies and enzyme compatibility are elucidated for the combined *in situ* reactive extraction and enzymatic metaraminol synthesis. In the previous chapter 3.2, section 3.2.3.1, the characterization of dissociation states of the reaction components and the determination of suitable extraction solvents were shown. Further required information for reactive *in situ* extraction of metaraminol were the applicable pH and the oleic acid concentration in the organic phase. Eventually, the determined reaction conditions are transferred to the transamination of (*S*)-3-OH-PAC using the amine transaminase *Bm*TA, thereby

assessing the transferability of the operational window to an alternative combination of enzyme and stereoisomer.

3.3.3 Results & Discussion

3.3.3.1 Designing a liquid-liquid reactive extraction concept

The herein presented reactive extraction strategy makes use of an organic phase containing a reactant (reactive extractant). As shown in chapter 3.2, the compatibility screening of different organic solvents with the amine transaminase suggested 1-octanol and 1-decanol as suitable solvents. In this approach, 1-octanol was used as diluent because it can be derived microbially and is ranked with a high health and safety score according to a general guide for biphasic biocatalytic reactions [198]. Additionally, 1-octanol offered improved phase separation compared to 1-decanol (personal communication with Moritz Doeker, Chair of Fluid Process Engineering, RWTH Aachen University). The extractant oleic acid can be obtained from bio-based waste streams as sustainable alternative to common crude-oil based solvents and extractants [199]. Based on previous investigations, the reactive extraction concept for metaraminol was designed using oleic acid as a cation exchanger [196]. Assuming only cationic metaraminol at the investigated neutral pH range and a negotiable decrease in the free oleic acid due to a high molar excess, the following equation describes the equilibrium distribution and equilibrium extraction constant K_{ex}. In this equation, MH^+_{aq} is the metaraminol cation, H^+ the hydrogen ion in the aqueous phase, MHR_{org} is the formed complex in the organic phase and HR_{org} is the free oleic acid concentration:

$$MH^+_{aq} + HR_{org} \leftrightarrow MHR_{org} + H^+$$

The oleic acid concentration and the pH must be determined experimentally to define an operational window for enzymatic synthesis and *in situ* reactive extraction of metaraminol. A schematic overview of the envisaged reactive extraction system and product recovery by back extraction is depicted in Figure 33.

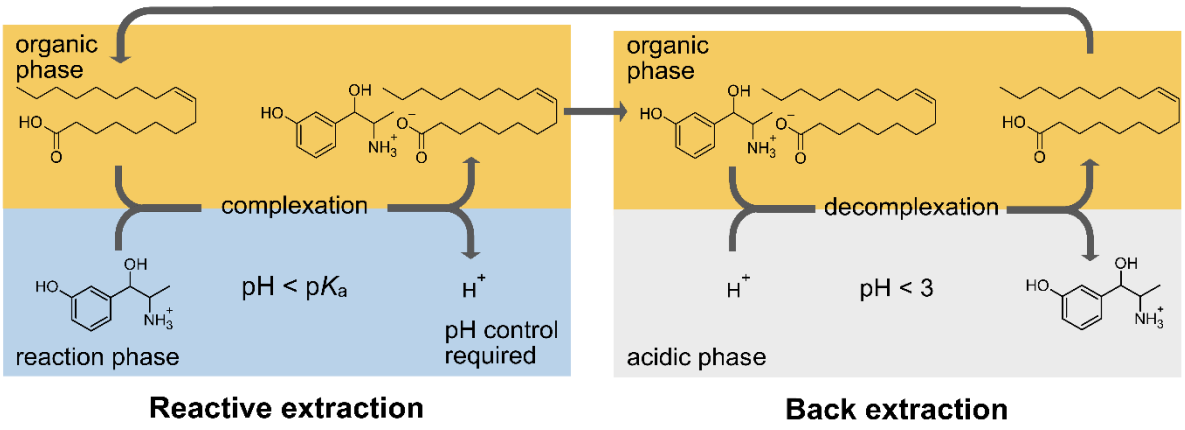

Figure 33 Process concept of *in situ* reactive extraction of metaraminol and product recovery by back extraction. Complexation and decomplexation are pH-driven. Upon dissociation of oleic acid, the formation of metaraminol oleate facilitates the distribution of metaraminol from the aqueous reaction phase to the organic extraction phase (1-octanol), requiring pH control. This figure was previously published and is reprinted in an adapted format with permission from Green Chemistry [124].

3.3.3.2 Defining an operational window for *in situ* reactive product extraction and enzyme catalysis

Liquid-liquid reactive extraction in pure substance systems without enzyme

To define an operational window for *in situ* reactive extraction of metaraminol, the reactive extraction behavior from an aqueous phase to an organic phase (1-octanol containing oleic acid) was first characterized for pure substance systems without addition of further side components nor enzyme. The pH dependent reactive extraction efficiency at different oleic acid concentrations is shown in Figure 34. As shown in chapter 3.2, physical extraction of metaraminol with pure 1-octanol as the extraction phase is only feasible at high pH values, with a maximum extraction efficiency at the isoelectric point of metaraminol (pH 9.55). The addition of oleic acid to the organic phase facilitates a complexation of the cationic metaraminol species in the organic phase, enabling superior extraction efficiencies compared to the physical extraction system and at a lower pH in the range of pH 5 to 8. No precipitation of solids was observed in the experiments, suggesting that the formed complex is stabilized in the organic phase. The results further illustrate that the reactive extraction is strongly dependent on the equilibrium pH of the aqueous phase. As metaraminol is mostly present as cationic species at neutral pH, this pH dependence cannot be explained by changes of the dissociation states. Therefore, the pH dependent extraction must be due to the oleic acid present in the system. Here, the oleic acid acts as liquid cation exchanger, which will exchange the initially bound proton with metaraminol forming ion pairs of metaraminol-oleate. In general, the exchange is commonly governed by the different concentrations of the involved species, which includes H^+ ions. As the H^+ ion concentration is linked to the pH *via* the activity coefficients, a change in pH significantly influences the ion

exchange and thus the reactive extraction efficiency. A second parameter influencing the liquid cation exchange is the concentration of oleic acid. With increased oleic acid concentrations higher extraction efficiencies are attainable. As the tested oleic acid concentrations between 0.1 M to 0.5 M facilitated very efficient extractions in the neutral pH range, these concentrations were chosen for further investigations in the following chapters.

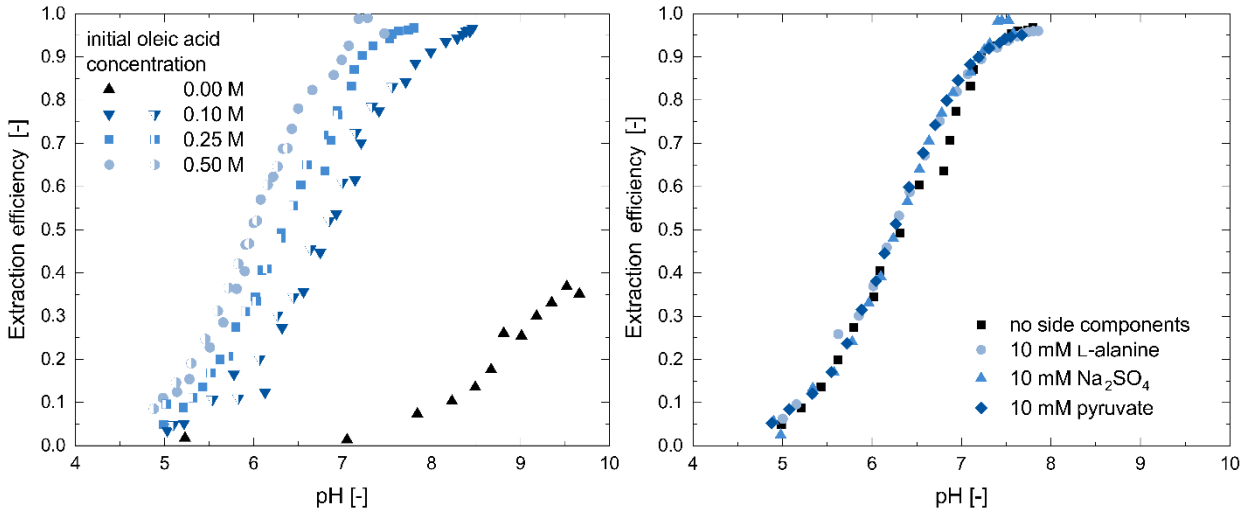

Figure 34 Left: Determination of the mole-related extraction efficiency for metaraminol at different pH values in equilibrium using different oleic acid concentrations in 1-octanol. The aqueous phase was prepared with commercial metaraminol bitartrate. Two independent reactive extraction experiments are shown for each reactant concentration. Right: The influence of L-alanine, Na_2SO_4 and pyruvate on the pH dependent extraction efficiency was investigated with 0.25 M oleic acid in 1-octanol as the organic extraction phase. The figures were originally designed by Moritz Doeker. The data was previously published [124] and was reprinted in an adapted form.

In the envisaged ISPR integrated transamination system, not only the product is present in the aqueous phase but also additional reaction components. Therefore, for an efficient integration, any putative influence of pyruvate (co-product), L-alanine (amine donor) and Na_2SO_4 (reflecting buffer salts) on the reactive extraction efficiency of metaraminol was tested in reactive extraction studies using 0.25 M oleic acid in 1-octanol as the organic extraction phase. The investigated components did not influence the reactive extraction of metaraminol and no further cationic side components are expected (Figure 34, right). However, the physical co-extraction of the substrate (*R*)-3-OH-PAC by 1-octanol (refer to Figure 27, section 3.2.3.2) remains existent. It can be concluded that the liquid cation exchange is highly selective for metaraminol at the investigated pH.

Identification of enzyme compatible process parameters for *Cv*2025

The extraction studies in the previous section revealed the pH of the aqueous phase and the oleic acid concentration in the organic phase as the two key process parameters for efficient reactive extraction of metaraminol. From the fundamental characterization studies in chapter 3.2, the enzymatically compatible pH was assessed by conversion and initial rate experiments, portraying pH 7.5 - 8.5 as a suitable pH range for *Cv*2025. As pH 7.6 facilitated high enzyme activity while keeping the reaction pH far below the first pK_a of metaraminol, it was used for the following experiments. In the next step, different oleic acid concentrations in the organic phase (1-octanol) were tested to completely define the operational window for reactive ISPR. To assess any influence of the reactant on the biocatalyst, the activity of *Cv*2025 in the presence of an organic overlay with oleic acid concentration between 0.1 M and 0.5 M was tested in the target reaction with isopropylamine (IPA) as amine donor. Using IPA in this reaction setup allowed for higher conversions than with L-alanine, resulting in better evaluation of any effects of the oleic acid on the enzyme (Figure 35). The results show that upon the increase of oleic acid concentrations to 0.25 M and 0.5 M, the conversion decreased slightly, suggesting that an upper optimal concentration of the reactant was found. In general, the influence of the oleic acid in 1-octanol was small. The addition of pure oleic acid, however, caused immediate inactivation of the biocatalyst (data not shown).

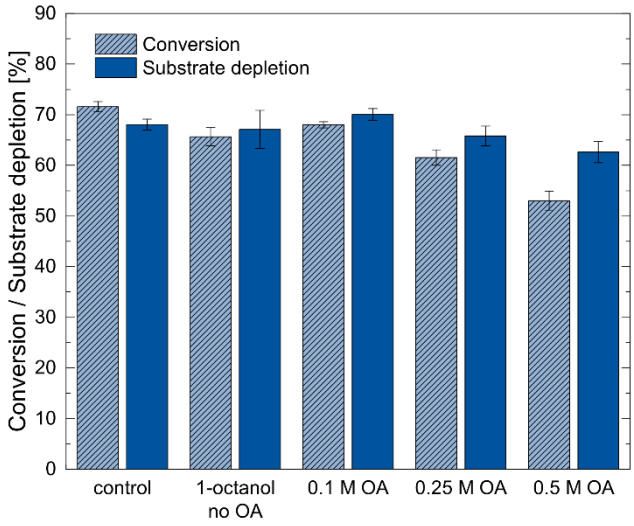

Figure 35 Determined mole-related conversion and substrate depletion in the transamination of (*R*)-3-OH-PAC to metaraminol in the presence of 10% (v/v) 1-octanol containing different oleic acid (OA) concentrations after 24 h. IPA was used as amine donor for screening purposes to facilitate high conversions (20 mM (*R*)-3-OH-PAC, 100 mM IPA, 100 mM HEPES buffer pH 7.6, 0.2 mM PLP, 10 mg mL^{-1} lyophilized whole cells (*Cv*2025). Error bars show standard deviation of technical triplicates. This figure was previously published [124] and is reprinted with permission from Green Chemistry.

To verify this influence of oleic acid on the enzyme activity, storage stability assays in the presence of oleic acid were performed. As shown in the previous chapter, *Cv*2025 exhibited substantial storage stability in buffer pre-saturated with 1-octanol or 1-decanol (refer to chapter 3.2.3.2).

Complementary to these results, now the objective was to test for stability when an organic overlay with the respective reactant concentrations (0.1 M, 0.25 M, and 0.5 M oleic acid in 1-octanol) was added to buffered enzyme stock solutions, forming a biphasic system. These enzyme solutions were incubated in the dark in an overhead shaker at 20 °C for 7 days. The initial activity of the incubated enzyme solution was measured after 1, 2 and 7 days (Figure 36). Compared to the control reactions without organic solvent, the enzyme activity was lowered upon addition of the second phase to the enzyme stock even before storage, directly correlating with oleic acid concentrations in the organic phase. Upon storage under these conditions, the enzyme retained this initial activity for 7 days for 1-octanol and with 0.1 M and 0.25 M oleic acid. In contrast, the enzyme stocks without organic solvent or with 0.5 M oleic acid in 1-octanol were inactive after 7 days. These results suggest a partly stabilizing effect of the organic overlay on *Cv*2025, which was shown before upon pre-saturation with organic solvent (refer to Figure 36). Here, this effect can be attributed to the exclusion of oxygen by the organic overlay, which might prevent enzyme destabilization by oxidation at the liquid-gas interface. Interestingly, the enzyme inactivation for 0.5 M oleic acid was also visibly evident by the formation of extensive protein precipitation at the end of the experiment (Figure 37, far right). While the enzyme stock solution without addition of an organic overlay did not present such precipitation, a decolorization of the typical yellow color of PLP was visible after 7 days (Figure 37, far left). Protein precipitation by organic solvents is well-described in literature and used, for example, for removal of proteins from analytical samples [200].

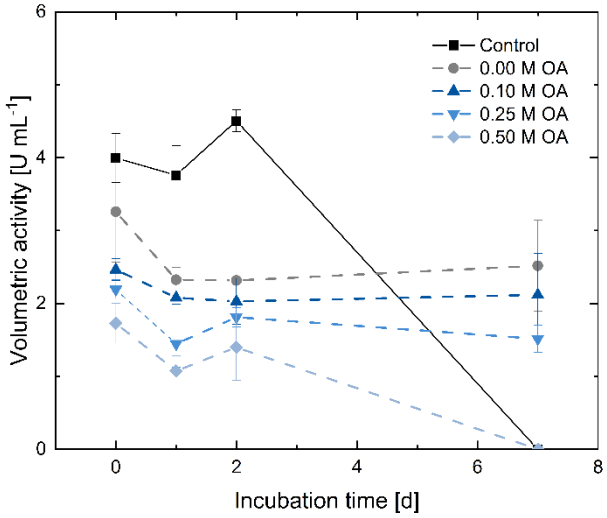

Figure 36 Storage stability of the amine transaminase *Cv*2025 in the presence of 10% (v/v) 1-octanol containing different oleic acid concentrations at pH 7.6. The control contains no organic solvent. The enzyme solutions were handled and incubated under exclusion of light. The initial activity was measured photometrically by the acetophenone production at 300 nm for 5 min. Reaction conditions: 100 mM HEPES, 0.1 mM PLP, 2.5 mM α-MBA, 5 mM pyruvate, 0.1 mg mL^{-1} *Cv*2025, 25 °C. Error bars show standard deviation of technical triplicates. This figure was previously published and is reprinted with permission from Green Chemistry [124].

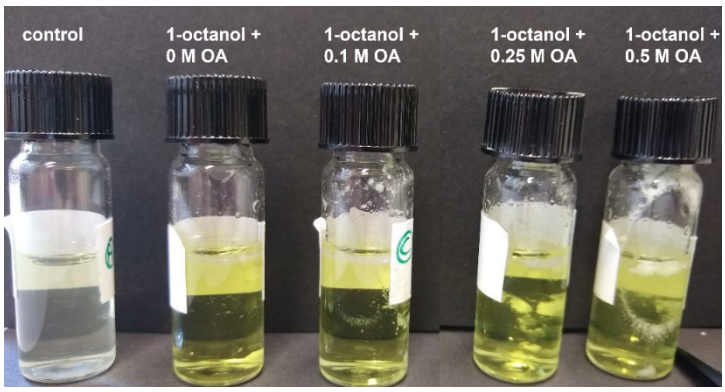

Figure 37 Picture of *Cv*2025 purified enzyme stocks solutions after incubation for 7 days without an organic overlay (control) and with 1-octanol containing 0.1 M, 0.25 M or 0.5 M oleic acid (OA), respectively.

Based on these results, 0.1 M and 0.25 M oleic acid in 1-octanol were selected as suitable reactant concentrations for *in situ* product removal in the final application.

3.3.3.3 Integration of *in situ* reactive product extraction for an equilibrium shift in the transamination reaction

Investigation of single-stage reactive extractions in the enzymatic production of metaraminol

To screen several parameters at once, the integration of *in situ* reactive product extraction within the enzymatic synthesis of metaraminol was first performed in a small-scale setup using 15 mL glass reaction vials. The results for the small-scale *in situ* reactive extraction experiments are shown in Figure 38, achieving 40% product yield with the initially selected reaction conditions (A). With half the L-alanine concentration (B), the product yield dropped to 33%, reflecting the direct link of amine donor concentration and reaction equilibrium. Another factor specifically for cost-contribution is the cofactor concentration. In this case, the reaction was tested with a fifth of the initial cofactor (pyridoxal-5'-phosphate, PLP) concentration (C), which slightly lowered the product yield to 38%. Accordingly, when increasing the substrate concentrations to 76 mM while keeping the relative molar excess of amine donor and the PLP concentration low, the product yield was drastically reduced (26%, condition D). The amine donor and oleic acid concentration was consequently increased, which facilitated 37% conversion for 80 mM (*R*)-3-OH-PAC (condition E). Resulting from this screening, 1 mM PLP and a 6.25-fold molar excess of amine donor were determined to be most favorable. This experiment was the first verification of the reactive ISPR design described in section 3.3.3.1. The product yields were increased successfully compared to previous reference reactions without the integration of ISPR (refer to Figure 31), indicating that *in situ* reactive product extraction achieves the desired equilibrium shift. The downside to this small-scale approach in a buffered system was that the buffer capacity seemed to be insufficient in this setup because manual pH adjustment with base was required twice after 3 h and 8 h reaction time. Therefore, the transamination reaction was conducted in a stirred-reactor setup to ensure

sufficient suspension of the biocatalyst and allow for automated pH control. To further characterize the effect of pH and oleic acid concentration, two varying conditions were tested in the ISPR integrated system (pH 7.3 or 7.6 and 0.1 M OA or 0.25 M OA, respectively, Figure 39).

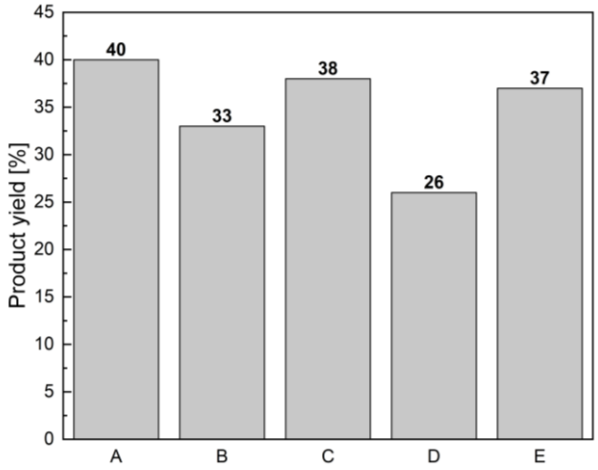

Figure 38 Small-scale *in situ* reactive product extraction of metaraminol under different reaction conditions. **A** 40 mM (*R*)-3-OH-PAC, 250 mM L-alanine, 1 mM PLP, 0.25 mM OA; **B** 40 mM (*R*)-3-OH-PAC, 120 mM L-alanine, 1 mM PLP, 0.25 mM OA; **C** 40 mM (*R*)-3-OH-PAC, 250 mM L-alanine, 0.2 mM PLP, 0.25 mM OA; **D** 76 mM (*R*)-3-OH-PAC, 230 mM L-alanine, 0.2 mM PLP, 0.25 mM OA; **E** 80 mM (*R*)-3-OH-PAC, 320 mM L-alanine, 0.2 mM PLP, 0.35 M OA. All reactions contained 100 mM Kpi buffer pH 7.6, 10 mg mL^{-1} lyophilized whole cells (*Cv*2025), 12 mL reaction phase, 3 mL 1-octanol containing oleic acid (OA). The reaction vessels were mixed by horizontal rocking at 30 °C for 24 h.

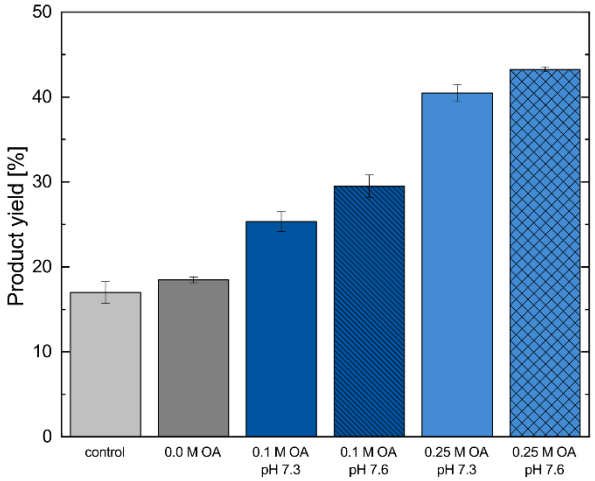

Figure 39 *In situ* product removal of metaraminol during the enzymatic transamination of (*R*)-3-OH-PAC using L-alanine as amine donor. The total mole-related product yield was calculated from the sum of metaraminol in the aqueous reaction and the organic extraction phase (after back extraction) after 48 h. Reaction conditions: 40 mM (*R*)-3-OH-PAC, 250 mM L-alanine, 1 mM PLP, 10 mg mL^{-1} lyophilized whole cells (*Cv*2025), 30 °C, 250 rpm, 40 mL reaction phase, 10 mL organic extraction phase, pH stat with 0.5 M NaOH. The control was without ISPR. The error bars show the variance between two independent experiments. This figure was previously published and is reprinted with permission from Green Chemistry [124].

The experimental results show that for the control without organic phase and the system with only 1-octanol, a reaction equilibrium of approximately 18% yield was achieved. A maximal conversion in equilibrium of 15 - 20% was already determined in prior investigations. No physical extraction occurred at the investigated pH with solely 1-octanol added. In contrast, the addition of oleic acid to the organic phase led to significantly higher product yields at both investigated pH values. Here, slightly higher product yields at pH 7.6 were observed when compared to the same oleic acid concentration at pH 7.3, which can be explained by the pH dependence of the reactive extraction. The addition of oleic acid to the organic phase allowed an increase in product yield of 10 - 15% for 0.1 M and 20 - 25% for 0.25 M oleic acid. This effect is due to the shift of the reaction equilibrium *via in situ* product removal, leading to higher overall product yields with an increase in oleic acid concentrations. Higher oleic acid concentrations also strongly influenced the maximal extraction equilibrium in pure substance extraction studies (section 3.3.3.1). Therefore, as a strategy to further increase product yield, the oleic acid concentration was increased to 0.5 M, yet without success (data not shown). Additionally, a larger organic phase volume was investigated. Likewise, no significant increase in product yields could be observed after 48 h. Due to the increased phase ratio, higher amounts of (*R*)-3-OH-PAC were probably co-extracted into the organic phase resulting in lower concentration of (*R*)-3-OH-PAC in the aqueous phase. Consequently, the conversion was slower and thereby counteracted the advantages of improved product extraction efficiency. The organic phase thus served as substrate reservoir with a constant re-feed if substrate is consumed in the aqueous reaction phase. In all conditions tested, an aqueous to organic phase ratio of 4 : 1 was most optimal to ensure sufficient aqueous substrate concentrations and higher enzymatic rates.

Implementing repeated reactive extraction steps with the enzymatic production of metaraminol

To overcome the observed maximal extraction equilibrium of the ISPR process described in the previous section, an alternative strategy was developed by implementing repeated extraction steps. The biotransformation thereby remained one batch, while the *in situ* product extraction was divided into three extractions. The organic phase was recovered by performing back extractions after 24 h, 48 h and 72 h hours with a tartaric acid aqueous phase at pH < 3. In this way, the extracted metaraminol is removed from the organic extraction phase, yielding a recovered organic phase, which was subsequently recycled in the following extraction step. During back extractions, the substrate (*R*)-3-OH-PAC remained largely in the organic phase and did not distribute significantly into the tartaric acid aqueous phase due to the low pH. Nevertheless, the volume of all three back extraction phase was kept low (10 mL) to minimize (*R*)-3-OH-PAC losses and to

concentrate the product. The results are shown in Figure 40, depicting both the product yield for the individual extraction steps and the total product yield comprising three repeated extractions and the remaining product in the aqueous reaction phase.

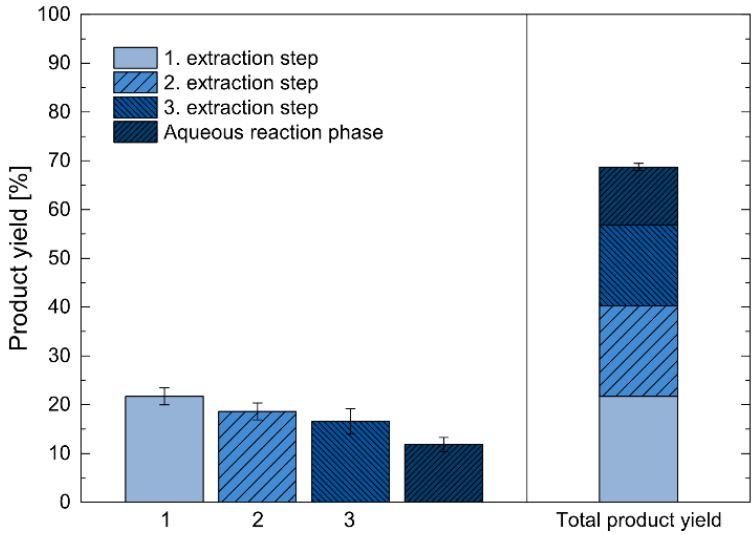

Figure 40 Mole-related product yield of *in situ* reactive extracted metaraminol during enzymatic transamination after three repeated ISPR extraction steps. The metaraminol amount in the back extraction phases for each of three repeated ISPR extraction steps (1-3) and the remaining product in the aqueous reaction phase (dark blue) are shown. Reaction conditions: 40 mM (*R*)-3-OH-PAC, 250 mM L-alanine, 1 mM PLP, 10 mg mL^{-1} lyophilized whole cells containing *Cv*2025, 30 °C, 250 rpm, 40 mL reaction phase, 10 mL organic extraction phase (1-octanol + 0.25 M oleic acid), pH stat (pH 7.6) with 0.5 M NaOH. The total product yield refers to the total amount of produced metaraminol from the initial amount of (*R*)-3-OH-PAC. Error bars show the variance of two independent experiments. The figure was previously published and is reprinted with permission from Green Chemistry [124].

The results show that in the first extraction step after 24 h, a product yield of 21% was achieved, referring only to the amount of extracted product in the first step. After back extraction of the organic phase, it was reused for two further extraction steps in the biphasic reaction system. Each time, the incubation was resumed for another 24 h. In the two following extraction steps, further product yields of 19% and 17% were obtained, respectively. The efficiency of the additional extraction steps decreased due to reduced substrate concentrations and enzymatic rates. As a result, the product formation and extraction in the second and third extraction step was slightly reduced, which was also observed by a lower titration of NaOH for pH control (Figure A2.6, appendix). After a total of three extraction steps, the total product yield of the enzymatic reaction reached 69%, corresponding to a 3.8-fold increase compared to the reaction without ISPR (refer to Figure 39). At the end of the process, the remaining aqueous concentration of metaraminol was 6 mM, corresponding to 12% product yield. Overall, 79% of the produced metaraminol was recovered in the acidic back extraction phase. During the experiments, no precipitation of solids was observed. This was also reflected by completely closed mass balances at the end of the processes (product selectivity > 90%).

3.3.3.4 Transfer of the ISPR strategy to further stereoisomers by alternative enzyme combination

To test the applicability of the developed reactive ISPR strategy to potentially other amino alcohols, the first step was the transfer to an alternative combination of enzyme and stereoisomer. For this purpose, an alternative set of ligase and amine transaminase was used to produce (1*S*,2*S*)-3-AHP. Specifically, the intermediate (*S*)-3-OH-PAC was produced by carboligation of 3-OH-BA and pyruvate using the pyruvate decarboxylase variant *Ap*PDC E469G. The intermediate was purified and subsequently aminated with L-alanine by the amine transaminase from *Bacillus megaterium* (*Bm*TA) (Figure 41). The amine transaminase is commonly characterized as (*S*)-selective and was shown to preferably convert (*S*)-enantiomeric substrates [91].

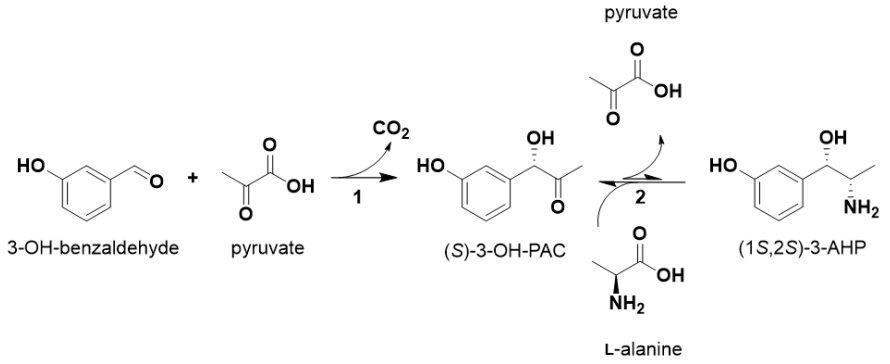

Figure 41 Reaction scheme of the enzymatic synthesis of (1*S*,2*S*)-3-AHP by combining an (*S*)-selective carboligase (*Ap*PDC E469G, 1) with the (*S*)-selective amine transaminase *Bm*TA (2) using L-alanine as amine donor.

The preparative-scale production of (*S*)-3-OH-PAC is shown in the appendix (Figure A2.1). This carboligation reaction was faster compared to the synthesis of (*R*)-3-OH-PAC and was routinely stopped upon complete aldehyde formation after 2.5 h for further product work-up (84% *ee*, 67% isolated yield, 92% HPLC purity). The *ee* after product work-up was further increased to > 98% by re-crystallization. The reaction conditions of the subsequent transamination reaction with *in situ* product removal were performed identically as described in the previous sections, assuming corresponding L-alanine acceptance and pH dependent activity of *Bm*TA. The tolerance of *Bm*TA to an organic overlay containing oleic acid was tested prior to the ISPR experiments to exclude potential enzyme inactivation by the reactant. The stability assay revealed substantial enzyme stability in the presence of an aqueous-organic interphase with 0.25 M oleic acid (Figure A2.5 in the appendix). The enzyme stock solution of *Bm*TA retained activity with and without an organic overlay (1-octanol + 0.25 M oleic acid) after 7 days, in contrast to the complete inactivation of *Cv*2025 with 0.5 M oleic acid and without an organic overlay (refer to Figure 36). While this might suggest a higher tolerance of *Bm*TA to oxidation, different handling and thereby different exposure to oxygen cannot be excluded. In addition, higher operational stability of tetramers (compared to

dimeric transaminases) was shown before, which is associated to the stabilizing effects of enhanced binding affinity to PLP [97, 201].

The integration of reactive product extraction with the transamination reaction was performed with 0.25 M oleic acid in 1-octanol. In reference reactions without ISPR, the yield after 24 h was 19%, which reflects the maximal equilibrium reached for metaraminol and *Cv*2025 (Figure 42). By repeated *in situ* reactive extraction steps, the yield was increased stepwise, reaching a total product yield of 56% after three extraction steps (72 h). In direct comparison with the metaraminol process, the absolute increase per extraction was notably reduced, as well as the maximal achievable yield (56% compared to 69% with 40 mM 2-hydroxy ketone). Furthermore, the isomeric content remained high in the aqueous phase and first back extraction phase (> 94%) but dropped to 84% in the third back extraction, showing only the (1*R*,2*S*)-stereoisomer as additional product. The reduced *ic* was due to racemization of the substrate, which was enhanced by L-alanine (Figure A2.8, appendix).

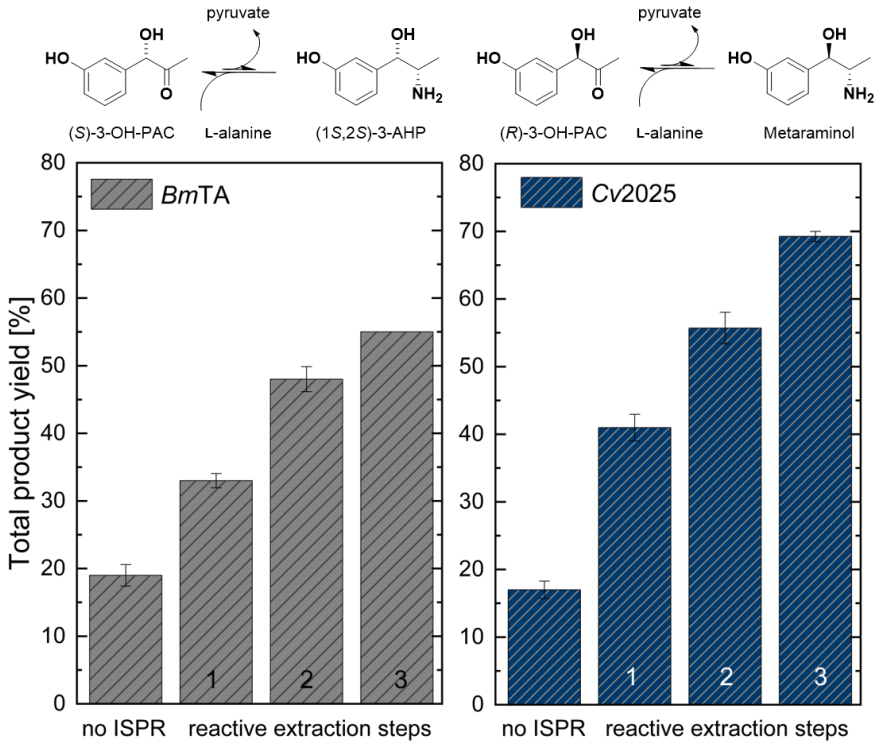

Figure 42 Total product yield after three repeated *in situ* reactive extraction of the product amino alcohol in transaminations with L-alanine. Reaction conditions: 40 mM 3-OH-PAC, 250 mM L-alanine, 1 mM PLP, 10 mg mL^{-1} lyophilized whole cells containing *Bm*TA or *Cv*2025, 30 °C, 250 rpm, 40 mL reaction phase, 10 mL organic extraction phase (1-octanol + 0.25 M oleic acid), pH stat (pH 7.6) with 0.5 M NaOH. The corresponding data for *Cv*2025 is taken from experiments shown in Figure 40 but visualized as total product yield after each reactive extraction step. The error bars show the variance of two independent experiments.

Any further adjustments of the reaction conditions, *e.g.* higher oleic acid concentrations or performing the back extraction with another acid isomer (D-(-)-tartaric acid) did not increase the yield per extraction step in the described process time, which can be explained by another

observation. Comparing the two ISPR-integrated reaction systems (Figure 42), another difference was observed in the formation of 3-hydroxybenzoate (3-OH-BZ) as a degradation product over the course of the reaction. Figure A2.9 in the appendix shows the accumulation of 3-OH-BZ for the reaction system with (*S*)-3-OH-PAC. Apparently, the substrate instability is more pronounced for the (*S*)-enantiomer. As a result, a reduced availability of the substrate limits the conversion towards the targeted amino alcohol in this reaction system. The degradation of 3-OH-PAC to 3-OH-BZ was verified before by GC-ToF-MS analysis. Possibly, the hydroxy ketone undergoes a spontaneous retro aldol reaction yielding the corresponding aldehyde, which subsequently oxidizes to the carboxylate. A similar retro-aldol mechanism was previously observed for other hydroxy ketones in the presence of L-alanine [45, 202]. In conclusion, the transfer of the ISPR concept to an alternative stereoisomer was achieved, demonstrating how the operational window was fitting for an alternative solute and transaminase. A system-specific degradation of the (*S*)-isomer of the substrate was identified as a central limitation resulting in a reduced overall product yield. As chirality does not affect the pK_a of a compound, the developed ISPR strategy is non-enantioselective, promoting a straight-forward transfer towards stereoisomers. The transferability of the ISPR strategy to further amino alcohols is discussed in detail in chapter 4.4.

3.3.3.5 Alternative reaction modes for ISPR-integrated transamination towards metaraminol with L-alanine as amine donor

To further improve the efficiency of the ISPR-integrated transamination to produce metaraminol, several adaptations of the reaction regime were tested. First, the established ISPR regime shown in section 3.3.3.3 was tested for the conversion of a higher substrate concentration (80 mM (*R*)-3-OH-PAC, Table 8). As small-scale ISPR experiments suggested that a higher L-alanine excess as well as higher oleic acid concentrations were favorable to retain the yield for higher substrate loadings, the experiment was conducted with 0.35 M oleic acid in 1-octanol and a 7-fold excess of L-alanine. After three repeated extraction steps, the product yield was comparable to the previous experiments (60%), implying a straightforward intensification with higher substrate concentrations in this setup.

As second variation, a two-step one-pot cascade reaction was performed in the EasyMax system (Figure 43). The carboligation of 3-OH-BA was achieved by pH stat titration of 1.5 M pyruvic acid (98%, 88.09 g mol^{-1}, 1.25 g mL^{-1}), titrating as much co-substrate as needed to avoid an excess of pyruvate in the reaction mixture, which would hamper the subsequent transamination equilibrium. The carboligation reached 99% conversion, providing 54 mM (*R*)-3-OH-PAC (99% *ee*) in the aqueous reaction mixture. Upon cell removal and addition of the organic extraction phase, the transamination of (*R*)-3-OH-PAC with L-alanine was performed with three repeated

extraction steps and one back extraction phase (instead of three separate back extraction phases as shown in section 3.3.3.3). The organic extraction was phase recycled. At the end of the cascade process, the obtained product yield was 61% with 94 mM (15.7 g L^{-1}) final metaraminol concentration in the back extraction phase (59% total conversion across both synthesis steps). Using a single back extraction phase (BE), metaraminol was concentrated to almost 100 mM final concentration. A high product concentration is particularly important for the feasibility of downstream processing, for example by subsequent crystallization of the product salt (metaraminol bitartrate). During the process, the formation of (*S*)-3-OH-PAC from racemization of the substrate was observed (Figures A2.7 and A2.8 in the appendix), which results in a reduced overall stereoselectivity, as previously described for the alternative substrate-enzyme combination in section 3.3.3.4.

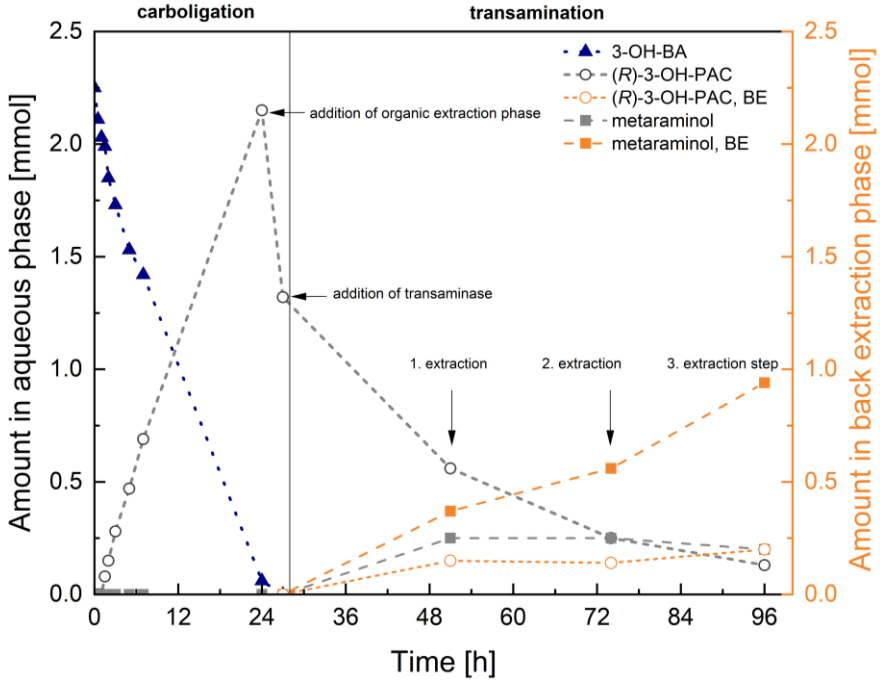

Figure 43 Two-step one-pot cascade towards metaraminol with integrated reactive ISPR. The carboligation was performed in a pH stat regime by titration of 1.5 M pyruvic acid. After 24 h, the cells were removed and organic extraction phase (10 mL 1-octanol + 0.25 M oleic acid) was added and equilibrated (to monitor the distribution of (*R*)-3-OH-PAC). Upon addition of whole cells containing *Cv*2025, the transamination was performed in a pH stat regime by titrating 0.5 M NaOH to counteract the acidifcation caused by reactive product extraction. Each extraction step was incubated for 24 h before the back extraction was performed (10 mL 100 mM L-(+)-tartaric acid). Reaction conditions carboligation: 60 mM 3-OH-BA, 2.5 mM $MgSO_4$, 0.1 mM ThDP, 10 mg mL^{-1} lyophilized whole cells (*Ap*PDC var), 40 mL, pH 6, 25 °C, 24 h. Transamination: 375 mM L-alanine (6.25-fold molar excess to initial substrate concentration), 1 mM PLP, pH 7.6, 10 mg mL^{-1} lyophilized whole cells (*Cv*2025), pH 7.6, 30 °C, 250 rpm.

Since the repeated extraction steps increased the extraction efficiency in the *in situ* reactive extraction of metaraminol (section 3.3.3.3), further reaction modes were investigated to further increase the overall product yield or reduce the manual intervention required for repeated extractions and back extractions. The continuous back extraction was achieved by contacting the organic extraction phase and the acidic back extraction phase in a membrane contactor module

(schematic setup is shown in Figure 16, section 2.2.9). The time course shows the decrease of the aqueous substrate concentration and accumulation of the product in the back extraction phase (Figure 44). Despite initiating the pumps for the first hours of the experiment to verify the equilibration of the membrane module and a leakproof setup, the pumping was only started continuously after 19 h, thereby delaying the extend of co-extraction and back extraction of the substrate.

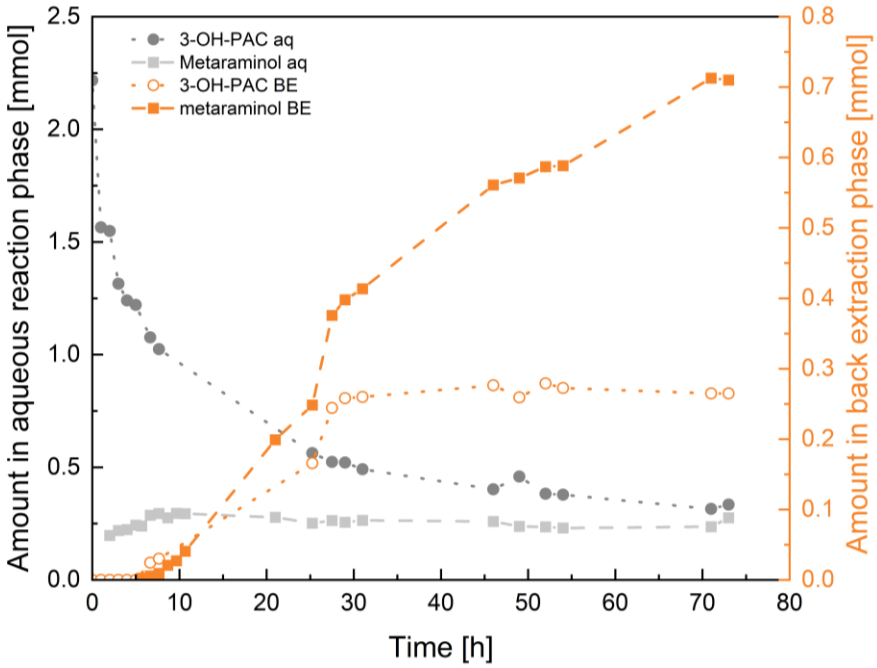

Figure 44 Time course of a semi-continuous reaction setup for reactive ISPR of metaraminol. The organic extraction phase and acidic back extraction phase (BE) where contacted in a membrane module. The pump was started after 4.5 h for 5 h, stopped over night and was thencontinuously run from 19 h on, except for during sampling. Reaction conditions: 60 mM (*R*)-3-OH-PAC, 6.25-fold molar excess L-alanine, 1 mM PLP, 40 mL aqueous phase (Kpi buffer pH 7.6), pH-stat with 0.5 M NaOH, 11.2 mL org (0.25 M OA in 1-octanol), 10 mg mL^{-1} LWC (*Cv*2025), stirred at 100 rpm, 30 °C, 72 h, 10 mL 100 mM L-(+)-tartaric acid for continuous back extraction of the organic phase *via* a membrane contactor (pumping rate was 0.6 mL min^{-1}). The final aqueous volume was 44.6 mL.

Between 30 h and the end of the experiment, the aqueous product concentration and the substrate concentration in the back extraction phase remained steady, while the product further accumulated in the back extraction phase. The final product yield, calculated over the total product in the reaction phase and back extraction phase was 58% (91% product selectivity). The *ic* value for the (1*R*,2*S*)-3-AHP in the back extraction of the process shown in Figure 44 was 82%, which was attributed to spontaneous racemization of (*R*)-3-OH-PAC during the reaction, as described previously. As only (1*S*,2*S*)-3-AHP was detected as additional product peak in chiral HPLC analysis, the stereoselectivity of the amine transaminase was unaltered under the applied conditions (refer to the appendix for further discussion). The overall performance was comparable to the two-step one-pot process, shown previously in Figure 43, regarding product yield and STY (Table 8 B, D). The product concentration in the back extraction phase was lower because a higher volume of tartaric acid had to be used to ensure a sufficient pumping volume.

During operation, slow phase separation behavior and the formation of an interphase between organic and aqueous phase were observed. This was traced back to cell debris and precipitated proteins and lipids, which accumulated at the organic-aqueous interface, potentially complicating large-scale applications of the presented process. To overcome this, a spatial separation of reaction and extraction and biocatalyst retention, *e.g., via* whole cell immobilization or enzyme gel carriers [203], could be used. Biocatalyst immobilization would thereby also expand the reusability of the biocatalyst and enhance the specific productivity. An overview of the described process regimes concerning yield, product concentration and productivity is shown in Table 8.

Table 8 Summary of process modifications for reactive *in situ* extraction of metaraminol using L-alanine as amine donor. 1, 3-OH-BA, 2, (*R*)-3-OH-PAC, 3, L-alanine, aq = aqueous phase, org = organic phase, OA = oleic acid, BE = back extraction phase (L-(+)-tartaric acid). All reactions were performed with 1 mM PLP, at pH 7.6 (pH stat with 0.5 M NaOH) and with 10 mg mL^{-1} LWC (*Cv*2025).

Process and experimental conditions	Yield [%]	Metaraminol in back extraction [g L^{-1}]	Productivity [g L^{-1} d^{-1}]
A Repeated extraction steps (Figure 40) 40 mM 2, 6.25-fold 3, 40 mL aq, 0.25 M OA in 10 mL org, 72 h, 3 x 10 mL BE (50 mM) for 3 extraction steps - after two extraction steps:	58	6.0	1.98
- after three extraction steps:	70	4.9	1.44
B Two-step one-pot cascade (Figure 42) 60 mM 1, 6.25-fold 3, 40 mL aq, 10 mL org (0.25 M OA in 1-octanol), 72 h, 1 x 10 mL BE (50 mM) for 3 extraction steps	61	15.7	1.64
C Higher substrate concentration (no figure) 80 mM 2, 6.25-fold 3, 40 mL aq, 10 mL org (0.35 M OA in 1-octanol), 72 h, 3 x 10 mL BE (100 mM) for 3 extraction steps	59	7.7	2.3
D Semi-continuous with membrane module (Figure 43) 60 mM 2, 6.25-fold 3, 40 mL aq (Kpi pH 7.6), 11.2 mL org (0.25 M OA in 1-octanol), 72 h, 1 x 10 mL BE (100 mM)	58	7.1	1.8
without ISPR (Figure 40) 40 mM 2, 6.25-fold 3, 40 mL aq, 24 h	14	-	0.9

Notably, the repeated extraction steps increased the total product yield while prolonging the overall process time, which is detrimental for STY and stereoselectivity (due to racemization of the substrate). In this chapter, the efficient equilibrium shift was targeted, which was quantified by the total product yield. If the optimization target focused on space time-yields, further alternative reaction regimes should be investigated. In this regard, continuous flow reactors in combination with efficient biocatalyst immobilization were previously shown to maximize space-time yields [204]. Although the total product yield was not further increased by the semi-continuous process shown here (Table 8, D), several aspects of the presented process can be highlighted. The organic

extraction phase can be recycled and reused at least three times, significantly reducing process waste streams and potentially adverse environmental impact of the process [52]. Furthermore, *Cv*2025 as lyophilized whole cell formulation remained active for up to 72 h, reflecting high operational stability under relevant process conditions additionally to the substantial storage stability in the presence of 1-octanol and oleic acid, which was shown in section 3.3.3.2. This good operational stability is a crucial factor when aiming for long-term application of the biocatalyst in multiple production cycles, which significantly reduces catalyst costs and ecological impact.

3.3.4 Conclusion

In conclusion, reactive extraction using oleic acid as reactant was shown to be a suitable strategy to improve enzymatic transaminations reactions with L-alanine and might contribute to the integration of more efficient and sustainable transaminase processes in future. In comparison to the physical extraction of metaraminol, the reactive extraction principle allowed for increased maximal extraction efficiencies in the neutral pH range, which was preferable for high amine transaminase activity and improved product selectivity, as no background reactions were observed. The reactive extraction strategy thereby facilitated a substantial increase in total product yield, which leverages the use of the bio-based amine donor. A clear advantage of this approach is the sustainable extraction system consisting of 1-octanol as the diluent, which can be produced microbially from renewable resources, and oleic acid as the reactant, which can be derived from (waste) plant oil. The possibility to recycle the extraction phase, as partly shown in the repeated extraction steps and semi-continuous reaction regime, further adds to a sustainable process concept. The main limitation in the presented process concerns the maximal loading of the oleic acid and the consequent reduction in free oleic acid in the organic extraction phase. The biphasic reaction system was hampered by poor phase separation with progressing process times, which is especially troublesome for (semi-)continuous processes.

Chapter 3.4

Enzyme immobilization as a tool in biocatalytic process intensification

Contributions:

For the results presented in chapter 3.4.3.1, Marianna Karava constructed the plasmids for the spore display and transformed *B. subtilis* KO7. Sarah Schmitz performed the cultivations and characterization experiments as part of her Bachelor thesis with supervision by Laura Grabowski [126]. For chapter 3.4.3.2, Anneke Strumpel performed the experiments as part of her Bachelor thesis, which was supervised by Laura Grabowski [205]. Laura Grabowski wrote this chapter, which was reviewed by Dörte Rother.

3.4 Enzyme immobilization as a tool in biocatalytic process intensification

3.4.1 Abstract

Immobilization offers potential benefits for biocatalyst stabilization and recycling, thereby reflecting a beneficial tool for biocatalytic process intensification. As the direct production, immobilization and purification of a biocatalyst offers the highest cost-benefit, strategies to combine these steps in as few process steps as possible are desired. In that regard, two different enzyme immobilization techniques were tested for their application in the two-step synthesis of chiral amino alcohols. The *in vivo* immobilization on the spore coat surface of *Bacillus subtilis* was used to produce immobilizates of *Ap*PDC var and *Bm*TA, revealing temperature-dependent production of the recombinant proteins on the spore surface. Due to low spore yield and activity, recycling of spore immobilizates was not efficient. In comparison, the affinity-based immobilization on porous glass bead carriers (EziG™, EnginZyme, Stockholm, Sweden) efficiently immobilized *Ap*PDC var and *Cv*2025 from crude cell extract, combining immobilization and purification in one step. The immobilization techniques were tested for biocatalyst activity and recyclability. The results suggested that the EziG™ technique was more favorable concerning activity and handling. In addition, it was found that the recycling efficiency of the immobilizates can largely be dependent on the tested reaction system.

3.4.2 Introduction

For an efficient biocatalytic process, the stability and reusability of the biocatalyst are of great importance to ensure high performance and cost-efficiency of the biocatalyst [206]. A simplified removal from the reaction mixture and subsequent recycling is only possible for heterogeneous catalysts. Hence, enzyme immobilization allows for alternative process modes and reactor types such as continuous flow applications or packed-bed reactors to improve a biocatalytic application in terms of space-time-yield and efficiency, especially for industrial applications [207]. In that way, biocatalyst immobilization can facilitate improved biocatalyst properties, as it was shown in industrial examples for the manufacturing of several specialty chemicals and APIs, specifically in the case of an engineered amine transaminase in sitagliptin synthesis [11, 206]. A facilitated downstream processing by catalyst removal or retention can be another advantage [208]. The different strategies to immobilize enzymes are commonly classified in three groups: the encapsulation or entrapment in permeable materials such as hydrogels [209], crosslinking *via* short molecular linkers to cross-linked enzyme aggregates (CLEAs) [210] or by binding to a carrier material [211]. The binding of the enzyme can be achieved by adsorption, ionic interactions, or

covalent binding [212]. One example for the covalent immobilization of various enzymes is *via* Halo-Tag, requiring Halo-Tag bead material and the respective modification of the enzyme [213, 214]. To conserve time and resources, the preparation of immobilized biocatalysts is ideally achieved in as little process steps as possible, for example by combining cultivation and immobilization (*in vivo* immobilization by spore display) or by achieving enzyme immobilization and purification in one step (*in vitro* carrier-based immobilization on EziG™). These two techniques are introduced in the following.

In contrast to immobilization on a specific carrier, (lyophilized) whole cell formulations can be regarded as the simplest "*in vivo*" immobilization, as the cell wall can act as natural entrapment and barrier, for example in organic solvents and in continuous flow processes [215, 216]. Similarly, *in situ* self-assembly to insoluble particles [212], also referred to as catalytic inclusion bodies (CatIBs), has been shown as an immobilization technique, which is directly integrated in the cultivation [217-219]. Recently, cross-linked *E. coli* spheroplasts were presented as an alternative *in vivo* immobilization technique of membranous enzymes like squalene-hopene cyclases [220]. Another *in vivo* immobilization technique is spore display, in which the target enzyme or protein is immobilized during sporulation and thereby exposed on the spore coat surface *via* an anchor protein, enabling the direct use of purified spores in biocatalytic transformations. This method was first shown for the display of a tetanus toxin fragment fused to the spore coat protein CotB by Isticato *et al.* in 2001 [221]. So far, various applications have been presented and the method was recently shown for the biocatalytic synthesis of hydrocarbons from lipids by immobilized photodecarboxylase [138]. Bartels *et al.* described CotY and CotZ as the most favorable anchor proteins [222]. In this recombinant approach, the target protein is fused *via* its N- or C-terminus to one spore-specific coat protein on molecular level, often connected by a linker to prevent steric hindrance of the target enzyme. The target enzyme, which is bound to the anchoring protein, is produced in the mother cell [223]. Subsequently, in the late sporulation phase, the target protein is bound to the mature spore surface with the help of the anchor protein and thus immobilized *in vivo* (Figure 45). To prevent contamination by germination, a knockout strain variant *B. subtilis* KO7 is used, which lacks the enzymes responsible for dissolving the spore membrane (Δ*cwlD* Δ*sleB*) [224]. *In vivo* immobilization on the surface of *B. subtilis* spores can provide an ecological, cost-effective, and robust immobilization technique without requiring addition materials [225]. At the same time, the spores as carriers are nontoxic, resistant to harsh conditions of industrial processes, and can be stored for long periods at room temperature [223].

The EziG™ immobilization technique makes use of porous silica beads (controlled-porosity glass, CPG) that are functionalized with Fe_3^+ ions, allowing for the selective immobilization of His-tagged proteins based on affinity adsorption. Additionally, three different surface modifications

are available, catering to different hydrophobicity requirements, depending on the target enzymes and reaction system. These are EziG™-Opal (silica surface, no polymer coating, hydrophilic), EziG™-Coral (Poly(vinylbenzylchloride) coating, hydrophobic) and EziG™-Amber (Co-polymer (polystyrene derivate) coating, semi-hydrophobic). The technique was first developed by Cassimjee *et al.* [226] and thus far applied for a variety of enzymes and applications [227, 228]. Specifically, EziG™-immobilized enzymes have been used in continuous flow applications, because the non-compressible, non-swelling and porous bead material exhibits advantageous fluid properties [229]. A schematic representation of the EziG™ immobilization and spore display is shown in Figure 45.

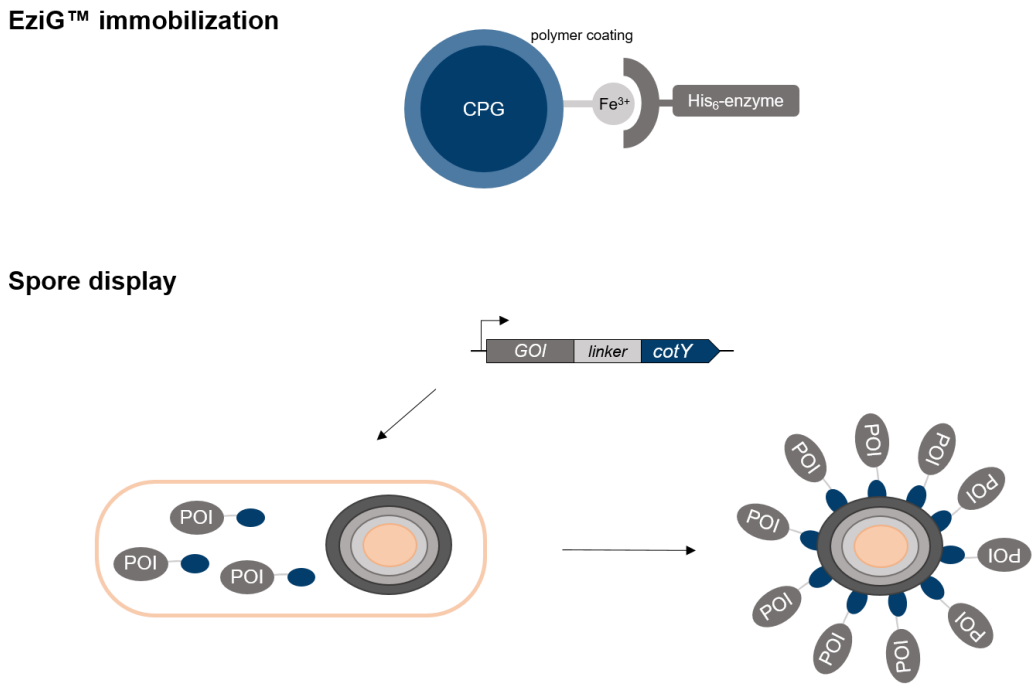

Figure 45 Schematic representation of EziG™ immobilization method and spore display on *B. subtilis* spores. Upper: The controlled-porosity glass (CPG) carrier beads have a polymer coating and Fe(III)-chelating derivatization to selectively bind His-tagged enzymes. Lower: The gene of interest (GOI) is genetically fused to a linker and the gene of the coat protein (CotY) downstream of a sporulation-inducible promoter PcotYZ (arrow). The protein of interest (POI) can be fused to the N-terminus (as depicted) or C-terminus of the coat protein. During sporulation, the fusion protein containing the protein of interest is displayed on the spore coat surface. The schematic representation of the spore display was originally designed by Marianna Karava [136], and was adapted with permission for the purpose of this thesis.

In chapter 3.3, it was shown that reactive ISPR in biphasic systems could benefit from efficient biocatalyst recycling and retention, especially in (semi-) continuous process regimes, prompting the investigation of simple (ideally one-step) enzyme immobilization. In this chapter, key results for two immobilization techniques, affinity adsorption on EziG carriers and *in vivo* spore display, are presented regarding biocatalyst activity and recyclability of a pyruvate decarboxylase variant (*Ap*PDC var) and two different amine transaminases (*Bm*TA or *Cv*2025). *Bm*TA was tested in the

spore display as reference data for alternative immobilization methods (EziG™-Opal, HaloTag) were available in literature. Finally, advantages and disadvantages of the respective immobilization techniques are discussed and conclusions concerning their applicability for process intensification are drawn.

3.4.3 Results & Discussion

3.4.3.1 *In vivo* spore display of *Ap*PDC var and *Bm*TA as novel immobilization technique

In collaboration with the computer-aided synthetic biology group from the Technical University Darmstadt (now located at the University of Trondheim) led by Prof. Dr. Johannes Kabisch, recombinant strains of *B. subtilis* KO7 for the spore display of *Ap*PDC var or *Bm*TA were constructed by Marianna Karava. The gene coding for the target enzymes were thereby integrated into a vector containing an origin of replication for *B. subtilis*, a kanamycin resistance, the sporulation-inducible promoter PcotYZ, and the gene sequence for the coat protein CotY (refer to the appendix, section A.3). During gene expression, the target enzyme is fused to the native anchor protein CotY and thereby bound to the spore coat surface in the late stages of sporulation [230].
To produce the spores, the *B. subtilis* KO7 strains were cultivated in 2xSG medium (Chapter 2.2, section 2.2.2.2). The growth behavior was determined by sampling and measuring the optical density at 600 nm (OD_{600}) at three different cultivation temperatures. The wildtype strain was cultivated for comparison. For all strains, growth was the slowest at 20 °C, requiring the longest cultivation time (52 h) with the highest final OD_{600}. Bs0242 (producing *Bm*TA as fusion protein) and Bs0243 (producing *Ap*PDC var as fusion protein) varied in optimal temperature and absolute growth rates. In addition to optical density measurements, the sporulation progress was monitored by microscopy (Figure 46). This allowed for monitoring the spore formation, which was also partly indicated by a drop in OD_{600} at the end of the cultivation, as the size and refractive index of spores changed compared to vegetative cells [231]. At the end of the cultivation, the spores were harvested, and vegetative cell debris was removed. After the spores were separated from the cell residues, the spores were used as biocatalyst in biotransformations, normalizing the number of spores by the final OD_{600} in the reaction because no absolute or relative protein determination was applicable for spore-displayed enzymes [136]. Notably, the obtained spore yield after purification did not correlate with growth behavior nor with the final OD_{600} in the cultivation. The key results considering growth, conversions, storage stability and recyclability are summarized in Table 9. The corresponding growth curves are shown in the appendix (Figure A2.10). Spores displaying *Bm*TA (from Bs0242) were tested in the transamination of (*S*)-3-OH-PAC with isopropylamine (IPA), reaching significantly higher conversion when produced at 20 °C compared to 30 °C. The production at 37 °C yielded less spores for the reaction (OD_{600} 34 instead of OD_{600} 50 could be

applied), therefore the immobilized enzyme was active, but the conversion is not directly comparable to the other two cultivation temperatures tested. With spores displaying *Ap*PDC var (from Bs0243 produced at 30 °C and 37 °C) comparable conversions in the carboligation of 3-hydroxybenzaldehyde (3-OH-BA) with pyruvate were observed. The storage stability compared to equally stored lyophilized whole cells (LWC) containing the respective enzyme was superior for spores displaying *Bm*TA than for *Ap*PDC var. Meanwhile, spore recycling was not applicable for neither of the tested enzymes as the conversion in the second reaction batch dropped substantially (Table 9).

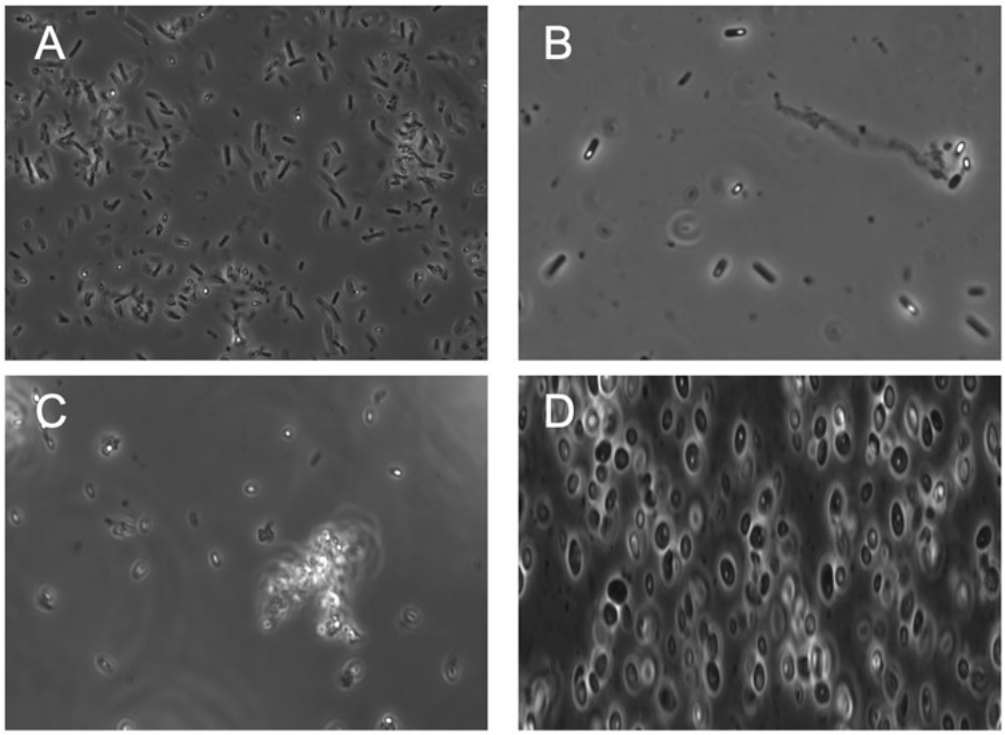

Figure 46 Microscopy images of recombinant *B. subtilis* KO7 in different cultivation stages. A – vegetative cells of a preculture, B – vegetative cells with forespores in main culture after 6 h, C – spores in main culture after 48 h, D – spores after purification. Pictures were taken in phase contrast microscopy (Eclipse Ti2, 1000x times magnification).

Table 9 Summary of results for the *in vivo* immobilization of *Bm*TA (Bs02042) and *Ap*PDC var (Bs02043) using purified spores from recombinant *B. subtilis* KO7 and wildtype strain without recombinant plasmid for spore display (Bs02003).

Strain	Growth rate[a] [h^{-1}]	Conversion[b] [%]	Residual activity after 7 days storage[c] [%]	Relative conversion in recycling step[d] [%]
Bs02003	n.d. (20 °C) 0.59 (30 °C) 0.87 (37 °C)	no activity	n.d.	n.d.
Bs02042	n.d. (20 °C) 0.72 (30 °C) 0.96 (37 °C)	86 ± 1 (20 °C) 53 ± 3 (30 °C) 31 ± 1 (37 °C)	> 99 (20 °C) LWC > 99	22 (20 °C)
Bs02043	n.d. (20 °C) 0.45 (30 °C) 0.81 (37 °C)	34 ± 1 (20 °C) 66 ± 4 (30 °C) 61 ± 3 (37 °C)	43 (30 °C) LWC > 99	18 (30 °C)

a Growth rates were derived *via* linear regressions of the natural logarithm of OD measurements at a wavelength of 600 nm in the first 3 h (37 °C) or 4 h (30 °C) of cultivation (growth curves and linear range in the appendix).
b Reaction conditions Bs02042 (*Bm*TA): OD_{600} 50 (30 °C, 20 °C) or OD_{600} 34 (37 °C) in 1 mL reaction volume, 10 mM (*S*)-3-OH-PAC, 50 mM IPA, 0.2 mM PLP, 100 mM HEPES pH 7.5, 30 °C, 1000 rpm, 24 h. Reaction conditions Bs02043 (*Ap*PDC var): OD_{600} 50 (37 °C, 30 °C) or OD_{600} 10 (20 °C) in 1 mL reaction volume, 10 mM 3-OH-BA, 50 mM pyruvate, 100 mM Kpi buffer pH 6.5, 1 mM ThDP, 2.5 mM $MgSO_4$, 25 °C, 1000 rpm, 24 h. Mean values and standard deviation from technical triplicates are shown.
c Residual activity reflect the relative conversion after 24 h after incubation of purified spores at 4 °C compared to the achieved conversion directly upon purification.
d Spore recycling for second reaction batch was achieved after centrifugation and washing steps as described in section 2.2.2.2

Several points of optimization can be emphasized for this system. One limitation of this system is that no absolute quantification of the amount of immobilized enzyme on the spore coat surface is possible. Protein detection and quantification methods such as Bradford assay, BCA or Western Blot were not suitable due to background staining of the spore coat, as verified by Marianna Karava [136]. Therefore, a direct comparison to the free enzyme in solution was not possible. Instead, the characterization of the spore display for different enzymes relied on activity determinations normalized by the spore amount in the assay. Thus, the cultivation optimization should aim for maximal spore production and activity. Here, a distinct influence of the cultivation temperature on the catalytic activity of the displayed enzymes was observed. It was previously shown that the temperature of growth and sporulation modulates the spore display efficiency [232]. The cultivation temperature predominantly affected the structure and function of *B. subtilis* spores, forming for instance more hydrophobic spores at lower temperatures [233]. The observed growth rates in complex medium were in the expected range for *B. subtilis* [234, 235]. However, no literature data for direct comparison of the knockout strain in sporulation media was available. In general, irregularities in the OD measurements and final spore yield after the purification were attributed to culture heterogeneities and extensive agglomeration of the spores, which was also visible in microscopy (Figure 46, C). Higher spore yields and a less hydrophobic spore surface can

be achieved by strain engineering [236]. For elucidating culture heterogeneity, a high-throughput flowcytometry-based method was developed by Marianna Karava, enabling the quantification and characterization of sporulation dynamics as well as the rapid separation of cells and spores [136]. In the performed biotransformations, only low substrate concentrations were applicable. First, despite extensive mixing and resuspension efforts, substantial agglomeration of the purified spores was observed, which likely influenced the mass transfer of catalyst and substrates. Second, the spore yield and activity were limited, requiring an entire cultivation and spore purification procedure for a triplicate reaction in 1 mL reaction volume. The preparative effort was therefore substantially more elaborate. In this context, a high storage stability for spores displaying *Bm*TA was observed, indicating that a large batch production could be prepared and stored for a longer time. The results further indicate that this method was not suitable for biocatalyst recycling as the conversions dropped drastically in the second reaction batch. The insufficient reusability could arise from spore losses during the centrifugation and washing steps or from inactivation over the course of the first reaction batch.

As such, *in vivo* immobilization by spore display represents a one-step production strategy for immobilized enzymes without dependence on the carrier material or chemical modifications such as cross-linking or the attachment to a solid support [212]. If the cultivation procedures can be optimized, the technique exhibits a high scalability compared to other immobilization methods. Nevertheless, other one-step immobilization strategies, in which the enzyme of interest is directly immobilized during production *in vivo* are already more established. For instance, catalytically active inclusion bodies (CatIBs) have been developed for various applications including flow chemistry [237-239]. The simplest form of *in vivo* immobilization is the formulation as (lyophilized) whole cells, which contains the enzyme of interest as heterogenous biocatalyst within the cell membrane. This formulation was shown in multi-phase flow applications [216, 240, 241] or in micro-aqueous reaction systems [242, 243]. In aqueous systems, however, proteins diffuse into the reaction solution, which impedes the reusability of the cells and causes emulsification and interphase formation in biphasic reaction systems as described in chapter 3.3. For that reason, an alternative immobilization strategy enabling catalyst recycling and reduced interphase formation in aqueous-organic reaction systems was explored, which is presented in the following chapter.

3.4.3.2 *In vitro* enzyme immobilization of *Ap*PDC var and *Cv*2025 using the EziG™ method

As a second immobilization strategy, the affinity adsorption on controlled-porosity glass (CPG)-carriers was tested for the immobilization of *Ap*PDC var and *Cv*2025, representing the enzyme combination used for metaraminol synthesis.

Characterization of suitable EziG™ carriers for *Ap*PDC var and *Cv*2025

Three different surface modifications of the CPG-carriers are available, catering to various catalyst requirements (hydrophilic, hydrophobic or semi-hydrophilic surface properties). First, a suitable EziG™ carrier had to be identified for immobilization of *Ap*PDC var or *Cv*2025, respectively. The results are summarized in Table 10. The data was obtained by separate carboligation or transamination experiments applying the reaction conditions as specified in the table description. The observed bead loadings were limited to 0.045 mg mg^{-1} (*Ap*PDC var with EziG™-Amber) and 0.09 mg mg^{-1} (*Cv*2025 with EziG™-Opal), when immobilized from purified enzyme solution, corresponding to a maximal mass specific loading of 10% (w/w) of the beads. Due to the interconnecting pore structure enlarging the overall surface of the carrier, the manufacturer specified 15-60% bead loading capacity [244]. The obtained bead loadings for both enzymes described in this work thus fall below this expected range. However, no further increase in the maximal bead loading was reached, even upon incubation with higher concentrated enzyme solutions. Seide *et al.* reported similar bead loadings for Fe(II)/α-ketoglutarate-dependent lysine hydroxylases [214]. The immobilization from crude cell extract (CCE) was tested for both enzymes, resulting in comparable bead loading and activity for *Ap*PDC var, whereas the immobilization from CCE containing *Cv*2025 gave a lowered bead loading and conversion with EziG™-Opal and EziG™-Amber. In transamination reactions, EziG™-Coral was not further considered as the hydrophobic bead surface caused substantial adsorption of the substrate 3-OH-PAC, which resulted in the overestimation of the apparent conversion.

Besides bead loading and overall conversion, the residual activity upon immobilization gives important insights into potential confirmational changes of the enzyme on the carriers and the resulting catalytic performance. For *Ap*PDC var, the initial activity was lowered compared to the free enzyme. Nevertheless, full conversion was achieved after 24 h for all three carriers, indicating that the operational stability of immobilized *Ap*PDC var was not impaired. However, as immobilization techniques based on affinity adsorption can suffer from protein leaching [245], a partial detachment of *Ap*PDC var from the carrier cannot be excluded, which would result in soluble enzyme contributing to the observed final conversion. The initial activity of *Cv*2025 was similar or higher compared to the free enzyme. Activity increase can be related to stabilization of the enzyme on a carrier [214, 246] or the selective immobilization of only intact, His-tagged

protein, because 1 mg of purified enzyme lyophilizate can contain a fraction of degraded, inactive protein. Enhanced activity of *Cv*2025 was also reported upon attachment of genetically encoded photosensitizers [247], indicating that the amine transaminase favors attachments of various forms and as a result frequently shows activity enhancements.

The stereoselectivity of the immobilized enzymes compared to the free enzyme was assessed. With immobilized *Ap*PDC var, high stereoselectivity was observed directly at the point of full conversion (< 95% *ee* after 9 h). Remarkably, a prolonged incubation caused a decrease in *ee* value to below 85% in reactions using EziG™-Amber or EziG™-Coral as enzyme carrier. For *Ap*PDC var immobilized on EziG™-Opal, this effect was less pronounced (91% *ee* after 24 h). While these results suggest an influence of the different surface properties on the stereoselectivity of the enzyme or the stability of the product itself, a similar reduction in the final *ee* was previously observed for longer incubation times with lyophilized whole cells containing *Ap*PDC var in fermentation supernatant (refer section 3.1.3.2). For *Cv*2025, the stereoselectivity was highest for EziG™-Opal. According to these results, EziG™-Opal was used as a suitable carrier for both, *Ap*PDC var and *Cv*2025, indicating a positive effect of the hydrophilic surface on bead loading, catalytic activity and stereoselectivity for both enzymes.

Table 10 Immobilization results for *Ap*PDC var and *Cv*2025 with different EziG™ carriers. n.d. = not determined, PE = purified enzyme, CCE = crude cell extract.

	***Ap*PDC var**		***Cv*2025**	
Bead loading [mg mg^{-1}]				
	from PE	**from CCE**	**from PE**	**from CCE**
Opal	0.038	0.039	0.09	0.04
Amber	0.045	0.024	0.06	0.05
Coral	0.034	0.029	0.10	n.d.
Conversion after 24 h[a] [%]				
	from PE	**from CCE**	**from PE**	**from CCE**
Opal	< 99	< 99	52	19
Amber	< 99	< 99	55	42
Coral	< 99	< 99	n.d.	n.d.
Relative activity to the same amount of free enzyme[b] [%]				
Opal	52		148	
Amber	54		> 99	
Stereoselectivity, *ee* after 6 h / 24 h [%]			***ic* after 24 h [%]**	
Opal	98 ± 0.3 / 91 ± 0.7		95 ± 0.0	
Amber	96 ± 0.6 / 84 ± 0.4		91 ± 0.3	
Coral	97 ± 0.4 / 84 ± 0.7		n.d.	
Free	97 ± 0.2 / 92 ± 0		97 [67]	

a Reaction conditions for ApPDC var: 1 mg mL^{-1} immobilized ApPDC var from crude cell extract, 20 mM 3-OH-BA, 100 mM pyruvate in 100 mM HEPES pH 7.5 with 0.1 mM ThDP, 2.5 mM $MgSO_4$, rotating incubation at 25 °C. Reaction conditions Cv2025: 20 mM (R)-3-OH-PAC, 100 mM IPA in 100 mM HEPES pH 7.5 with 0.1 mM PLP, rotating incubation (closed reaction vial) at 30 °C. Mean values and standard deviation from technical triplicates are shown.
b Relative activities were derived from product formation rate in the first 2 h of the reaction compared to the same amount of free, purified enzyme.

Recycling studies with EziG™-immobilized *Ap*PDC var and *Cv*2025

A central advantage of enzyme immobilization is the possibility to reuse the heterogenous biocatalyst for multiple reaction cycles, which is ecologically and economically favorable. The reusability of the immobilized *Ap*PDC var or *Cv*2025 was studied by repetitive batch studies, in which the EziG™ beads were separated from the first reaction batch by centrifugation and subsequently recycled for further consecutive reactions. The recycling of the EziG™-Opal-immobilized *Ap*PDC var achieved high conversion and enantiomeric excess for the (*R*)-enantiomer in three consecutive reactions (Figure 47). It becomes obvious that both, the conversion and the

ee value, decreased slightly with increasing reaction time. In the following three reactions, the conversion dropped further to 30%, 21% and 10%, respectively after 24 h. Thus, at first sight, a sharp drop in the conversion was apparent after the third reaction batch. Instead, a steadily declining enzymatic activity was observed as reflected by prolonged reaction times to reach a certain conversion (Figure A2.11, appendix). Thus, a combination of inactivation and leaching is likely causing the decrease in performance upon multiple recycling steps with the immobilized *Ap*PDC var.

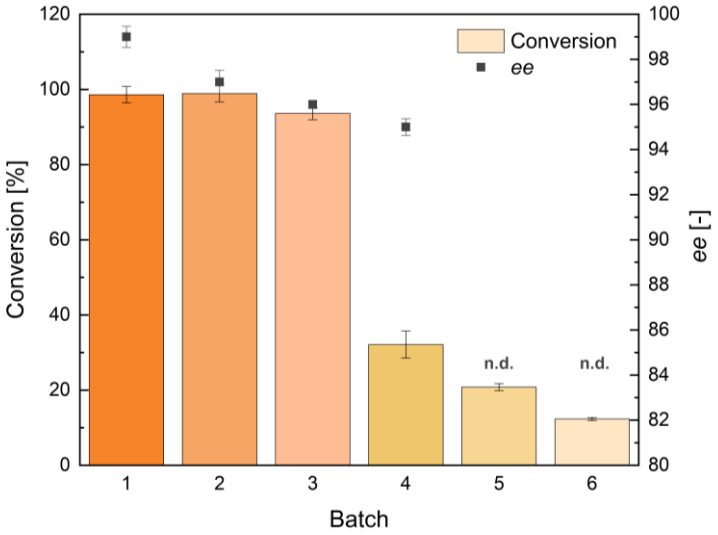

Figure 47 Conversion of 3-OH-BA and pyruvate to (*R*)-3-OH-PAC catalyzed by Opal-immobilized *Ap*PDC var in a repeated batch approach. Reaction conditions: 1 mg mL^{-1} EziG™-Opal-immobilized *Ap*PDC var from crude cell extract, 20 mM 3-OH-BA, 100 mM pyruvate in 100 mM HEPES pH 7.5 with 0.1 mM ThDP, 2.5 mM $MgSO_4$, rotating incubation at 25 °C for 9 h (Batch 1) or 24 h (Batch 2 - 6). The error bars show the standard deviation of technical triplicates. Data associated with this figure were taken from Anneke Strumpel's Bachelor thesis [205]

Likewise, the recycling of *Cv*2025 immobilized on EziG™-Opal or EziG™-Amber was tested in repeated batch transamination reactions towards metaraminol using IPA as the amine donor. A two-step one-pot approach consisting of consecutive carboligation (with *Ap*PDC var immobilized on EziG™-Opal) and transamination step resulted in only 20% conversion in the transamination step (data not shown). Therefore, a sequential reaction regime was chosen by using purified 3-OH-PAC as the starting substrate as previously shown for L-alanine as amine donor in chapter 3.1 - 3.3. Additionally, the evaporation of the by-product acetone from an opened reaction vial during incubation allowed for an equilibrium shift, reaching 73% conversion (Opal) or 67% (Amber) in the first batch (Figure 48, 1). Thus, the conversion was increased by improved acetone removal compared to the closed, rotating incubation shown in Table 10. In addition, to counteract possible leaching of the amine transaminase from the carrier, the pH and cofactor concentration were elevated slightly, as recommended by the manufacturer's protocol. The recycling of EziG™-

immobilized *Cv*2025 was however not successful as the conversion in the second and third reaction batch decreased to 20% and 10%, respectively (Figure 48, 2 and 3).

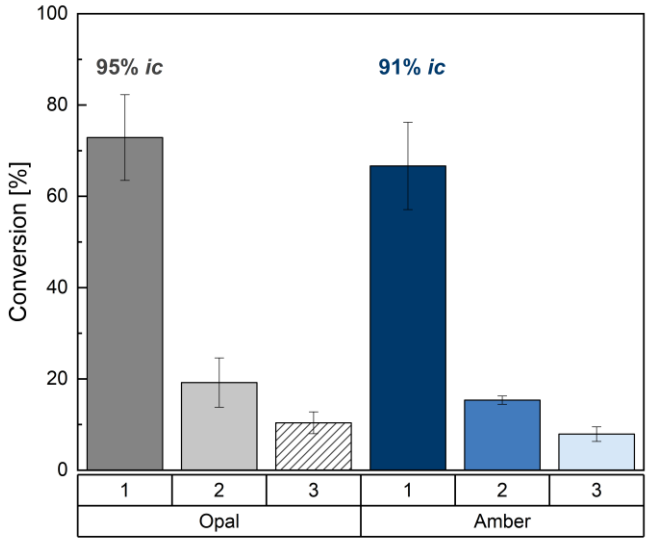

Figure 48 Conversion in three consecutive reaction batches with EziG™-Opal-immobilized *Cv*2025 in the transamination of (*R*)-3-OH-PAC with IPA as amine donor. Reaction conditions: 20 mM (*R*)-3-OH-PAC, 250 mM IPA in 100 mM HEPES pH 8.0 with 1 mM PLP, incubation shaking at 700 rpm at 30 °C for 24 h in an open reaction vial. The error bars show the difference of technical duplicates. Data associated with this figure were taken from Anneke Strumpel's Bachelor thesis [205].

Remarkably, the recycling of *Cv*2025 immobilized on EziG™-Opal or EziG™-Amber in an alternative reaction system with α-methylbenzylamine and pyruvate allowed for at least five consecutive reaction batches with stable conversion (Figure A2.12, appendix). Consequently, the recycling efficiency was dependent on the reaction system, indicating an inactivating or leaching-promoting component in the target reaction towards metaraminol. The successful recycling of the amine transaminase *Bm*TA immobilized on EziG™-Opal was previously shown in transamination reaction towards 1-amino-1-phenylpropan-2-ol (APP), retaining high conversion and stereoselectivity across 11 consecutive reaction cycles [248]. Böhmer *et al.* reported the efficient immobilization *Cv*2025 on EziG™-Amber, allowing for the recycling of the immobilized enzyme in four cycles of amination of 1-phenoxypropan-2-one with IPA and the application in neat organic solvents in flow or for the kinetic resolution of α-MBA [249]. This suggests an influence of specific reaction components of the herein tested system, causing an inactivation of the attached enzyme itself or its leaching from the carrier [250]. In a control experiment, the desorption from the carrier was studies after incubation with different additives. While the incubation with (*R*)-3-OH-PAC caused minor protein leaching from the carrier over 17 h incubation time, the presence of IPA or metaraminol resulted in a reduction in bead loading by 50% (Figure A2.13, appendix). Even though this might suggest that amine compounds promote enzyme leaching, a

combinatorial effect of inactivation and enzyme leaching is more likely, limiting the applicability of EziG™ immobilization in this reaction system.

Biphasic transamination of (*R*)-3-OH-PAC with *Cv*2025 immobilized on EziG™-Opal and L-alanine as amine donor

In chapter 3.3, the integration of reactive *in situ* product extraction was shown to facilitate the use of the bio-based amine donor L-alanine in the transamination of (*R*)-3-OH-PAC by shifting the previously unfavorable reaction equilibrium. In the experiments, lyophilized whole cells containing *Cv*2025 were used as robust and simple biocatalyst formulation. One downside of using whole cells in a biphasic aqueous-organic reaction system was interphase formation and emulsification because denatured proteins at the interface prevented coalescence of the emulsified phases [251]. This not only aggravates ISPR steps, but also complicates further product purification, as extractions and crystallization steps require efficient protein removal to obtain sufficient purity of the product. In that regard, a carrier-bound transaminase could be removed more easily from the reaction mixture and possibly circumvent interphase formation to overcome these challenges, which motivated the application study of EziG™-immobilized *Cv*2025 in a 15 mL biphasic reaction system with repeated reactive product extraction (the procedure is described in section 2.2.7.2). To examine the performance of the EziG™ immobilization in this system, a second batch with lyophilized crude cell extract containing *Cv*2025 was applied as direct comparison, as this formulation contains mostly soluble proteins and thus homogenous biocatalyst, not allowing a simple protein removal, nor enzyme recycling. After two extraction steps, the product yield with immobilized and free *Cv*2025 was comparable (48% EziG™, 45% CCE), indicating an overall better performance of lyophilized whole cells in this reaction system (58% after two extraction steps, refer to section 3.3.3.3). Furthermore, the phase separation behavior after 48 h differed visibly (Figure 48, A). For immobilized TA, two clear liquid phases were observed. In contrast, for CCE, droplets in the organic phase indicated poor coalescence and a visible interphase. After the transamination reaction was finished, the immobilized catalyst was removed by centrifugation. To assess whether the transaminase was removed completely, the aqueous reaction supernatant was used for a subsequent carboligation reaction, in which the co-produced pyruvate was recycled. Upon addition of *Ap*PDC var, the aldehyde was completely converted, forming around 5 mM additional (*R*)-3-OH-PAC (Figure 48, C). However, also substantial conversion of 3-OH-BA in the absence of the carboligase was observed, but no additional (*R*)-3-OH-PAC was formed. This indicated that remaining transaminase was left in the aqueous reaction phase, which converted 3-OH-BA to 3-hydroxybenzylamine. Therefore, the

amine transaminase had leached from the carrier in the preceding transamination step and remained as active, soluble enzyme in the aqueous reaction phase.

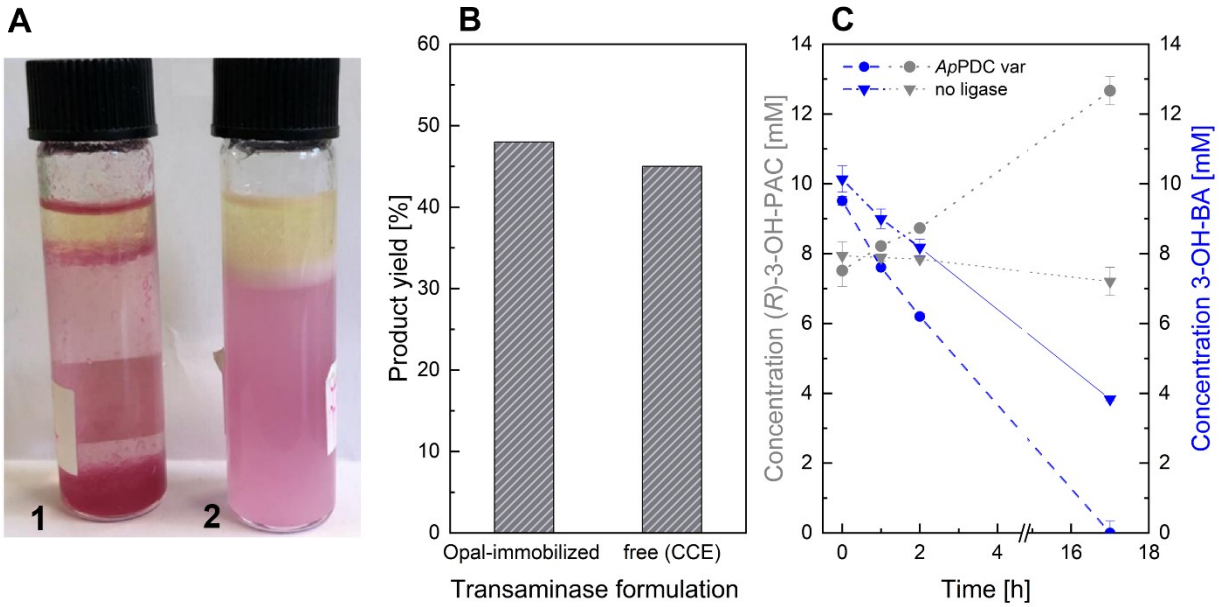

Figure 49 A – Biphasic reaction system for *in situ* reactive extraction of metaraminol catalyzed by (1) 2 mg mL^{-1} EziG™-Opal-immobilized *Cv*2025 or (2) 9 mg mL^{-1} crude cell extract (CCE) containing 10% *Cv*2025 (0.85 U mg^{-1}) after 48 h. B – Product yield after 48 h. C – Conversion of 3-OH-BA with recycled pyruvate from aqueous supernatant of A1. Reaction conditions: 6 mL reaction phase (40 mM (*R*)-3-OH-PAC, 250 mM L-alanine, 1 mM PLP, 100 mM Kpi buffer pH 7.6, 0.1 mM ThDP, 2.5 mM $MgSO_4$), 1.5 mL organic extraction phase (1-octanol, 0.25 M OA), incubation swaying at 30 °C in the dark for 24 h, back extraction with of 1 mL organic overlay with 1 mL 50 mM tartaric acid for 25 °C rotating for 45 min. The second extraction step was performed with 0.7 mL of the original organic overlay and 0.3 mL added organic phase. The EziG™-Opal-immobilized *Cv*2025 was replaced for fresh beads the second extraction step. C: The beads were removed by centrifugation and the supernatant was supplemented with 20 mM 3-OH-BA, 10 mM additional sodium pyruvate, 1 mM ThDP, 2.5 mM $MgSO_4$ and added to 1 mg mL^{-1} EziG™-Opal-immobilized *Ap*PDC var. Data associated with this figure were taken from Anneke Strumpel's Bachelor thesis [205].

In summary, the application of EziG™-immobilized *Cv*2025 caused less emulsification and therefore enabled a rapid phase separation in the biphasic transamination reaction system. This can be especially advantageous in continuous flow applications, in which aqueous and organic liquid phases are contacted for integrated product removal [215, 252]. Nevertheless, substantial enzyme leaching was verified in this system, indicating that the detaching from the carrier was not only observed in the presence of IPA (refer to Figure A2.13, appendix), but also for L-alanine. The lack of reusability is thereby a result of enzyme leaching and inactivation. Several studies have suggested that amine transaminase inactivation is caused by PMP-leakage from the enzyme-cofactor intermediate state and subsequent dissociation of the protein subunits, which was explained as an amine donor-induced mechanism [99, 201, 253]. This effect is enhanced by incubation with amine substrates, proving that Schiff base disruption causes an irreversible inactivation of *Cv*2025 [254]. However, this seems to be highly dependent on the substrate system and tertiary structure of the amine transaminases [255].

3.4.4 Conclusion

In conclusion, two immobilization techniques were tested for carboligation and transamination purposes, revealing several advantages and disadvantages of the respective methods. The number of process steps required to obtain the final biocatalyst was comparable, comprising pre-culture, main culture, cell or spore harvest, spore purification or immobilization from crude cell extract. The *in vivo* immobilization by spore display developed by Karava *et al*. was successfully adapted to display *Ap*PDC var or *Bm*TA, requiring no additional material. While this represents a promising new tool for the immobilization of recombinant proteins, the application for *in vitro* biotransformations was limited by low spore yield and considerable preparative effort. In addition, due to the lack of absolute quantitative protein determination, the direct comparison across *in vivo* immobilization and non-immobilized biocatalysts remains challenging. The EziG™ immobilization was shown to be a straight-forward immobilization technique for *Ap*PDC var from crude cell extract. For *Cv*2025, the immobilization from purified enzyme solution was more efficient, requiring an additional purification procedure. In aqueous-organic two-phase systems, EziG™-immobilized *Cv*2025 was favorable to facilitate sufficient phase separation compared to using crude cell extract, demonstrating how the identification of beneficial biocatalyst formulations represents a key factor in biocatalytic process development. A central bottleneck of this method for both enzymes was the leaching from the carrier, resulting in low or complete lack of reusability, which was dependent on the reaction system. The findings imply that neither of the investigated immobilization techniques are directly applicable to (large-scale) synthesis of metaraminol. Therefore, further experimental elucidations of the underlying effects were required to understand putative enzyme destabilization or inactivation in the transamination of (*R*)-3-OH-PAC with IPA, which are presented in chapter 3.5.

Chapter 3.5

Process intensification by further reaction parameter optimization

Contributions:

Laura Grabowski planned and evaluated all experiments in this chapter. Nina Klos performed the experiments and analyzed the results as part of her Master thesis, which was supervised and reviewed by Laura Grabowski [256]. Where indicated, figures from Nina Klos' Master thesis were adapted and included in this chapter. Laura Grabowski wrote this chapter, which was reviewed by Dörte Rother.

3.5 Process intensification by further reaction parameter optimization

3.5.1 Abstract

Isopropylamine (IPA) is commonly used as amine donor in amine transaminase-catalyzed reactions to shift the thermodynamic equilibrium by removal of the volatile co-product acetone. To intensify the metaraminol synthesis with IPA, increased product concentrations were targeted. Stability assays in the presence of different substrate concentrations were performed to elucidate potential inhibitory effects and draw conclusions for the intensification potential of this reaction. The results revealed a substrate inhibition by (*R*)-3-OH-PAC, indicating that the reaction is both limited by an unfavorable equilibrium and inhibition phenomena. In contrast, upon incubation with PAC derivatives with different hydroxylation, (*R*)-PAC and (*R*)-4-OH-PAC, *Cv*2025 retained high activity. The amine donor IPA showed minor to no adverse effects on the enzyme up to a concentration of 1 M. The substrate inhibition was partly overcome by increasing the total enzyme loading in the reaction, however, feeding experiments and varying setups for improved acetone removal failed to increase the final metaraminol concentration above 20 mM. These results indicated that an additional product inhibition of *Cv*2025 by metaraminol is probable. The scalability of the metaraminol synthesis with IPA is therefore hampered by the operational stability of *Cv*2025 in this specific reaction system.

3.5.2 Introduction

In the previous chapter, the recycling of the amine transaminase *Cv*2025 immobilized on (polymer-coated) controlled-porosity glass (CPG) carriers was heavily dependent on the reaction system, suggesting a combination of enzyme leaching and inactivation in the transamination reaction of (*R*)-3-OH-PAC to metaraminol with IPA as amine donor (section 3.4.3.2). For this reason, the objective was to identify the bottlenecks present in the metaraminol synthesis and deduce optimization strategies to scale the reaction towards higher product concentrations. Enzymatic transamination in industry often makes use of IPA as the amine donor as a non-chiral and consequently cheaper reagent as for example L-alanine, making this a factor in application-oriented screening and engineering of suitable amine transaminases [257]. The herein applied amine transaminase *Cv*2025 previously showed good acceptance of IPA in various reactions with aliphatic and aromatic ketones [85, 258, 259]. The reaction equilibrium can be shifted by evaporation of the co-product acetone. Nonetheless, applying reaction engineering methods to displace the equilibrium is especially crucial when transitioning from small scale (large surface-to-volume ratio) to larger scale processes beyond the laboratory scale (small surface-to-volume

and reduced mixing efficiency). Several measures for enhanced acetone removal can be found in literature, *e.g.*, purging with inert gas, evaporation (enhanced by high temperature and reduced pressure) or *in situ* product removal (enzymatic or by process engineering) [105, 259]. For the industrial production of sitagliptin, a combination of methods was applied, shifting the reaction equilibrium through a surplus in amine donor (four-fold, > 1 M) and enhancing acetone removal by reduced pressure (400 mbar), high temperature (> 40 °C) and a nitrogen flow in the head space [11]. To withstand the high substrate loadings and reaction conditions, the amine transaminase was engineered for high operational stability and stereoselectivity (> 99%).

In this chapter, the objective was to describe opportunities and possible pitfalls for scaling the metaraminol synthesis with IPA to compare the performance of this reaction system with the previously presented ISPR-integrated synthesis with L-alanine as the amine donor (chapter 3.3). For this purpose, the starting points for reaction engineering comprised the PLP concentration, the biocatalyst concentration and the reaction setup. Further, as substrate inhibition is a common phenomenon for amine transaminases [34], stability assays with different substituted PAC substrates were performed to assess possible inactivating and destabilizing factors of the reaction systems on the amine transaminase *Cv*2025.

3.5.3 Results & Discussion

3.5.3.1 Shifting the reaction equilibrium towards metaraminol with IPA as amine donor

High conversions in a transamination with IPA are commonly achieved by a molar excess of amine donor and sufficient removal of the co-product acetone. In the following investigations, the reaction optimization was pursued with Kpi buffer as it enabled comparable transaminase activity as in HEPES buffer (refer to Figure 28, section 3.2.3.2), but simplifies product purification as potassium phosphate is not extractable with organic solvents. To assess the scalability towards higher substrate concentrations, the reaction was performed with 40 mM, 80 mM, 120 mM and 160 mM (*R*)-3-OH-PAC, while keeping the molar excess of IPA constant (Figure 50). Independent of the applied substrate concentration in a range of 40 mM to 120 mM (*R*)-3-OH-PAC, the product concentration approached 20 mM after 24 h in all reaction systems, except for the reaction system with 160 mM (*R*)-3-OH-PAC and 1 M IPA, in which the product concentration only reached 6 mM. This translates to decreasing yields with increasing substrate concentrations after 24 h (Figure 50).

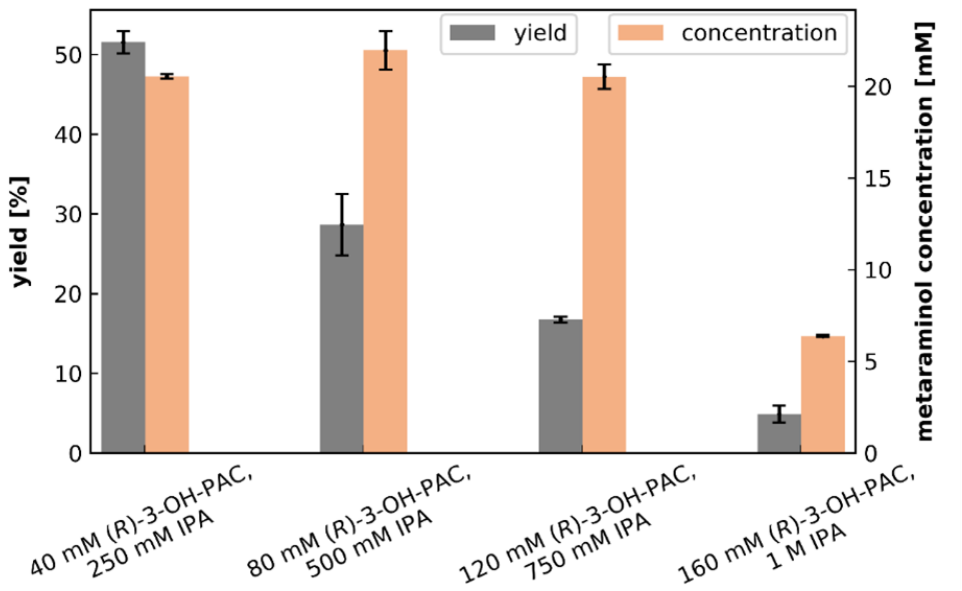

Figure 50 Yield and metaraminol concentrations for different initial substrate concentrations. Reaction conditions: 40 mM/80 mM/120 mM/160 mM (*R*)-3-OH-PAC, 250 mM/500 mM/750 mM/1 M IPA, 1 mM PLP, 100 mM Kpi buffer pH 7.5, 10 mg mL^{-1} lyophilized whole cells containing *Cv*2025, 1 mL, open glass reaction vial, 30 °C, 850 rpm, 24 h. The error bars represent the variance of technical duplicates. This figure originates from Nina Klos's Master thesis [256].

If the reaction was solely limited by the thermodynamic reaction equilibrium, the yield in equilibrium should be retained across the substrate increase. Possibly, at the determined endpoint of 24 h, the reaction systems were not yet in equilibrium, meaning that the equilibrium yield is only reached after reaction times > 24 h. The product concentration of 20 mM was reached for 40 - 120 mM (*R*)-3-OH-PAC, indicating that reaction rate was similar across increasing substrate concentrations in this range. However, for 160 mM 3-OH-PAC and 1 M IPA, the lower product concentration suggests inhibitory effects of the substrates on the enzymatic rate.

To elucidate the influence of the individual reaction components on *Cv*2025, a stability assay was developed (refer to section 2.2.5.2 for the method description). Lyophilized whole cells containing *Cv*2025 were incubated with the respective compound and the initial product formation rate was determined in the linear range of the subsequent conversion progress. The reference refers to an incubation in buffer without the putative inhibitors (Figure 51). The relative initial product formation rate negatively correlated with concentrations of (*R*)-3-OH-PAC in the incubation solution. This effect was more pronounced after 3 h of incubation than after 10 min of incubation. After 3 incubation with 160 mM (*R*)-3-OH-PAC, the initial product formation rate was reduced by 60%. Remarkably, this effect could be partly resolved by supplying a higher cofactor concentration during the incubation step (10 mM from initially 1 mM PLP), because the initial product formation rate in the subsequent assay (which was always performed with 1 mM PLP) was increased (Figure A2.14, appendix). In contrast, performing the reaction assay with 10 mM

PLP inhibited the conversion significantly (data not shown). These findings suggest that, while high cofactor excess is beneficial for *Cv*2025 (storage) stability, it acts inhibiting in the reaction itself and is thus not suitable to counteract inhibitions by the main substrate. A similar correlation was previously shown for a tetrameric amine transaminase, which was inhibited by ≥ 5 mM PLP in the reaction [201]. Additionally, PLP has chromophoric properties and is light-sensitive. Under illumination und oxygen it can disaggregate into benzoin-like PLP dimers and 4-pyrodoxic acid 5'-phosphate [260]. These degradation components can irreversibly inactivate the enzyme through a reaction with the histidines in the active site [261]. The influence of light on PLP-dependent enzymes, including *Cv*2025, was previously studied by Gerlach *et al.* [262]. Consequently, the observed performance loss with 10 mM PLP could be partly caused by PLP-based inactivation of the enzyme, as this experiment was not performed under full light exclusion.

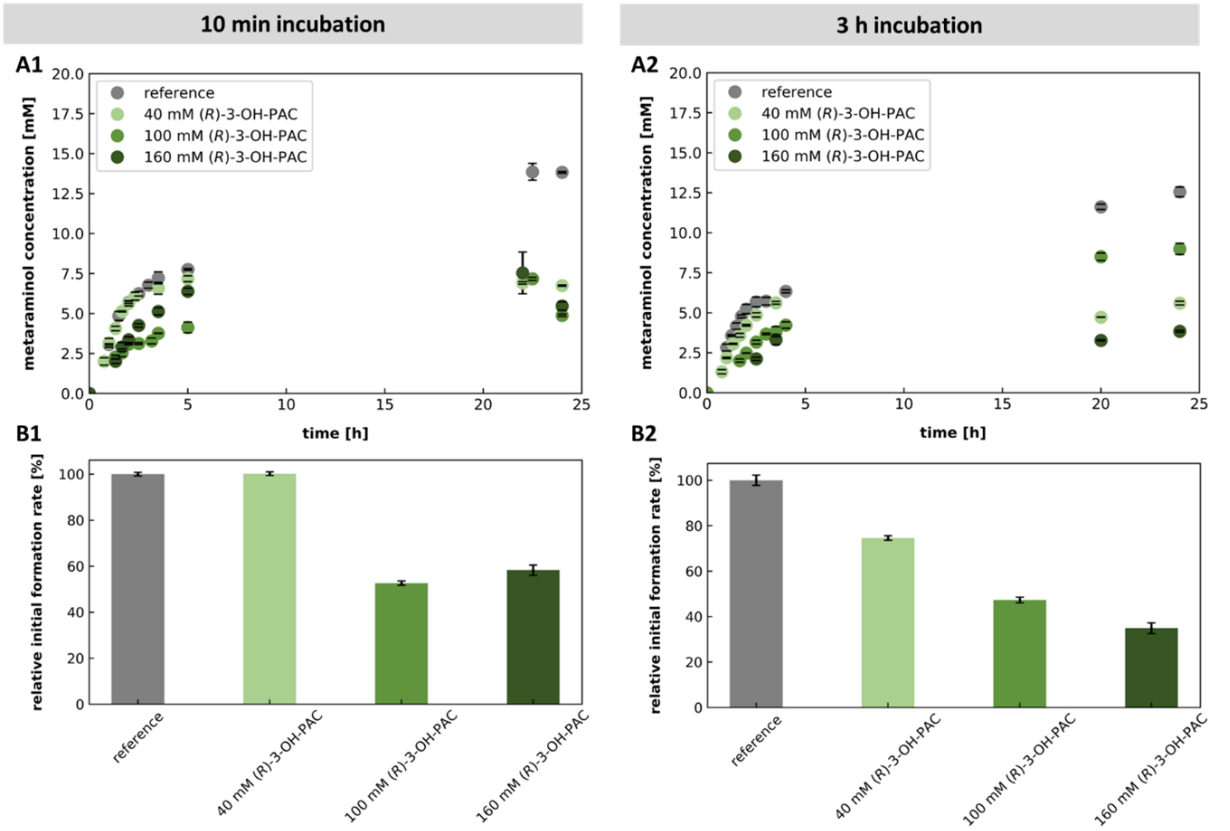

Figure 51 Stability of *Cv*2025 in the presence (*R*)-3-OH-PAC after 10 min of incubation (A1 and B1) and 3 h of incubation (A2 and B2). The relative initial product formation rate after incubation with different (*R*)-3-OH-PAC concentrations was determined from the slope in the linear range up to 180 min of the assay reaction. The reference reflects the same incubation procedure without addition of the tested compound and the subsequent initital product formation rate was set to 100%. Reaction conditions in the assay reaction: 20 mM (*R*)-3-OH-PAC, 125 mM IPA, 1 mM PLP, 100 mM Kpi buffer pH 7.5, 10 mg mL^{-1} lyophilized whole cells containing *Cv*2025, 1 mL, open glass vial, 30 °C, 850 rpm, 24 h. The error bars show the variance of technical duplicates. This figure originates from Nina Klos's Master thesis [256].

The stability assay was also performed with the co-substrate IPA. The incubation with 125 - 500 mM IPA allowed to retain similar product formation rates compared to the reference, whereas incubation with 1 M IPA caused the initial product formation rate to drop to 53% relative to the reference (Figure 52). These results suggest that *Cv*2025 is inhibited by substrate concentrations of ≥ 40 mM (*R*)-3-OH-PAC and > 500 M IPA.

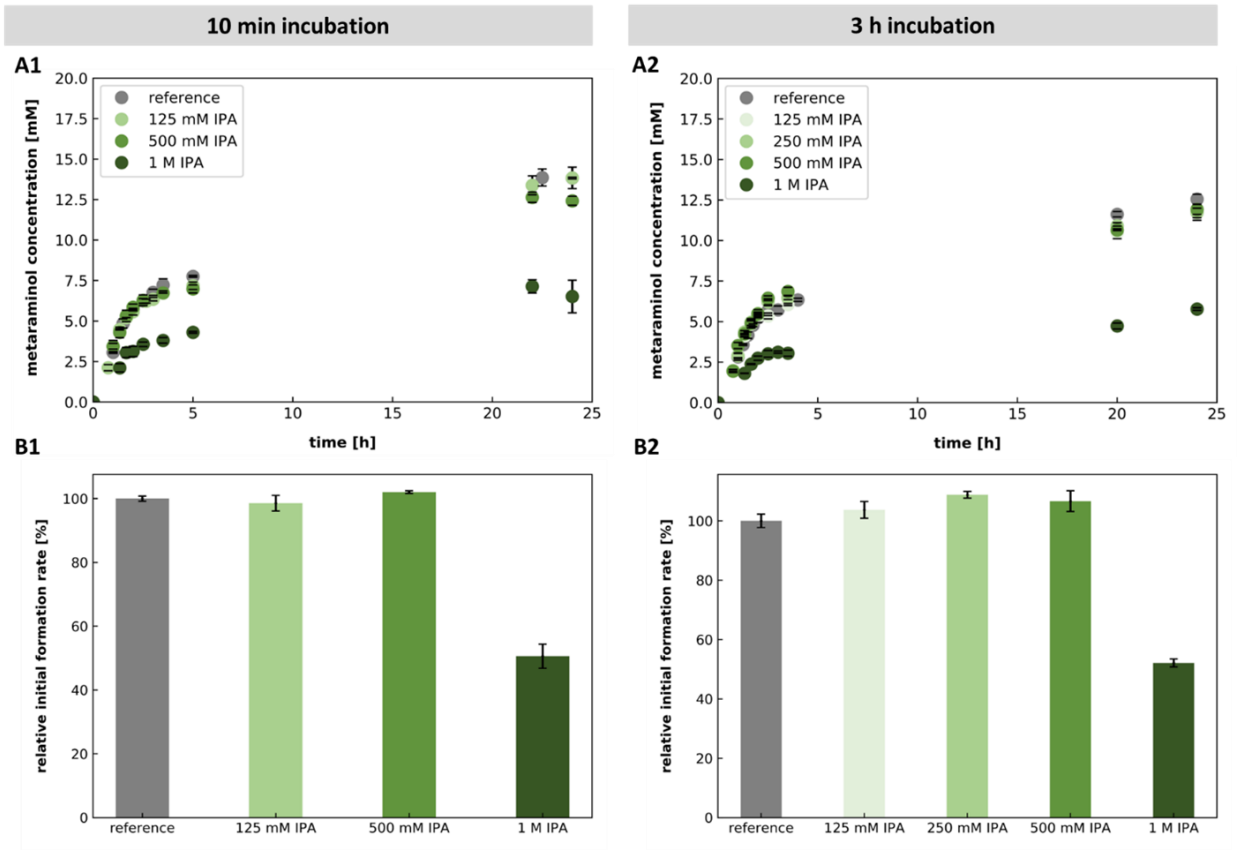

Figure 52 Stability of *Cv*2025 in the presence of IPA after 10 min of incubation (A1 and B1) and 3 h of incubation (A2 and B2). The relative initial product formation rate after incubation with different IPA concentrations was determined from the slope in the linear range of the assay reaction (up to 180 min). The reference reflects the same incubation procedure without addition of the tested compound and the subsequent initital product formation rate was set to 100%. Reaction conditions: 20 mM (*R*)-3-OH-PAC, 125 mM IPA, 1 mM PLP, 100 mM Kpi buffer pH 7.5, 10 mg mL^{-1}, lyophilized whole cells (*Cv*2025), 1 mL, open glass vial, 30 °C, 850 rpm, 24 h. The error bars show the variance of technical duplicates. This figure originates from Nina Klos's Master thesis [256].

To possibly overcome the apparent inhibition of the biocatalyst in the presence of the substrate, a reaction with 80 mM substrate was performed with different catalyst concentrations (Figure 53). Due to the higher enzyme loading, the reaction with 30 mg mL^{-1} lyophilized whole cells showed a faster reaction progress and reached 33% conversion after 4 h reaction time, compared to 28% with 20 mg mL^{-1} and 12% with 10 mg mL^{-1} cell concentration.

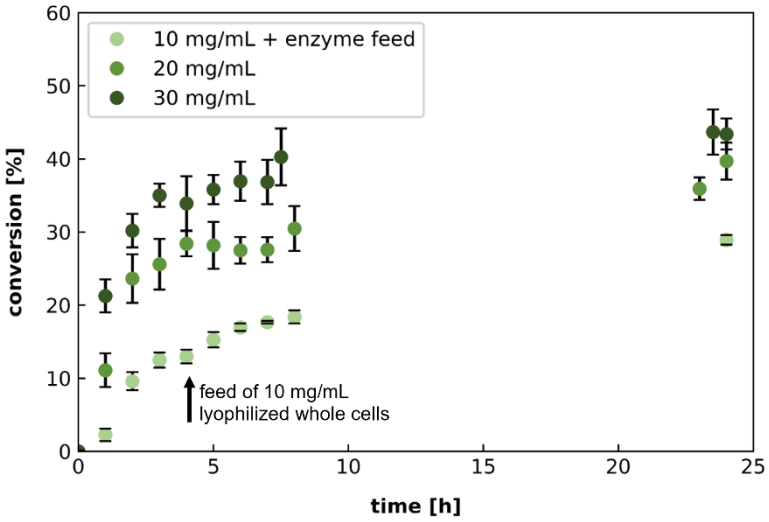

Figure 53 Variation of enzyme loading in the transamination towards metaraminol. Reaction conditions: 80 mM (*R*)-3-OH-PAC, 500 mM IPA, 1 mM PLP, 100 mM Kpi buffer pH 7.5, varied concentration of lyophilized whole cells (containing *Cv*2025), additional supplementation of 10 mg mL^{-1} cells after 4 h, 1 mL, open glass vial, 30 °C, 850 rpm, 24 h. The error bars show the variance of technical duplicates. This figure originates from Nina Klos's Master thesis [256].

This experiment showed that a higher enzyme loading can partly overcome inhibitory effects by the substrate, as the total activity and thus the initial reaction rate is significantly enhanced. Nonetheless, addition of fresh biocatalyst at a later point in the reaction (feed of 10 mg mL^{-1} after 4 h, Figure 53, light green dots) only led to a slight increase in conversion, indicating a potential additional inhibition.

In general, the space-time yield (STY) and final conversion was improved by increasing the total enzyme loading. Eventually, a tradeoff between higher STY or biocatalyst-specific yield must be chosen carefully. A higher enzyme loading also entails implications for the required unit operations for downstream processing and raises the catalyst costs, especially if recycling of the biocatalyst is not possible. In a separate experiment, a repeated batch was tested by reusing the lyophilized whole cells for a second reaction. The second reaction batch yielded significantly less product (9 mM compared to 16 mM metaraminol in the first reaction, after 18 h incubation from 20 mM (*R*)-3-OH-PAC, 250 mM IPA, 1 mM PLP, 10 mg mL^{-1} lyophilized whole cells containing *Cv*2025). This result indicates that some of the enzyme was already irreversibly inactivated with 20 mM substrate concentration, which corresponds to the lack of reusability observed for EziG™-immobilized *Cv*2025 in this reaction system (refer to chapter 3.4.3.2).

Circumventing the apparent substrate inhibition was pursued by feeding strategies in a stirred reactor setup. However, product concentrations remained limited to 20 mM (data not shown). Strikingly, neither the additional feeding of IPA nor fresh cells resulted in an increase in conversion. As these results in addition to the previously obtained ones strongly imply a possible

product inhibition, further investigations in the combinatorial effects of substrate and product inhibitions on *Cv*2025 should be pursued. An inhibition by dissolved acetone in the reaction was excluded because no acetone was detectable by GC measurements in all reaction setups and incubation at reduced pressure (750 mbar in a rotary evaporator) did not increase conversions.

These findings allow a direct comparison with the previously established metaraminol synthesis with L-alanine as amine donor, which was facilitated by extractive *in situ* product removal (chapter 3.2 and 3.3). Comparing the reaction performances, comparable yields after 24 h were obtained with 40 mM substrate concentration (43% with L-alanine as amine donor, refer to Figure 39 in section 3.3.3.3; 41 - 51% with IPA as amine donor in 20 mL and 1 mL reaction volume). However, upon increasing the total substrate concentration to 80 mM, the transamination with L-alanine in a biphasic reaction system resulted in 60% yield by repeated *in situ* extraction steps (Table 8 in section 3.3.3.5), whereas yields were limited to 25 - 28% with IPA. Notably, this comparison is valid for the similar compound concentrations (1 mM PLP, 6.25-fold molar excess of amine donor, 10 mg mL^{-1} lyophilized whole cells containing *Cv*2025), whereas the reaction conditions differed because it was a monophasic reaction setup for IPA and a biphasic, ISPR-integrated reaction system, when L-alanine was used as the amine donor. This comparison emphasizes how reactive ISPR afforded enhanced yields even with higher substrate load, because the aqueous concentration of both substrate and products were maintained low due to the biphasic system (< 40 mM 3-OH-PAC and ≤ 6 mM metaraminol). As substrate inhibition is a common phenomenon in enzymes, investigations to explain the mechanism behind the inhibitory effects should be pursued. In dehalogenases, inhibitions were a result of the substrate binding to the enzyme-product complex, preventing product release and thus further catalysis [263]. In amine transaminases, the formation of dead-end complexes during the catalytic cycle (in this case by binding of the 2-hydroxy ketone to the enzyme-PLP form (E-PLP) or by binding of the amine donor to E-PMP) have been reported as a probable cause of substrate inhibitions [92, 97, 264, 265]. One option to overcome substrate and product inhibitions is to develop a selective ISPR method that is applicable with IPA as amine donor, in combination with a feeding strategy, which keeps the substrate concentration below a certain threshold. In a follow-up Master thesis proceeding from the herein presented data, metaraminol concentrations as low as 8 mM were discovered to inhibit *Cv*2025 in buffered reaction systems (data not shown) [266]. Therefore, the reactive extraction strategy described in chapter 3.3 in this thesis was likely responsible to circumvent additional product inhibitions by metaraminol, as further discussed in chapter 4. This ISPR strategy is, however, not applicable with IPA due to co-extraction of the amine donor. Nonetheless, the integration of ISPR with enzymatic reactions can be a potent strategy to mitigate inhibition effects [267, 268]. Recently, several

transamination reactions with L-alanine as amine donor were improved by another ISPR strategy that made use of ion exchange resins to minimize inhibitory effects of the products [269].

3.5.3.2 Overcoming substrate inhibition by PAC derivatives

Based on the results from the previous section, stability assays with *Cv*2025 were performed with (*R*)-PAC and (*R*)-4-OH-PAC, to assess how the lack of hydroxylation ((*R*)-PAC) or an alternative hydroxylation position ((*R*)-4-OH-PAC) affects the substrate inhibition. The alternative reaction system with (*R*)-4-OH-PAC has previously not been investigated, thus a two-step enzymatic synthesis of the respective amino alcohol product 2-amino-1-(4-hydroxyphenyl)propan-1-ol (4-AHP) was developed as part of this thesis. The enzyme identification for both reaction steps as well as the preparative synthesis of (*R*)-4-OH-PAC is described in chapter 3.6.

When incubating *Cv*2025 with 1 M IPA or 160 mM (*R*)-4-OH-PAC for 3 h prior to starting the assay reaction, the initial formation rate of 4-AHP was not negatively affected, indicating high enzyme stability and activity in this reaction system (Figure 54 A). Upon incubation with (*R*)-PAC, the relative formation rate of norephedrine was reduced to 66% of the reference (Figure 54 B). In contrast, the initial formation rate of norephedrine remained unchanged after incubation with 1 M IPA. The final conversion in this reaction system was > 99%, indicating that solely the initial activity of the cells was lowered but full conversion was reached after 24 h. The findings were verified in two independent experiments with technical duplicates, respectively.

These results are essential to evaluate the observed inactivation of *Cv*2025 in the reaction system with (*R*)-3-OH-PAC, shown in the previous section (Figures 51 and 52). Besides a substantial inactivation by already 20 mM (*R*)-3-OH-PAC, a reduced metaraminol formation rate was also observed after incubation with 1 M IPA. This effect was, however, not verified in the herein presented assays with (*R*)-4-OH-PAC nor (*R*)-PAC. It can be concluded that the 2-hydroxy ketone substrate is the decisive factor for *Cv*2025 activity and stability, whereas a combinatorial, detrimental effect of substrate and amine donor cannot be fully excluded. Altogether, the experiments reflect a vast influence of the hydroxylation pattern for overall performance of *Cv*2025 as biocatalyst, in which the 3-hydroxylated substrate is least favorable. With these novel insights it can be reinforced that the recyclability of EziG™-immobilized *Cv*2025 (presented in section 3.4.3.2, Figure 48) was drastically hampered due to enzyme inactivation by the substrate. Clarification of the responsible mechanism should be pursued in the future. Based on the direct comparison between reaction systems shown here, it might be beneficial to intensify the enzymatic synthesis of 4-hydroxylated amino alcohols with *Cv*2025, which is further discussed in the following chapter.

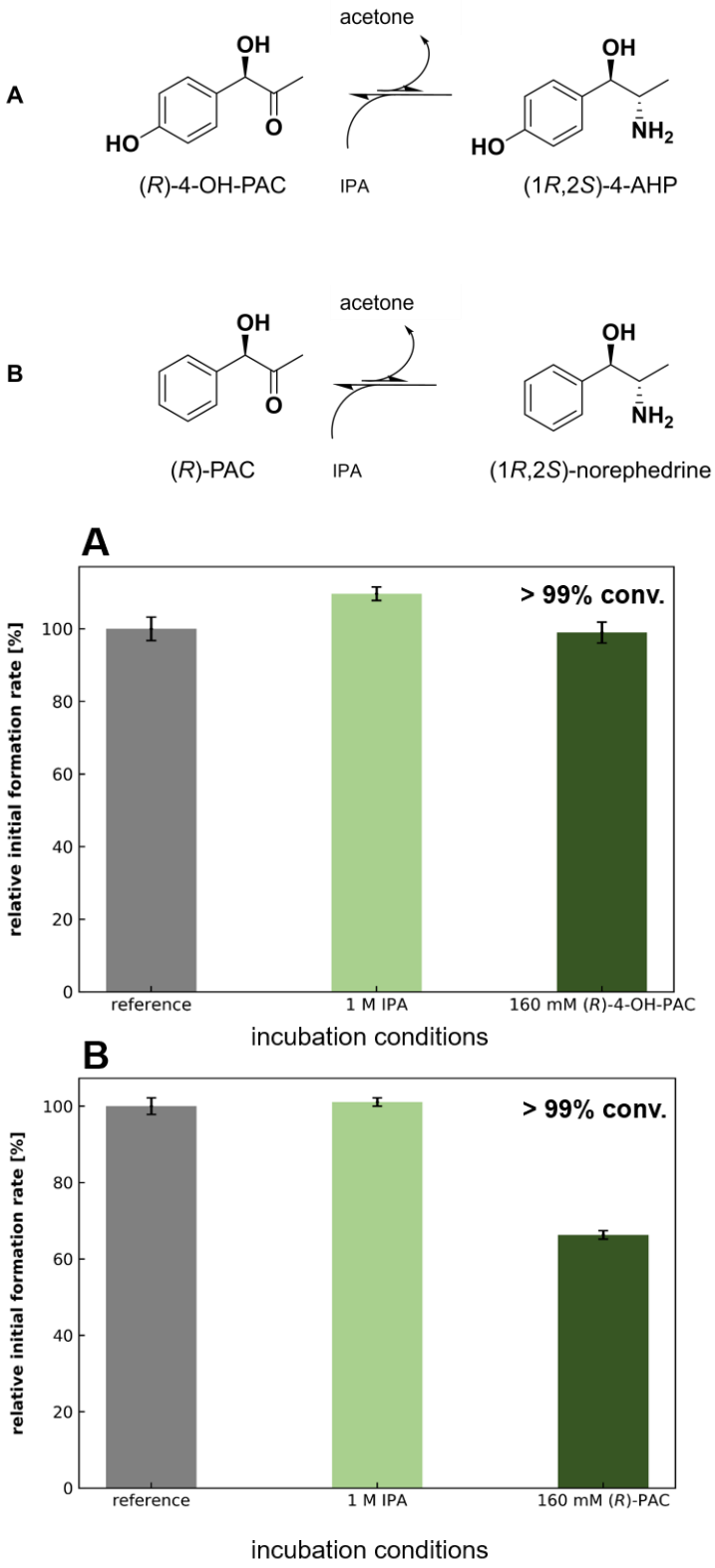

Figure 54 Relative initial product formation rate after incubation with (A) 1 M IPA or 160 mM (*R*)-4-OH-PAC or (B) 1 M IPA or 160 mM (*R*)-PAC for 3 h. The conversion after 24 h is indicated. The reference reflects the same incubation procedure without addition of the tested compound and the subsequent initial product formation rate in the respective reaction system was set to 100%. Reaction conditions: 20 mM (*R*)-4-OH-PAC, 125 mM IPA (A) or 20 mM (*R*)-PAC, 125 mM IPA (B), 1 mM PLP, 100 mM Kpi buffer pH 7.5, 10 mg mL^{-1} lyophilized whole cells containing *Cv*2025, 1 mL, open glass vial, 30 °C, 850 rpm. The error bars show the variance of technical duplicates. This figure originates from Nina Klos's Master thesis [256].

3.5.4 Conclusion

The investigations revealed substantial inhibition of *Cv*2025 by (*R*)-3-OH-PAC. While the evaporation of acetone was efficient in the reaction setups and concentration ranges tested, a special focus on acetone removal in suitable reaction setups must be placed when transitioning to higher reaction volumes and substrate concentration ranges. The results further imply additional inhibition by metaraminol. Surprisingly, these effects were not observed in the reaction systems towards (1*R*,2*S*)-norephedrine or (1*R*,2*S*)-4-AHP with *Cv*2025. Several further research objectives can be deduced from these findings. First, the operational stability of *Cv*2025 could be increased by rational enzyme engineering, possibly supported by computational approaches to clarify the underlying effects of different hydroxylation patterns of aromatic substrates on *Cv*2025. *In situ* product removal of metaraminol should be developed to remove the product from the reaction phase, which was implemented in this thesis with L-alanine as amine donor (chapter 3.2 and 3.3). However, these ISPR strategies are not directly applicable with IPA in the reaction system (refer to chapter 4.4).

Chapter 3.6

Enlarging the product spectrum to 4-hydroxylated amino alcohols

Contributions:

Laura Grabowski planned and co-performed all experiments in collaboration with Lilia Arnold (technician in the Biocatalysis group at IBG-1). Lilia Arnold established the instrumental analytics, conducted the carboligase screening and performed experimental optimization of the carboligation reaction. Laura Grabowski performed the preparative-scale reactions, intermediate work-up, transaminase reactions and cascade experiments. All results were finally evaluated and visualized by Laura Grabowski. The chapter was written by Laura Grabowski and revised by Dörte Rother.

3.6 Enlarging the product spectrum to 4-hydroxylated amino alcohols

3.6.1 Abstract

Microbial synthesis of substituted benzoates in combination with the enzymatic reduction to aldehydes represents a way to provide starting substances for sustainable production of chiral, value-added products. So far, the enzymatic synthesis of 4-hydroxylated chiral amino alcohols (2-amino-1-(4-hydroxyphenyl)propan-1-ol), 4-AHP) from 4-hydroxybenzaldehyde (4-OH-BA) remained challenging as an efficient carboligase accepting 4-OH-BA as substrate was missing. Consequently, the identification of efficient and stereocomplementary enzyme combinations was targeted. The branched-chain keto decarboxylase from *Lactococcus lactis* (*Ll*KdcA) was shown to catalyze the desired carboligation reaction of 4-OH-BA and pyruvate with high conversions and stereoselectivity. Upon reaction optimization with lyophilized *E. coli* BL21 (DE3) cells containing *Ll*KdcA, (*R*)-4-OH-PAC was synthesized in preparative scale and further transformed by two complementary transaminases, namely *Cv*2025 and *As*TA, to (1*R*,2*S*)-4-AHP and (1*R*,2*R*)-4-AHP, respectively. The carboligation and transamination steps were characterized by high conversion rates and yield, especially compared to the transamination of (*R*)-3-OH-PAC to metaraminol. In this way, a promising synthesis route for precursors of potential active pharmaceutical ingredients was found.

3.6.2 Introduction

Carbon-carbon bond forming chemistry build up the molecular frameworks of organic molecules. Several enzyme classes capable of performing C-C coupling reactions have been studied extensively as biocatalytic tools in organic synthesis [270, 271]. Enzyme discovery and protein engineering as well as substrate engineering have led to advances in this field, broadening the product scope in the past years [272]. One group of enzymes are ThDP-dependent carboligases, which differ in their substrate acceptance, stereo- and chemoselectivity [273, 274]. In the past, asymmetric carboligation reactions of (substituted) benzaldehyde were shown with stereoselective enzyme variants (pyruvate decarboxylase, PDC, branched-chain keto acid decarboxylase, KdcA or acetohydroxyacid synthase, AHAS) [270, 275, 276]. The findings led to a comprehensive enzymatic toolbox of complementary functionalities and selectivity, which in turn allowed to exploit an entire product platform of 2-hydroxy ketone derivatives [274]. In combination with complementary amine transaminases, synthetic enzyme cascades towards a variety of chiral amino alcohols were developed starting from simple, achiral precursors [39, 41, 67, 90] . Recently, it was shown that the respective aldehyde substrates can also be derived enzymatically from microbially

produced benzoates using carboxylate reductases (CARs, E.C.1.2.1.30) [162, 277-279]. CARs catalyze a one-step reduction of carboxylic acids to aldehydes using NADPH as cofactor [280, 281]. The known enzyme variants are characterized by a broad substrate acceptance, catalyzing the reduction of various substituted benzaldehydes. In that way, the utilization of bio-based, substituted aromatic carboxylic acids in combination with enzymatic catalysis uncloses a starting point of sustainable syntheses from renewable resources as already described in chapter 3.1. Similarly, the production of 4-hydroxybenzoate was achieved using engineered *Escherichia coli*, *Pseudomonas taiwanensis* or *Corynebacterium glutamicum* [129, 282, 283]. The highest titer was achieved by Kitade *et al.* using metabolically engineered *C. glutamicum* in an aerobic fed-batch process (36.6 g L^{-1}) [284], outperforming the highest titers for other microbially produced benzoic acids so far [129, 161, 285, 286]. The microbially produced 4-hydroxybenzoate can be reduced efficiently to the respective aldehyde by NoCAR [70]. Following this reduction step, the desired chiral amino alcohols ((2-amino-1-(4-hydroxyphenyl)propan-1-ol), 4-AHP) should be synthesized in a two-step process, involving the further transformation of 4-OH-BA by ligation, with (bio-based) pyruvate, yielding the 2-hydroxy ketone [150]. In contrast to the enzymatic reduction step, the hydroxylation in 4'-position remains a challenging substrate for asymmetric carboligation. Afterwards, the 2-hydroxy ketone must be aminated using a suitable amine donor. The resulting vicinal amino alcohol can serve as precursor for potential active pharmaceutical ingredients like ritodrine and ritobegron, which could be used in the treatment of premature labor or overactive bladder, respectively [59, 60].

In this chapter, the objective was to identify enzyme combinations for the chemo- and stereoselective synthesis of 4-hydroxylated chiral amino alcohols (2-amino-1-(4-hydroxyphenyl)propan-1-ol)) to offer a method to close the missing link between microbial precursor production of 4-OH-BA and value-added products in form of chiral amino alcohols.

3.6.3 Results & Discussion

3.6.3.1 Identification of a carboligase catalyzing the asymmetric ligation of 4-hydroxybenzaldehyde and pyruvate

Targeting the mixed carboligation of 4-hydroxybenzaldehyde (4-OH-BA) with pyruvate as co-substrate, initially a first screening with five carboligases was performed, namely *Zm*PDC, *Sc*PDC, *Sc*PhePDC, *Ap*PDC var, *Ll*KdcA (data not shown). The pyruvate decarboxylase variant from *Acetobacter pasteurianus* *Ap*PDC var and the branched-chain keto decarboxylase from *Lactococcus lactis* showed the desired substrate acceptance. In addition, minor activity was identified for *Sc*PDC, which was however not quantifiable. In the initial tests, 86% and 35% conversion were achieved with 20 mM 4-OH-BA and a 3-fold molar excess of sodium pyruvate

for *Ll*KdcA and *Ap*PDC var, respectively (Figure 55). For both catalysts, the obtained product peak was analyzed by GC-MS (method section 2.2.10.4), revealing a parent peak with 166 m/z. The spectrum provided a first confirmation of the desired product configuration (4-OH-PAC), which was later verified by further structural elucidation of the purified product (see 3.6.3.2). No side-product formation (such as 4-OH-HPP, HPP is 1-hydroxy-1-phenylpropan-2-one) was detected. In the next step, the reaction was further optimized with *Ll*KdcA as the most promising catalyst. Increasing the substrate concentration to 40 or 60 mM 4-OH-BA showed similar or higher conversions (Figure 56).

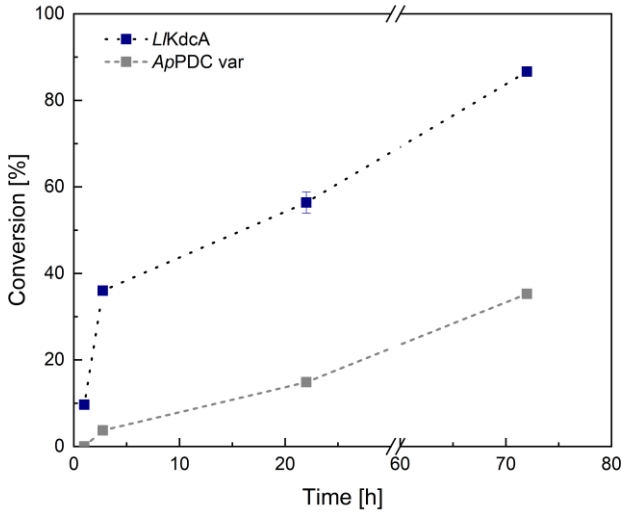

Figure 55 Carboligation reaction of 4-OH-BA and pyruvate catalyzed by *Ap*PDC var or *Ll*KdcA. Reaction conditions: 20 mM 4-OH-BA, 60 mM sodium pyruvate, 100 mM Kpi buffer pH 6.5, 2.5 mM $MgSO_4$, 0.1 mM ThDP, 1 mL reaction volume, 1 mg mL^{-1} purified enzyme *Ap*PDC var; 0.16 mg mL^{-1} purified enzyme *Ll*KdcA, 1 mL reaction volume, 25 °C, 750 rpm. GC-MS measurements were used for analysis. Error bars show the variance of technical duplicates.

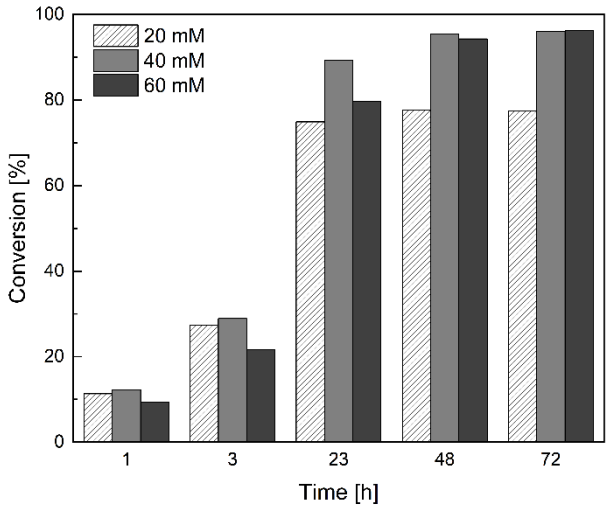

Figure 56 Carboligation reaction of varying concentrations of 4-OH-BA with pyruvate catalyzed by *Ll*KdcA. Reaction conditions: 20 mM/ 40 mM/ 60 mM 4-OH-BA, 3-fold molar excess of sodium pyruvate, 100 mM Kpi buffer pH 6.5, 2.5 mM $MgSO_4$, 0.1 mM ThDP, 1 mL reaction volume, 0.16 mg mL^{-1} purified enzyme *Ll*KdcA, 1 mL reaction volume, 25 °C, 750 rpm.

In previous characterization studies of *Ll*KdcA, a substrate dependent chemoselectivity was described for mixed carboligation reactions. For benzaldehyde and acetaldehyde, a 60:40 ratio of HPP to PAC was observed, with 92% and 94% *ee* for the (*R*)-isomer, respectively [287]. With increasing side chain length of the donor, the product ratio shifted to mainly PAC formation with excellent stereoselectivity. The substrate that is bound first to ThDP acts as the donor molecule. In case of PAC formation, acetaldehyde acts as donor and benzaldehyde binds second and serves as acceptor. If the substrates bind *vice versa*, the HPP product is formed. The herein observed highly chemoselective formation of 4-OH-PAC indicates that *Ll*KdcA first decarboxylates pyruvate to acetaldehyde, before catalyzing the ligation with 4-OH-BA, possibly due to the bulkier structure of 4-hydroxylated benzaldehyde. Surprisingly, a complete lack of conversion of 4-OH-BA with acetaldehyde as co-substrate was observed.

3.6.3.2 Preparative-scale production of 4-OH-PAC for product identification and further enzymatic conversion

Formerly, characterization and applications of *Ll*KdcA were mainly performed with purified enzyme formulation, requiring time- and resource-intensive purification procedures. Especially in large-scale applications, whole cell formulations or (lyophilized) crude cell extract are preferred due to cost and time savings [146]. Using the previously selected reaction conditions, 40 mM 4-OH-BA were converted in 3 h with 94% conversion (data not shown), indicating a fast reaction progress with lyophilized whole cells containing *Ll*KdcA. When the reaction was incubated up to 24 h, the reverse reaction was observed, lowering the overall conversion. Interestingly, with lyophilized whole cells, some activity was also detected with acetaldehyde as co-substrate (18%

conversion after 22 h, data not shown). In contrast, with purified *Ll*KdcA, no conversion was detected for 4-OH-BA and acetaldehyde as described in the previous section. The main product of this reaction was 4-OH-PAC. Acetoin was not detected. The observed activity of whole cells on the alternative substrate combination (4-OH-BA and acetaldehyde) was compared to the target reaction very slow and can therefore be attributed to unidentified enzymatic activity on 4-OH-BA, stemming from the cell background of *E. coli*. Although several ThDP-dependent enzymes from *E. coli* have been characterized for their application in synthetic carbon-carbon coupling reactions, the enzyme responsible for the observed background reactivity was not identified [288, 289].

The absolute configuration of 4-OH-PAC was assessed by chiral HPLC analysis in analogy to (*R*)- and (*S*)-3-OH-PAC as reference substances, revealing a selective formation of (*R*)-4-OH-PAC. In addition, the complementary product enantiomer (*S*)-4-OH-PAC was synthesized with the (*S*)-selective enzyme variant *Ap*PDC E469G, obtaining 30 - 40% conversion and 73-78% *ee* after 23 h in 1 mL test experiments (data not shown) and 64% *ee* in 100 mL reaction batch after 22 h (Figure A2.1, C in the appendix). While these results did not allow scale-up of the reaction due to poor conversion and optical purity, it allowed to confirm baseline separation of the 4-OH-PAC enantiomers in chiral HPLC analysis. The stereoselectivity of *Ll*KdcA towards the (*R*)-product enantiomer in the conversion of 4-OH-BA with pyruvate therefore corresponded with previously described (*R*)-selectivity of *Ll*KdcA [287].

With excellent stereo- and chemoselectivity proven, the next step was to transfer the reaction system to a preparative scale. To facilitate an efficient synthesis process, further adaptions of the reaction conditions were made. For product work-up, complete depletion of the substrate aldehyde is preferable. By increasing the pyruvate excess to 5-fold, the residual substrate concentration was reduced to < 1 mM. Second, by lowering the pH of the reaction solution slightly to pH 6.25 a faster reaction progress was achieved. Finally, with the optimized reaction conditions, the synthesis of (*R*)-4-OH-PAC was performed in a 100 mL stirred reaction vessels (66 mM substrate concentration, Figure 57).

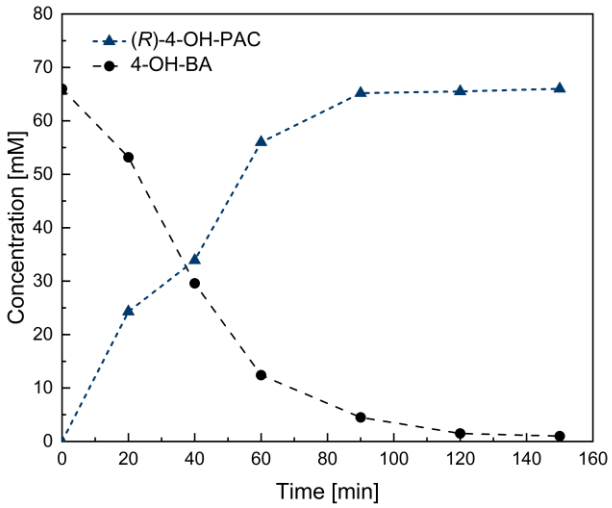

Figure 57 Preparative-scale enzymatic synthesis of (*R*)-4-OH-PAC. Reaction conditions: 66 mM 4-OH-BA, 300 mM sodium pyruvate, 2.5 mM $MgSO_4$, 0.1 mM ThDP, 100 mM Kpi buffer pH 6.25, 10 mg mL^{-1} lyophilized whole cells containing *Ll*KdcA, 25 °C, 100 mL reaction volume (EasyMax 402), stirred at 250 rpm. The reaction was stopped after 2.5 h and the product was purified as described in method section 2.2.4.4.

The reaction was complete after 2.5 h reaching 99% conversion. Furthermore, with these reaction conditions, the cells could be recycled in a second batch, which afforded 87% conversion after 3 h (data not shown). This indicates good operational stability of the lyophilized whole cells containing *Ll*KdcA. Product work-up from the reaction supernatant was performed by extraction with ethyl acetate as described in section 2.2.3.7. After solvent evaporation, minor residues of the substrate remained, which was subsequently completely removed by re-crystallization, obtaining a crystalline product with 83% isolated yield (96% HPLC purity). The product was confirmed by ^{1}H-NMR (Figure A2.15, appendix). In summary, the production of (*R*)-4-OH-PAC was possible in a robust enzymatic synthesis using *Ll*KdcA as lyophilized whole cell formulation. In comparison to the enzymatic production of (*R*)-3-OH-PAC using *Ap*PDC var, the reaction times were much faster (refer to Figure A2.1, A in the appendix). Possibly, the high activity and stereoselectivity allow for a straight-forward scalability of the reaction towards economically feasible concentration ranges. As the substrate solubility was limited to around 69 mM in aqueous buffer systems, a feeding approach should be investigated for further process intensification.

3.6.3.3 Identification of an amine transaminase accepting 4-OH-PAC as substrate

Having the desired 2-hydroxy ketone in hand, the next step was to identify amine transaminases capable of performing the subsequent transamination towards 4-hydroxylated, vicinal amino alcohols. Therefore, three (*S*)-selective amine transaminases and one putative (*R*)-selective enzyme were tested in the transamination reactions with (*R*)-4-OH-PAC and IPA as amine donor. In an initial test, the amine transaminase from *Chromobacterium violaceum* ATCC 12472 (*Cv*2025) converted 10 mM in 2.66 h (data not shown). In contrast, the amine transaminases from

Bacillus megaterium (*Bm*TA) or *Arthrobacter citreus* (*Ac*TA, [290]) did not accept the substrate, suggesting a significantly altered substrate preferences for bulky aromatic compounds with a substitution in *para*-position [291]. Complementary, the commonly as (*R*)-selective characterized amine transaminase from *Arthrobacter spec.* (*As*TA) converted 10 - 40 mM 4-OH-PAC with excellent conversion after 24 h (Figure 59, left). Remarkably, *Cv*2025 exhibited significantly higher substrate acceptance for (*R*)-4-OH-PAC compared to (*R*)-3-OH-PAC, reaching 90% conversion after 6 h (Figure 59, right). The differing performance between hydroxylated PAC derivatives was discussed in chapter 3.5.

Chiral HPLC analysis revealed one distinct product peak for each amine transaminase, respectively, with baseline separation of the complementary products (Figure A2.16, appendix). No side-products were detected. Regarding the previously characterized stereoselectivity of both amine transaminases [292], and in analogy to 3-OH-AHP (both enantiomers as reference substances), the obtained products were defined as (1*R*,2*S*)-4-OH-AHP for *Cv*2025 and (1*R*,2*R*)-4-OH-AHP for *As*TA (Figure 58).

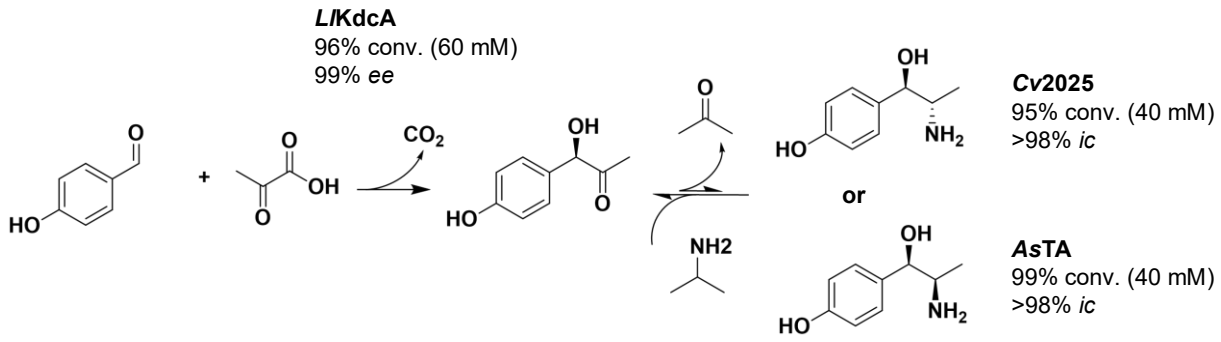

Figure 58 Two-step enzymatic synthesis of two diastereomers of 4-AHP. *Ll*KdcA catalyzes the highly chemo- and stereoselective carboligation of 4-OH-BA and pyruvate, yielding (*R*)-4-OH-PAC. The transamination with IPA as amine donor yields (1*R*,2*S*)-4-OH-AHP with *Cv*2025 and (1*R*,2*R*)-4-OH-AHP with *As*TA (final conversions after 24 h are shown).

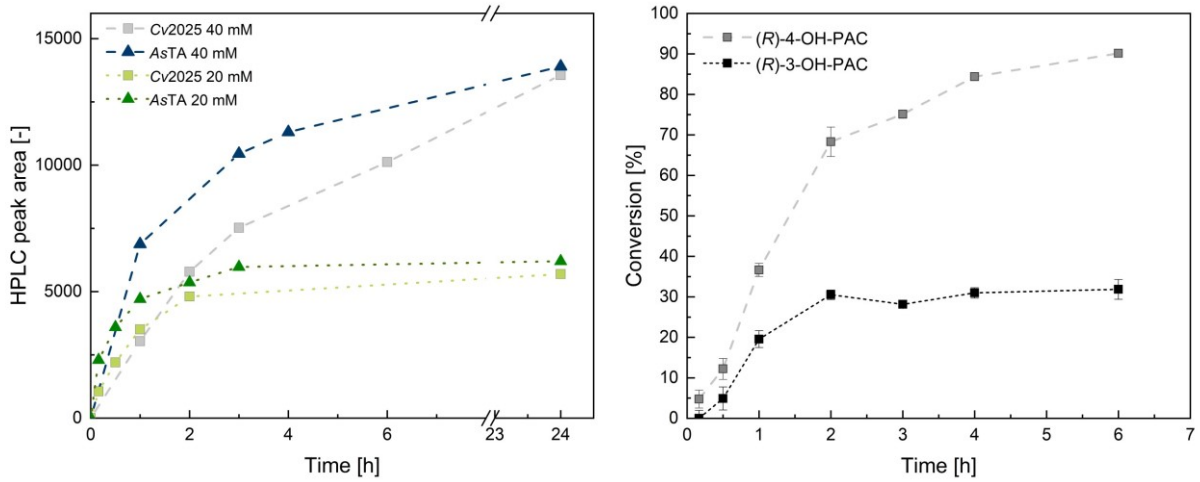

Figure 59 Left: Transamination of 4-OH-PAC with IPA as amine donor. Reaction conditions: 20 mM or 40 mM (*R*)-4-OH-PAC, 250 mM or 500 mM IPA, 1 mM PLP, 100 mM HEPES pH 7.5, 10 mg mL^{-1} lyophilized whole cells. (*Cv*2025 or *As*TA), 30 °C, 850 rpm, 1 mL reaction volume, open reaction vial. The HPLC peak area corresponds to one single product peak, which was not calibrated as no standard reference was available. Right: Comparison of the transamination of (*R*)-3-OH-PAC or (*R*)-4-OH-PAC with IPA towards the respective amino alcohol catalyzed by *Cv*2025. Reaction conditions: 40 mM 3- or 4-OH-PAC, 500 mM IPA, 1 mM PLP, 100 mM HEPES pH 7.5, 10 mg mL^{-1} lyophilized whole cells (*Cv*2025), 30 °C, 850 rpm, 1 mL reaction volume, open reaction vial. The error bars show the variance of technical duplicates.

In these experiments, a 12.5-fold molar excess of IPA was used as amine donor to shift the commonly unfavorable thermodynamic equilibrium of the transamination reaction by evaporation of acetone in an open reaction vial. Although IPA is not gained from renewables, it was feasible to use it for an initial enzyme screening, even though efforts to utilize renewable amine donors such as L-alanine are worthwhile. Notably, the microbial production of acetone and isopropanol in gas fermentations could signify a promising route towards these platform chemicals. In future, this technology could generate IPA from cost-efficient waste gas (or syngas), which can be produced with renewable energy [293]. Likewise, the reaction could be based on bio-based 4-hydroxybenzoate (4-OH-BZ) by including a reduction of 4-OH-BZ to 4-OH-BA as a preliminary step [70]. The carboxylate reductase from *Nocardia otitidiscaviarum* (*No*CAR) was shown to catalyze this reaction [279]. Previously, a one-pot cascade for direct reduction and carboligation of 3-OH-BZ to (*R*)-3-OH-PAC was implemented with *No*CAR and *Ap*PDC var, obtaining 98% yield (not isolated) from 15 mM 3-OH-BZ [70]. However, first experiments in this direction resulted in very low conversions in a one-pot system starting from 4-OH-BZ. For the one-pot two-step enzymatic cascade from 4-OH-BZ to 4-OH-PAC, two biocatalysts were combined in the reaction mixture according to Weber *et al.* (both were lyophilized whole cell formulations of *E. coli* K-12 MG1655 RARE with confirmed production of either *No*CAR or *Ll*KdcA, respectively). The results suggested an incompatibility of the combined reduction-ligation system with *Ll*KdcA, presumably due to the various additives required for the NAD(P)H recycling in the reduction step. As a variation of buffers and cell ratios were thus far not successful to synthesize

4-OH-PAC in a one-pot approach, the reaction steps should be separated by intermediate purification of the aldehyde (4-OH-BA), which was not further pursued within the scope of this thesis. Finally, the direct utilization of microbially produced 4-OH-BZ from fermentation supernatants would possibly require additional reaction engineering efforts, as previously shown in chapter 3.1 for the application of fermentation supernatants as substrate reservoir in an enzymatic carboligation.

3.6.4 Conclusion

An efficient and stereoselective two-step synthesis of 4-hydroxylated aromatic amino alcohols was found. In this way, valuable chiral amino alcohols were derived, which can serve as synthons for APIs. An additional N-alkylation step can provide the APIs ritodrine and ritobegron from the herein synthesized (1*R*,2*S*)-4-OH-AHP. The high chemo- and stereoselectivity and high conversion rate provide a strong alternative to chemically catalyzed syntheses of these compounds. To replace petroleum-based resources with renewable starting materials, the combination with enzymatic reduction of microbially produced 4-hydroxybenzoates should be established. Moreover, the further modification of the 4-hydroxylated amino alcohols by Pictet-Spengler reactions with different derivatized aldehydes might be an interesting way to gain molecular complexity and valorization. In future, increased substrate concentrations would need to reach feasible limits to demonstrate industrial relevance. The obtained results indicate that *Ll*KdcA as lyophilized whole cell formulation is a stable and highly selective biocatalyst for this application.

Chapter 4

General Discussion & Outlook

Contributions:

This chapter was written by Laura Grabowski and revised by Dörte Rother.

4 General Discussion & Outlook

4.1 Opportunities of hybrid processes for bio-based syntheses of chiral products

Hybrid approaches as conceptualized in the "HyImPAct" project combine microbial transformations, (chemo-)enzymatic syntheses and process engineering concepts to establish interdisciplinary processes with economic and ecological benefits. Microbial transformations offer a unique possibility to establish process chains towards platform chemicals from renewable carbon and energy sources. However, some synthetic steps require (engineered) enzymes working at non-physiological pH and high substance loads, which is not suitable for cell growth [122], or step-separation due to undesired cross reactivity. Thus, by combining microbial cell factories (*in vivo*) and biocatalysis (*in vitro*), the efficient production of value-added products from renewable resources can be realized [294]. Although hybrid approaches thereby hold great promise to replace non-sustainable processes in the long-term goal of establishing a circular bioeconomy, few examples have been published or readily implemented thus far [295-297].

In this thesis, the integration of renewable, microbially produced aliphatic precursors (L-alanine and pyruvate) with an enzyme cascade towards the active pharmaceutical ingredient (API) metaraminol was shown. As pyruvate and L-alanine have broad applications in the pharmaceutical, food and feed industry, these compounds are interesting products for engineered microbial cell factories. Here, the combined production of catalyst and product formation in a one-pot process is favorable for bulk platform chemicals. Further conversion towards the API can then be achieved in two stereoselective, enzymatic steps. This approach allowed the replacement of the non-renewable and polluting amine donor isopropylamine (IPA), as well as the enhancement of the overall achievable atom economy through a possible pyruvate recycling step. Several advantages for greener synthesis are certainly evident in this process, including non-toxic and biodegradable biocatalysts, that are active under ambient temperatures and pressure. The technological advances in targeted strain and process engineering in combination with the flexible linkage of enzymes from toolboxes allow for highly selective, atom- and step-efficient synthesis of bio-based, chiral products. In future, by modulating biocatalyst of different selectivity in hybrid cascade concepts, entire isomeric product platforms can be made accessible. The wide range of possible products can be even enlarged by incorporating additional chemical reaction steps [298].

Eventually, the entire synthesis of metaraminol should be based on renewables, specifically also with the bio-derived starting aldehyde. However, instead of producing the starting aldehydes *in vivo*, the microbial production of the corresponding carboxylate was targeted in the HyImPAct

project. This strategy is favorable due to several reasons. First, the carboxylates can be reduced to the respective aldehydes by carboxylate reductases (CARs) [278, 299]. As *in vivo* recycling of cofactors in whole cells was shown, this transformation step could be scalable in a straight-forward way. Second, the accumulation of aldehydes is challenging in living microbes, often imposing toxicity and growth limitations [127]. Furthermore, aldehydes tend to be very reactive (chemically) and are a potential substrate for undesired enzymatic cross reactivity within living cells. In contrast, with various metabolic engineering strategies at hand, high concentrations of substituted aromatic compounds have been produced with engineered *Pseudomonas*, *S. cerevisiae* or *C. glutamicum* [300]. Hence, the microbial production of hydroxybenzoic acids can provide a versatile, bio-based starting point for the production of value-added compounds by further enzymatic and chemical catalysis [301]. As a different starting point, novel technologies utilize one-carbon metabolism, in which complex carbon scaffolds are derived from single-carbon sources, ideally from industrial emissions or syngas, using appropriate enzymes such as carboligases and reductases [302]. Along this line, another promising starting point for hybrid processes could be carbon-negative biosynthesis, which enables carbon fixation and valorization *via* gas fermentations with autotrophic organisms [293, 303].

When designing bio-based hybrid processes, potential pitfalls such as thermodynamic limitations, incompatible reaction conditions or contrary performance optimization goals must be considered. For instance, in microbial bioreactor cultivations, standard metrics to assess the efficiency of the process are the carbon-specific product yields (*e.g.* $mol_{product}\ mol_{substrate}^{-1}$) or the product concentration. However, it is not always possible to maximize both, which requires a tradeoff. For subsequent purification or direct enzymatic utilization of the produced precursors, the product concentration is usually the determining factor, as heavily diluted product in the fermentation broth counteracts efficient downstream processing (DSP), and high concentrations are desired for direct further enzymatic conversion in the fermentation supernatant, as shown in chapter 3.1. This example illustrates, how pivotal performance indicators should be predefined early in the process development. In a recent article, Prof. John Woodley stressed the importance of product concentration (for facilitated DSP) and long-term enzyme stability (for high biocatalyst-specific yields) as the two key factors determining the economic and ecologic feasibility of a biocatalytic process [304]. As these factors are, however, often closely linked (high substrate and product concentration can cause inactivation and instability of enzyme, in turn low stability limits final product concentrations), process engineering methods such as enzyme immobilization, *in situ* substrate supply and direct product recovery can provide powerful means to overcome these challenges, which was demonstrated for the enzymatic, bio-based metaraminol production in this thesis.

Finally, the actual "greenness" of any hybrid process should be evaluated by life cycle assessment (LCA) to assess the footprint and efficiency of the process concept quantitatively or disclose possible bottlenecks. For instance, high energy and water consumption, and waste generation of the overall process must be considered, especially for fermentation processes [305]. Likewise, for enzymatic steps requiring cofactor recycling, the cost and emission contribution of the respective recycling technique must be assessed [306]. Especially in an academic setting, this is rarely possible due to a lack of data availability. However, it is an important pillar for (hybrid) process development in industry. Conclusively, hybrid processes might portray an economically favorable and sustainable alternative if the individual process steps are efficient and smart solutions for interconnections are found. Most likely, an increased complexity does not correspond to a higher process efficiency nor sustainability. Due to this interdependence, every novel hybrid approach must undergo repeated optimization as a one-fits-all solution is not feasible. Nevertheless, as more examples are presented in this direction, general design principles could be derived to pave the way to more sustainable manufacturing.

4.2 Evaluation of process intensification methods presented in this thesis

In recent years, process intensification (PI) has been a growing subject in biochemical engineering research, both in academia and industry, to eventually meet certain process benchmarks [35, 307, 308]. In the field of biocatalysis, PI can be divided into four complementary approaches as depicted in Figure 60: cascade design, enzyme optimization, reaction engineering and process development. Different PI methods were applied in this thesis for the enzymatic multi-step synthesis of chiral amino alcohols, focussing on reaction and process engineering. Reaction engineering of the enzymatic transaminations was pursued with two different amine donors, L-alanine (chapter 3.1 - 3.3) or isopropylamine (chapter 3.4 - 3.6).

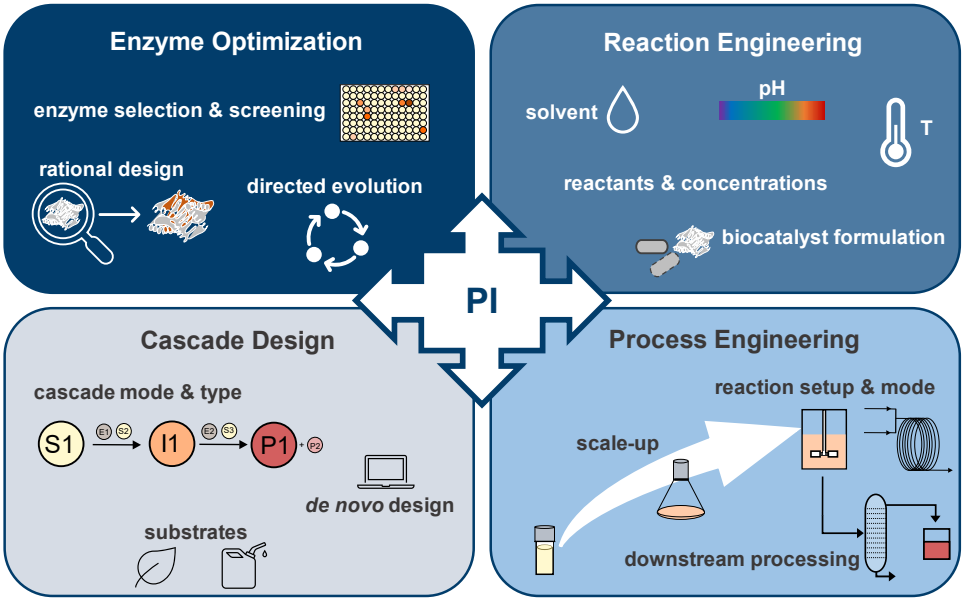

Figure 60 Overview of different approaches for biocatalytic process intensification (PI). The experimental optimization can be divided into cascade design, enzyme optimization, reaction engineering and process development [35].

The reaction mode was of particular importance in the enzymatic synthesis of metaraminol. Precisely, the sequential two-step synthesis consisting of carboligation and transamination (separated reactions with intermediate purification) was a prerequisite to thermodynamically decouple the two reaction steps and thus achieve higher conversions with microbially produced precursors (chapter 3.1). In addition, reducing exceeding incubation times and intermediate purification were effective measures to ensure high stereoselectivity and stability of the intermediate (*R*)-3-OH-PAC.

An aspect that was only partially considered in this work is the reactor selection, which is a crucial step in process intensification [309]. A suitable reactor setup will be especially important for semi-continuous reactive product extraction presented in chapter 3.3. Likewise, it will be crucial for scaling the transamination with IPA as amine donor to allow for sufficient acetone evaporation, as discussed in chapter 3.5. Especially at large scales, headspace and surface-to-volume ratio will be limited, requiring further means to strip acetone from the reaction [105].

Regarding the solvent system, asymmetric syntheses catalyzed by amine transaminases are often restricted to aqueous reaction systems to prevent imine formation and retain enzyme activity and stereoselectivity. However, it is advisable to consider all possible solvent systems beyond aqueous buffer systems for biocatalytic process intensification, as shown previously [52, 310]. The solvent system can have significant impact on the solubility of the substrate or product and consequently on the final concentration and productivity. For this reason, amine transaminase has been applied in disperse systems for conversion of more hydrophobic substrates [311]. Furthermore, the solvent also determines suitable DSP strategies or further connection to chemical reaction steps [312]. For

ISPR, the removal of the product from the reaction phase is required. In *in situ* product crystallization (ISPC), this phase transition of the product occurs from the soluble to the insoluble, solid state [107], whereas in ISPR strategies that are based on liquid-liquid extraction (described in chapter 3.2 and 3.3), the phase transition of the product from the aqueous reaction phase to an organic extraction phase requires a biphasic solvent system. Here, the selection of a suitable extraction solvent that serves both, extractive properties for the target product and biocompatible conditions for high enzyme activity, was of utmost importance. The integration of reactive *in situ* product extraction enabled an equilibrium shift in transamination reactions with L-alanine, leveraging the application of the bio-based amine donor for similar transamination reactions and initiating product recovery, thereby providing an efficient recovery step to commonly challenging purification procedures of amine products (refer to chapter 4.3 for detailed discussion of presented ISPR strategies). The reactive ISPR strategy further reduced enzyme inhibition by both, the substrate (*R*)-3-OH-PAC and the product metaraminol, whereby good product yields were retained also with increased substrate concentrations (chapter 3.3 and 3.5).

Another important consideration for intensifying biocatalytic syntheses is the choice of biocatalyst formulation. In this thesis, lyophilized whole cells were used as simple and cost-effective catalysts, as especially the biocatalyst production must be considered in process design [313]. In industry, the reuse of (bio)catalyst as well as their retention is desired to develop, for example, efficient continuous flow applications, which are beneficial for high space-time yields, especially for *in situ* reactive extractions [142]. The spore display described in chapter 3.4 is a novel *in vivo* immobilization strategy to combine production and immobilization of the biocatalyst. However, considerable improvements of immobilization efficiency and scalability are required to compete with (lyophilized) whole cells. In contrast, a carrier-based method was suitable to immobilize the amine transaminase *Cv*2025 and gave first promising indications for its application in an aqueous-organic reaction system (chapter 3.4). While not within the scope of this thesis, several further approaches concerning enzyme optimization can leverage biocatalytic metaraminol production in the future. In chapter 3.5, it was shown that the reaction system, specifically the 3-hydroxylated 2-hydroxy ketone and the resulting amino alcohol product, likely inactivates the amine transaminase *Cv*2025. The enzyme was additionally compromised by high oleic acid concentrations after implementing reactive product extraction. Therefore, enzyme engineering by rational design or directed evolution approaches can generate new enzyme variants with improved operational stability [314], presenting unique possiblities for further research on this topic.

4.3 Challenges and prospects of ISPR strategies

Two alternative ISPR strategies for the enzymatic synthesis of metaraminol were investigated in this thesis, namely physical and reactive extraction. The specific capabilities and future potential of the extraction-based ISPR of metaraminol can be examined from different point of views.

The physical ISPR strategy allowed to recover metaraminol from the aqueous phase while reducing the amount of co-extracted substrate by performing the reaction at an alkaline pH value. Nevertheless, as the extraction efficiency of the substrate was still equal or higher than that of the product, the overall effectiveness of physical ISPR was limited for metaraminol synthesis. Potentially, this is a common limitation for transamination reactions, in which the substrate and product are structurally similar, and the product is very hydrophilic. A low single-stage extraction efficiency can likely be overcome by measures of process engineering, for example, by multiple extraction stages. However, in this reaction system, reduced enzymatic activity and considerable chemical side reactivity of the product in the alkaline pH range further diminished the feasibility of the ISPR strategy. This illustrates how a compromise-oriented approach is a common prerequisite for the development of ISPR-integrated biotransformations [315].

In turn, the reactive ISPR strategy facilitated high enzymatic activity and stability, high extraction efficiency and selectivity for metaraminol. This ISPR strategy thereby served multiple purposes. First, it allowed for the application of the renewable amine donor L-alanine by shifting the reaction equilibrium, thereby offering a well-performing alternative to the common, oil-based amine donor IPA. Second, metaraminol was recovered in an aqueous acid phase, allowing for easy purification or further synthesis without tremendous energy input required by other DSP operations. Third, the biphasic reaction system seemed to mitigate substrate and product inhibition phenomena, enabling the conversion of higher substrate concentrations with stable yields. These aspects illustrate how, in this reaction system, reactive *in situ* product removal with oleic acid as the reactant was more beneficial. As an environmentally friendly and recyclable solvent system was used, this ISPR strategy is also compatible with the rationale of green chemistry. The non-extractability of L-alanine imposes an additional inherent advantage compared to using IPA as amine donor in extractive ISPR-integrated systems [108, 112].

From a different point of view, several aspects can be stressed regarding its industrial feasibility. The reactive extraction system, which makes use of oleic acid as an inexpensive reactant, meets standard safety requirements for industrial applications, for example concerning flammability and toxicity [164]. The cost-contribution of the chiral, bio-based amine donor L-alanine is substantial (by a factor of 5 compared to IPA when assuming similar molar excess), potentially limiting its economic viability in comparison to other amine donors [104]. A further associated challenge is

the scalability of the reactive ISPR strategy that was herein developed in laboratory (preparative) scale, owing to physicochemical constraints and process costs. In general, liquid-liquid extraction techniques can be favorable as the handling of liquids in apparatuses is easier than solids [316]. Nonetheless, in case of substantial emulsification, the applicability of biphasic reaction systems in industrial scales can be restricted. Measures to mitigate insufficient phase separation and allow for biocatalyst retention have involved membrane-based strategies [108, 184, 317, 318]. The spatial segregation achieved by membrane extraction can retain the (immobilized) biocatalyst, separate process streams and facilitate higher yields by *in situ* product recovery, all while increasing the overall process complexity. A semi-continuous setup using a membrane contactor was presented for metaraminol recovery in chapter 3.3.3.5. In literature, techno-economic assessment of biocatalytic chiral amine production with membrane-based *in situ* product extraction revealed the final product amine concentration (and ratio of product amine to amine donor) in the extractant solution and the membrane flux of the product amine as decisive key factors for the resulting manufacturing costs of different ISPR-integrated process scenarios [319]. In this regard, the thus far achieved metaraminol concentration in the back extraction phase must be further increased to achieve an economically feasible process. Here, several degrees of freedom are conceivable such as increasing the enzymatic activity and stability through enzyme engineering, cell immobilization *via* chitosan flocculation and utilization of different membranes and experimental setups.

4.4 Transfer of reactive extraction for (*in situ*) recovery of other amine products

As part of this thesis, the transfer of reactive *in situ* product removal towards an alternative product stereoisomer was shown (chapter 3.3.3.4). The previously determined optimal conditions could thereby be transferred to the synthesis of (1*S*,2*S*)-2-amino-1-(3-hydroxyphenyl)propan-1-ol (3-AHP), revealing a robust ISPR system for L-alanine as amine donor. In this way, the previously published production of (1*S*,3*S*,4*S*)-tetrahydroisoquinoline based on (1*S*,2*S*)-3-AHP could potentially be realized from sustainable co-substrates [247]. For an *in situ* application in entirely different reaction systems, a thorough characterization of enzyme compatibility, operating pH and solvent composition is inevitable to ensure optimal process parameters within the potentially narrow operational window. Most likely, trade-offs must be found, depending on predefined benchmarks and ascertained constraints.

Besides its application for *in situ* product removal, the herein presented reactive extraction concept could be included as initial recovery method in the DSP strategy for a variety of chiral amines under certain prerequisites. The characterization of this method showed that the achievable extraction efficiencies were heavily dependent on the pK_a value and hydrophobicity of the specific

amine product [141, 196]. Therefore, while reactive extraction with oleic acid might be applicable to other aromatic amines and vicinal amino alcohols with only one or two alcohol groups, the extraction of more hydrophilic compounds could remain challenging as the affinity towards the organic phase decreases. Furthermore, the efficiency of the recovery method as well as the overall purity of the final product in this case highly depends on the presence of cationic side components in the reaction system, which would be similarly extracted. This would result in additional purifications steps. Therefore, the choice of amine donor not only determines process costs and reaction equilibrium, but it also affects the applicable reaction engineering concepts. For example, a common challenge with α-MBA as amine donor is, that although the equilibrium can be easily shifted by an excess of amine donor, subsequent recovery of the amine product by reactive extraction is heavily compromised by the co-extraction of α-MBA and acetophenone [141]. Likewise, if a high excess of IPA is supplied to shift the reaction equilibrium in transamination reactions by acetone evaporation (chapter 3.5 and 3.6), considerable amounts of IPA would be co-extracted, complicating the product recovery by reactive extraction. This underlines that the bio-based and non-extractable amine donor L-alanine offers an additional advantage in combination with the here presented reactive extraction strategy.

4.5 Outlook

Several future perspectives can be drawn from the results of this work. To overcome solubility limitations in aqueous systems or inhibitions by 3-hydroxylated substrate and products, alternative feeding experiments should be evaluated as a strategy to enhance the product concentrations in transamination reactions to chiral amino alcohols. In this context, automation technology and online-analytics offer great potential to establish efficient and self-regulated enzymatic cascades, especially in combination with selective enzyme regulation.

To transition from laboratory to economically feasible scales, further measures of process intensifcation should be considered. First, the operational stability of both, transaminase and carboligase enzymes used in this study, was compromised by organic solvents, substrate and product concentration or upon immobilization. To engineer biocatalysts for industrial processes, rational design or directed evolution approaches can generate new enzyme variants with improved stability or tolerance towards reaction components, presenting unique possiblities for further research in this direction [320]. In this context, computational approaches for targeted enzyme engineering as well as mathematical modeling of reaction kinetics are promising technologies to leverage these bio-based enzymatic transformations [10, 321]. Based on the findings of this thesis, these approaches will be pursued in the consortium project “MetaProcess” of the Bioeconomy Science Center. Second, robust, large-scale production of biocatalysts is a prerequisite for up-scaling of biotransformations. Hence, fermentation processes meeting both, high cell density and specific activity, have to be developed. In this way, the application of enzymatic carboligation and transamination chemistry in multi-enzyme catalyzed processes from bio-based resources can contribute to efficient and synergistic value chains in a circular bioeconomy.

References

1. Sheldon, R.A. and D. Brady, Green Chemistry, Biocatalysis, and the Chemical Industry of the Future. ChemSusChem, 2022. **15**(9): e202102628.
2. Sheldon, R.A. and J.M. Woodley, Role of Biocatalysis in Sustainable Chemistry. Chemical Reviews, 2018. **118**(2): 801-838.
3. Anastas, P.T. and J.C. Warner, Green Chemistry: theory and practice. 1998, New York: Oxford University Press.
4. García-Serna, J., L. Pérez-Barrigón, and M.J. Cocero, New trends for design towards sustainability in chemical engineering: Green engineering. Chemical Engineering Journal, 2007. **133**(1): 7-30.
5. Sheldon, R.A., The E factor 25 years on: the rise of green chemistry and sustainability. Green Chemistry, 2017. **19**(1): 18-43.
6. Heckmann, C.M. and F. Paradisi, Looking Back: A Short History of the Discovery of Enzymes and How They Became Powerful Chemical Tools. ChemCatChem, 2020. **12**(24): 6082-6102.
7. Bell, E.L., W. Finnigan, S.P. France, A.P. Green, M.A. Hayes, L.J. Hepworth, S.L. Lovelock, H. Niikura, S. Osuna, E. Romero, K.S. Ryan, N.J. Turner, and S.L. Flitsch, Biocatalysis. Nature Reviews Methods Primers, 2021. **1**(1): 46.
8. Abdelraheem, E.M.M., H. Busch, U. Hanefeld, and F. Tonin, Biocatalysis explained: from pharmaceutical to bulk chemical production. Reaction Chemistry & Engineering, 2019. **4**(11): 1878-1894.
9. Lancaster, L., W. Abdallah, S. Banta, and I. Wheeldon, Engineering enzyme microenvironments for enhanced biocatalysis. Chemical Society Reviews, 2018. **47**(14): 5177-5186.
10. Yi, D., T. Bayer, C.P.S. Badenhorst, S. Wu, M. Doerr, M. Höhne, and U.T. Bornscheuer, Recent trends in biocatalysis. Chemical Society Reviews, 2021. **50**(14): 8003-8049.
11. Savile, C.K., J.M. Janey, E.C. Mundorff, J.C. Moore, S. Tam, W.R. Jarvis, J.C. Colbeck, A. Krebber, F.J. Fleitz, J. Brands, P.N. Devine, G.W. Huisman, and G.J. Hughes, Biocatalytic asymmetric synthesis of chiral amines from ketones applied to sitagliptin manufacture. Science, 2010. **329**(5989): 305-309.
12. Kinner, A., P. Nerke, R. Siedentop, T. Steinmetz, T. Classen, K. Rosenthal, M. Nett, J. Pietruszka, and S. Lütz, Recent Advances in Biocatalysis for Drug Synthesis. Biomedicines, 2022. **10**(5): 964.
13. Jiang, J., X. Chen, D. Zhang, Q. Wu, and D. Zhu, Characterization of (*R*)-selective amine transaminases identified by in silico motif sequence blast. Applied Microbiology and Biotechnology, 2015. **99**(6): 2613-2621.
14. Brooks, W.H., W.C. Guida, and K.G. Daniel, The significance of chirality in drug design and development. Current Topics in Medicinal Chemistry, 2011. **11**(7): 760-770.
15. Malik, M.S., E.-S. Park, and J.-S. Shin, Features and technical applications of ω-transaminases. Applied Microbiology and Biotechnology, 2012. **94**(5): 1163-1171.
16. Trost, B.M., Asymmetric catalysis: An enabling science. Proceedings of the National Academy of Sciences, 2004. **101**(15): 5348-5355.
17. Kamanna, K., Organocatalysts based on natural and modified amino acids for asymmetric reactions. Physical Sciences Reviews, 2022. **7**(4-5): 429-467.
18. Qu, G., Y. Bi, B. Liu, J. Li, X. Han, W. Liu, Y. Jiang, Z. Qin, and Z. Sun, Unlocking the stereoselectivity and substrate acceptance of enzymes: proline-induced loop engineering test. Angewandte Chemie International Edition, 2022. **61**(1): e202110793.

19. Bergmeier, S.C., The synthesis of vicinal amino alcohols. Tetrahedron, 2000. **56**(17): 2561-2576.
20. Lee, H.-K., S. Kang, and E.B. Choi, Stereoselective synthesis of norephedrine and norpseudoephedrine by using asymmetric transfer hydrogenation accompanied by dynamic kinetic resolution. The Journal of Organic Chemistry, 2012. **77**(12): 5454-5460.
21. Gollapudy Subrahmanyam, S.V.J., Ashutosh Digambar Gupte, Minal Madhukar Butala, Venkat Padmanabha Dendukuri, Amit Hari Pakhurde, Novel process for reductive amination of prochiral ketones, 2012, India, 1477/MUM/2012.
22. Cwik, A., A. Fuchs, Z. Hell, and J.-M. Clacens, Nitroaldol-reaction of aldehydes in the presence of non-activated Mg:Al 2:1 hydrotalcite; a possible new mechanism for the formation of 2-aryl-1,3-dinitropropanes. Tetrahedron, 2005. **61**(16): 4015-4021.
23. Lang, K., J. Park, and S. Hong, Urea/transition-metal cooperative catalyst for anti-selective asymmetric nitroaldol reactions. Angewandte Chemie International Edition, 2012. **51**(7): 1620-1624.
24. Satianegara, G., M. Breuer, B. Hauer, P.L. Rogers, and B. Rosche, Enzymatic (*R*)-phenylacetylcarbinol production in a benzaldehyde emulsion system with *Candida utilis* cells. Applied Microbiology and Biotechnology, 2006. **70**(2): 170-175.
25. Pimparkar, K.P., D.J. Miller, and J.E. Jackson, Hydrogenation of amino acid mixtures to amino alcohols. Industrial & Engineering Chemistry Research, 2008. **47**(20): 7648-7653.
26. Tamura, M., R. Tamura, Y. Takeda, Y. Nakagawa, and K. Tomishige, Catalytic hydrogenation of amino acids to amino alcohols with complete retention of configuration. Chemical Communications, 2014. **50**(50): 6656-6659.
27. Gao, W.-T., Q. Chen, M.-G. Du, W.-M. Zhang, C.-Y. Cao, and W.-G. Song, Enabling an atom-economic production of chiral amino alcohols by electrodialysis with bipolar membranes. Green Chemistry, 2020. **22**(7): 2213-2224.
28. Domínguez de María, P., G. de Gonzalo, and A. Alcántara, Biocatalysis as useful tool in asymmetric synthesis: an assessment of recently granted patents (2014–2019). Catalysts, 2019. **9**(10): 802.
29. Schwarz, J.L., R. Kleinmans, T.O. Paulisch, and F. Glorius, 1,2-Amino alcohols *via* Cr/photoredox dual-catalyzed addition of α-amino carbanion equivalents to carbonyls. Journal of the American Chemical Society, 2020. **142**(5): 2168-2174.
30. Pan, S., M. Jiang, J. Hu, R. Xu, X. Zeng, and G. Zhong, Synthesis of 1,2-amino alcohols by decarboxylative coupling of amino acid derived α-amino radicals to carbonyl compounds *via* visible-light photocatalyst in water. Green Chemistry, 2020. **22**(2): 336-341.
31. Ward, J. and R. Wohlgemuth, High-yield biocatalytic amination reactions in organic synthesis. Current Organic Chemistry, 2010. **14**(17): 1914-1927.
32. Hanefeld, U., F. Hollmann, and C.E. Paul, Biocatalysis making waves in organic chemistry. Chemical Society Reviews, 2022. **51**(2): 594-627.
33. Rudroff, F., M.D. Mihovilovic, H. Gröger, R. Snajdrova, H. Iding, and U.T. Bornscheuer, Opportunities and challenges for combining chemo- and biocatalysis. Nature Catalysis, 2018. **1**(1): 12-22.
34. Gomm, A. and E. O'Reilly, Transaminases for chiral amine synthesis. Current Opinion in Chemical Biology, 2018. **43**: 106-112.
35. Siedentop, R., C. Claaßen, D. Rother, S. Lütz, and K. Rosenthal, Getting the most out of enzyme cascades: strategies to optimize *in vitro* multi-enzymatic reactions. Catalysts, 2021. **11**(10): 1183.
36. McDonald, A.D., S.K. Bruffy, A.T. Kasat, and A.R. Buller, Engineering enzyme substrate scope complementarity for promiscuous cascade synthesis of 1,2-amino alcohols. Angewandte Chemie International Edition. **61**(46): e202212637.

37. Villegas-Torres, M.F., R.J. Martinez-Torres, A. Cázares-Körner, H. Hailes, F. Baganz, and J. Ward, Multi-step biocatalytic strategies for chiral amino alcohol synthesis. Enzyme and Microbial Technology, 2015. **81**: 23-30.
38. Zhang, J.-D., Y.-W. Chang, R. Dong, X.-X. Yang, L.-L. Gao, J. Li, S.-P. Huang, X.-M. Guo, C.-F. Zhang, and H.-H. Chang, Enantioselective cascade biocatalysis for deracemization of racemic β-amino alcohols to enantiopure (*S*)-*β*-amino alcohols by employing cyclohexylamine oxidase and ω-transaminase. ChemBioChem, 2021. **22**(1): 124-128.
39. Sehl, T., H.C. Hailes, J.M. Ward, U. Menyes, M. Pohl, and D. Rother, Efficient 2-step biocatalytic strategies for the synthesis of all nor(pseudo)ephedrine isomers. Green Chemistry, 2014. **16**(6): 3341-3348.
40. Sehl, T., H.C. Hailes, J.M. Ward, R. Wardenga, E. von Lieres, H. Offermann, R. Westphal, M. Pohl, and D. Rother, Two steps in one pot: enzyme cascade for the synthesis of nor(pseudo)ephedrine from inexpensive starting materials. Angewandte Chemie International Edition, 2013. **52**(26): 6772-6775.
41. Corrado, M.L., T. Knaus, and F.G. Mutti, High regio- and stereoselective multi-enzymatic synthesis of all phenylpropanolamine stereoisomers from β-methylstyrene. ChemBioChem, 2021. **22**(13): 2345-2350.
42. Gruber, P., F. Carvalho, M.P.C. Marques, B. O'Sullivan, F. Subrizi, D. Dobrijevic, J. Ward, H.C. Hailes, P. Fernandes, R. Wohlgemuth, F. Baganz, and N. Szita, Enzymatic synthesis of chiral amino-alcohols by coupling transketolase and transaminase-catalyzed reactions in a cascading continuous-flow microreactor system. Biotechnology and Bioengineering, 2018. **115**(3): 586-596.
43. Ingram, C.U., M. Bommer, M.E.B. Smith, P.A. Dalby, J.M. Ward, H.C. Hailes, and G.J. Lye, One-pot synthesis of amino-alcohols using a *de-novo* transketolase and β-alanine: Pyruvate transaminase pathway in *Escherichia coli.* Biotechnology and Bioengineering, 2007. **96**(3): 559-569.
44. Corrado, M.L., T. Knaus, U. Schwaneberg, and F.G. Mutti, High-yield synthesis of enantiopure 1,2-amino alcohols from L-phenylalanine *via* linear and divergent enzymatic cascades. Organic Process Research & Development, 2022. **26**(7): 2085-2095.
45. Kohls, H., M. Anderson, J. Dickerhoff, K. Weisz, A. Córdova, P. Berglund, H. Brundiek, U.T. Bornscheuer, and M. Höhne, Selective access to all four diastereomers of a 1,3-amino alcohol by combination of a keto reductase- and an amine transaminase-catalysed reaction. Advanced Synthesis & Catalysis, 2015. **357**(8): 1808-1814.
46. Busto, E., R.C. Simon, N. Richter, and W. Kroutil, Enzymatic synthesis of chiral amines using ω-transaminases, amine oxidases, and the berberine bridge enzyme, in Green Biocatalysis, R.N. Patel, Editor. 2016, John Wiley & Sons, Inc. p. 17-57.
47. Ducrot, L., M. Bennett, A.A. Caparco, J.A. Champion, A.S. Bommarius, A. Zaparucha, G. Grogan, and C. Vergne-Vaxelaire, Biocatalytic reductive amination by native amine dehydrogenases to access short chiral alkyl amines and amino alcohols. Frontiers in Catalysis, 2021. **1**: 781284.
48. Chen, F.-F., S.C. Cosgrove, W.R. Birmingham, J. Mangas-Sanchez, J. Citoler, M.P. Thompson, G.-W. Zheng, J.-H. Xu, and N.J. Turner, Enantioselective synthesis of chiral vicinal amino alcohols using amine dehydrogenases. ACS Catalysis, 2019. **9**(12): 11813-11818.
49. Maugeri, Z. and D. Rother, Reductive amination of ketones catalyzed by whole cell biocatalysts containing imine reductases (IREDs). Journal of Biotechnology, 2017. **258**: 167-170.
50. Grogan, G. and N.J. Turner, InspIRED by nature: NADPH-dependent imine reductases (IREDs) as catalysts for the preparation of chiral amines. Chemistry – A European Journal, 2016. **22**(6): 1900-1907.

51. Li, Y., N. Hu, Z. Xu, Y. Cui, J. Feng, P. Yao, Q. Wu, D. Zhu, and Y. Ma, Asymmetric synthesis of *N*-substituted 1,2-amino alcohols from simple aldehydes and amines by one-pot sequential enzymatic hydroxymethylation and asymmetric reductive amination. Angewandte Chemie International Edition, 2022. **61**(17): e202116344.
52. van Schie, M.M.C.H., J.-D. Spöring, M. Bocola, P. Domínguez de María, and D. Rother, Applied biocatalysis beyond just buffers – from aqueous to unconventional media. Options and guidelines. Green Chemistry, 2021. **23**(9): 3191-3206.
53. Jaffery, S.M.F., M.A. Khan, S. Ullah, Atia-tul-Wahab, M.I. Choudhary, and F.Z. Basha, Synthesis of new valinol-derived sultam triazoles as α-glucosidase inhibitors. ChemistrySelect, 2021. **6**(37): 9780-9786.
54. Fuchs, C.S., R.C. Simon, W. Riethorst, F. Zepeck, and W. Kroutil, Synthesis of (*R*)- or (*S*)-valinol using ω-transaminases in aqueous and organic media. Bioorganic & Medicinal Chemistry, 2014. **22**(20): 5558-5562.
55. Villegas-Torres, M.F., J.M. Ward, and F. Baganz, Optimisation of enzyme cascades for chiral amino alcohol synthesis in aid of host cell integration using a statistical experimental design approach. Journal of Biotechnology, 2018. **281**: 150-160.
56. Malkov, A.V., M.A. Kabeshov, M. Bella, O. Kysilka, D.A. Malyshev, K. Pluháčková, and P. Kočovský, Vicinal amino alcohols as organocatalysts in asymmetric cross-aldol reaction of ketones: application in the synthesis of convolutamydine A. Organic Letters, 2007. **9**(26): 5473-5476.
57. Flavahan, N.A., Phenylpropanolamine constricts mouse and human blood vessels by preferentially activating α_2-adrenoceptors. Journal of Pharmacology and Experimental Therapeutics, 2005. **313**(1): 432-439.
58. Kalyanasundar, B., C.I. Perez, B. Arroyo, M.G. Moreno, and R. Gutierrez, The appetite suppressant D-norpseudoephedrine (cathine) acts *via* D1/D2-like dopamine receptors in the nucleus accumbens shell. Frontiers in Neuroscience, 2020. **14**: 572328.
59. Yaju, Y. and T. Nakayama, Effectiveness and safety of ritodrine hydrochloride for the treatment of preterm labour: a systematic review. Pharmacoepidemiology and Drug Safety, 2006. **15**(11): 813-822.
60. Maruyama, I., S. Tatemichi, Y. Goi, K. Maruyama, Y. Hoyano, Y. Yamazaki, and H. Kusama, Effects of ritobegron (KUC-7483), a novel selective β_3-adrenoceptor agonist, on bladder function in cynomolgus monkey. Journal of Pharmacology and Experimental Therapeutics, 2012. **342**(1): 163-168.
61. Ngan Kee, Warwick D., Tze K. Lau, Kim S. Khaw, and Bee B. Lee, Comparison of metaraminol and ephedrine infusions for maintaining arterial pressure during spinal anesthesia for elective cesarean section. Anesthesiology, 2001. **95**(2): 307-313.
62. Estafanous, F.G., P.G. Barash, and J.G. Reves, Cardiac anesthesia: principles and clinical practice. 1994, Philadelphia, USA: J.B. Lippincott Company.
63. Brik, A. and C.-H. Wong, HIV-1 protease: mechanism and drug discovery. Organic & Biomolecular Chemistry, 2003. **1**(1): 5-14.
64. Merrill, A.H., Jr., M.C. Sullards, E. Wang, K.A. Voss, and R.T. Riley, Sphingolipid metabolism: roles in signal transduction and disruption by fumonisins. Environmental Health Perspectives, 2001. **109**(2): 283-289.
65. Astrup, A., L. Breum, and S. Toubro, Pharmacological and clinical studies of ephedrine and other thermogenic agonists. Obesity Research, 1995. **3**(4): 537-540.
66. Gupta, P. and N. Mahajan, Biocatalytic approaches towards the stereoselective synthesis of vicinal amino alcohols. New Journal of Chemistry, 2018. **42**(15): 12296-12327.
67. Erdmann, V., B.R. Lichman, J. Zhao, R.C. Simon, W. Kroutil, J.M. Ward, H.C. Hailes, and D. Rother, Enzymatic and chemoenzymatic three-step cascades for the synthesis of stereochemically complementary trisubstituted tetrahydroisoquinolines. Angewandte Chemie International Edition, 2017. **56**(41): 12503-12507.

68. Wilson, R.J., E. Jecs, E.J. Miller, H.H. Nguyen, Y.A. Tahirovic, V.M. Truax, M.B. Kim, K.M. Kuo, T. Wang, C.S. Sum, M.E. Cvijic, A.A. Paiva, G.M. Schroeder, L.J. Wilson, and D.C. Liotta, Synthesis and SAR of 1,2,3,4-tetrahydroisoquinoline-based CXCR4 antagonists. ACS Medicinal Chemistry Letters, 2018. **9**(1): 17-22.
69. Ye, K., Y. Ke, N. Keshava, J. Shanks, J.A. Kapp, R.R. Tekmal, J. Petros, and H.C. Joshi, Opium alkaloid noscapine is an antitumor agent that arrests metaphase and induces apoptosis in dividing cells. Proceedings of the National Academy of Sciences, 1998. **95**(4): 1601-1606.
70. Weber, D., Biocatalytic reduction of carboxylic acids - production and application of carboxylate reductases in synthetic enzyme cascades. Doctoral thesis, 2022. RWTH Aachen University.
71. Brovetto, M., D. Gamenara, P. Saenz Méndez, and G.A. Seoane, C−C bond-forming lyases in organic synthesis. Chemical Reviews, 2011. **111**(7): 4346-4403.
72. Chandra Raj, K., L.O. Ingram, and J.A. Maupin-Furlow, Pyruvate decarboxylase: a key enzyme for the oxidative metabolism of lactic acid by *Acetobacter pasteurianus*. Archives of Microbiology, 2001. **176**(6): 443-451.
73. Nemeria, N.S., S. Chakraborty, A. Balakrishnan, and F. Jordan, Reaction mechanisms of thiamin diphosphate enzymes: defining states of ionization and tautomerization of the cofactor at individual steps. The FEBS Journal, 2009. **276**(9): 2432-3446.
74. Frank, R.A., F.J. Leeper, and B.F. Luisi, Structure, mechanism and catalytic duality of thiamine-dependent enzymes. Cellular and Molecular Life Sciences, 2007. **64**(7-8): 892-905.
75. Rother , D., G. Kolter, T. Gerhards, C.L. Berthold, E. Gauchenova, M. Knoll, J. Pleiss, M. Müller, G. Schneider, and M. Pohl, *S*-selective mixed carboligation by structure-based design of the pyruvate decarboxylase from *Acetobacter pasteurianus*. ChemCatChem, 2011. **3**(10): 1587-1596.
76. Wechsler, C., Intermediates in the carboligation of the ThDP-dependent pyruvate decarboxylase - Tailor-made enzyme catalysts for industrial applications. Doctoral thesis, 2014. Georg August University of Göttingen.
77. Jansonius, J.N., Structure, evolution and action of vitamin B6-dependent enzymes. Current Opinion in Structural Biology, 1998. **8**(6): 759-769.
78. Taylor, P.P., D.P. Pantaleone, R.F. Senkpeil, and I.G. Fotheringham, Novel biosynthetic approaches to the production of unnatural amino acids using transaminases. Trends in Biotechnology, 1998. **16**(10): 412-418.
79. Skalden, L., M. Thomsen, M. Höhne, U.T. Bornscheuer, and W. Hinrichs, Structural and biochemical characterization of the dual substrate recognition of the (*R*)-selective amine transaminase from *Aspergillus fumigatus*. The FEBS Journal, 2015. **282**(2): 407-415.
80. Mehta, P.K., T.I. Hale, and P. Christen, Aminotransferases: demonstration of homology and division into evolutionary subgroups. European Journal of Biochemistry, 1993. **214**(2): 549-561.
81. Cassimjee, K.E., M.S. Humble, V. Miceli, C.G. Colomina, and P. Berglund, Active site quantification of an ω-transaminase by performing a half transamination reaction. ACS Catalysis, 2011. **1**(9): 1051-1055.
82. Cassimjee, K.E., B. Manta, and F. Himo, A quantum chemical study of the ω-transaminase reaction mechanism. Organic & Biomolecular Chemistry, 2015. **13**(31): 8453-8464.
83. Telzerow, A., J. Paris, M. Håkansson, J. González-Sabín, N. Ríos-Lombardía, H. Gröger, F. Morís, M. Schürmann, H. Schwab, and K. Steiner, Expanding the toolbox of *R*-selective amine transaminases by identification and characterization of new members. ChemBioChem, 2021. **22**(7): 1232-1242.

84. Guan, L.-J., J. Ohtsuka, M. Okai, T. Miyakawa, T. Mase, Y. Zhi, F. Hou, N. Ito, A. Iwasaki, Y. Yasohara, and M. Tanokura, A new target region for changing the substrate specificity of amine transaminases. Scientific Reports, 2015. **5**(1): 10753.
85. Kaulmann, U., K. Smithies, M.E.B. Smith, H.C. Hailes, and J.M. Ward, Substrate spectrum of ω-transaminase from *Chromobacterium violaceum* DSM30191 and its potential for biocatalysis. Enzyme and Microbial Technology, 2007. **41**(5): 628-637.
86. Humble, M.S., K.E. Cassimjee, M. Håkansson, Y.R. Kimbung, B. Walse, V. Abedi, H.J. Federsel, P. Berglund, and D.T. Logan, Crystal structures of the *Chromobacterium violaceum* ω-transaminase reveal major structural rearrangements upon binding of coenzyme PLP. The FEBS Journal, 2012. **279**(5): 779-792.
87. Smithies, K., M.E.B. Smith, U. Kaulmann, J.L. Galman, J.M. Ward, and H.C. Hailes, Stereoselectivity of an ω-transaminase-mediated amination of 1,3-dihydroxy-1-phenylpropane-2-one. Tetrahedron: Asymmetry, 2009. **20**(5): 570-574.
88. Du, C., L. Rios-Solis, J. Ward, P. Dalby, and G. Lye, Evaluation of CV2025 *ω*-transaminase for the bioconversion of lignin breakdown products into value-added chemicals: Synthesis of vanillylamine from vanillin. Biocatalysis and Biotransformation 2014. **32**.
89. Hanson, R.L., B.L. Davis, Y. Chen, S.L. Goldberg, W.L. Parker, T.P. Tully, M.A. Montana, and R. Patel, Preparation of (*R*)-amines from racemic amines with an (*S*)-amine transaminase from *Bacillus megaterium.* Advanced Synthesis & Catalysis, 2008. **350**: 1367-1375.
90. Erdmann, V., T. Sehl, I. Frindi-Wosch, R.C. Simon, W. Kroutil, and D. Rother, Methoxamine synthesis in a biocatalytic 1-pot 2-step cascade approach. ACS Catalysis, 2019. **9**(8): 7380-7388.
91. van Oosterwijk, N., S. Willies, J. Hekelaar, A.C. Terwisscha van Scheltinga, N.J. Turner, and B.W. Dijkstra, Structural basis of the substrate range and enantioselectivity of two (*S*)-selective ω-transaminases. Biochemistry, 2016. **55**(31): 4422-4431.
92. Shin, J.S. and B.G. Kim, Substrate inhibition mode of omega-transaminase from *Vibrio fluvialis* JS17 is dependent on the chirality of substrate. Biotechnology and Bioengineering, 2002. **77**(7): 832-837.
93. Guo, F. and P. Berglund, Transaminase biocatalysis: optimization and application. Green Chemistry, 2017. **19**(2): 333-360.
94. Weiß, M.S., I.V. Pavlidis, P. Spurr, S.P. Hanlon, B. Wirz, H. Ding, and U.T. Bornscheuer, Amine transaminase engineering for spatially bulky substrate acceptance. ChemBioChem, 2017. **18**(11): 1022-1026.
95. Dawood, A.W.H., M.S. Wei, C. Schulz, I.V. Pavlidis, H. Iding, R.O.M.A. de Souza, and U.T. Bornscheuer, Isopropylamine as amine donor in transaminase-catalyzed reactions: better acceptance through reaction and enzyme engineering. ChemCatChem, 2018. **10**(18): 3943-3949.
96. Chen, S., H. Land, P. Berglund, and M.S. Humble, Stabilization of an amine transaminase for biocatalysis. Journal of Molecular Catalysis B: Enzymatic, 2016. **124**: 20-28.
97. Börner, T., S. Rämisch, E.R. Reddem, S. Bartsch, A. Vogel, A.-M.W.H. Thunnissen, P. Adlercreutz, and C. Grey, Explaining operational instability of amine transaminases: substrate-induced inactivation mechanism and influence of quaternary structure on enzyme–cofactor intermediate stability. ACS Catalysis, 2017. **7**(2): 1259-1269.
98. Roura Padrosa, D., R. Alaux, P. Smith, I. Dreveny, F. López-Gallego, and F. Paradisi, Enhancing PLP-binding capacity of Class-III ω-transaminase by single residue substitution. Frontiers in Bioengineering and Biotechnology, 2019. **7**: 282.
99. Meng, Q., N. Capra, C.M. Palacio, E. Lanfranchi, M. Otzen, L.Z. van Schie, H.J. Rozeboom, A.-M.W.H. Thunnissen, H.J. Wijma, and D.B. Janssen, Robust ω-transaminases by computational stabilization of the subunit interface. ACS Catalysis, 2020. **10**(5): 2915-2928.

100. Velasco-Lozano, S., E. Jackson, M. Ripoll, F. López-Gallego, and L. Betancor, Stabilization of ω-transaminase from *Pseudomonas fluorescens* by immobilization techniques. International Journal of Biological Macromolecules, 2020. **164**: 4318-4328.
101. Gundersen, M.T., R. Abu, M. Schürmann, and J.M. Woodley, Amine donor and acceptor influence on the thermodynamics of ω-transaminase reactions. Tetrahedron: Asymmetry, 2015. **26**(10): 567-570.
102. Hillert, M., Le Chatelier's principle - restated and illustrated with phase diagrams. Journal of Phase Equilibria, 1995. **16**(5): 403-410.
103. Tufvesson, P., J.S. Jensen, W. Kroutil, and J.M. Woodley, Experimental determination of thermodynamic equilibrium in biocatalytic transamination. Biotechnology and Bioengineering, 2012. **109**(8): 2159-2162.
104. Tufvesson, P., M. Nordblad, U. Krühne, M. Schürmann, A. Vogel, R. Wohlgemuth, and J.M. Woodley, Economic considerations for selecting an amine donor in biocatalytic transamination. Organic Process Research & Development, 2015. **19**(6): 652-660.
105. Tufvesson, P., C. Bach, and J.M. Woodley, A model to assess the feasibility of shifting reaction equilibrium by acetone removal in the transamination of ketones using 2-propylamine. Biotechnology and Bioengineering, 2013. **111**(2): 309-319.
106. Satyawali, Y., D.F. del Pozo, P. Vandezande, I. Nopens, and W. Dejonghe, Investigating pervaporation for *in situ* acetone removal as process intensification tool in ω-transaminase catalyzed chiral amine synthesis. Biotechnology Progress, 2019. **35**(1): e2731.
107. Hülsewede, D., M. Tänzler, P. Süss, A. Mildner, U. Menyes, and J. von Langermann, Development of an *in situ*-product crystallization (ISPC)-concept to shift the reaction equilibria of selected amine transaminase-catalyzed reactions. European Journal of Organic Chemistry, 2018. **2018**(18): 2130-2133.
108. Rehn, G., P. Adlercreutz, and C. Grey, Supported liquid membrane as a novel tool for driving the equilibrium of ω-transaminase catalyzed asymmetric synthesis. Journal of Biotechnology, 2014. **179**: 50-55.
109. Heintz, S., T. Börner, R.H. Ringborg, G. Rehn, C. Grey, M. Nordblad, U. Krühne, K.V. Gernaey, P. Adlercreutz, and J.M. Woodley, Development of *in situ* product removal strategies in biocatalysis applying scaled-down unit operations. Biotechnology and Bioengineering, 2017. **114**(3): 600-609.
110. Shin, J.S. and B.G. Kim, Asymmetric synthesis of chiral amines with omega-transaminase. Biotechnology and Bioengineering, 1999. **65**(2): 206-211.
111. Shin, J.S. and B.G. Kim, Kinetic modeling of ω-transamination for enzymatic kinetic resolution of *α*-methylbenzylamine. Biotechnology and Bioengineering, 1998. **60**(5): 534-540.
112. Börner, T., G. Rehn, C. Grey, and P. Adlercreutz, A process concept for high-purity production of amines by transaminase-catalyzed asymmetric synthesis: combining enzyme cascade and membrane-assisted ISPR. Organic Process Research & Development, 2015. **19**(7): 793-799.
113. Telzerow, A., M. Hobisch, M. Müller, M. Schürmann, H. Schwab, and K. Steiner, A co-expression system to shift the equilibrium of transamination reactions toward the synthesis of enantiomerically pure amines. Molecular Catalysis, 2019. **471**: 38-43.
114. Koszelewski, D., I. Lavandera, D. Clay, D. Rozzell, and W. Kroutil, Asymmetric synthesis of optically pure pharmacologically relevant amines employing ω-transaminases. Advanced Synthesis & Catalysis, 2008. **350**(17): 2761-2766.
115. Hyungdon, Y. and B.G. Kim, Asymmetric synthesis of (*S*)-*α*-methylbenzylamine by recombinant *Escherichia coli* co-expressing omega-transaminase and acetolactate synthase. Bioscience, Biotechnology, and Biochemistry, 2008. **72**(11): 3030-3033.

116. Truppo, M.D., J.D. Rozzell, and N.J. Turner, Efficient production of enantiomerically pure chiral amines at concentrations of 50 g/L using transaminases. Organic Process Research & Development, 2010. **14**(1): 234-237.
117. Keil, F.J., Process intensification. Reviews in Chemical Engineering, 2018. **34**(2): 135-200.
118. Van Gerven, T. and A. Stankiewicz, Structure, energy, synergy, time - the fundamentals of process intensification. Industrial & Engineering Chemistry Research, 2009. **48**(5): 2465-2474.
119. Woodley, J.M., Bioprocess intensification for the effective production of chemical products. Computers & Chemical Engineering, 2017. **105**: 297-307.
120. Wohlgemuth, R., T. Twardowski, and A. Aguilar, Bioeconomy moving forward step by step - A global journey. New Biotechnology, 2021. **61**: 22-28.
121. (BioSC), B.S.C. FocusLab HyImPAct. 2023 [cited 2023 May 27]; Available from: https://www.biosc.de/HyImPAct.
122. Wu, S., R. Snajdrova, J.C. Moore, K. Baldenius, and U.T. Bornscheuer, Biocatalysis: enzymatic synthesis for industrial applications. Angewandte Chemie International Edition, 2021. **60**(1): 88-119.
123. Labib, M., L. Grabowski, C. Brüsseler, N. Kallscheuer, L. Wachtendonk, T. Fuchs, A. Jupke, W. Wiechert, J. Marienhagen, D. Rother, and S. Noack, Toward the sustainable production of the active pharmaceutical ingredient metaraminol. ACS Sustainable Chemistry & Engineering, 2022. **10**(16): 5117-5128.
124. Doeker, M., L. Grabowski, D. Rother, and A. Jupke, *In situ* reactive extraction with oleic acid for process intensification in amine transaminase catalyzed reactions. Green Chemistry, 2022. **24**(1): 295-304.
125. Mack, K., M. Doeker, L. Grabowski, A. Jupke, and D. Rother, Extractive *in situ* product removal for the application of naturally produced L-alanine as an amine donor in enzymatic metaraminol production. Green Chemistry, 2021. **23**: 4892-4901.
126. Schmitz, S., Charakterisierung der *in-vivo* Immobilisierung einer Carboligase und einer Amintransaminase über die Sporenoberfläche von *Bacillus subtilis*. Bachelor thesis, 2021. FH Aachen University of Applied Sciences.
127. Kunjapur, A.M., Y. Tarasova, and K.L.J. Prather, Synthesis and accumulation of aromatic aldehydes in an engineered strain of *Escherichia coli*. Journal of the American Chemical Society, 2014. **136**(33): 11644-11654.
128. Kortmann, M., V. Kuhl, S. Klaffl, and M. Bott, A chromosomally encoded T7 RNA polymerase-dependent gene expression system for *Corynebacterium glutamicum*: construction and comparative evaluation at the single-cell level. Microbial Biotechnology, 2015. **8**(2): 253-265.
129. Kallscheuer, N. and J. Marienhagen, *Corynebacterium glutamicum* as platform for the production of hydroxybenzoic acids. Microbial Cell Factories, 2018. **17**(1): 70.
130. Smit, B.A., J.E. van Hylckama Vlieg, W.J. Engels, L. Meijer, J.T. Wouters, and G. Smit, Identification, cloning, and characterization of a *Lactococcus lactis* branched-chain alpha-keto acid decarboxylase involved in flavor formation. Applied Environmental Microbiology, 2005. **71**(1): 303-311.
131. Schäfer, A., A. Tauch, W. Jäger, J. Kalinowski, G. Thierbach, and A. Pühler, Small mobilizable multi-purpose cloning vectors derived from the *Escherichia coli* plasmids pK18 and pK19: selection of defined deletions in the chromosome of *Corynebacterium glutamicum*. Gene, 1994. **145**(1): 69-73.
132. van Ooyen, J., S. Noack, M. Bott, A. Reth, and L. Eggeling, Improved L-lysine production with *Corynebacterium glutamicum* and systemic insight into citrate synthase flux and activity. Biotechnology and Bioengineering, 2012. **109**(8): 2070-2081.

133. Marienhagen, J., N. Kennerknecht, H. Sahm, and L. Eggeling, Functional analysis of all aminotransferase proteins inferred from the genome sequence of *Corynebacterium glutamicum.* Journal of Bacteriology, 2005. **187**(22): 7639-7646.
134. Litsanov, B., M. Brocker, and M. Bott, Toward homosuccinate fermentation: metabolic engineering of *Corynebacterium glutamicum* for anaerobic production of succinate from glucose and formate. Applied Environmental Microbiology, 2012. **78**(9): 3325-3337.
135. Bradford, M.M., A rapid and sensitive method for the quantitation of microgram quantities of protein utilizing the principle of protein-dye binding. Analytical Biochemistry, 1976. **72**(1-2): 248-254.
136. Karava, M., Development of a platform for immobilization of proteins based on *Bacillus subtilis* spores. Doctoral thesis, 2021. Technische Universität Darmstadt.
137. Leighton, T.J. and R.H. Doi, The stability of messenger ribonucleic acid during sporulation in *Bacillus subtilis.* Journal of Biological Chemistry, 1971. **246**(10): 3189-3195.
138. Karava, M., P. Gockel, and J. Kabisch, *Bacillus subtilis* spore surface display of photodecarboxylase for the transformation of lipids to hydrocarbons. Sustainable Energy & Fuels, 2021. **5**(6): 1727-1733.
139. Schätzle, S., M. Höhne, E. Redestad, K. Robins, and U.T. Bornscheuer, Rapid and sensitive kinetic assay for characterization of ω-transaminases. Analytical Chemistry, 2009. **81**(19): 8244–8248.
140. Keilhauer, C., L. Eggeling, and H. Sahm, Isoleucine synthesis in *Corynebacterium glutamicum*: molecular analysis of the ilvB-ilvN-ilvC operon. Journal of Bacteriology, 1993. **175**(17): 5595-5603.
141. Doeker, M., V. Hüttche, and A. Jupke, Reactive extraction for the recovery of primary amines from aqueous streams. Separation and Purification Technology, 2021. **277**: 118229.
142. Clayton, A.D., L.A. Power, W.R. Reynolds, C. Ainsworth, D.R.J. Hose, M.F. Jones, T.W. Chamberlain, A.J. Blacker, and R.A. Bourne, Self-optimising reactive extractions: towards the efficient development of multi-step continuous flow processes. Journal of Flow Chemistry, 2020. **10**(1): 199-206.
143. Tenhaef, N., C. Brüsseler, A. Radek, R. Hilmes, P. Unrean, J. Marienhagen, and S. Noack, Production of d-xylonic acid using a non-recombinant *Corynebacterium glutamicum* strain. Bioresource Technology, 2018. **268**: 332-339.
144. Schnell, S., "Reproducible" research in mathematical sciences requires changes in our peer review culture and modernization of our current publication approach. Bulletin of Mathematical Biology, 2018. **80**(12): 3095-3105.
145. Kelly, S.A., S. Pohle, S. Wharry, S. Mix, C.C.R. Allen, T.S. Moody, and B.F. Gilmore, Application of ω-transaminases in the pharmaceutical industry. Chemical Reviews, 2017. **118**(1): 349-367.
146. Tufvesson, P., J. Lima-Ramos, M. Nordblad, and J.M. Woodley, Guidelines and cost analysis for catalyst production in biocatalytic processes. Organic Process Research & Development, 2011. **15**(1): 266-274.
147. Eggeling, L. and M. Bott, A giant market and a powerful metabolism: L-lysine provided by *Corynebacterium glutamicum.* Applied Microbiology and Biotechnology, 2015. **99**(8): 3387-3394.
148. Tsuge, Y. and H. Matsuzawa, Recent progress in production of amino acid-derived chemicals using *Corynebacterium glutamicum.* World Journal of Microbiology and Biotechnology, 2021. **37**(3): 1-13.
149. Wieschalka, S., B. Blombach, M. Bott, and B.J. Eikmanns, Bio-based production of organic acids with *Corynebacterium glutamicum.* Microbial Biotechnology, 2013. **6**(2): 87-102.

150. Wieschalka, S., B. Blombach, and B.J. Eikmanns, Engineering *Corynebacterium glutamicum* for the production of pyruvate. Applied Microbiology and Biotechnology, 2012. **94**(2): 449-459.
151. Jojima, T., M. Fujii, E. Mori, M. Inui, and H. Yukawa, Engineering of sugar metabolism of *Corynebacterium glutamicum* for production of amino acid L-alanine under oxygen deprivation. Applied Microbiology and Biotechnology, 2010. **87**(1): 159-165.
152. Yamamoto, S., W. Gunji, H. Suzuki, H. Toda, M. Suda, T. Jojima, M. Inui, and H. Yukawa, Overexpression of genes encoding glycolytic enzymes in *Corynebacterium glutamicum* enhances glucose metabolism and alanine production under oxygen deprivation conditions. Applied Environmental Microbiology, 2012. **78**(12): 4447-4457.
153. Okino, S., M. Inui, and H. Yukawa, Production of organic acids by *Corynebacterium glutamicum* under oxygen deprivation. Applied Microbiology and Biotechnology, 2005. **68**(4): 475-480.
154. Tenhaef, N., J. Kappelmann, A. Eich, M. Weiske, L. Brieß, C. Brüsseler, J. Marienhagen, W. Wiechert, and S. Noack, Microaerobic growth-decoupled production of *α*-ketoglutarate and succinate from xylose in a one-pot process using *Corynebacterium glutamicum*. Biotechnology Journal, 2021. **16**(9): 2100043.
155. Kataoka, N., A.S. Vangnai, T. Pongtharangkul, T. Yakushi, M. Wada, A. Yokota, and K. Matsushita, Engineering of *Corynebacterium glutamicum* as a prototrophic pyruvate-producing strain: characterization of a *ramA*-deficient mutant and its application for metabolic engineering. Bioscience, Biotechnology, and Biochemistry, 2019. **83**(2): 372-380.
156. Zelić, B., T. Gerharz, M. Bott, D. Vasic-Racki, C. Wandrey, and R. Takors, Fed-batch process for pyruvate production by recombinant *Escherichia coli* YYC202 strain. Engineering in Life Sciences, 2003. **3**: 299-305.
157. Liu, P., H. Xu, and X. Zhang, Metabolic engineering of microorganisms for L-alanine production. Journal of Industrial Microbiology and Biotechnology, 2021. **49**(2): kuab057.
158. Baraibar, Á.G., E. von Lieres, W. Wiechert, M. Pohl, and D. Rother, Effective Production of (*S*)-α-hydroxy ketones: an reaction engineering approach. Top. Catal., 2014. **57**(5): 401-411.
159. Gerhards, T., U. Mackfeld, M. Bocola, E. von Lieres, W. Wiechert, M. Pohl, and D. Rother, Influence of organic solvents on enzymatic asymmetric carboligations. Advanced Synthesis & Catalysis, 2012. **354**(14-15): 2805-2820.
160. Wagner, R., D.H. Gonzalez, F.E. Podesta, and C.S. Andreo, Changes in the quaternary structure of phosphoenolpyruvate carboxylase induced by ionic strength affect its catalytic activity. European Journal of Biochemistry, 1987. **164**(3): 661-666.
161. Zhou, Y., Z. Li, X. Wang, and H. Zhang, Establishing microbial co-cultures for 3-hydroxybenzoic acid biosynthesis on glycerol. Engineering in Life Sciences, 2019. **19**: 389-395.
162. Weber, D., D. Patsch, A. Neumann, M. Winkler, and D. Rother, Production of the carboxylate reductase from *Nocardia otitidiscaviarum* in a soluble, active form for *in vitro* applications. ChemBioChem, 2021. **22**(10): 1823-1832.
163. Tufvesson, P., J. Lima-Ramos, J.S. Jensen, N. Al-Haque, W. Neto, and J.M. Woodley, Process considerations for the asymmetric synthesis of chiral amines using transaminases. Biotechnology and Bioengineering, 2011. **108**(7): 1479-1493.
164. Demling, P., M. von Campenhausen, C. Grütering, T. Tiso, A. Jupke, and L.M. Blank, Selection of a recyclable *in situ* liquid–liquid extraction solvent for foam-free synthesis of rhamnolipids in a two-phase fermentation. Green Chemistry, 2020. **22**(23): 8495-8510.
165. Neuburger, J., F. Helmholz, S. Tiedemann, P. Lehmann, P. Süss, U. Menyes, and J. von Langermann, Implementation and scale-up of a semi-continuous transaminase-catalyzed reactive crystallization for the preparation of (*S*)-(3-methoxyphenyl)ethylamine. Chemical Engineering and Processing - Process Intensification, 2021. **168**: 108578.

166. Gorden, J., E. Geiser, N. Wierckx, L.M. Blank, T. Zeiner, and C. Brandenbusch, Integrated process development of a reactive extraction concept for itaconic acid and application to a real fermentation broth. Engineering in Life Sciences, 2017. **17**(7): 809-816.
167. Kaur, G., A.K. Srivastava, and S. Chand, Debottlenecking product inhibition in 1,3-propanediol fermentation by *in-situ* product recovery. Bioresource Technology, 2015. **197**: 451-457.
168. Eggert, A., T. Maßmann, D. Kreyenschulte, M. Becker, B. Heyman, J. Büchs, and A. Jupke, Integrated *in-situ* product removal process concept for itaconic acid by reactive extraction, pH-shift back extraction and purification by pH-shift crystallization. Separation and Purification Technology, 2019. **215**: 463-472.
169. Park, E.-S. and J.-S. Shin, Biocatalytic cascade reactions for asymmetric synthesis of aliphatic amino acids in a biphasic reaction system. Journal of Molecular Catalysis B: Enzymatic, 2015. **121**: 9-14.
170. Hülsewede, D., J.-N. Dohm, and J. von Langermann, Donor amine salt-based continuous *in situ*-product crystallization in amine transaminase-catalyzed reactions. Advanced Synthesis & Catalysis, 2019. **361**(11): 2727-2733.
171. Settimo, L., K. Bellman, and R.M.A. Knegtel, Comparison of the accuracy of experimental and predicted pKa values of basic and acidic compounds. Pharmaceutical Research, 2014. **31**(4): 1082-1095.
172. Newton, D.W. and R.B. Kluza, pKa Values of edicinal compounds in pharmacy practice. Drug Intelligence & Clinical Pharmacy, 1978. **12**(9): 546-554.
173. Schell, U., R. Wohlgemuth, and J.M. Ward, Synthesis of pyridoxamine 5′-phosphate using an MBA:pyruvate transaminase as biocatalyst. Journal of Molecular Catalysis B: Enzymatic, 2009. **59**(4): 279-285.
174. Brabander, P., E. Uitterhaegen, E. Verhoeven, C. Cruyssen, K. Winter, and W. Soetaert, *In situ* product recovery of bio-based industrial platform chemicals: a guideline to solvent selection. Fermentation, 2021. **7**: 26.
175. Wang, S., X. Meng, H. Zhou, Y. Liu, F. Secundo, and Y. Liu, Enzyme stability and activity in non-aqueous reaction systems: a mini review. Catalysts, 2016. **6**(2): 32.
176. Halling, P.J., A.C. Ross, and G. Bell, Inactivation of enzymes at the aqueous-organic interface, in Progress in Biotechnology. 1998, Elsevier: Amsterdam, The Netherlands. p. 365-372.
177. Akhtar, M.K., H. Dandapani, K. Thiel, and P.R. Jones, Microbial production of 1-octanol: a naturally excreted biofuel with diesel-like properties. Metabolic Engineering Communications, 2015. **2**: 1-5.
178. Rutter, C.D. and C.V. Rao, Production of 1-decanol by metabolically engineered *Yarrowia lipolytica.* Metabolic Engineering 2016. **38**: 139-147.
179. Grabowski, L., Characterization and process intensification of the enzymatic metaraminol production by implementing liquid-liquid *in situ* product removal. Master thesis, 2019. RWTH Aachen University.
180. Fuchs, M., J.E. Farnberger, and W. Kroutil, The industrial age of biocatalytic transamination. European Journal of Organic Chemistry, 2015. **2015**(32): 6965-6982.
181. Godoy-Alcántar, C., A.K. Yatsimirsky, and J.M. Lehn, Structure-stability correlations for imine formation in aqueous solution. Journal of Physical Organic Chemistry, 2005. **18**(10): 979-985.
182. Castiglione, K., Y. Fu, I. Polte, S. Leupold, A. Meo, and D. Weuster-Botz, Asymmetric whole-cell bioreduction of (*R*)-carvone by recombinant *Escherichia coli* with *in situ* substrate supply and product removal. Biochemical Engineering Journal, 2017. **117**: 102-111.

183. Schmölzer, K., K. Mädje, B. Nidetzky, and R. Kratzer, Bioprocess design guided by *in situ* substrate supply and product removal: process intensification for synthesis of (*S*)-1-(2-chlorophenyl)ethanol. Bioresource Technology, 2012. **108**: 216-223.
184. Matassa, C., A. Romani, D. Ormerod, U.T. Bornscheuer, M. Höhne, and Y. Satyawali, Jeffamine® ED-600: a polyether amine donor for enzymatic transamination in organic solvent/solvent-free medium with membrane-assisted product extraction. Journal of Chemical Technology & Biotechnology, 2019. **95**(3): 604-613.
185. Vázquez-Villegas, P., O. Aguilar, and M. Rito-Palomares, Continuous enzyme aqueous two-phase extraction using a novel tubular mixer-settler in multi-step counter-current arrangement. Separation and Purification Technology, 2015. **141**: 263-268.
186. Ritter, E. and I. Smirnova, Continuous countercurrent extractive biocatalysis in aqueous surfactant two-phase systems. Chemie Ingenieur Technik, 2018. **90**(3): 348-357.
187. Datta, D., S. Kumar, and H. Uslu, Status of the reactive extraction as a method of separation. Journal of Chemistry, 2015. **2015**: 1-16.
188. Toth, A., M. Siebenhofer, and S. Lux, Reactive distillation for solvent regeneration after biphasic carboxylic acid esterification. Chemie Ingenieur Technik, 2021. **93**(10): 1493-1501.
189. Buchbender, F. and M. Wiese, Efficient concentration of an amino acid using reactive extraction coupled with bipolar electrodialysis. Chemical Engineering & Technology, 2018. **41**(12): 2298-2305.
190. De, B., K. Wasewar, V. Dhongde, and T. Mishra, A step forward in the development of *in-situ* product recovery by reactive separation of protocatechuic acid: equilibrium modelling and column design. Reaction Chemistry & Engineering, 2019. **4**(1): 78-89.
191. Steensma, M., N.J.M. Kuipers, A.B. de Haan, and G. Kwant, Influence of process parameters on extraction equilibria for the chiral separation of amines and amino-alcohols with a chiral crown ether. Journal of Chemical Technology & Biotechnology, 2006. **81**(4): 588-597.
192. Steensma, M., N.J. Kuipers, A.B. De Haan, and G. Kwant, Identification of enantioselective extractants for chiral separation of amines and aminoalcohols. Chirality, 2006. **18**(5): 314-328.
193. Tso, W.-W., W.-P. Fung, and M.-Y.W. Tso, Variability of crown ether toxicity. Journal of Inorganic Biochemistry, 1981. **14**(3): 237-244.
194. Krzyżaniak, A., B. Schuur, and D. Haan, Extractive recovery of aqueous diamines for bio-based plastics production. Journal of Chemical Technology & Biotechnology, 2013. **88**: 1937-1945.
195. Utomo, R.N.C., W.-J. Li, T. Tiso, C. Eberlein, M. Doeker, H.J. Heipieper, A. Jupke, N. Wierckx, and L.M. Blank, Defined microbial mixed culture for utilization of polyurethane monomers. ACS Sustainable Chemistry & Engineering, 2020. **8**(47): 17466-17474.
196. Bednarz, A., A.C. Spieß, and A. Pfennig, Reactive and physical extraction of bio-based diamines from fermentation media. Journal of Chemical Technology & Biotechnology, 2017. **92**(7): 1817-1824.
197. Wang, Y., Z. Zhang, X. lu, H. Zong, and B. Zhuge, Genetic engineering of an industrial yeast *Candida glycerinogenes* for efficient production of 2-phenylethanol. Applied Microbiology and Biotechnology, 2020. **104**: 1-11.
198. Grundtvig, I.P.R., S. Heintz, U. Krühne, K.V. Gernaey, P. Adlercreutz, J.D. Hayler, A.S. Wells, and J.M. Woodley, Screening of organic solvents for bioprocesses using aqueous-organic two-phase systems. Biotechnology Advances, 2018. **36**(7): 1801-1814.
199. Elkacmi, R., N. Kamil, M. Bennajah, and S. Kitane, Extraction of oleic acid from moroccan olive mill wastewater. BioMed Research International, 2016. **2016**: 1-9.
200. French, D., Chapter Five - Advances in clinical mass spectrometry, in Advances in Clinical Chemistry, G.S. Makowski, Editor. 2017, Elsevier: Amsterdam, The Netherlands. p. 153-198.

201. Börner, T., S. Rämisch, S. Bartsch, A. Vogel, P. Adlercreutz, and C. Grey, Three in one: temperature, solvent and catalytic stability by engineering the cofactor-binding element of amine transaminase. ChemBioChem, 2017. **18**(15): 1482-1486.
202. Anderson, M., S. Afewerki, P. Berglund, and A. Córdova, Total synthesis of capsaicin analogues from lignin-derived compounds by combined heterogeneous metal, organocatalytic and enzymatic cascades in one pot. Advanced Synthesis & Catalysis, 2014. **356**(9): 2113-2118.
203. Fellechner, O. and I. Smirnova, Process design of a continuous biotransformation with *in situ* product removal by cloud point extraction. The Canadian Journal of Chemical Engineering, 2021. **99**(5): 1035-1049.
204. Peschke, T., P. Bitterwolf, S. Hansen, J. Gasmi, K.S. Rabe, and C.M. Niemeyer, Self-immobilizing biocatalysts maximize space-time yields in flow reactors. Catalysts, 2019. **9**(2): 164.
205. Strumpel, A., Efficiency increase of the synthesis of metaraminol by catalyst recycling using immobilized carboligase and amine transaminase. Bachelor thesis, 2022. FH Darmstadt University of Applied Sciences.
206. Basso, A. and S. Serban, Industrial applications of immobilized enzymes—a review. Molecular Catalysis, 2019. **479**: 110607.
207. Singh, R.K., M.K. Tiwari, R. Singh, and J.-K. Lee, From protein engineering to immobilization: promising strategies for the upgrade of industrial enzymes. International Journal of Molecular Sciences, 2013. **14**(1): 1232-1277.
208. Salvi, H.M. and G.D. Yadav, Process intensification using immobilized enzymes for the development of white biotechnology. Catalysis Science & Technology, 2021. **11**(6): 1994-2020.
209. Kappauf, K., N. Majstorovic, S. Agarwal, D. Rother, and C. Claaßen, Modulation of transaminase activity by encapsulation in temperature-sensitive poly(N-acryloyl glycinamide) hydrogels. ChemBioChem, 2021. **22**(24): 3452-3461.
210. Velasco-Lozano, S., F. López-Gallego, J.C. Mateos-Díaz, and E. Favela-Torres, Cross-linked enzyme aggregates (CLEA) in enzyme improvement – a review. Biocatalysis, 2016. **1**(1): 166-177.
211. Neto, W., M. Schürmann, L. Panella, A. Vogel, and J. Woodley, Immobilisation of ω-transaminase for industrial application: Screening and characterisation of commercial ready to use enzyme carriers. Journal of Molecular Catalysis B: Enzymatic, 2015. **117**: 54-61.
212. Rehm, F.B., S. Chen, and B.H. Rehm, Enzyme engineering for *in situ* immobilization. Molecules, 2016. **21**(10): 1370.
213. Döbber, J., T. Gerlach, H. Offermann, D. Rother, and M. Pohl, Closing the gap for efficient immobilization of biocatalysts in continuous processes: HaloTag™ fusion enzymes for a continuous enzymatic cascade towards a vicinal chiral diol. Green Chemistry, 2018. **20**(2): 544–552.
214. Seide, S., L. Arnold, S. Wetzels, M. Bregu, J. Gätgens, and M. Pohl, From enzyme to preparative cascade reactions with immobilized enzymes: tuning Fe(II)/α-ketoglutarate-dependent lysine hydroxylases for application in biotransformations. Catalysts, 2022. **12**(4): 354.
215. Andrade, L.H., W. Kroutil, and T.F. Jamison, Continuous flow synthesis of chiral amines in organic solvents: immobilization of *E. coli* cells containing both ω-transaminase and PLP. Organic Letters, 2014. **16**(23): 6092-6095.
216. Molnár, Z., E. Farkas, Á. Lakó, B. Erdélyi, W. Kroutil, B.G. Vértessy, C. Paizs, and L. Poppe, Immobilized whole-cell transaminase biocatalysts for continuous-flow kinetic resolution of amines. Catalysts, 2019. **9**(5): 438.

217. Küsters, K., M. Pohl, U. Krauss, G. Ölçücü, S. Albert, K.-E. Jaeger, W. Wiechert, and M. Oldiges, Construction and comprehensive characterization of an EcLDCc-CatIB set—varying linkers and aggregation inducing tags. Microbial Cell Factories, 2021. **20**(1): 49.
218. Pei, X., J. Wang, H. Zheng, Q. Xiao, A. Wang, and W. Su, Catalytically active inclusion bodies (CatIBs) induced by terminally attached self-assembling coiled-coil domains: to enhance the stability of (*R*)-hydroxynitrile lyase. Enzyme and Microbial Technology, 2022. **153**: 109915.
219. Kloss, R., M.H. Limberg, U. Mackfeld, D. Hahn, A. Grünberger, V.D. Jäger, U. Krauss, M. Oldiges, and M. Pohl, Catalytically active inclusion bodies of L-lysine decarboxylase from *E. coli* for 1,5-diaminopentane production. Scientific Reports, 2018. **8**(1): 5856.
220. Benítez-Mateos, A.I., A. Schneider, E. Hegarty, B. Hauer, and F. Paradisi, Spheroplasts preparation boosts the catalytic potential of a squalene-hopene cyclase. Nature Communications, 2022. **13**(1): 6269.
221. Isticato, R., G. Cangiano, H.T. Tran, A. Ciabattini, D. Medaglini, M.R. Oggioni, M. De Felice, G. Pozzi, and E. Ricca, Surface display of recombinant proteins on *Bacillus subtilis* spores. Journal of Bacteriology, 2001. **183**(21): 6294-6301.
222. Bartels, J., S. López Castellanos, J. Radeck, and T. Mascher, Sporobeads: The Utilization of the *Bacillus subtilis* Endospore Crust as a Protein Display Platform. ACS Synthetic Biology, 2018. **7**(2): 452-461.
223. Chen, L., M. Holmes, E. Schaefer, A. Mulchandani, and X. Ge, Highly active spore biocatalyst by self-assembly of co-expressed anchoring scaffoldin and multimeric enzyme. Biotechnology and Bioengineering, 2018. **115**(3): 557-564.
224. Li, Y., X.Y. Butzin, A. Davis, B. Setlow, G. Korza, F.I. Üstok, G. Christie, P. Setlow, and B. Hao, Activity and regulation of various forms of CwlJ, SleB, and YpeB proteins in degrading cortex peptidoglycan of spores of *Bacillus* species *in vitro* and during spore germination. Journal of Bacteriology, 2013. **195**(11): 2530-2540.
225. Ugwuodo, C.J. and T.N. Nwagu, Stabilizing enzymes by immobilization on bacterial spores: a review of literature. International Journal of Biological Macromolecules, 2021. **166**: 238-250.
226. Engelmark Cassimjee, K., M. Kadow, Y. Wikmark, M. Svedendahl Humble, M.L. Rothstein, D.M. Rothstein, and J.E. Bäckvall, A general protein purification and immobilization method on controlled porosity glass: biocatalytic applications. Chemical Communications, 2014. **50**(65): 9134-9137.
227. Coloma, J., T. Lugtenburg, M. Afendi, M. Lazzarotto, P. Bracco, P.-L. Hagedoorn, L. Gardossi, and U. Hanefeld, Immobilization of *Arabidopsis thaliana* hydroxynitrile lyase (AtHNL) on EziG Opal. Catalysts, 2020. **10**(8): 899.
228. Thompson, M.P., S.R. Derrington, R.S. Heath, J.L. Porter, J. Mangas-Sanchez, P.N. Devine, M.D. Truppo, and N.J. Turner, A generic platform for the immobilisation of engineered biocatalysts. Tetrahedron, 2019. **75**(3): 327-334.
229. Thompson, M.P., I. Peñafiel, S.C. Cosgrove, and N.J. Turner, Biocatalysis using immobilized enzymes in continuous flow for the synthesis of fine chemicals. Organic Process Research & Development, 2018. **23**(1): 9–18.
230. Pan, J.-G., S.-K. Choi, H.-C. Jung, and E.-J. Kim, Display of native proteins on *Bacillus subtilis* spores. FEMS Microbiology Letters, 2014. **358**(2): 209-217.
231. Katz, A., A. Alimova, M. Xu, E. Rudolph, P. Gottlieb, and J. Steiner, Refractive index changes during germination of *Bacillus subtilis* spores. Proceedings of SPIE - The International Society for Optical Engineering, 2005. **5692**.
232. Petrillo, C., S. Castaldi, M. Lanzilli, A. Saggese, G. Donadio, L. Baccigalupi, E. Ricca, and R. Isticato, The temperature of growth and sporulation modulates the efficiency of spore-display in *Bacillus subtilis*. Microbial Cell Factories, 2020. **19**(1): 185.

233. Isticato, R., M. Lanzilli, C. Petrillo, G. Donadio, L. Baccigalupi, and E. Ricca, *Bacillus subtilis* builds structurally and functionally different spores in response to the temperature of growth. Environmental Microbiology, 2020. **22**(1): 170-182.
234. Liu, Y., A. Su, R. Tian, J. Li, L. Liu, and G. Du, Developing rapid growing *Bacillus subtilis* for improved biochemical and recombinant protein production. Metabolic Engineering Communications, 2020. **11**: e00141.
235. Errington, J. and L.T.V. Aart, Microbe Profile: *Bacillus subtilis*: model organism for cellular development, and industrial workhorse. Microbiology (Reading), 2020. **166**(5): 425-427.
236. Shuster, B., M. Khemmani, Y. Nakaya, G. Holland, K. Iwamoto, K. Abe, D. Imamura, N. Maryn, A. Driks, T. Sato, and P. Eichenberger, Expansion of the spore surface polysaccharide layer in *Bacillus subtilis* by deletion of genes encoding glycosyltransferases and glucose modification enzymes. Journal of Bacteriology, 2019. **201**(19): e00321-00319.
237. Ölçücü, G., B. Baumer, K. Küsters, K. Möllenhoff, M. Oldiges, J. Pietruszka, K.-E. Jaeger, and U. Krauss, Catalytically active inclusion bodies─benchmarking and application in flow chemistry. ACS Synthetic Biology, 2022. **11**(5): 1881-1896.
238. Jäger, V.D., R. Kloss, A. Grünberger, S. Seide, D. Hahn, T. Karmainski, M. Piqueray, J. Embruch, S. Longerich, U. Mackfeld, K.E. Jaeger, W. Wiechert, M. Pohl, and U. Krauss, Tailoring the properties of (catalytically)-active inclusion bodies. Microbial Cell Factories, 2019. **18**(1): 33.
239. Kloss, R., T. Karmainski, V.D. Jäger, D. Hahn, A. Grünberger, M. Baumgart, U. Krauss, K.-E. Jaeger, W. Wiechert, and M. Pohl, Tailor-made catalytically active inclusion bodies for different applications in biocatalysis. Catalysis Science & Technology, 2018. **8**(22): 5816-5826.
240. De Vitis, V., F. Dall'Oglio, F. Tentori, M.L. Contente, D. Romano, E. Brenna, L. Tamborini, and F. Molinari, Bioprocess intensification using flow reactors: stereoselective oxidation of achiral 1,3-diols with immobilized *Acetobacter aceti*. Catalysts, 2019. **9**(3): 208.
241. Dreßen, A., T. Hilberath, U. Mackfeld, J. Rudat, and M. Pohl, Phenylalanine ammonia lyase from *Arabidopsis thaliana* (AtPAL2): a potent MIO-enzyme for the synthesis of non-canonical aromatic alpha-amino acids.: Part II: Application in different reactor concepts for the production of (*S*)-2-chloro-phenylalanine. Journal of Biotechnology, 2017. **258**: 158-166.
242. Jakoblinnert, A. and D. Rother, A two-step biocatalytic cascade in micro-aqueous medium: using whole cells to obtain high concentrations of a vicinal diol. Green Chemistry, 2014. **16**(7): 3472-3482.
243. Maugeri, Z. and D. Rother, Application of imine reductases (IREDs) in micro-aqueous reaction systems. Advanced Synthesis & Catalysis, 2016. **358**(17): 2745-2750.
244. EnginZyme. EziG Product Data Sheet. 2017 [cited 2022, 4th of October]; Available from: https://enginzyme.com/wp-content/uploads/2017/03/EziG%E2%84%A2-Product-Data-Sheet.pdf.
245. Gardossi, L., P.B. Poulsen, A.O. Ballesteros, K. Hult, V.K. Svedas, D. Vasić-Rački, G. Carrea, A.O. Magnusson, A. Schmid, R. Wohlgemuth, and P.J. Halling, Guidelines for reporting of biocatalytic reactions. Trends in Biotechnology, 2010. **28** (4): 171-180.
246. Mateo, C., J.M. Palomo, G. Fernandez-Lorente, J.M. Guisan, and R. Fernandez-Lafuente, Improvement of enzyme activity, stability and selectivity *via* immobilization techniques. Enzyme and Microbial Technology, 2007. **40**(6): 1451-1463.
247. Gerlach, T., Avoiding cross-reactivities in multi-step enzyme cascades by light-induced enzyme inactivation using genetically encoded photosensitizer fusion tags. Doctoral thesis (to be submitted), 2023. RWTH Aachen University.

248. Mack, K., V. Erdmann, J. Döbber, M. Pohl, H.C. Hailes, W. Kroutil, U.T. Bornscheuer, and D. Rother, Modular enzyme cascades to novel chiral amino alcohols, from screening to atom- and step efficient processes (manuscript in preparation).
249. Böhmer, W., A. Volkov, K. Engelmark Cassimjee, and F.G. Mutti, Continuous flow bioamination of ketones in organic solvents at controlled water activity using immobilized ω-transaminases. Advanced Synthesis & Catalysis, 2020. **362**(9): 1858-1867.
250. Böhmer, W., T. Knaus, A. Volkov, T.K. Slot, N.R. Shiju, K. Engelmark Cassimjee, and F.G. Mutti, Highly efficient production of chiral amines in batch and continuous flow by immobilized ω-transaminases on controlled porosity glass metal-ion affinity carrier. Journal of Biotechnology, 2019. **291**: 52-60.
251. Wilde, P., A. Mackie, F. Husband, P. Gunning, and V. Morris, Proteins and emulsifiers at liquid interfaces. Advances in Colloid and Interface Science, 2004. **108-109**: 63-71.
252. Santi, M., L. Sancineto, V. Nascimento, J. Braun Azeredo, E.V.M. Orozco, L.H. Andrade, H. Gröger, and C. Santi, Flow biocatalysis: a challenging alternative for the synthesis of APIs and natural compounds. International Journal of Molecular Sciences 2021. **22**(3): 990.
253. Chen, S., P. Berglund, and M.S. Humble, The effect of phosphate group binding cup coordination on the stability of the amine transaminase from *Chromobacterium violaceum*. Molecular Catalysis, 2018. **446**: 115-123.
254. Ruggieri, F., J.C. Campillo-Brocal, S. Chen, M.S. Humble, B. Walse, D.T. Logan, and P. Berglund, Insight into the dimer dissociation process of the *Chromobacterium violaceum* (*S*)-selective amine transaminase. Scientific Reports, 2019. **9**(1): 16946.
255. Merz, L.M., L.M. van Langen, and P. Berglund, The role of buffer, pyridoxal 5'-phosphate and light on the stability of the *Silicibacter pomeroyi* transaminase. ChemCatChem, 2022: e202201174.
256. Klos, N., Investigation of factors influencing the enzymatic transamination towards chiral amino alcohols and resulting reaction engineering concepts. Master thesis, 2023. RWTH Aachen University.
257. Kelly, S.A., S. Mix, T.S. Moody, and B.F. Gilmore, Transaminases for industrial biocatalysis: novel enzyme discovery. Applied Microbiology and Biotechnology, 2020. **104**(11): 4781-4794.
258. Smith, M.E.B., B.H. Chen, E.G. Hibbert, U. Kaulmann, K. Smithies, J.L. Galman, F. Baganz, P.A. Dalby, H.C. Hailes, G.J. Lye, J.M. Ward, J.M. Woodley, and M. Micheletti, A multidisciplinary approach toward the rapid and preparative-scale biocatalytic synthesis of chiral amino alcohols: a concise transketolase-/ω-transaminase-mediated synthesis of (2*S*,3*S*)-2-aminopentane-1,3-diol. Organic Process Research & Development, 2010. **14**(1): 99-107.
259. Kelefiotis-Stratidakis, P., T. Tyrikos-Ergas, and I.V. Pavlidis, The challenge of using isopropylamine as an amine donor in transaminase catalysed reactions. Organic & Biomolecular Chemistry, 2019. **17**(7): 1634-1642.
260. Reiber, H., Photochemical reactions of vitamin B6 compounds, isolation and properties of products. Biochimica et Biophysica Acta (BBA) - General Subjects, 1972. **279**(2): 310-315.
261. Rippa, M. and S. Pontremoli, Pyridoxal 5′-phosphate as a specific photosensitizer for histidine residue at the active site of 6-phosphogluconate dehydrogenase. Archives of Biochemistry and Biophysics, 1969. **133**(1): 112-118.
262. Gerlach, T., D.L. Nugroho, and D. Rother, The effect of visible light on the catalytic activity of PLP-dependent enzymes. ChemCatChem, 2021. **13**(10): 2398-2406.
263. Kokkonen, P., A. Beier, S. Mazurenko, J. Damborsky, D. Bednar, and Z. Prokop, Substrate inhibition by the blockage of product release and its control by tunnel engineering. RSC Chemical Biology, 2021. **2**(2): 645-655.

264. Rios-Solis, L., N. Bayir, M. Halim, C. Du, J.M. Ward, F. Baganz, and G.J. Lye, Non-linear kinetic modelling of reversible bioconversions: Application to the transaminase catalyzed synthesis of chiral amino-alcohols. Biochemical Engineering Journal, 2013. **73**: 38-48.
265. Sowa, M.A., Transaminase-mediated synthesis of ß-chiral amines. Doctoral thesis, 2019. Greifswald University.
266. Schmitz, S., Reaction engineering for the enzymatic synthesis of metaraminol as an active pharmaceutical ingredient. Master thesis, 2023. FH Aachen University of Applied Sciences.
267. Gruber, P., M. Marques, B. O'Sullivan, F. Baganz, R. Wohlgemuth, and N. Szita, Conscious coupling: The challenges and opportunities of cascading enzymatic microreactors. Biotechnology Journal, 2017. **12**: 1700030.
268. Winkler, C.K., D. Clay, E. van Heerden, and K. Faber, Overcoming co-product inhibition in the nicotinamide independent asymmetric bioreduction of activated C=C-bonds using flavin-dependent ene-reductases. Biotechnology and Bioengineering, 2013. **110**(12): 3085-3092.
269. Han, S.-W. and J.-S. Shin, *In situ* removal of inhibitory products with ion exchange resins for enhanced synthesis of chiral amines using ω-transaminase. Biochemical Engineering Journal, 2020. **162**: 107718.
270. Schmidt, N.G., E. Eger, and W. Kroutil, Building bridges: biocatalytic C–C-bond formation toward multifunctional products. ACS Catalysis, 2016. **6**(7): 4286-4311.
271. Domínguez de María, P., M. Pohl, D. Gocke, H. Gröger, H. Trauthwein, T. Stillger, L. Walter, and M. Müller, Asymmetric synthesis of aliphatic 2-hydroxy ketones by enzymatic carboligation of aldehydes. European Journal of Organic Chemistry, 2007. **2007**(18): 2940-2944.
272. Zetzsche, L.E. and A.R.H. Narayan, Broadening the scope of biocatalytic C–C bond formation. Nature Reviews Chemistry, 2020. **4**(7): 334-346.
273. Demir, A., P. Ayhan, and S. Sopaci, Thiamine pyrophosphate dependent enzyme catalyzed reactions: stereoselective C–C bond formations in water. CLEAN – Soil, Air, Water, 2007. **35**: 406-412.
274. Müller, M., D. Gocke, and M. Pohl, Thiamin diphosphate in biological chemistry: exploitation of diverse thiamin diphosphate-dependent enzymes for asymmetric chemoenzymatic synthesis. The FEBS Journal, 2009. **276**(11): 2894-2904.
275. Benítez-Mateos, A.I., D. Roura Padrosa, and F. Paradisi, Multistep enzyme cascades as a route towards green and sustainable pharmaceutical syntheses. Nature Chemistry, 2022. **14**(5): 489-499.
276. Hailes, H.C., D. Rother, M. Müller, R. Westphal, J.M. Ward, J. Pleiss, C. Vogel, and M. Pohl, Engineering stereoselectivity of ThDP-dependent enzymes. The FEBS Journal, 2013. **280**(24): 6374-6394.
277. Napora-Wijata, K., G.A. Strohmeier, and M. Winkler, Biocatalytic reduction of carboxylic acids. Biotechnology Journal, 2014. **9**(6): 822-843.
278. Winkler, M., Carboxylic acid reductase enzymes (CARs). Current Opinion in Chemical Biology, 2018. **43**: 23-29.
279. Weber, D., L. de Souza Bastos, M. Winkler, Y. Ni, A.E. Aliev, H.C. Hailes, and D. Rother, Multi-enzyme catalysed processes using purified and whole-cell biocatalysts towards a 1,3,4-substituted tetrahydroisoquinoline. RSC Advances, 2023. **13**(15): 10097-10109.
280. Qu, G., J. Guo, D. Yang, and Z. Sun, Biocatalysis of carboxylic acid reductases: phylogenesis, catalytic mechanism and potential applications. Green Chemistry, 2018. **20**(4): 777-792.
281. Strohmeier, G.A., I.C. Eiteljörg, A. Schwarz, and M. Winkler, Enzymatic one-step reduction of carboxylates to aldehydes with cell-free regeneration of ATP and NADPH. Chemistry, 2019. **25**(24): 6119-6123.

282. Lenzen, C., B. Wynands, M. Otto, J. Bolzenius, P. Mennicken, L.M. Blank, and N. Wierckx, High-yield production of 4-hydroxybenzoate from glucose or glycerol by an engineered *Pseudomonas taiwanensis* VLB120. Frontiers in Bioengineering and Biotechnology, 2019. **7**: 130.
283. Chen, Y., Y. Chen, L. Liu, Y. Zhang, and J. Yuan, Microbial synthesis of 4-hydroxybenzoic acid from renewable feedstocks. Food Chemistry: Molecular Sciences, 2021. **3**: 100059.
284. Kitade, Y., R. Hashimoto, M. Suda, K. Hiraga, and M. Inui, Production of 4-hydroxybenzoic acid by an aerobic growth-arrested bioprocess using metabolically engineered *Corynebacterium glutamicum.* Applied Environmental Microbiology, 2018. **84**(6): e02587-02517.
285. Zhou, Y., B.S. Sekar, S. Wu, and Z. Li, Benzoic acid production *via* cascade biotransformation and coupled fermentation-biotransformation. Biotechnology and Bioengineering, 2020. **117**(8): 2340-2350.
286. Otto, M., B. Wynands, J. Marienhagen, L.M. Blank, and N. Wierckx, Benzoate synthesis from glucose or glycerol using engineered *Pseudomonas taiwanensis.* Biotechnology Journal, 2020. **15**(11): 2000211.
287. Gocke, D., C.L. Nguyen, M. Pohl, T. Stillger, L. Walter, and M. Müller, Branched-chain keto acid decarboxylase from *Lactococcus lactis* (KdcA), a valuable thiamine diphosphate-dependent enzyme for asymmetric C-C bond formation. Advanced Synthesis & Catalysis, 2007. **349**(8-9): 1425-1435.
288. Marsden, S.R., D.G.G. McMillan, and U. Hanefeld, Assessing the thiamine diphosphate dependent pyruvate dehydrogenase E1 subunit for carboligation reactions with aliphatic ketoacids. International Journal of Molecular Sciences, 2020. **21**(22): 8641.
289. Vinogradov, V., M. Vyazmensky, S. Engel, I. Belenky, A. Kaplun, O. Kryukov, Z.e. Barak, and D.M. Chipman, Acetohydroxyacid synthase isozyme I from *Escherichia coli* has unique catalytic and regulatory properties. Biochimica et Biophysica Acta (BBA) - General Subjects, 2006. **1760**(3): 356-363.
290. Martin, A.R., R. DiSanto, I. Plotnikov, S. Kamat, D. Shonnard, and S. Pannuri, Improved activity and thermostability of (*S*)-aminotransferase by error-prone polymerase chain reaction for the production of a chiral amine. Biochemical Engineering Journal, 2007. **37**(3): 246-255.
291. Cassimjee, K.E., M.S. Humble, H. Land, V. Abedi, and P. Berglund, *Chromobacterium violaceum* ω-transaminase variant Trp60Cys shows increased specificity for (*S*)-1-phenylethylamine and 4′-substituted acetophenones, and follows Swain–Lupton parameterisation. Organic & Biomolecular Chemistry, 2012. **10**(28): 5466-5470.
292. Erdmann, V., Synthetic enzyme cascades for the synthesis of amino alcohols and tetrahydroisoquinolines. Doctoral thesis, 2018. RWTH Aachen University.
293. Liew, F.E., R. Nogle, T. Abdalla, B.J. Rasor, C. Canter, R.O. Jensen, L. Wang, J. Strutz, P. Chirania, S. De Tissera, A.P. Mueller, Z. Ruan, A. Gao, L. Tran, N.L. Engle, J.C. Bromley, J. Daniell, R. Conrado, T.J. Tschaplinski, R.J. Giannone, R.L. Hettich, A.S. Karim, S.D. Simpson, S.D. Brown, C. Leang, M.C. Jewett, and M. Köpke, Carbon-negative production of acetone and isopropanol by gas fermentation at industrial pilot scale. Nature Biotechnology, 2022. **40**(3): 335-344.
294. Kazimírová, V. and M. Rebroš, Production of aldehydes by biocatalysis. International Journal of Molecular Sciences, 2021. **22**(9): 4949.
295. Delhomme, C., S.L.M. Goh, F.E. Kühn, and D. Weuster-Botz, Esterification of bio-based succinic acid in biphasic systems: comparison of chemical and biological catalysts. Journal of Molecular Catalysis B-enzymatic, 2012. **80**: 39-47.
296. Oberleitner, N., A.K. Ressmann, K. Bica, P. Gärtner, M.W. Fraaije, U.T. Bornscheuer, F. Rudroff, and M.D. Mihovilovic, From waste to value – direct utilization of limonene from

orange peel in a biocatalytic cascade reaction towards chiral carvolactone. Green Chemistry, 2017. **19**(2): 367-371.
297. Ütkür, F.Ö., T. Thanh Tran, J. Collins, C. Brandenbusch, G. Sadowski, A. Schmid, and B. Bühler, Integrated organic–aqueous biocatalysis and product recovery for quinaldine hydroxylation catalyzed by living recombinant *Pseudomonas putida.* Journal of Industrial Microbiology and Biotechnology, 2012. **39**(7): 1049-1059.
298. Heuson, E. and F. Dumeignil, The various levels of integration of chemo- and bio-catalysis towards hybrid catalysis. Catalysis Science & Technology, 2020. **10**(21): 7082-7100.
299. Gahloth, D., M.S. Dunstan, D. Quaglia, E. Klumbys, M.P. Lockhart-Cairns, A.M. Hill, S.R. Derrington, N.S. Scrutton, N.J. Turner, and D. Leys, Structures of carboxylic acid reductase reveal domain dynamics underlying catalysis. Nature Chemical Biology, 2017. **13**(9): 975-981.
300. Braga, A. and N. Faria, Bioprocess optimization for the production of aromatic compounds with metabolically engineered hosts: recent developments and future challenges. Frontiers in Bioengineering and Biotechnology, 2020. **8**: 96.
301. Wang, S., M. Bilal, H. Hu, W. Wang, and X. Zhang, 4-Hydroxybenzoic acid-a versatile platform intermediate for value-added compounds. Applied Microbiology and Biotechnology, 2018. **102**(8): 3561-3571.
302. Nattermann, M., S. Burgener, P. Pfister, A. Chou, L. Schulz, S.H. Lee, N. Paczia, J. Zarzycki, R. Gonzalez, and T.J. Erb, Engineering a highly efficient carboligase for synthetic one-carbon metabolism. ACS Catalysis, 2021. **11**(9): 5396-5404.
303. Fackler, N., B.D. Heijstra, B.J. Rasor, H. Brown, J. Martin, Z. Ni, K.M. Shebek, R.R. Rosin, S.D. Simpson, K.E. Tyo, R.J. Giannone, R.L. Hettich, T.J. Tschaplinski, C. Leang, S.D. Brown, M.C. Jewett, and M. Köpke, Stepping on the gas to a circular economy: accelerating development of carbon-negative chemical production from gas fermentation. Annual Review of Chemical and Biomolecular Engineering, 2021. **12**(1): 439-470.
304. Woodley, J.M., Ensuring the sustainability of biocatalysis. ChemSusChem, 2022. **15**(9): e202102683.
305. Pothakos, V., N. Debeer, I. Debonne, A. Rodriguez, J.N. Starr, and T. Anderson, Fermentation titer optimization and impact on energy and water consumption during downstream processing. Chemical Engineering & Technology, 2018. **41**(12): 2358-2365.
306. Burnett, J.W.H., Z. Sun, J. Li, X. Wang, and X. Wang, Comparative life cycle assessment of NAD(P)H regeneration technologies. Green Chemistry, 2021. **23**(18): 7162-7169.
307. Burek, B.O., A.W.H. Dawood, F. Hollmann, A. Liese, and D. Holtmann, Process intensification as game changer in enzyme catalysis. Frontiers in Catalysis, 2022. **2**: 858706.
308. Lutze, P., R. Gani, and J.M. Woodley, Process intensification: a perspective on process synthesis. Chemical Engineering and Processing: Process Intensification, 2010. **49**(6): 547-558.
309. Lindeque, R.M. and J.M. Woodley, Reactor selection for effective continuous biocatalytic production of pharmaceuticals. Catalysts, 2019. **9**(3): 262.
310. W. Zhuhong, W.Z.K., Y. Huang, J. Wang, C. Baoqin,, L.J. Z. Ying, M. Zhipeng, Z. Baohua, Z. Huaihao,, and L.Y. M. Bocora, S. Baoguo and L. Zhenlin, Production method and equipment of phenylethylamine, 2020, US20200332321A1.
311. Fiorati, A., P. Berglund, M.S. Humble, and D. Tessaro, Application of transaminases in a disperse system for the bioamination of hydrophobic substrates. Advanced Synthesis & Catalysis, 2020. **362**(5): 1156-1166.
312. Spöring, J.-D., W. Graf von Westarp, C.R. Kipp, A. Jupke, and D. Rother, Enzymatic cascade in a simultaneous, one-pot approach with *in situ* product separation for the asymmetric production of (4*S*,5*S*)-octanediol. Organic Process Research & Development, 2022. **26**(7): 2038-2045.

313. Becker, M., S. Lütz, and K. Rosenthal, Environmental assessment of enzyme production and purification. Molecules, 2021. **26**(3): 573.
314. Land, H., J.C. Campillo-Brocal, M. Svedendahl Humble, and P. Berglund, B-factor guided proline substitutions in *Chromobacterium violaceum* amine transaminase: evaluation of the proline rule as a method for enzyme stabilization. ChemBioChem, 2019. **20**(10): 1297-1304.
315. Sánchez-Castañeda, A.K., M. Moussa, L. Ngansop, I.C. Trelea, and V. Athès, Organic phase screening for in-stream reactive extraction of bio-based 3-hydroxypropionic acid: biocompatibility and extraction performances. Journal of Chemical Technology & Biotechnology, 2020. **95**(4): 1046-1056.
316. Fellechner, O., M. Blatkiewicz, and I. Smirnova, Reactive separations for *in situ* product removal of enzymatic reactions: a Review. Chemie Ingenieur Technik, 2019. **91**(11): 1522-1543.
317. Fernandes, P., D.M.F. Prazeres, and J.M.S. Cabral, Membrane-assisted extractive bioconversions, in Process Integration in Biochemical Engineering. 2003, Springer Berlin Heidelberg. p. 115-148.
318. Shin, J.S., B.G. Kim, A. Liese, and C. Wandrey, Kinetic resolution of chiral amines with ω-transaminase using an enzyme-membrane reactor. Biotechnology and Bioengineering, 2001. **73**(3): 179-187.
319. Yang, J., A. Buekenhoudt, M.V. Dael, P. Luis, Y. Satyawali, R. Malina, and S. Lizin, A techno-economic assessment of a biocatalytic chiral amine production process integrated with *in situ* membrane extraction. Organic Process Research & Development, 2022. **26**(7): 2052-2066.
320. Arnold, F.H., Innovation by evolution: bringing new chemistry to life (Nobel lecture). Angewandte Chemie International Edition, 2019. **58**(41): 14420-14426.
321. Santacoloma, P.A., G. Sin, K.V. Gernaey, and J.M. Woodley, Multienzyme-catalyzed processes: next-generation biocatalysis. Organic Process Research & Development, 2011. **15**(1): 203-212.
322. Sambrook, J. and D.W. Russel, Molecular cloning - A laboratory manual. 3rd ed. Vol. 1. 2001, Cold Spring Harbor, New York: Cold Spring Harbor Laboratory Press.
323. Gustafsson, C., L. Whitman, M. Gore, J. Ness, E. Theodorou, and J. Minshull, Rapid, scarless cloning of gene fragments using the electra vector system. Genetic engineering & biotechnology news: GEN, 2013. **33**: 42.
324. Eggeling, L. and M. Bott, Handbook of *Corynebacterium glutamicum*. 2005, Boca Raton: CRC Press.
325. Abe, S., K.-I. Takayama, and S. Kinoshita, Taxonomical studies on glutamic acid-producing bacteria. The Journal of General and Applied Microbiology, 1967. **13**(3): 279-301.
326. Bertani, G., Studies on lysogenesis. I. The mode of phage liberation by lysogenic *Escherichia coli.* Journal of Bacteriology, 1951. **62**(3): 293-300.

Appendix

A.1 Appendix for Chapter 2

Plasmid and strain construction for microbial cell factory

The oligonucleotides used in this study were synthesized by Eurofins genomics (Ebersfeld, Germany) and are listed in Table A1.1. The methodology for plasmid and strain construction of *C. glutamicum* have been published before in supplementary information [123].

Table A1.1 Oligonucleotides used for metabolic engineering of *C. glutamicum* (chapter 3.1). The codon-optimized gene *alaD* was synthesized with flanking restriction sites and immediately cloned into pMKEx2 without any PCR-based amplification step.

Primer name	Sequence (5' → 3')
Seq_*gltA*_for	ATGAGTCCGAAGGTTGCTGCAT
Seq_*gltA*_rev	TCGAGTGGGTTCAGCTGGTCC
Co_del_*alaT*_for	CTGGGTATTCGCCACGGACGT
Co_del_*alaT*_rev	TCGGCGGTGTCAAAAGCATTGC
Co_del_*ldhA*_for	GCACCAGTTGCGATGTGGGTGG
Co_del_*ldhA*_rev	CGTTGTCGATCATCTGCTTCCAG
Co_del_*pqo*_for	GAGTTGTCTACACCGATCAGAAAG
Co_del_*pqo*_rev	GCATACCTGCTGCCCAGCGCC
Co_del_*ppc*_for	GGAATAGACTCGCTCGGC
Co_del_*ppc*_rev	GTGAACAGGCTCTCGATGC

All enzymes for cloning purposes were purchased from Thermo Scientific (Schwerte, Germany). The codon-optimized synthetic gene *alaD* for expression in *C. glutamicum* was obtained from GeneArt (Thermo Fisher Scientific). For standard molecular cloning work, such as PCR or restriction cloning, standard protocols were used [322]. The construction of pMKEx2_*alaD* was performed by using Electra Cloning, which relies on the activity of the class IIS restriction enzyme *Sap*I, generating customizable 5'-overhangs [323]. For verification of the constructed plasmids both, restriction analysis and DNA sequencing, were performed (Eurofins Genomics, Ebersberg, Germany). *E. coli* DH5α was routinely transformed using the RbCl-method, whereas specific techniques for *C. glutamicum*, e.g. electroporation were performed as described previously [324]. In-frame deletions of the genes encoding lactate dehydrogenase (*ldhA)*, phosphoenolpyruvate carboxylase (*ppc*), alanine transaminase (*alaT)*, and pyruvate:quinone oxidoreductase (*pqo)* were performed by two-step homologous recombination using the pK19*mobsacB* system [131]. All

C. glutamicum strains are derived from the wild-type strain ATCC 13032 [325], whereas *E. coli* DH5α was used for cloning purposes. *C. glutamicum* was cultivated aerobically at 30 °C in Brain Heart Infusion (BHI) medium (Difco Laboratories, Detroit, USA) or defined CGXII medium with D-glucose or combinations of D-glucose and sodium acetate as sole carbon and energy source [325]. For recombinant DNA work *E. coli* was cultivated in Lysis broth (LB) medium [326] at 37 °C. If appropriate, kanamycin (30 µg mL^{-1} for *C. glutamicum*, 50 µg mL^{-1} for *E. coli*) and 1 mM isopropyl-β-D-thiogalactoside (IPTG) for induction of heterologous gene expression were added to the medium.

Enzyme production in *E. coli* BL21 (DE3) as purified biocatalyst or crude biocatalyst formulations

Exemplary SDS-PAGE (section 2.2.1.6) of cultivation broth, whole cells, crude cell extract or IMAC purification for selected enzymes are shown in Figure A1.1.

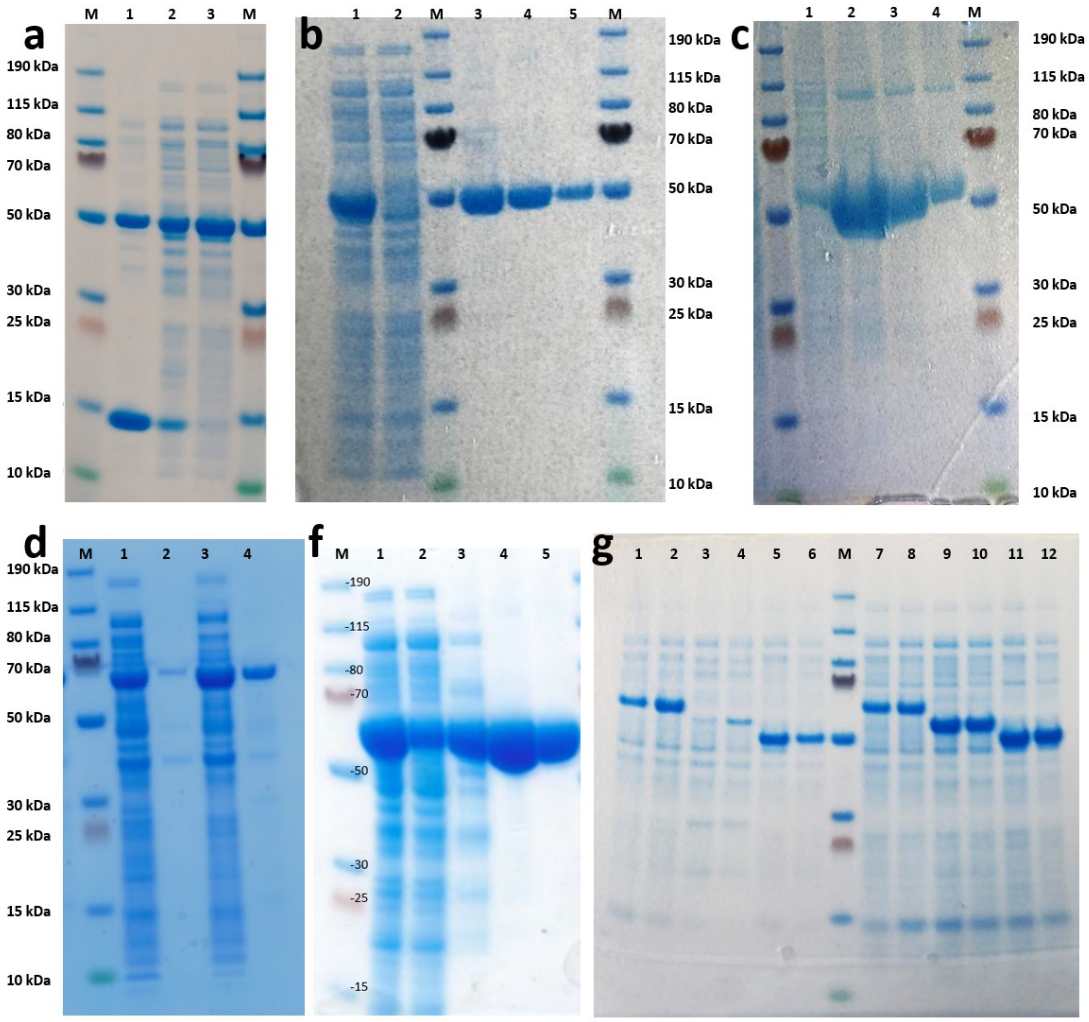

Figure A1.1 SDS-PAGE of selected enzymes and enzyme formulations. M = PageRuler Prestained Plus protein marker. (a) Line 1-2: soluble and insoluble fractions of cells producing *Cv*2025, 3: crude cell extract containing *Cv*2025 (b) IMAC purification fractions of *Cv*2025 in Tris buffer, fractions from 1-5: crude cell extract, flow trough, wash, elution, desalting. (c) IMAC purification fractions of *Bm*TA with Kpi buffer, fractions from 1-4: flow trough, wash, elution, desalting. (d) Soluble and pellet fraction of *Ll*KdcA from cultivations in AI (1, supernatant; 2, pellet) and LB medium (3, supernatant; 4, pellet). (f) IMAC purification fractions of *Ap*PDC var with Kpi buffer, fractions from 1-4: crude cell extract, flow trough, wash, elution, desalting. (g) Soluble (left) and insoluble (right) fractions of *E. coli* BL21 (DE3) producing amine transaminases *Ac*TA (1 - 2, 7 - 8), *Bm*TA (2 - 3, 9 - 10) and *Cv*2025 (4 - 5, 11 - 12). The electrophoresis was performed in MES buffer for 60 min, 200 V and 100 mA. The gel was dyed with Coomassie brilliant blue for 60 min and destained with water. Expected molecular masses: *Cv*2025 52.23 kDa, *Bm*TA 54.48 kDa, *Ac*TA 65.84 kDa, *Ap*PDC var 61.14 , *Ll*KdcA 63.35 kDa. The band at approximately 14 kDa is lysozyme.

HPLC analytics with online derivatization for determination of metaraminol in pure substance systems

The metaraminol in the pure substance systems shown in chapter 3.2 and 3.3 was quantified *via* HPLC measurement using the online derivatization method with orthophtalic aldehyde (OPA) and mercaptoethanol (as previously published in supplementary information of [124]). The used inline derivatization procedure is given in Table A1.2, where vial 99 contained 0.1 mL OPA reagent and 0.9 mL of 0.4 M borate buffer at pH 10.4 and vial 100 contained distilled water. The derivatized samples were injected onto the HPLC and the method was run for 6 minutes. The eluents were (A) 2.5 mM acetic acid in water with 10% methanol at pH 6 and (B) methanol. The gradient elution is given in Table A1.3.

Table A1.2 Derivatization procedure for quantification of metaraminol in pure substance systems.

Derivatization procedure	
1.	DRAW 4.5 µL from vial 100
2.	DRAW 1.5 µL from sample
3.	DRAW 0.5 µL from air
4.	NEEDLE wash in vial 99
5.	DRAW 4.5 µL from vial 100
6.	MIX 11.0 µL in seat
7.	WAIT 1.00 min
8.	INJECT
9.	DRAW and EJECT 100 µL from vial 99

Table A1.3 Gradient elution used in the quantification of metaraminol in pure substance systems.

Time [min]	**Eluent A [%]**	**Flow [mL min^{-1}]**
0.00	90	0.4
1.00	10	0.4
2.00	10	0.4
5.00	90	0.4

The calibration curve for metaraminol is shown in Figure A1.2 (Agilent 1200, DAD 334 nm, Machery Nagel Nucleodur C18ec pre-column, 2 x 4 mm, 40 °C).

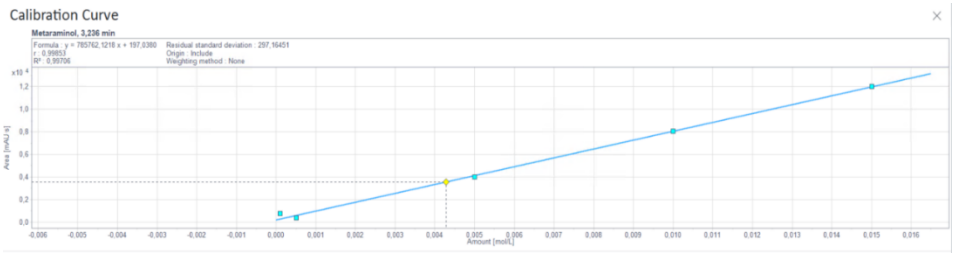

Figure A1.2 Calibration curve for metaraminol bitartrate used in pure substance extraction studies.

(U)HPLC calibration curves

The reaction components were quantified using different (U)HPLC methods as stated in section 2.2.10, Table 5 (refer to table for retention times and specifications of application). For quantitative analysis, external calibrations were prepared in triplicate serial dilutions from two separate standard stock solution and repeated for eventual column and guard column replacements. For better overview, only one calibration curve is shown in the following. For chiral detection of amino alcohols (section 2.2.10, Table 5, Method IV), only HPLC peak areas were considered. Figures A1.7 to A1.12 originate from Nina Klos's Master thesis [256].

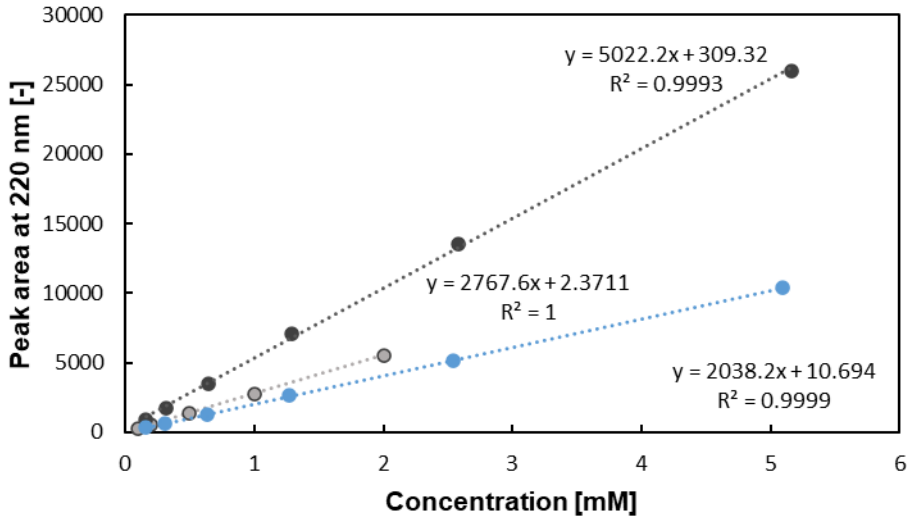

Figure A1.3 Calibrations for chiral HPLC quantification of (*R*)-3-OH-PAC (light blue), (*S*)-3-OH-PAC (light grey) and 3-OH-BA (dark grey) on Agilent Infinity 1260. Method I: Chiralpak IE column (4.6 x 250 mm, 5 µm), 20 °C, 5 µL injection, isocratic flow of 25% ACN in purified water, flow rate 0.9 mL min^{-1} , 10 min total, DAD 220 nm.

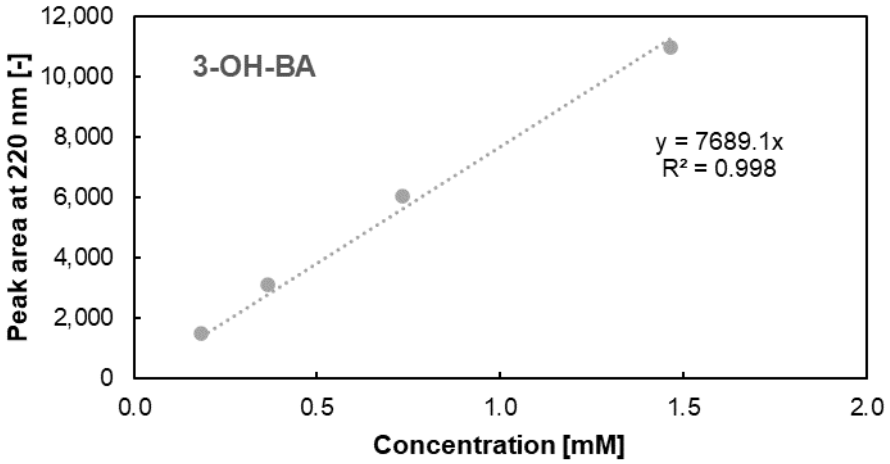

Figure A1.4 Calibration for HPLC quantification of 3-OH-BA on Agilent Infinity II 1290 (achiral). Method II: Zorbax Eclipse plus C18 column (2 x 100 mm, 1.8 µm), 20 °C, 5 µL injection, DAD 220 nm, 10% ACN and 90% water + 0.1% DEA + 0.075% TFA up to 90% ACN in 5 min, 6 min total, 0.5 mL min^{-1}.

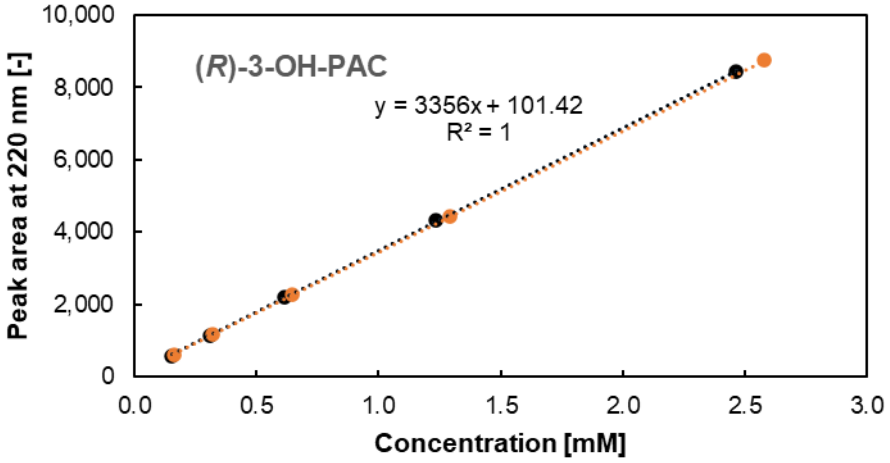

Figure A1.5 Calibration for HPLC quantification of 3-OH-PAC on Agilent Infinity II 1290 (achiral). Method II: Zorbax Eclipse plus C18 column (2 x 100 mm, 1.8 µm), 20 °C, 5 µL injection, DAD 220 nm, 10% ACN and 90% water + 0.1% DEA + 0.075% TFA up to 90% ACN in 5 min, 6 min total, 0.5 mL min^{-1}.

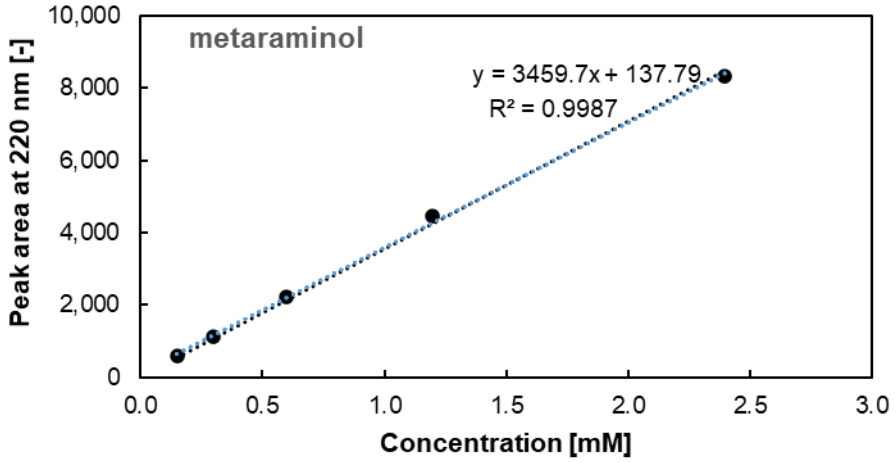

Figure A1.6 Calibration for HPLC quantification of metaraminol on Agilent Infinity II 1290 (achiral). Method III: Zorbax Eclipse plus C18 column (2 x 100 mm, 1.8 µm), 20 °C, 5 µL injection, DAD 220 nm, isocratic flow of and 15% ACN and 85% purified water + 0.1% DEA + 0.075% TFA, 0.3 mL min^{-1}, 10 min total.

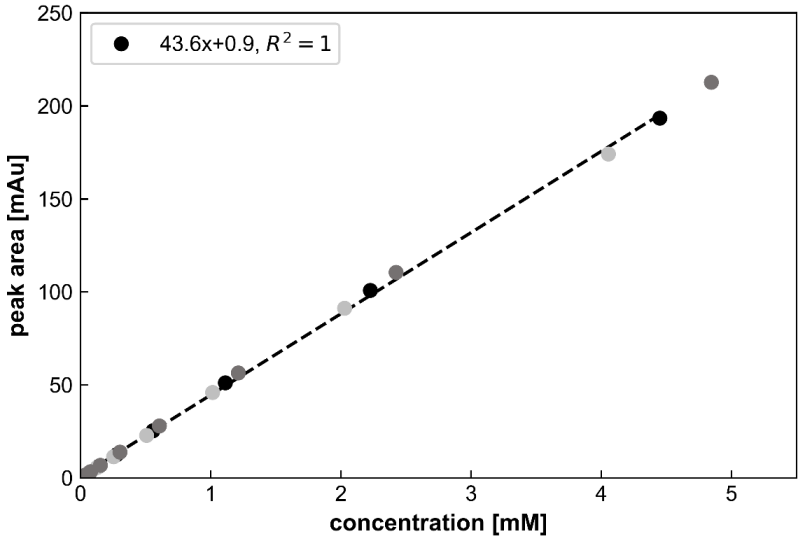

Figure A1.7 Calibration curve of acetophenone measured on Thermo Scientific Dionex UltiMate 3000 HPLC. Method V: LiChrospher 100 RP-18 (25 cm x 4 mm, 5 µm), 25 °C, 10 µL injection volume, isocratic flow of 45% ACN and 55% purified water, flow rate 1.5 mL min^{-1}, 10 min, UV-VIS, detection of acetophenone at 254 nm.

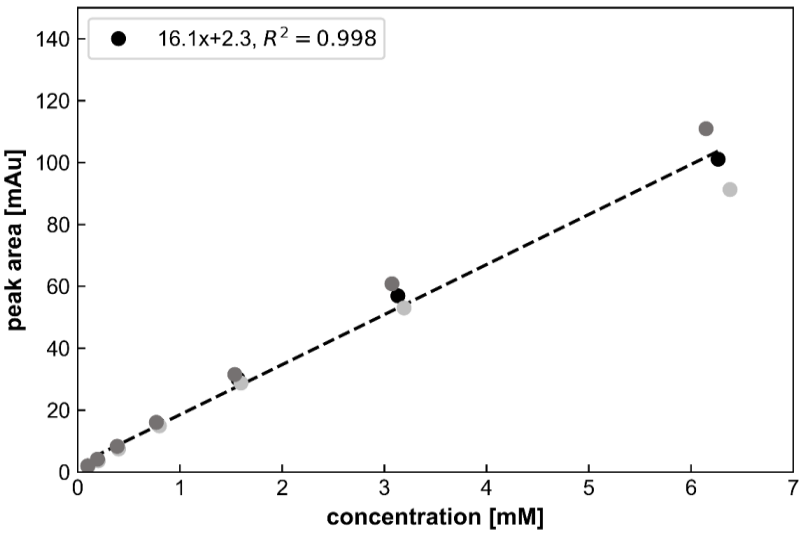

Figure A1.8 Calibration curve of (*S*)-α-MBA measured on Thermo Scientific Dionex UltiMate 3000 HPLC. Method V: LiChrospher 100 column (RP-18, 25 cm x 4 mm, 5 µm, achiral), 25 °C, 10 µL injection volume, isocratic flow of 45% ACN/ 55% H_2O, flow rate 1.5 mL min^{-1}, 10 min, UV-VIS, detection of (*S*)-α-MBA at 213 nm.

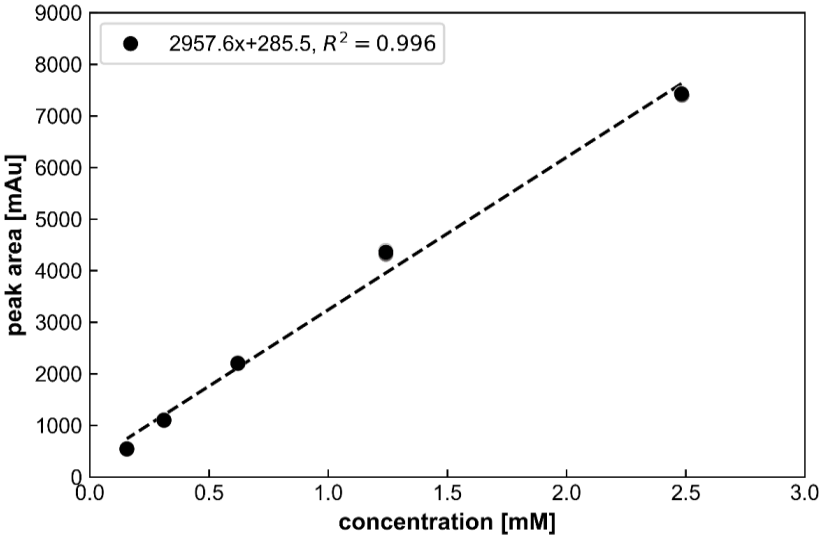

Figure A1.9 Calibration curve of metaraminol measured on Agilent 1290 Infinity II HPLC. Method VIII: Poroshell 120 column (EC-C18, 2.1 x 100 mm, 1.9 µm), 20 °C, 5 µL injection volume, isocratic flow of 15% ACN and 85% purified water + 0.1% DEA + 0.075% TFA, flow rate 0.3 mL min^{-1}, 10 min total, DAD detection of metaraminol at 220 nm.

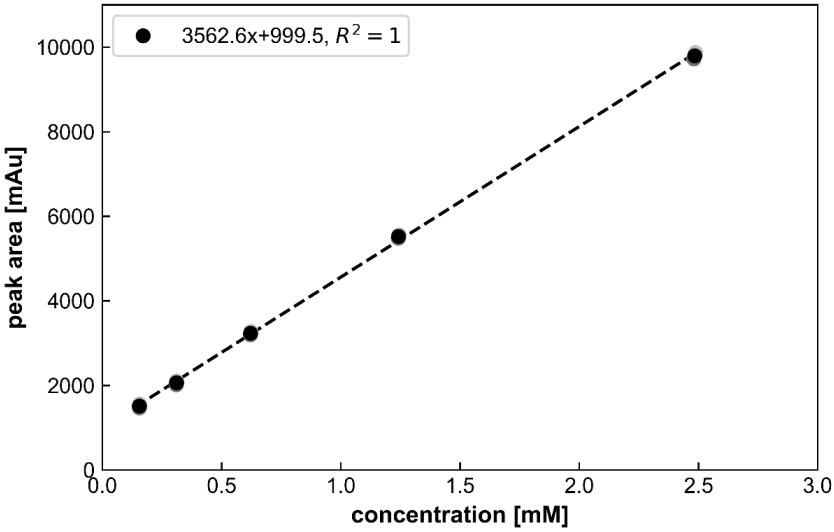

Figure A1.10 Calibration curve of (*R*)-3-OH-PAC measured on Agilent 1290 Infinity II HPLC. Method VIII: Poroshell 120 (EC-C18, 2.1 x 100 mm, 1.9 µm), 20 °C, 5 µL injection volume, gradient elution with 5% ACN, 95% purified water + 0.1% DEA + 0.075% TFA up to 95% ACN in 6 min, 6 min total, 0.5 mL min^{-1}, DAD detection of (*R*)-3-OH-PAC at 220 nm.

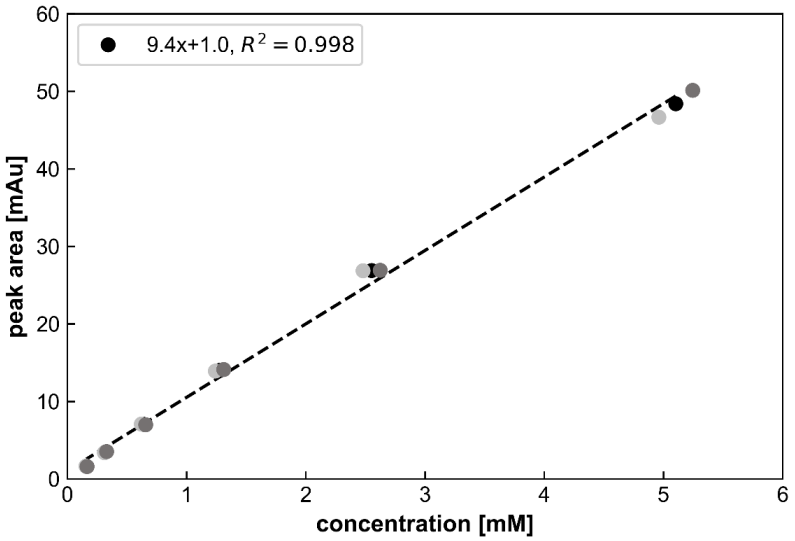

Figure A1.11 Calibration curve of (1*S*,2*R*)-norephedrine measured on Thermo Scientific Dionex UltiMate 3000 HPLC. Method VII: LiChrospher 100 column (RP-18, 250 mm x 4 mm, 5 µm), 25 °C, 10 µL injection volume, gradient elution with solvent A (ACN + 0.1% TFA, 3 - 97%) and solvent B (H_2O + 0.1% TFA), flow rate 0.5 mL min^{-1}, 25 min total, UV-VIS detection of norephedrine (achiral) at 220 nm.

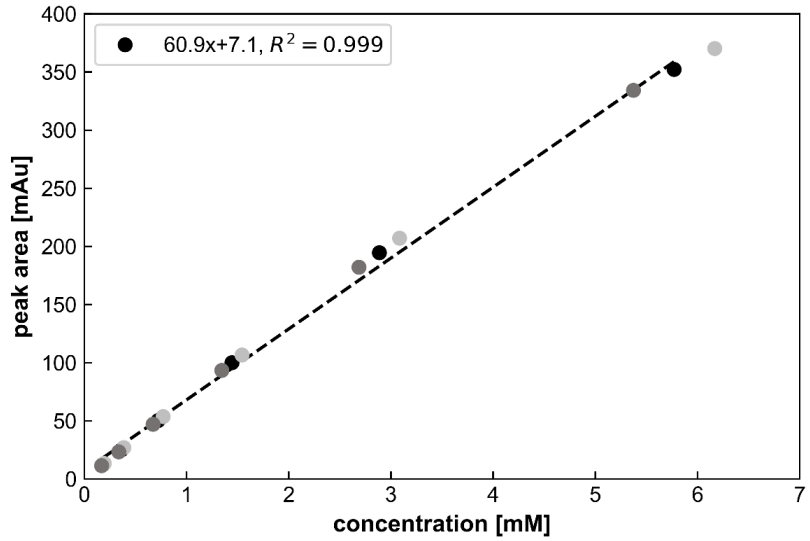

Figure A1.12 Calibration curve of (*R*)-PAC measured on measured on Thermo Scientific Dionex UltiMate 3000 HPLC. Method VII: LiChrospher 100 column (RP-18, 250 mm x 4 mm, 5 µm), 25 °C, 10 µL injection volume, gradient elution with solvent A (ACN + 0.1% TFA, 3 - 97%) and solvent B (H_2O + 0.1% TFA), flow rate 0.5 mL min^{-1}, 25 min total, UV-VIS detection of PAC (achiral) at 220 nm.

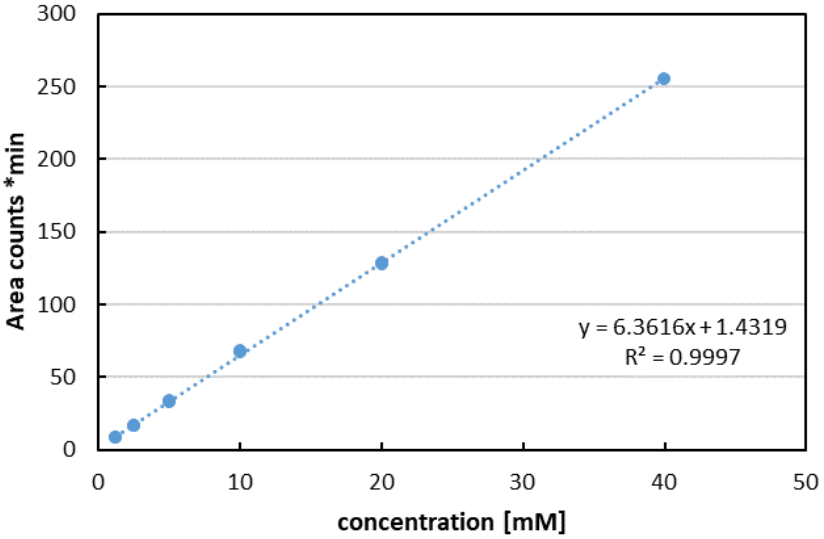

Figure A1.13 Calibration curve of 4-OH-BA measured on Thermo Scientific Dionex UltiMate 3000 HPLC. Method VI: LiChrospher 100 column (RP-18, 250 mm x 4 mm, 5 µm), 25 °C, 10 µL injection volume, isocratic flow of 20% ACN and 80% purified water, 1.5 mL min^{-1}, 10 min total, UV-VIS detection of 4-OH-BA at 200 nm.

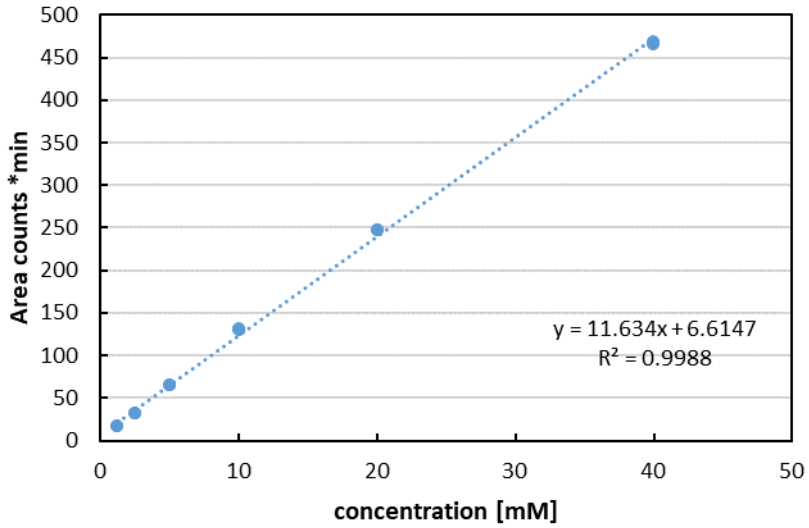

Figure A1.14 Calibration curve of 4-OH-PAC measured on Thermo Scientific Dionex UltiMate 3000 HPLC. Method VI: LiChrospher 100 column (RP-18, 250 mm x 4 mm, 5 µm), 25 °C, 10 µL injection volume, isocratic flow of 20% ACN and 80% purified water, 1.5 mL min^{-1}, 10 min total, UV-VIS detection of 4-OH-PAC at 200 nm.

A.2 Appendix for Chapter 3

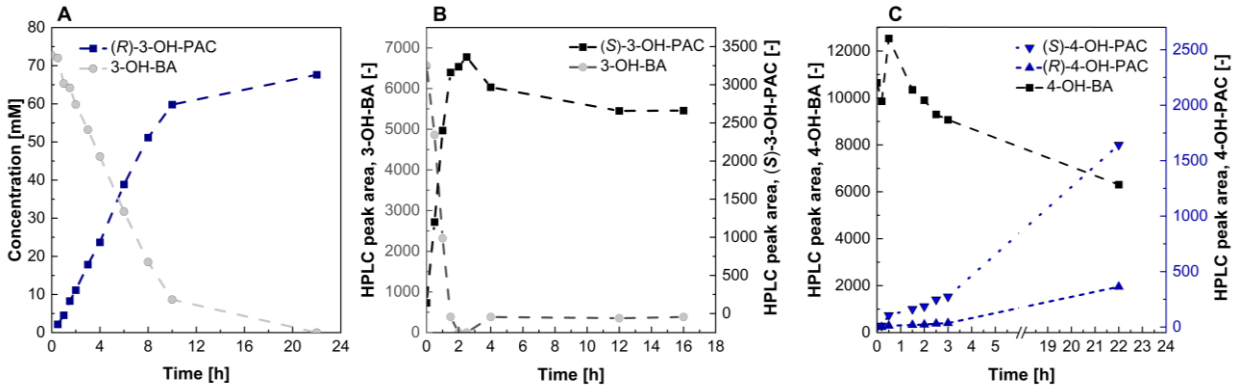

Figure A2.1 Typical conversion curves of preparative-scale reactions towards substituted PAC with carboligase variants from *Acetobacter pasteurianus* (*Ap*PDC). Reaction conditions **A**: 60 mM 3-OH-BA, 180 mM sodium pyruvate, 2.5 mM $MgSO_4$, 0.1 mM ThDP, 100 mM Kpi buffer pH 6.5, 10 mg mL^{-1} lyophilized whole cells containing *Ap*PDC var, 25 °C, 100 mL reaction volume (EasyMax 402), stirred at 250 rpm. Reaction conditions **B**: 60 mM 3-OH-BA, 180 mM sodium pyruvate, 2.5 mM $MgSO_4$, 0.1 mM ThDP, 100 mM Kpi buffer pH 6.5, 10 mg mL^{-1} lyophilized whole cells containing *Ap*PDC E469G, 25 °C, 100 mL reaction volume (EasyMax 402), stirred at 250 rpm. The synthesis of (*S*)-3-OH-PAC was terminated directly at the point of full conversion (2.5 h), whereas for (*R*)-3-OH-PAC no reverse reaction was observed also for longer reaction times. Reaction conditions C: 60 mM 4-OH-BA, 180 mM sodium pyruvate, 2.5 mM $MgSO_4$, 0.1 mM ThDP, 100 mM Kpi buffer pH 6.5, 10 mg mL^{-1} lyophilized whole cells *Ap*PDC E469G, 25 °C, 100 mL reaction volume, stirred at 350 rpm. The produced (*S*)-4-OH-PAC was not purified due to poor conversion (ca. 40% substrate depletion) and low stereoselectivity (64% *ee*). Chiral analysis with Chiralpak IE column (analogous to HPLC method I, Table 5, section 2.2.10.2, but with a flow rate of 0.9 mL min^{-1} and without calibration). The retention times were 4.6 min for (*S*)-4-OH-PAC, 4.8 min for (*R*)-4-OH-PAC and 6.2 min for 4-OH-BA.

Supplementary information for Chapter 3.1

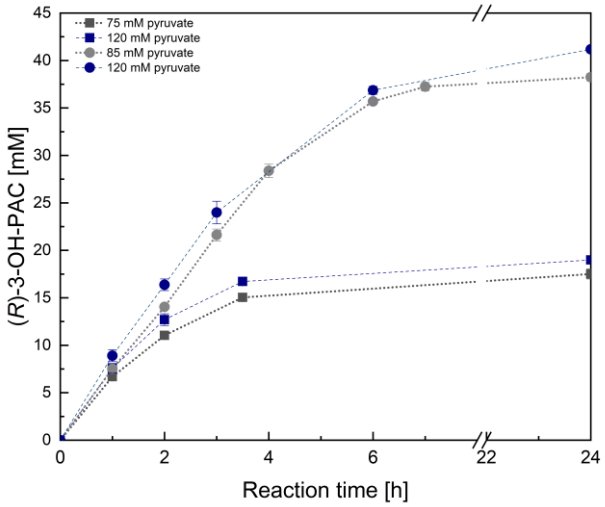

Figure A2.2 Carboligation of 3-OH-BAand pyruvate to (*R*)-3-OH-PAC in a buffered system. Reaction conditions: 20 mM (squares) or 40 mM (circles) 3-OH-BA, the indicated pyruvate concentrations, 1 mM ThDP, 2.5 mM $MgCl_2$, 10 mg mL^{-1} lyophilized whole cells containing *Ap*PDC var, 25 °C, 700 rpm, 1 mL, 24 h. Error bars show the range of two independent reactions.

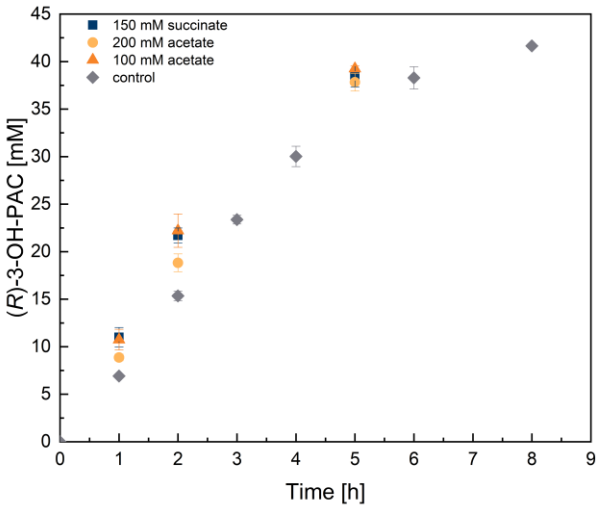

Figure A2.3 Carboligation reaction of 3-OH-BA and pyruvate with the addition of succinate and acetate. Control reaction without addition of side components. Reaction conditions: 40 mM 3-OH-benzaldehyde, 120 mM sodium pyruvate, 1 mM ThDP, 2.5 mM $MgCl_2$, 50 mM Kpi buffer pH 6.5, 10 mg mL^{-1} *Ap*PDC var (lyophilized whole cells), 25 °C, 700 rpm, 1 mL. Error bars show standard deviation of technical triplicates. This figure was previously published [123], and is reprinted with permission from American Chemical Society.

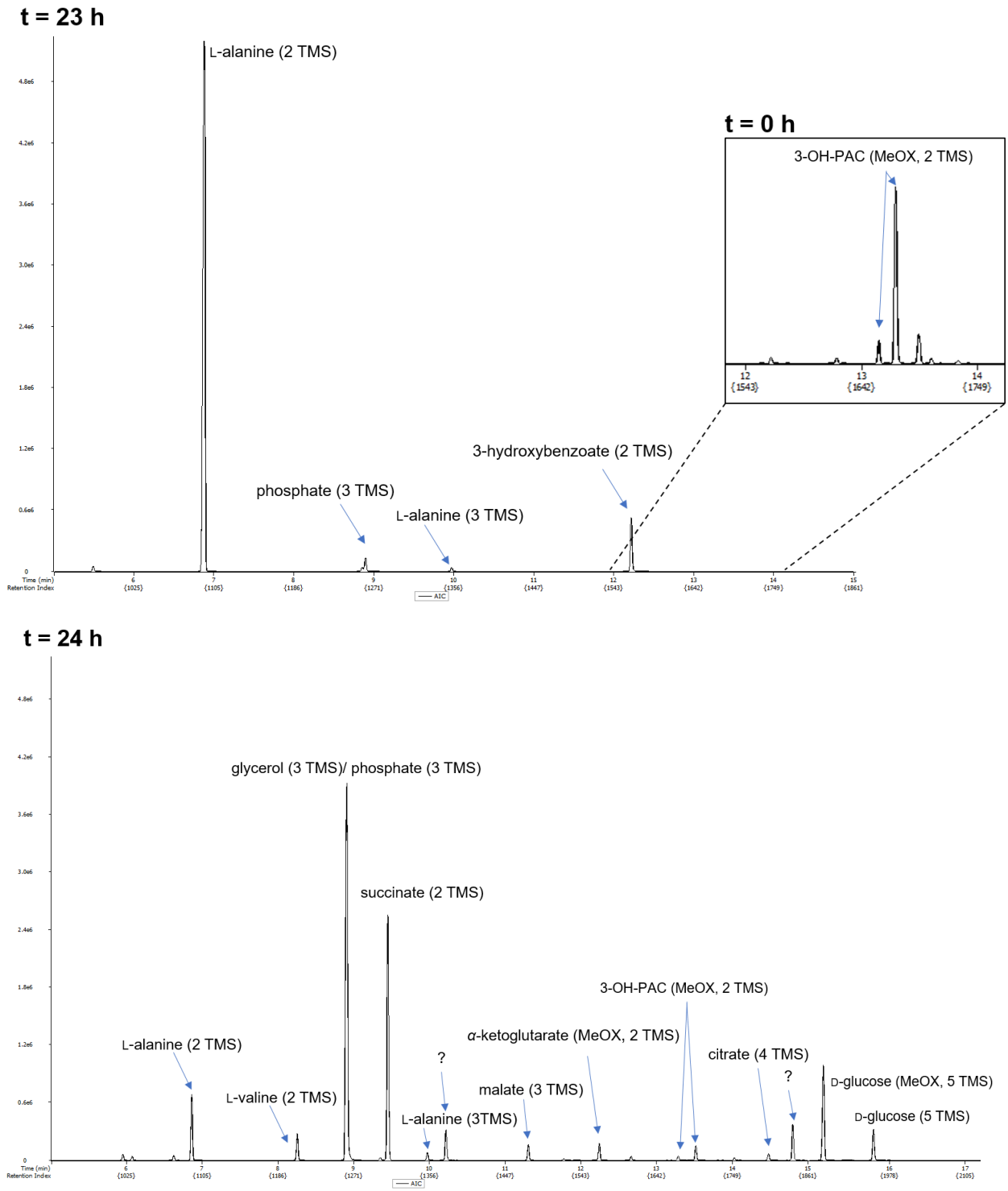

Figure A2.4 Upper: GC-ToF-MS spectrum of alkaline reaction solution for transamination of (*R*)-3-OH-PAC to metaraminol using L-alanine as amine donor. After 23 h, the substrate solution had a pH > 9.5 and had a dark brown color because the substrate (*R*)-3-OH-PAC degraded to 3-hydroxybenzoate. Lower: GC-ToF-MS spectrum of fermentation supernatant PYR_ALA_8_R1 (without heat inactivation) after carboligation and transamination steps were performed in the supernatant.

Supplementary information for chapter 3.3

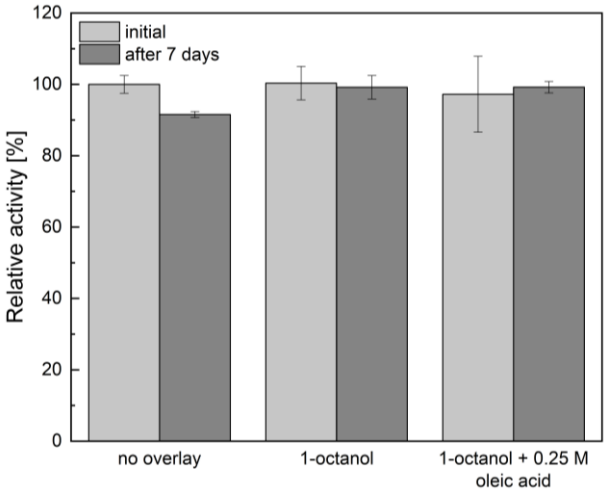

Figure A2.5 Storage stability of purified *Bm*TA in the presence of 10% (v/v) 1-octanol and 1-octanol containing 0.25 M oleic acid. The relative activity is shown in relation to the initial specific activity without overlay (100%). All enzymes solutions were incubated rotating at 20 °C under exclusion of light and the activity was measured photometrically as described before (section 2.2.5.1). The error bars show standard deviations of technical triplicates.

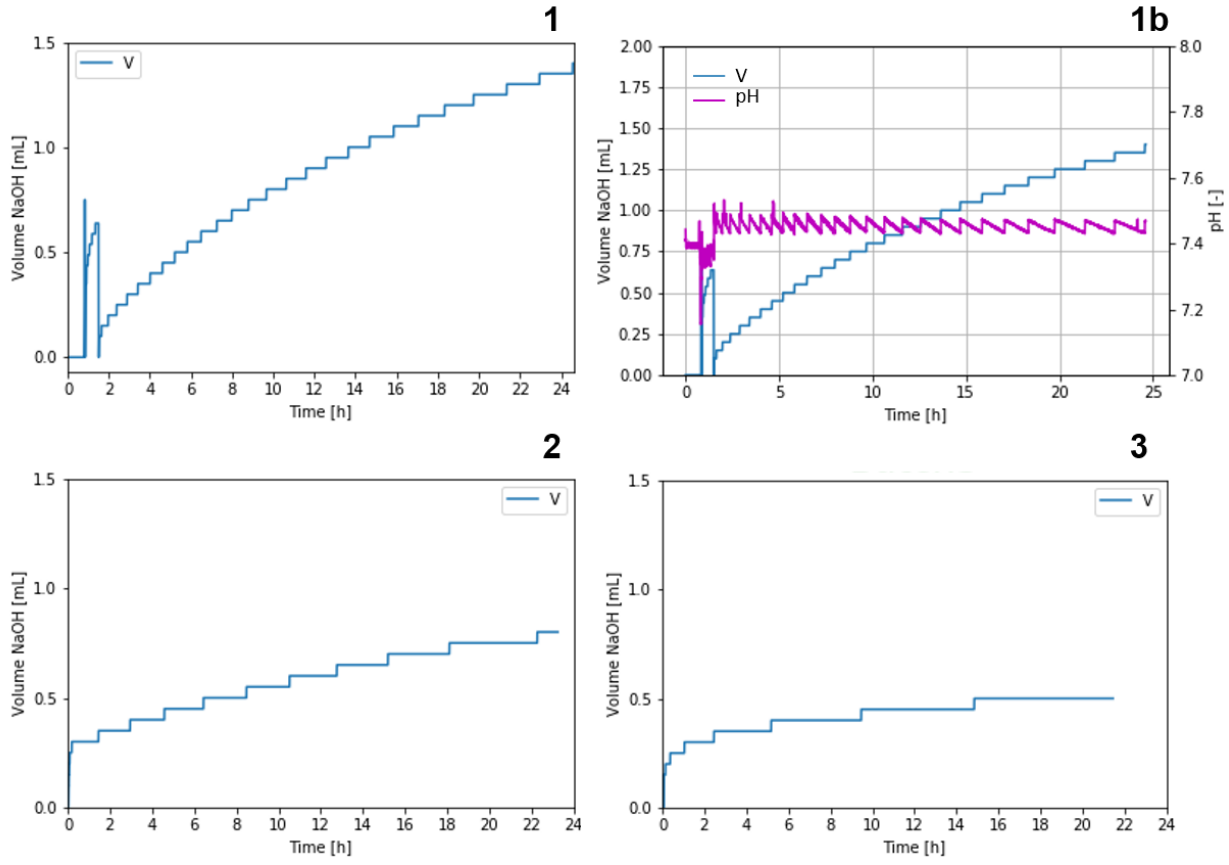

Figure A2.6 Titration pattern of 0.5 NaOH during three repeated reactive extraction steps. The pH stat regime was necessary to control the pH during metaraminol extraction and associated dissociation of the reactant oleic acid, refer to Figure 33. 1-3 show the volume of added NaOH for the three extraction steps, 1b shows the corresponding reaction pH in the first extraction step (with stirring), which was set to pH 7.6 (without stirring).

Additional information on stereoselectivity in the repeated reactive *in situ* extractions

In the repeated reactive extraction steps (section 3.3.3.3), a decrease in *ee* of the substrate (*R*)-3-OH-PAC was observed. Already after 24 h (representing the first extraction step), the formation of the complementary enantiomer (*S*)-3-OH-PAC was observed (Figure A2.7). Additional experiments could show that this racemization was caused by the amine donor L-alanine. This effect was observed for both enantiomeric starting compounds, (*S*)-3-OH-PAC or (*R*)-3-OH-PAC (Figure A2.8). An influence of the whole cell formulation or the organic overlay for *in situ* product extraction was excluded as determining factors, because the *ee* for (*S*)-3-OH-PAC dropped in the reaction with L-alanine from 90% to 60% in 48 h with purified *Bm*TA and without ISPR (data not shown). As a result of the substrate racemization, also the *ic* of the amino alcohol product was reduced over time (as specified in the main text), although not as drastic compared to the *ee* of the substrate. This indicates that the substrate specificity and stereoselectivity of the applied amine transaminases was retained, as only one additional product stereoisomer was detected *via* chiral HPLC analysis ((1*R*,2*S*)-3-AHP and (1*S*,2*S*)-3-AHP).

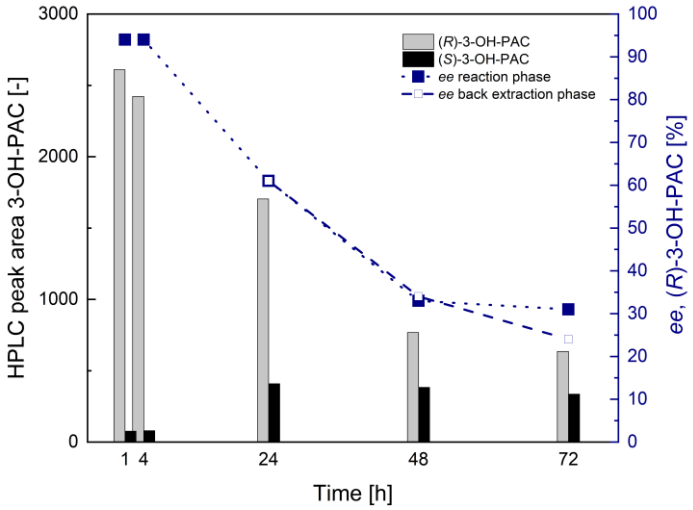

Figure A2.7 Decrease in the enantiomeric excess for (*R*)-3-OH-PAC in the reactive ISPR experiments over three repeated extraction steps (after 24 h, 48 h and 72 h, respectively).

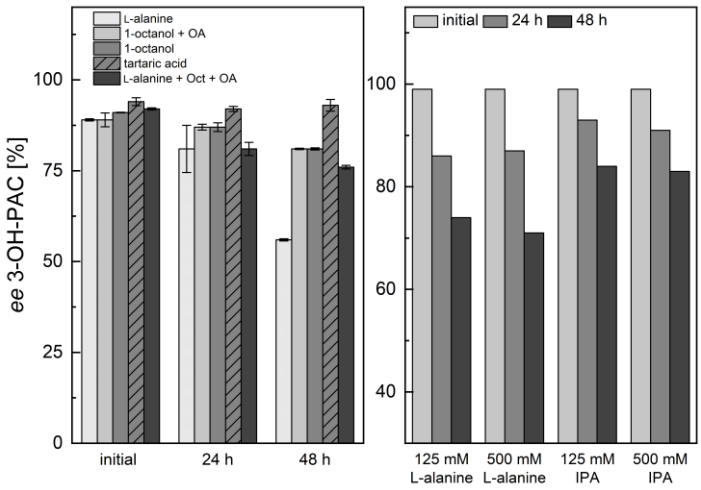

Figure A2.8 Incubation of (*S*)-3-OH-PAC (left) or (*R*)-3-OH-PAC (right) in the presence of different components of the reactive ISPR system. Racemization 3-OH-PAC was observed in the presence of the amine donors L-alanine and IPA. Left: the (*S*)-3-OH-PAC was not recrystallized after production, hence the initial *ee* was slighly lower (cira 90% *ee*) as for the bioconversion experiments shown in section 3.3.3.4. Right: Only slight effects of increased amine donor concentrations (500 mM compared to 125 mM L-alanine or IPA, respectively) were observed. Incubation conditions: 20 mM (*S*)- or (*R*)-3-OH-PAC in 100 mM Kpi buffer pH 7.5 containing 1 mM PLP or 100 mM tartaric acid, 125 mM L-alanine, where indicated 250 µL of 1-octanol containing 0.25 M oleic acid (Oct-OA) was added, 30 °C, shaken in a closed glass vial at 750 rpm**.**

In the reaction system with (S)-3-OH-PAC as substrate, an additional substrate degradation was observed (Figure A2.9), which lowered the overall achievable product yield (refer to the main text in section 3.3.3.4).

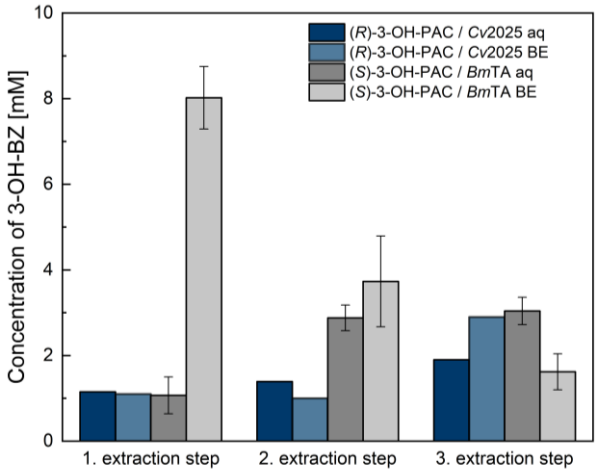

Figure A2.9 Concentration of 3-hydroxybenzoate (3-OH-BZ) as degradation product of the substrate 3-OH-PAC in three repeated reactive *in situ* extraction steps. Separate back extraction phases (BE) and one aqueous reaction phase (aq) are shown. Overall, higher formation of 3-OH-BZ were observed in the reaction system with (*S*)-3-OH-PAC and *Bm*TA as biocatalyst.

Supplementary information for chapter 3.4

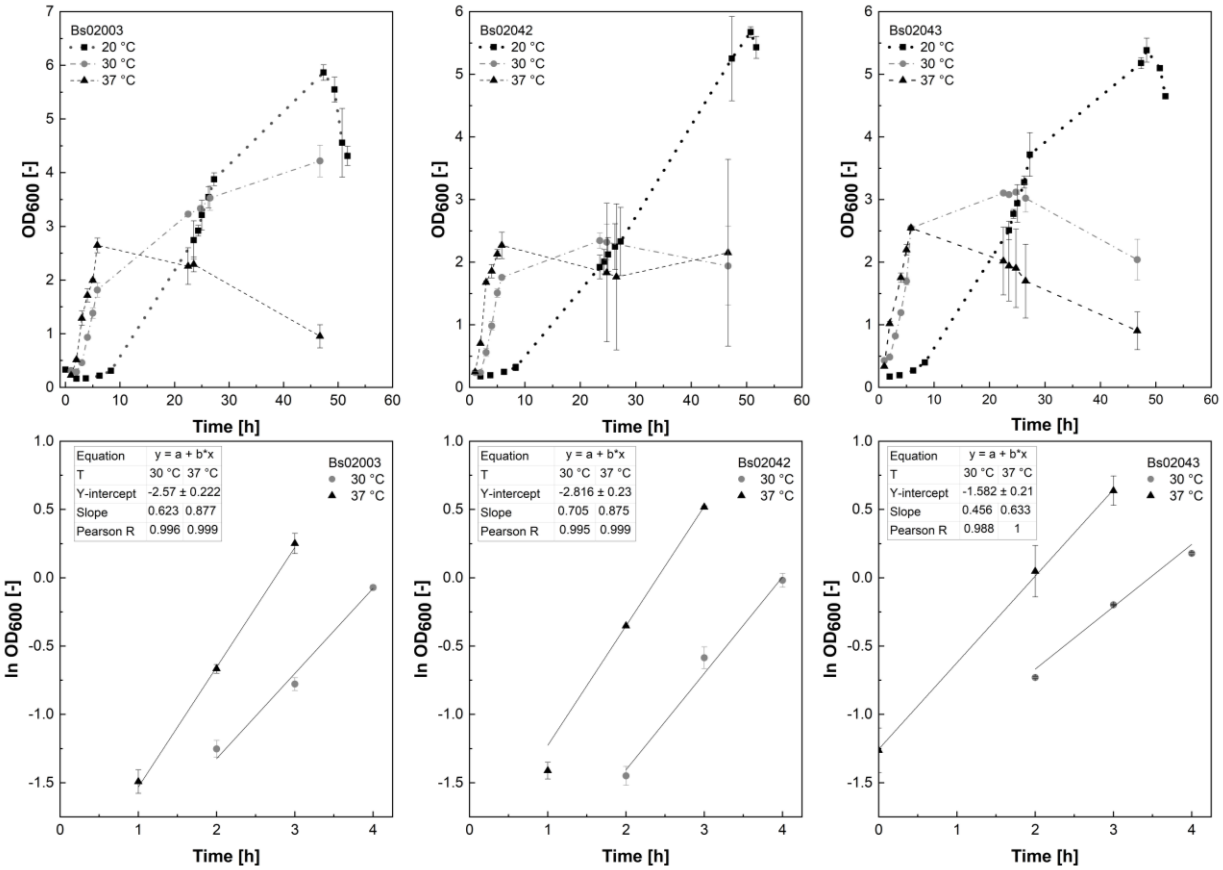

Figure A2.10 Growth curves of *B. subtilis* strains at different cultivation temperatures. The cultivated strains were the wildtype (Bs02003, left) and recombinant strains for spore display of *Bm*TA (Bs02042, middle) and *Ap*PDC var (Bs02043, right). The growth rates were determined from the linear range of ln(OD_{600}), which are shown in the lower row.

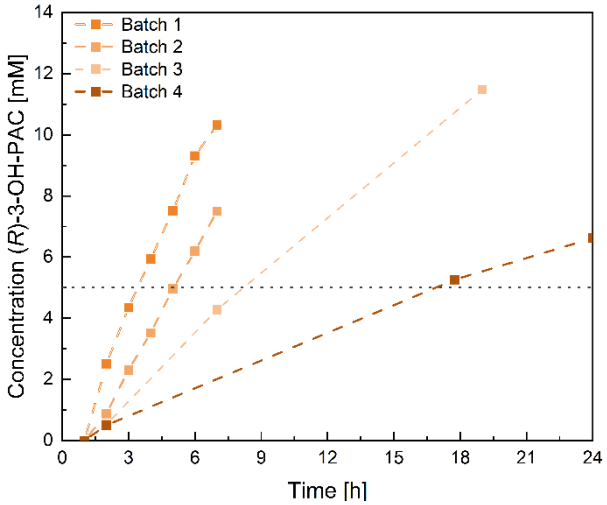

Figure A2.11 Time-resolved carboligation reactions with recycling of EziG™-Opal immobilized *Ap*PDC var for four consecutive reaction cycles. It becomes obvious that the overall reaction rate decreased upon repeated recycling of the immobilized carboligase.

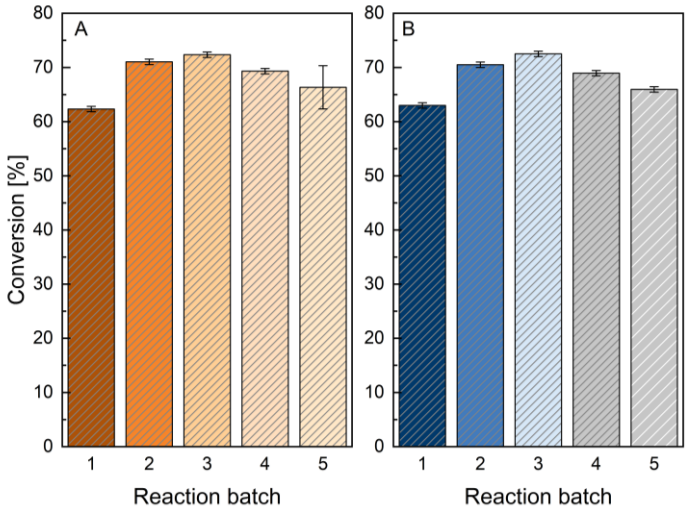

Figure A2.12 Recycling of *Cv*2025 immobilized on EziG™-Opal in a model reaction with α-MBA and pyruvate in five consecutive reaction cycles. In contrast to the reaction system to metaraminol, the recycling of the immobilized amine transaminase was possible in this reaction system.

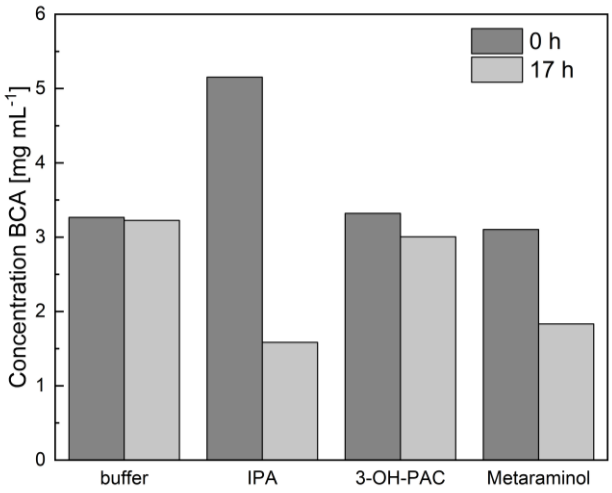

Figure A2.13 Protein determination of *Cv*2025 immobilized on EziG™-Opal before and after incubation in buffer (100 mM HEPES pH 8.0, 0.1 mM PLP) or in the same buffer containing IPA (250 mM), (*R*)-3-OH-PAC (20 mM) or metaraminol bitartrate (20 mM), respectively. The protein concentration was determined by BCA. The incubation was performed in closed 1.5 mL glass reaction vials at 1000 rpm and 30 °C for 17 h and the beads were washed three times with buffer before measuring BCA again.

Supplementary information for chapter 3.5

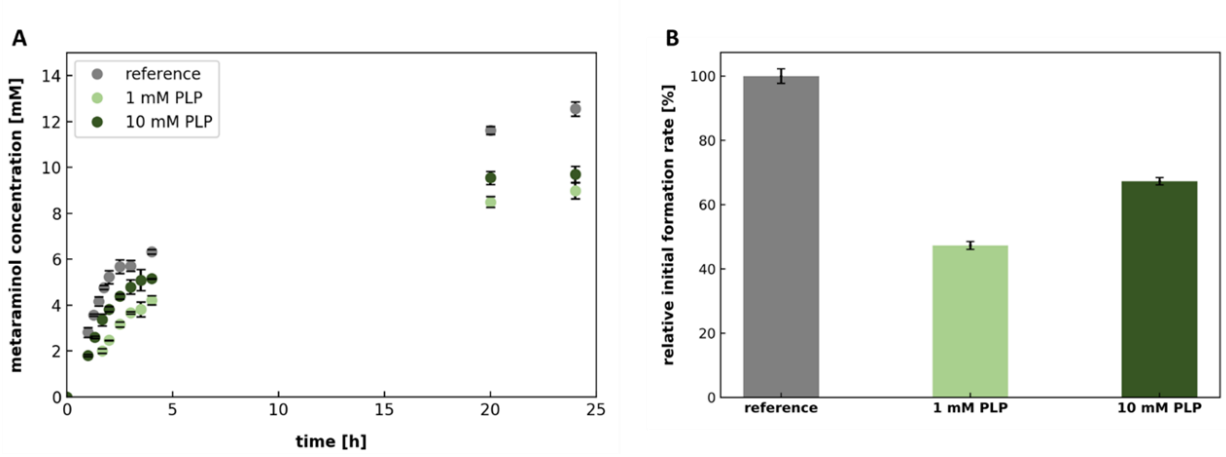

Figure A2.14 Influence of the cofactor PLP on the stability of *Cv*2025 upon incubation with (*R*)-3-OH-PAC for 3 h. Incubation solutions: ● reference, ● 100 mM (*R*)-3-OH-PAC and 1 mM PLP, ● 100 mM (*R*)-3-OH-PAC and 10 mM PLP. **A** illustrates the time-dependent metaraminol concentration course and **B** the relative initial formation rate. The relative initial formation rate was calculated with the slope of the linear equation in the linear part of the time-dependent concentration course. Error bars indicate the variance of technical duplicates. Only the metaraminol concentration was measured. Incubation solution of the reference consisted of 100 mM Kpi buffer pH 7.5, 1 mM PLP, 10 mg mL^{-1} lyophilized whole cells (*Cv*2025, 0.78 ± 0.06 U/mg). Reaction conditions in assay: 20 mM (*R*)-3-OH-PAC, 125 mM IPA, 1 mM PLP, 100 mM Kpi buffer pH 7.5, 10 mg mL^{-1} lyophilized whole cells, 30 °C, 850 rpm, 1 mL, open reaction vial, 24 h.

Supplementary information for chapter 3.6

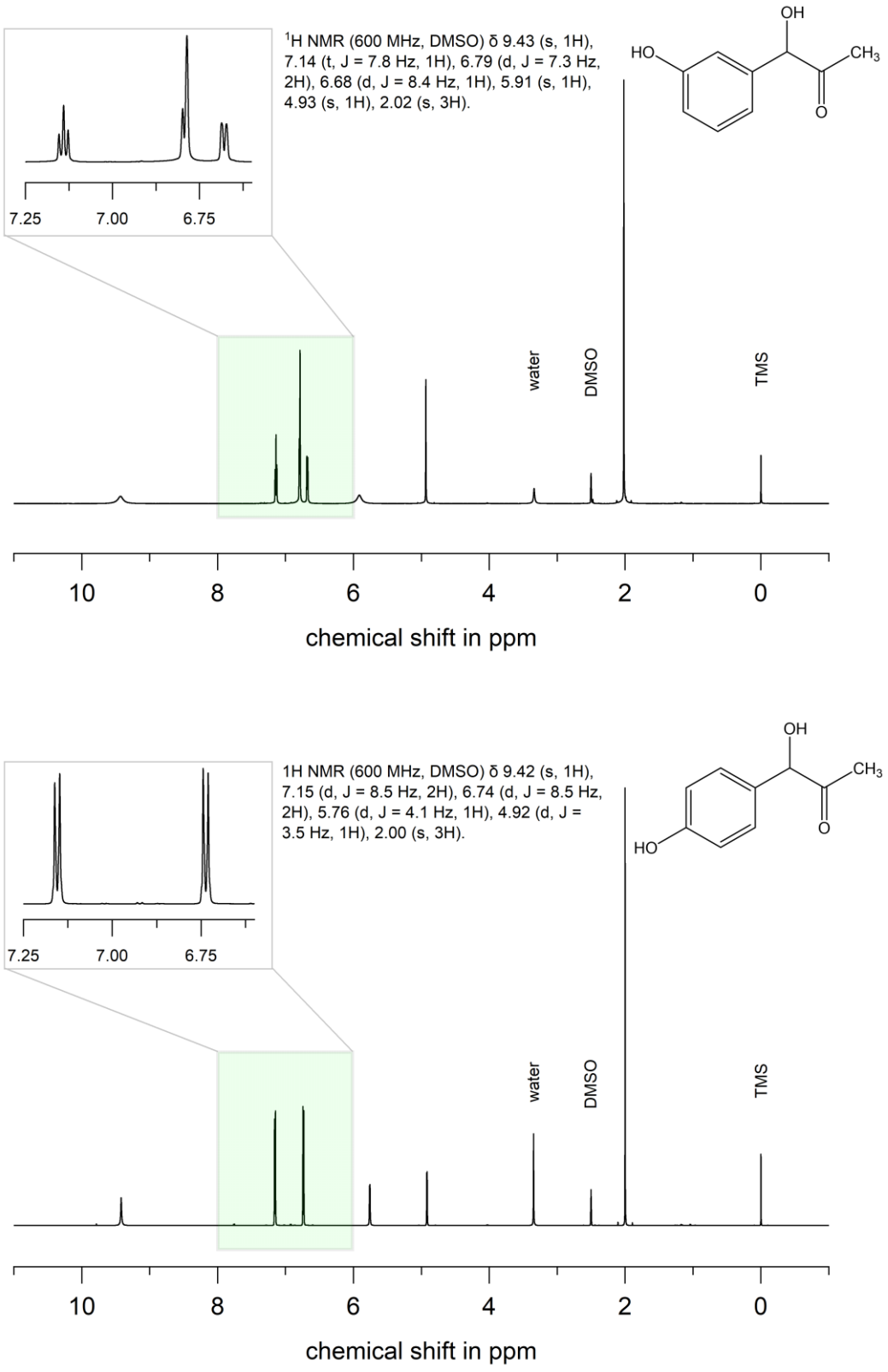

Figure A2.15 ^{1}H-NMR spectra of purified 3-OH-PAC (upper) and 4-OH-PAC (lower).

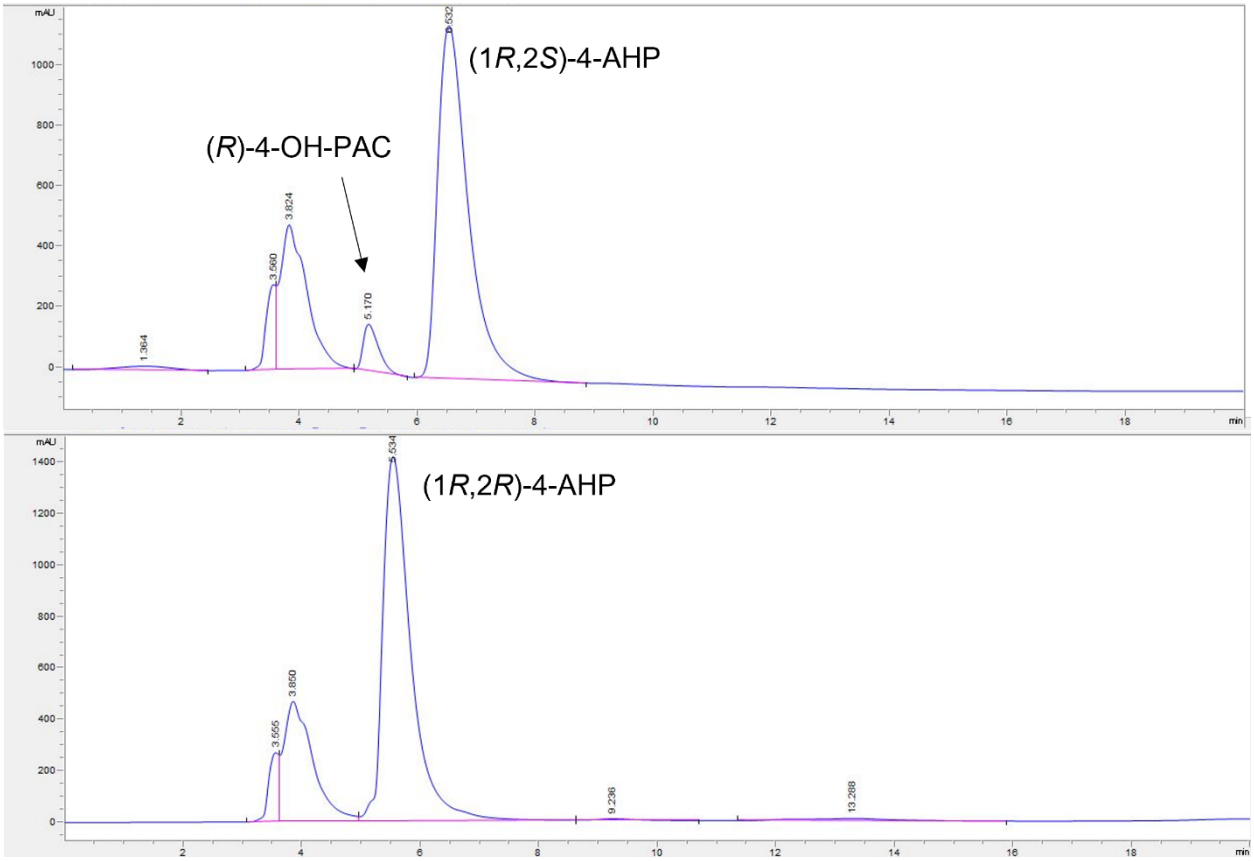

Figure A2.16 HPLC chromatogram of chiral analysis of (1*R*,2S)-4-AHP (transamination of (*R*)-4-OH-PAC and *Cv*2025 as catalyst) and (1*R*,2*R*)-4-AHP (transamination of (*R*)-4-OH-PAC and *As*TA as catalyst). Method IV: Crownpak CR-I (+) (3 x 150 mm, 5 µm), 15 °C, 5 µL injection, 80% 0.1 M $HClO_4$/20% ACN, 0.3 mL min^{-1}, 20 min, DAD detection at 210 nm. Retention times: (1*R*,2*S*)-4-AHP 6.5 min, (1*R*,2*R*)-4-AHP 5.5 min, 4-OH-PAC 5.1 min. The samples were taken after 5 h reaction time.

A.3 Plasmids

A.3.1 Gene sequences of fusion constructs for spore display with *B. subtilis* KO7

Gene sequence of amine transaminase from *Bacillus megaterium* SC6394 (*Bm*TA, codon-optimized for *B. subtilis*) as fusion construct in pCASCADEv1.0 (7417 bps):

Entire plasmid: coat protein Y (Cot Y), linker, *Bm*TA

TACGAGGGAAGAGTTCATCTGACTAACTGATAAGCGTTGGTTTGGCAATCTTATCGGGCTATGCATCCAAGCATATGATGAATAT
ATAGACGTTCACCCACACCAAGTGGGGCACGGGTACATATGTTGTTAAGGACTAAAGTCAAATACCCTATAAAGAAGGAGCTGA
AATCAATGAGCTGCGGAAAAACCCATGGCCGGCATGAGAACTGTGTATGCGATGCAGTGGAAAAGATTTTAGCAGAGCAGGAG
GCAGTTGAAGAACAGTGTCCGACTGGCTGCTATACCAACCTTTTAAACCCTACGATTGCTGGAAAAGACACAATTCCGTTTCTC
GTTTTTGATAAAAAAGGCGGATTGTTCTCCACATTCGGAAACGTAGGGGGATTTGTGGATGATATGCAATGCTTTGAATCCATTT
TCTTCCGCGTCGAAAAATTATGCGATTGCTGTGCAACACTGTCTATTTTACGCCCGGTCGATGTCAAAGGCGATACCTTAAGTGT
TTGCCACCCTTGCGACCCGGATTTCTTCGGGCTAGAAAAAACAGATTTCTGCATTGAAGTGGATCTCGGATGCTTCTGCGCGAT
TCAGTGCCTGTCACCAGAGCTAGTTGACAGAACATCGCCTCACAAAGATAAAAAGCATCATCACAATGGAGGTGGAGGTGGTG
GAAGTGGTGGAGGTGGTGGAAGTATGGCTAGCAGAGGATCGCATCACCATCACCATCACGGCGCCAGCCTGACCGTGCAGAA
AATTAATTGGGAACAGGTGAAAGAATGGGATCGCAAATATCTGATGCGTACCTTTAGCACCCAGAATGAATATCAGCCGGTTCC
GATTGAAAGCACCGAAGGCGATTATCTGATTATGCCGGATGGCACCCGTCTGCTGGATTTTTTTAATCAGCTGTATTGCGTTAAT
CTGGGCCAGAAAAACCAGAAAGTGAACGCAGCAATTAAAGAAGCACTGGATCGTTACGGTTTTGTGTGGGATACCTATGCCAC
CGATTATAAAGCAAAAGCCGCAAAAATTATTATTGAAGATATTCTGGGCGATGAAGATTGGCCTGGTAAAGTTCGTTTTGTTAGC
ACCGGTAGCGAAGCAGTTGAAACCGCACTGAATATTGCACGTCTGTATACCAATCGTCCGCTGGTTGTTACCCGTGAACATGAT
TATCATGGTTGGACCGGTGGTGCAGCAACCGTTACCCGTCTGCGTAGCTATCGTAGCGGTCTGGTTGGTGAAAATAGCGAAAG
CTTTAGCGCACAGATTCCGGGTAGCAGCTATAATAGCGCAGTTCTGATGGCACCGAGCCCGAATATGTTTCAGGATTCCGATG
GTAATCTGCTGAAAGATGAAAATGGTGAACTGCTGTCCGTTAAATATACCCGTCGCATGATTGAAAATTATGGTCCGGAACAGG
TTGCAGCAGTTATTACCGAAGTTAGCCAGGGTGCAGGTAGCGCAATGCCTCCGTATGAATATATTCCGCAGATTCGTAAAATGA
CCAAAGAACTGGGTGTTCTGTGGATTAATGATGAAGTGCTGACCGGTTTTGGTCGTACCGGTAAATGGTTTGGCTATCAGCATT
ATGGTGTTCAGCCGGATATTATTACCATGGGTAAAGGTCTGAGCAGCAGCAGCCTGCCTGCAGGTGCAGTTCTGGTTAGCAAA
GAAATCGCAGCCTTTATGGATAAACATCGTTGGGAAAGCGTTAGCACCTATGCAGGTCATCCGGTTGCAATGGCAGCAGTTTGT
GCAAATCTGGAAGTGATGATGGAAGAAAATTTTGTGGAACAGGCCAAAGATAGCGGTGAATATATCCGTAGCAAACTGGAACTG
CTGCAGGAAAAACATAAAAGCATTGGCAATTTTGATGGTTATGGCCTGCTGTGGATTGTTGATATTGTGAATGCCAAAACCAAAA
CCCCGTATGTTAAACTGGATCGCAATTTTACCCATGGCATGAATCCGAATCAGATTCCGACCCAGATTATCATGAAAAAAGCCCT
GGAAAAAGGTGTTCTGATTGGTGGTGTTATGCCGAATACCATGCGTATTGGTGCAAGCCTGAATGTTAGCCGTGGCGATATTGA
TAAAGCAATGGATGCACTGGATTATGCCCTGGATTATCTGGAAAGCGGTGAATGGCAGTAATAACACGCGTTGATCAGGCGCCT
CGTTCCACTGAGCGTCAGACCCCGTAGAAAAGATCAAAGGATCTTCTTGAGATCCTTTTTTTCTGCGCGTAATCTGCTGCTTGCA
AACAAAAAAACCACCGCTACCAGCGGTGGTTTGTTTGCCGGATCAAGAGCTACCAACTCTTTTTCCGAAGGTAACTGGCTTCAG
CAGAGCGCAGATACCAAATACTGTTCTTCTAGTGTAGCCGTAGTTAGGCCACCACTTCAAGAACTCTGTAGCACCGCCTACATA
CCTCGCTCTGCTAATCCTGTTACCAGTGGCTGCTGCCAGTGGCGATAAGTCGTGTCTTACCGGGTTGGACTCAAGACGATAGTT
ACCGGATAAGGCGCAGCGGTCGGGCTGAACGGGGGGTTCGTGCACACAGCCCAGCTTGGAGCGAACGACCTACACCGAACT
GAGATACCTACAGCGTGAGCTATGAGAAAGCGCCACGCTTCCCGAAGGGAGAAAGGCGGACAGGTATCCGGTAAGCGGCAGG
GTCGGAACAGGAGAGCGCACGAGGGAGCTTCCAGGGGGAAACGCCTGGTATCTTTATAGTCCTGTCGGGTTTCGCCACCTCT
GACTTGAGCGTCGATTTTTGTGATGCTCGTCAGGGGGGCGGAGCCTATGGAAAAACGCCAGCAACGCGGCCTTTTTACGGTTC
CTGGCCTTTTGCTGGCCTTTTGCTCACATGTTCTTTCCTGCGTTATCCCCTGATTCTGTGGATAACCGTATTACCGCCTTTGAGT
GAGCTGATACCGCTCGCCGCAGCCGAACGACCGAGCGCAGCGAGTCAGTGAGCGAGGAAGCGGAAGAGCGCCCAATACGCA
AACCGCCTCTCCCCGCGCGTTGGCCGATTCATTAATGCAGGTTGATCACCTAGAGGATCCCCCAAAGCATAAAAACTTGCATGG
ACTAATGCTTGAAACCCAGGACAATAACCTTATAGCTTGTAAATTCTATCATAATTGTGGTTTCAAAATCGGCTCCGTCGATACTA
TGTTATACGCCAACTTTGAAAACAACTTTGAAAAAGCTGTTTTCTGGTATTTAAGGTTTTAGAATGCAAGGAACAGTGAATTGGAG
TTCGTCTTGTTATAATTAGCTTCTTGGGGTATCTTTAAATACTGTAGAAAAGAGGAAGGAAATAATAAATGGCTAAAATGAGAATA
TCACCGGAATTGAAAAAACTGATCGAAAAATACCGCTGCGTAAAAGATACGGAAGGAATGTCTCCTGCTAAGGTATATAAGCTG
GTGGGAGAAAATGAAAACCTATATTTAAAAATGACGGACAGCCGGTATAAAGGGACCACCTATGATGTGGAACGGGAAAAGGA
CATGATGCTATGGCTGGAAGGAAAGCTGCCTGTTCCAAAGGTCCTGCACTTTGAACGGCATGATGGCTGGAGCAATCTGCTCA
TGAGTGAGGCCGATGGCGTCCTTTGCTCGGAAGAGTATGAAGATGAACAAAGCCCTGAAAAGATTATCGAGCTGTATGCGGAG
TGCATCAGGCTCTTTCACTCCATCGACATATCGGATTGTCCCTATACGAATAGCTTAGACAGCCGCTTAGCCGAATTGGATTACT
TACTGAATAACGATCTGGCCGATGTGGATTGCGAAAACTGGGAAGAAGACACTCCATTTAAAGATCCGCGCGAGCTGTATGATT
TTTTAAAGACGGAAAAGCCCGAAGAGGAACTTGTCTTTTCCCACGGCGACCTGGGAGACAGCAACATCTTTGTGAAAGATGGCA
AAGTAAGTGGCTTTATTGATCTTGGGAGAAGCGGCAGGGCGGACAAGTGGTATGACATTGCCTTCTGCGTCCGGTCGATCAGG
GAGGATATCGGGGAAGAACAGTATGTCGAGCTATTTTTTGACTTACTGGGGATCAAGCCTGATTGGGAGAAAATAAAATATTATA
TTTTACTGGATGAATTGTTTTAGTACCTAGATTTAGATGTCTAAAAAGCCTGCAGTCGCGAGGCCTCGACGGATCCCCAAAGCA
CTTGCATAGGCTAATGCCTGGCTTGGTTTTTCAGCTAAAATAACCGTACTCATTAACTATCCCTCTTTTCATTGTTTTTTCTTTGAT
CGACTGTCACGTTGTATCTTGATCGATACCTTCTAAACGTTCGGCGATTAATTCCAGTTTGTTCTTCAACTTCTTTATCGGATAAA
CCGTTCAAAAACAAATCGAAAGCGTGTTGTAAACGTGGATCATTTTCTTTGAATTTCAGTTGTCGCCCTTTGAATTTTCCTTTTTT
CTTAGCAATTTCAATTCCTTGGGCTTGGCGTTCTTTAATTCGTTTGCGTTCAGATTCCGCTTGGTACTTATACAATTCAATCACTA
AATTATTAATCAGCCGTCTTAAATTTTCATCTTCAATACCATTCATTGAGGGTAAATTTAAGACTTCCAGGGTTGCCCCCTTAATTT
GAATTTGATTCATCAATTCTGTTAATTCTTTATTATTTCGTCCTAATCGATCTAATTCAGTAACAACAACTATATCCCCTTCACGAA
TATAGTTAAGCATAGCTTGTAATTGTGGGCGTTCGACCGATTGACCGCTTGCTTTGTCTGAAAAGACCTTAGAAACGCCCTCTAA
CGCTTTCAGTTGTCTATCTAAGTTCTGTTCTTTGCTACTGACACGTGCATACCCTACTTTAGTCATGTTAAAAAACACCTCCCTTG
TTAAGAAAAAAATAAATTGGATATGAATTGGGAATTCTATTTAATCACTTTGACTAGCAAATACTAACAACAAGACACACACACCA
AAAATCAAAAATTCACTACTTTTAGTTAAAAACCACGTAACCACAAGAACTAATCCAATCCATGTAATCGGGTTCTTCAAATATTTC
TCCAAGATTTTCCTCCTCTAATATGCTCAACTTAAATGACCTATTCAATAAATCTATTATGCTGCTAAATAGTTTATAGGACAAATA
AGTATACTCTAATGACCTATAAAAGATAGAAAATTAAAAAATCAAGTGTTCGCTTCGCTCTCACTGCCCCTCGACGTTTTAGTAGC
CTTTCCCTCACTTCGTTCAGTCCAAGCCAACTAAAAGTTTTCGGGCTACTCTCTCCTTCTCCCCCTAATAATTAATTAAAATCTTA
CTCTGTATATTTCTGCTAATCATTCGCTAAACAGCAAAGAAAAAACAAACACGTATCATAGATATAAATGTAATGGCATAGTGCGG
GTTTTATTTTCAGCCTGTATCATAGCTAAACAAATCGAGTTGTGTGTCCGTTTTAGGGCGTTCTGCTAGCTTGTTTAAAGTCTCTT

GAATGAATGTATGCTCTAAGTCAAAAGAATTTGTCAGCGCCTTTATATAGCTTTCTTTTTCTTCTTTTTTTACTTTAATGATCGATA
GCAACAATGATTTAACACTAGCAAGTTGAATGCCACCATTTCTTCCTGGTTTAATCTTAAAGAAAATTTCCTGATTCGCCTTCAGT
ACCTTCAGCAATTTATCTAATGTCCGTTCAGGAATGCCTAGCACTTCTCTAATCTCTTTTTTGGTCGTCACTAAATAAGGCTTGTA
TACATCGCTTTTTTCGCTAATATAAGCCATTAAATCTTCTTTCCATTCTGACAAATGAACACGTTGACGTTCGCTTCTTTTTTTCTT
GAATTTAAACCACCCTTGACGGACAAATAAATCTTTACTGGTTAAATCACTTGATACCCAAGCTTTGCAAAGAATGGTAATGTATT
CCCTATTAGCCCCTTGATAGTTTTCTGAATAGGCACTTCTAACAATTTTGATTACTTCTTTTTCTTCTAAGGGTTGATCTAATCGAT
TATTAAACTCAAACATATTATATTCGCACGTTTCGATTGAATAGCCTGAACTAAAGTAGGCTAAAGAGAGGGTAAACATGACGTT
ATTACGCCCTATTAAACCCTTTTCTCCTGAAAATTTCGTTTCGTGCAATAAGAGATTAAACCAGGGTTCATCTACTTGTTTTTTGC
CTTCTGTACCGCTTAAAACCGTTAGACTTGAACGAGTAAAGCCCTTATTATCTGTTTGTTTGAAAGACCAATCTTGCCATTCTTTG
AAAGAATAACGGTAATTAGGATCAAAAAATTCTACATTGTCCGTTCTTGGTATGCGAGCAATACCAAAATGATTACACGTTAGATC
AACTGGCAAAGACTTTCCAAAATATTCTCGGATATTTTGCGAAATTATTTTGGCTGCTTTGACAGATTTAAATTCTGATTTTGAAGT
CACATAGACTGGCGTTTCTAAAACAAAATATGCTTGATAACCTTTATCAGATTTGATAATCATAGTAGGCATAAAACCTAAATCAA
TAGCGGTTGTTAAAATATCGCTTGCTGAAATAGTTTCTTTTGCCGTGTGAATATCAAAATCAATAAAGAAGGTATTGATTTGTCTT
AAATTGTTTTCAGAATGTCCTTTCGTGTATGAACGGTTTTCGTCTGCATACGTTCCATAACGATAAACGTTGGGTGTCCAATGTG
TAAATGTATCTTGATTTTCTTGAATCGCTTCCTCGGAAGTCAGAACAACACCACGACCGCCAATCATGCTTGATTTTGAGCGATA
CGCAAAAATAGCCCCTTTGCTTTTACCTGGCTTGGTAGTGATTGAGCGAATTTTACTATTTTTAAATTTGTACTTTAACAAGCCGT
CATGAAGCACAGTTTCTACAACAAAAGGGATATTCATTCAGCTGTTCTCCTTTCCTATAAATCCTATAAAATAGGTTGTTTAATTAA
CTTGGTTTGCTTTTTCATTCAACTGTTTCAATATTGCATGTTTTGAAAAAGATTTTTTTCCTTTATAAGTCAATTTTTTTCCACTAAT
CGAATAAATTATTTTGTTATTTTCTATTAACTTATATATATAATCTTCCCCCTCCGAAGAAAAATACTTATCTGATTTTGTTTCTAAG
TAGATATTTCTCTTTTCTAACTCTTTCTTAAACGTTTCTAGTGTATAGATATTTGCTAATTTTCTTATCTCCAATAAACTATTTTTTAT
ATAAGTTTTACATTCATCATGATTCATACAAACTCCACCTTCTATAAATGAATACAAAAAAAGCAATCAAACGATTTCCGATTGATT
GCTTAACAATTCTTAAATTCAGTAGCTTAGATACTTGAAAACTCTCTGATTTCCCTATATAATGATAGTACGGTTATATACCGTCTT
CAAACAAAGTTAATTAAATAACTTCT

Amino acid sequence of fusion protein: CotY, linker, *Bm*TA

MLLRTKVKYPIKKELKSMSCGKTHGRHENCVCDAVEKILAEQEAVEEQCPTGCYTNLLNPTIAGKDTIPFLVFDKKGGLFSTFGNVGG
FVDDMQCFESIFFRVEKLCDCCATLSILRPVDVKGDTLSVCHPCDPDFFGLEKTDFCIEVDLGCFCAIQCLSPELVDRTSPHKDKKHH
HNGGGGGGSGGGGGSMASRGSHHHHHHGASLTVQKINWEQVKEWDRKYLMRTFSTQNEYQPVPIESTEGDYLIMPDGTRLLDFF
NQLYCVNLGQKNQKVNAAIKEALDRYGFVWDTYATDYKAKAAKIIIEDILGDEDWPGKVRFVSTGSEAVETALNIARLYTNRPLVVTRE
HDYHGWTGGAATVTRLRSYRSGLVGENSESFSAQIPGSSYNSAVLMAPSPNMFQDSDGNLLKDENGELLSVKYTRRMIENYGPEQ
VAAVITEVSQGAGSAMPPYEYIPQIRKMTKELGVLWINDEVLTGFGRTGKWFGYQHYGVQPDIITMGKGLSSSSLPAGAVLVSKEIAA
FMDKHRWESVSTYAGHPVAMAAVCANLEVMMEENFVEQAKDSGEYIRSKLELLQEKHKSIGNFDGYGLLWIVDIVNAKTKTPYVKLD
RNFTHGMNPNQIPTQIIMKKALEKGVLIGGVMPNTMRIGASLNVSRGDIDKAMDALDYALDYLESGEWQ

Gene sequence of pyruvate decarboxylase variant from *Acetobacter pasteurianus* (*Ap*PDC var) as fusion construct in pCASCADEv1.0:

Entire plasmid: ApPDC var, linker, coat protein Y (CotY)

TACGAGGGAAGAGTTCATCTGACTAACTGATAAGCGTTGGTTTGGCAATCTTATCGGGCTATGCATCCAAGCATATGATGAATAT
ATAGACGTTCACCCACACCAAGTGGGGCACGGGTACATATGTTGTTAAGGACTAAAGTCAAATACCCTATAAAGAAGGAGCTGA
AATCAATGACCTATACTGTTGGCATGTATCTTGCAGAACGCCTTGTACAGATCGGGCTGAAGCATCACTTCGCCGTGGCGGGC
GACTACAATCTCGTTCTTCTGGATCAGTTGCTCCTCAACAAGGACATGAAACAGATCTATTGCTGCAATGAGTTGAACTGTGGCT
TCAGCGCGGAAGGCTACGCCCGTTCTAACGGGGCTGCGGCAGCGGTTGTCACCTTCAGCGTTGGCGCCATTTCCGCCATGAA
CGCCCTCGGCGGCGCCTATGCCGAAAACCTGCCGGTTATCCTGATTTCCGGCGCGCCCAACAGCAATGATCAGGGCACAGGT
CATATCCTGCATCACACAATCGGCAAGACGGATTACAGCTACCAGCTTGAAATGGCCCGTCAGGTCACCTGTGCCGCCGAAAG
CATTACCGACGCTCACTCCGCCCCGGCCAAGATTGACCACGTCATTCGCACGGCGCTGCGCGAGCGTAAGCCGGCCTATCTG
GACATCGCGTGCAACATTGCCTCCGAGCCCTGCGTGCGGCCTGGCCCTGTCAGCAGCCTGCTGTCCGAGCCTGAAATCGACC
ACACGAGCCTGAAGGCCGCAGTGGACGCCACGGTTGCCTTGCTGGAAAAATCGGCCAGCCCCGTCATGCTGCTGGGCAGCAA
GCTGCGGGCCGCCAACGCACTGGCCGCAACCGAAACGCTGGCAGACAAGCTGCAATGCGCGGTGACCATCATGGCGGCCGC
GAAAGGCTTTTTCCCCGAAGACCACGCGGGTTTCCGCGGCCTGTACTGGGGCGAAGTCTCGAACCCCGGCGTGCAGGAACTG
GTGGAGACCTCCGACGCACTGCTGTGCATCGCCCCCGTATTCAACGACTATTCAACAGTCGGCTGGTCGGCATGGCCCAAGG
GCCCCAATGTGATTCTGGCTGAGCCCGACCGCGTAACGGTCGATGGCCGCGCCTATGACGGCTTTACCCTGCGCGCCTTCCT
GCAGGCTCTGGCGGAAAAAGCCCCCGCGCCCGGCCTCCGCACAGAAAAGCAGCGTCCCGACGTGCTCGCTCACCGCGAC
ATCCGATGAAGCCGGTCTGACGAATGACGAAATCGTCCGTCATATCAACGCCCTGCTGACATCAAACACGACGCTGGTGGCAG
AAACCGGCGATTCATGGTTCAATGCCATGCGCATGACCCTGCCGCGCGGTGCGCGCGTGGAACTGGAAATGCAGTGGGGCCA
TATCGGCTGGTCCGTGCCCTCCGCCTTCGGCAATGCCATGGGCTCGCAGGACCGCCAGCATGTGGTGATGGTAGGCGATGGC
TCCTTCCAGCTTACCGCGCAGGAAGTGGCTCAGATGGTGCGCTACGAACTGCCCGTCATTATCTTTCTGATCAACAACCGTGG
CTATGTCATTCAAATCGCCATTCATGACGGCCCGTACAACTATATCAAGAACTGGGATTACGCCGGCCTGATGGAAGTCTTCAA
CGCCGGAGAAGGCCATGGACTTGGCCTGAAAGCCACCACCCCGAAGGAACTGACAGAAGCCATCGCCAGGGCAAAAGCCAAT
ACCCGCGGCCCGACGCTGATCGAATGCCAGATCGACCGCACGGACTGCACGGATATGCTGGTTCAATGGGGCCGCAAGGTTG
CCTCAACCAACGCGCGCAAGACCACTCTGGCCCTCGAGCACCACCACCACCACCACGGTGGAGGTGGTGGAAGTGGTGGAG
GTGGTGGAAGTATGAGCTGCGGAAAAACCCATGGCCGGCATGAGAACTGTGTATGCGATGCAGTGGAAAAGATTTTAGCAGAG
CAGGAGGCAGTTGAAGAACAGTGTCCGACTGGCTGCTATACCAACCTTTTAAACCCTACGATTGCTGGAAAAGACACAATTCCG
TTTCTCGTTTTTGATAAAAAAGGCGGATTGTTCTCCACATTCGGAAACGTAGGGGGATTTGTGGATGATATGCAATGCTTTGAAT
CCATTTTCTTCCGCGTCGAAAAATTATGCGATTGCTGTGCAACACTGTCTATTTTACGCCCGGTCGATGTCAAAGGCGATACCTT
AAGTGTTTGCCACCCTTGCGACCCGGATTTCTTCGGGCTAGAAAAAACAGATTTCTGCATTGAAGTGGATCTCGGATGCTTCTG
CGCGATTCAGTGCCTGTCACCAGAGCTAGTTGACAGAACATCGCCTCACAAAGATAAAAAGCATCATCACAATGGATAACACGC
GTTGATCAGGCGCCTCGTTCCACTGAGCGTCAGACCCCGTAGAAAAGATCAAAGGATCTTCTTGAGATCCTTTTTTTCTGCGCG
TAATCTGCTGCTTGCAAACAAAAAAACCACCGCTACCAGCGGTGGTTTGTTTGCCGGATCAAGAGCTACCAACTCTTTTTCCGA
AGGTAACTGGCTTCAGCAGAGCGCAGATACCAAATACTGTTCTTCTAGTGTAGCCGTAGTTAGGCCACCACTTCAAGAACTCTG
TAGCACCGCCTACATACCTCGCTCTGCTAATCCTGTTACCAGTGGCTGCTGCCAGTGGCGATAAGTCGTGTCTTACCGGGTTG
GACTCAAGACGATAGTTACCGGATAAGGCGCAGCGGTCGGGCTGAACGGGGGGTTCGTGCACACAGCCCAGCTTGGAGCGAA

CGACCTACACCGAACTGAGATACCTACAGCGTGAGCTATGAGAAAGCGCCACGCTTCCCGAAGGGAGAAAGGCGGACAGGTA
TCCGGTAAGCGGCAGGGTCGGAACAGGAGAGCGCACGAGGGAGCTTCCAGGGGGAAACGCCTGGTATCTTTATAGTCCTGTC
GGGTTTCGCCACCTCTGACTTGAGCGTCGATTTTTGTGATGCTCGTCAGGGGGGCGGAGCCTATGGAAAAACGCCAGCAACGC
GGCCTTTTTACGGTTCCTGGCCTTTTGCTGGCCTTTTGCTCACATGTTCTTTCCTGCGTTATCCCCTGATTCTGTGGATAACCGT
ATTACCGCCTTTGAGTGAGCTGATACCGCTCGCCGCAGCCGAACGACCGAGCGCAGCGAGTCAGTGAGCGAGGAAGCGGAAG
AGCGCCCAATACGCAAACCGCCTCTCCCCGCGCGTTGGCCGATTCATTAATGCAGGTTGATCACCTAGAGGATCCCCCAAAGC
ATAAAAACTTGCATGGACTAATGCTTGAAACCCAGGACAATAACCTTATAGCTTGTAAATTCTATCATAATTGTGGTTTCAAAATC
GGCTCCGTCGATACTATGTTATACGCCAACTTTGAAAACAACTTTGAAAAAGCTGTTTTCTGGTATTTAAGGTTTTAGAATGCAAG
GAACAGTGAATTGGAGTTCGTCTTGTTATAATTAGCTTCTTGGGGTATCTTTAAATACTGTAGAAAAGAGGAAGGAAATAATAAAT
GGCTAAAATGAGAATATCACCGGAATTGAAAAAACTGATCGAAAAATACCGCTGCGTAAAAGATACGGAAGGAATGTCTCCTGC
TAAGGTATATAAGCTGGTGGGAGAAAATGAAAACCTATATTTAAAAATGACGGACAGCCGGTATAAAGGGACCACCTATGATGT
GGAACGGGAAAAGGACATGATGCTATGGCTGGAAGGAAAGCTGCCTGTTCCAAAGGTCCTGCACTTTGAACGGCATGATGGCT
GGAGCAATCTGCTCATGAGTGAGGCCGATGGCGTCCTTTGCTCGGAAGAGTATGAAGATGAACAAAGCCCTGAAAAGATTATC
GAGCTGTATGCGGAGTGCATCAGGCTCTTTCACTCCATCGACATATCGGATTGTCCCTATACGAATAGCTTAGACAGCCGCTTA
GCCGAATTGGATTACTTACTGAATAACGATCTGGCCGATGTGGATTGCGAAAACTGGGAAGAAGACACTCCATTTAAAGATCCG
CGCGAGCTGTATGATTTTTTAAAGACGGAAAAGCCCGAAGAGGAACTTGTCTTTTCCCACGGCGACCTGGGAGACAGCAACAT
CTTTGTGAAAGATGGCAAAGTAAGTGGCTTTATTGATCTTGGGAGAAGCGGCAGGGCGGACAAGTGGTATGACATTGCCTTCT
GCGTCCGGTCGATCAGGGAGGATATCGGGGAAGAACAGTATGTCGAGCTATTTTTTGACTTACTGGGGATCAAGCCTGATTGG
GAGAAAATAAAATATTATATTTTACTGGATGAATTGTTTTAGTACCTAGATTTAGATGTCTAAAAAGCCTGCAGTCGCGAGGCCTC
GACGGATCCCCAAAGCACTTGCATAGGCTAATGCCTGGCTTGGTTTTTCAGCTAAAATAACCGTACTCATTAACTATCCCTCTTT
TCATTGTTTTTTCTTTGATCGACTGTCACGTTGTATCTTGATCGATACCTTCTAAACGTTCGGCGATTAATTCCAGTTTGTTCTTCA
ACTTCTTTATCGGATAAACCGTTCAAAAACAAATCGAAAGCGTGTTGTAAACGTGGATCATTTTCTTTGAATTTCAGTTGTCGCCC
TTTGAATTTTCCTTTTTTCTTAGCAATTTCAATTCCTTGGGCTTGGCGTTCTTTAATTCGTTTGCGTTCAGATTCCGCTTGGTACTT
ATACAATTCAATCACTAAATTATTAATCAGCCGTCTTAAATTTTCATCTTCAATACCATTCATTGAGGGTAAATTTAAGACTTCCAG
GGTTGCCCCCTTAATTTGAATTTGATTCATCAATTCTGTTAATTCTTTATTATTTCGTCCTAATCGATCTAATTCAGTAACAACAAC
TATATCCCCTTCACGAATATAGTTAAGCATAGCTTGTAATTGTGGGCGTTCGACCGATTGACCGCTTGCTTTGTCTGAAAAGACC
TTAGAAACGCCCTCTAACGCTTTCAGTTGTCTATCTAAGTTCTGTTCTTTGCTACTGACACGTGCATACCCTACTTTAGTCATGTT
AAAAAACACCTCCCTTGTTAAGAAAAAAATAAATTGGATATGAATTGGGAATTCTATTTAATCACTTTGACTAGCAAATACTAACAA
CAAGACACACACCAAAAATCAAAAATTCACTACTTTTAGTTAAAAACCACGTAACCACAAGAACTAATCCAATCCATGTAATCG
GGTTCTTCAAATATTTCTCCAAGATTTTCCTCCTCTAATATGCTCAACTTAAATGACCTATTCAATAAATCTATTATGCTGCTAAAT
AGTTTATAGGACAAATAAGTATACTCTAATGACCTATAAAAGATAGAAAATTAAAAAATCAAGTGTTCGCTTCGCTCTCACTGCCC
CTCGACGTTTTAGTAGCCTTTCCCTCACTTCGTTCAGTCCAAGCCAACTAAAAGTTTTCGGGCTACTCTCTCCTTCTCCCCCTAA
TAATTAATTAAAATCTTACTCTGTATATTTCTGCTAATCATTCGCTAAACAGCAAAGAAAAAACAAACACGTATCATAGATATAAAT
GTAATGGCATAGTGCGGGTTTTATTTTCAGCCTGTATCATAGCTAAACAAATCGAGTTGTGTGTCCGTTTTAGGGCGTTCTGCTA
GCTTGTTTAAAGTCTCTTGAATGAATGTATGCTCTAAGTCAAAAGAATTTGTCAGCGCCTTTATATAGCTTTCTTTTTCTTCTTTTT
TTACTTTAATGATCGATAGCAACAATGATTTAACACTAGCAAGTTGAATGCCACCATTTCTTCCTGGTTTAATCTTAAAGAAAATTT
CCTGATTCGCCTTCAGTACCTTCAGCAATTTATCTAATGTCCGTTCAGGAATGCCTAGCACTTCTCTAATCTCTTTTTTGGTCGTC
ACTAAATAAGGCTTGTATACATCGCTTTTTTCGCTAATATAAGCCATTAAATCTTCTTTCCATTCTGACAAATGAACACGTTGACG
TTCGCTTCTTTTTTTCTTGAATTTAAACCACCCTTGACGGACAAATAAATCTTTACTGGTTAAATCACTTGATACCCAAGCTTTGCA
AAGAATGGTAATGTATTCCCTATTAGCCCCTTGATAGTTTTCTGAATAGGCACTTCTAACAATTTTGATTACTTCTTTTTCTTCTAA
GGGTTGATCTAATCGATTATTAAACTCAAACATATTATATTCGCACGTTTCGATTGAATAGCCTGAACTAAAGTAGGCTAAAGAGA
GGGTAAACATGACGTTATTACGCCCTATTAAACCCTTTTCTCCTGAAAATTTCGTTTCGTGCAATAAGAGATTAAACCAGGGTTC
ATCTACTTGTTTTTTGCCTTCTGTACCGCTTAAAACCGTTAGACTTGAACGAGTAAAGCCCTTATTATCTGTTTGTTTGAAAGACC
AATCTTGCCATTCTTTGAAAGAATAACGGTAATTAGGATCAAAAAATTCTACATTGTCCGTTCTTGGTATGCGAGCAATACCAAAA
TGATTACACGTTAGATCAACTGGCAAAGACTTTCCAAAATATTCTCGGATATTTTGCGAAATTATTTTGGCTGCTTTGACAGATTT
AAATTCTGATTTTGAAGTCACATAGACTGGCGTTTCTAAAACAAAATATGCTTGATAACCTTTATCAGATTTGATAATCATAGTAG
GCATAAAACCTAAATCAATAGCGGTTGTTAAAATATCGCTTGCTGAAATAGTTTCTTTTGCCGTGTGAATATCAAAATCAATAAAG
AAGGTATTGATTTGTCTTAAATTGTTTTCAGAATGTCCTTTCGTGTATGAACGGTTTTCGTCTGCATACGTTCCATAACGATAAAC
GTTGGGTGTCCAATGTGTAAATGTATCTTGATTTTCTTGAATCGCTTCCTCGGAAGTCAGAACAACACCACGACCGCCAATCATG
CTTGATTTTGAGCGATACGCAAAAATAGCCCCTTTGCTTTTACCTGGCTTGGTAGTGATTGAGCGAATTTTACTATTTTTAAATTT
GTACTTTAACAAGCCGTCATGAAGCACAGTTTCTACAACAAAAGGGATATTCATTCAGCTGTTCTCCTTTCCTATAAATCCTATAA
AATAGGTTGTTTAATTAACTTGGTTTGCTTTTTCATTCAACTGTTTCAATATTGCATGTTTTGAAAAAGATTTTTTTCCTTTATAAGT
CAATTTTTTTCCACTAATCGAATAAATTATTTTGTTATTTTCTATTAACTTATATATATAATCTTCCCCCTCCGAAGAAAAATACTTA
TCTGATTTTGTTTCTAAGTAGATATTTCTCTTTTCTAACTCTTTCTTAAACGTTTCTAGTGTATAGATATTTGCTAATTTTCTTATCT
CCAATAAACTATTTTTTATATAAGTTTTACATTCATCATGATTCATACAAACTCCACCTTCTATAAATGAATACAAAAAAAGCAATCA
AACGATTTCCGATTGATTGCTTAACAATTCTTAAATTCAGTAGCTTAGATACTTGAAAACTCTCTGATTTCCCTATATAATGATAGT
ACGGTTATATACCGTCTTCAAACAAAGTTAATTAAATAACTTCT

Amino acid sequence of fusion protein: *Ap*PDC var, linker, CotY

MLLRTKVKYPIKKELKSMTYTVGMYLAERLVQIGLKHHFAVAGDYNLVLLDQLLLNKDMKQIYCCNELNCGFSAEGYARSNGAAAAVV
TFSVGAISAMNALGGAYAENLPVILISGAPNSNDQGTGHILHHTIGKTDYSYQLEMARQVTCAAESITDAHSAPAKIDHVIRTALRERKP
AYLDIACNIASEPCVRPGPVSSLLSEPEIDHTSLKAAVDATVALLEKSASPVMLLGSKLRAANALAATETLADKLQCAVTIMAAAKGFFP
EDHAGFRGLYWGEVSNPGVQELVETSDALLCIAPVFNDYSTVGWSAWPKGPNVILAEPDRVTVDGRAYDGFTLRAFLQALAEKAPA
RPASAQKSSVPTCSLTATSDEAGLTNDEIVRHINALLTSNTTLVAETGDSWFNAMRMTLPRGARVELEMQWGHIGWSVPSAFGNAM
GSQDRQHVVMVGDGSFQLTAQEVAQMVRYELPVIIFLINNRGYVIQIAIHDGPYNYIKNWDYAGLMEVFNAGEGHGLGLKATTPKELT
EAIARAKANTRGPTLIECQIDRTDCTDMLVQWGRKVASTNARKTTLALEHHHHHHGGGGGSGGGGGSMSCGKTHGRHENCVCDAV
EKILAEQEAVEEQCPTGCYTNLLNPTIAGKDTIPFLVFDKKGGLFSTFGNVGGFVDDMQCFESIFFRVEKLCDCCATLSILRPVDVKGD
TLSVCHPCDPDFFGLEKTDFCIEVDLGCFCAIQCLSPELVDRTSPHKDKKHHHNG

A.3.2 Gene sequences for enzyme production in *E. coli* BL21 (DE3)

All enzymes were produced as His-tagged variants.

Gene sequence of amine transaminase from *Chromobacterium violaceum (Cv*2025) in pET29a:

TGGCGAATGGGACGCGCCCTGTAGCGGCGCATTAAGCGCGGCGGGTGTGGTGGTTACGCGCAGCGTGACCGCTACACTTGC
CAGCGCCCTAGCGCCCGCTCCTTTCGCTTTCTTCCCTTCCTTTCTCGCCACGTTCGCCGGCTTTCCCCGTCAAGCTCTAAATCG
GGGGCTCCCTTTAGGGTTCCGATTTAGTGCTTTACGGCACCTCGACCCCAAAAAACTTGATTAGGGTGATGGTTCACGTAGTGG
GCCATCGCCCTGATAGACGGTTTTTCGCCCTTTGACGTTGGAGTCCACGTTCTTTAATAGTGGACTCTTGTTCCAAACTGGAAC
AACACTCAACCCTATCTCGGTCTATTCTTTTGATTTATAAGGGATTTTGCCGATTTCGGCCTATTGGTTAAAAAATGAGCTGATTT
AACAAAAATTTAACGCGAATTTTAACAAAATATTAACGTTTACAATTTCAGGTGGCACTTTTCGGGGAAATGTGCGCGGAACCCC
TATTTGTTTATTTTTCTAAATACATTCAAATATGTATCCGCTCATGAATTAATTCTTAGAAAAACTCATCGAGCATCAAATGAAACT
GCAATTTATTCATATCAGGATTATCAATACCATATTTTTGAAAAAGCCGTTTCTGTAATGAAGGAGAAAACTCACCGAGGCAGTTC
CATAGGATGGCAAGATCCTGGTATCGGTCTGCGATTCCGACTCGTCCAACATCAATACAACCTATTAATTTCCCCTCGTCAAAAA
TAAGGTTATCAAGTGAGAAATCACCATGAGTGACGACTGAATCCGGTGAGAATGGCAAAAGTTTATGCATTTCTTTCCAGACTTG
TTCAACAGGCCAGCCATTACGCTCGTCATCAAAATCACTCGCATCAACCAAACCGTTATTCATTCGTGATTGCGCCTGAGCGAG
ACGAAATACGCGATCGCTGTTAAAAGGACAATTACAAACAGGAATCGAATGCAACCGGCGCAGGAACACTGCCAGCGCATCAA
CAATATTTTCACCTGAATCAGGATATTCTTCTAATACCTGGAATGCTGTTTTCCCGGGGATCGCAGTGGTGAGTAACCATGCATC
ATCAGGAGTACGGATAAAATGCTTGATGGTCGGAAGAGGCATAAATTCCGTCAGCCAGTTTAGTCTGACCATCTCATCTGTAAC
ATCATTGGCAACGCTACCTTTGCCATGTTTCAGAAACAACTCTGGCGCATCGGGCTTCCCATACAATCGATAGATTGTCGCACC
TGATTGCCCGACATTATCGCGAGCCCATTTATACCCATATAAATCAGCATCCATGTTGGAATTTAATCGCGGCCTAGAGCAAGAC
GTTTCCCGTTGAATATGGCTCATAACACCCCTTGTATTACTGTTTATGTAAGCAGACAGTTTTATTGTTCATGACCAAAATCCCTT
AACGTGAGTTTTCGTTCCACTGAGCGTCAGACCCCGTAGAAAAGATCAAAGGATCTTCTTGAGATCCTTTTTTTCTGCGCGTAAT
CTGCTGCTTGCAAACAAAAAAACCACCGCTACCAGCGGTGGTTTGTTTGCCGGATCAAGAGCTACCAACTCTTTTTCCGAAGGT
AACTGGCTTCAGCAGAGCGCAGATACCAAATACTGTCCTTCTAGTGTAGCCGTAGTTAGGCCACCACTTCAAGAACTCTGTAGC
ACCGCCTACATACCTCGCTCTGCTAATCCTGTTACCAGTGGCTGCTGCCAGTGGCGATAAGTCGTGTCTTACCGGGTTGGACT
CAAGACGATAGTTACCGGATAAGGCGCAGCGGTCGGGCTGAACGGGGGGTTCGTGCACACAGCCCAGCTTGGAGCGAACGA
CCTACACCGAACTGAGATACCTACAGCGTGAGCTATGAGAAAGCGCCACGCTTCCCGAAGGGAGAAAGGCGGACAGGTATCC
GGTAAGCGGCAGGGTCGGAACAGGAGAGCGCACGAGGGAGCTTCCAGGGGGAAACGCCTGGTATCTTTATAGTCCTGTCGG
GTTTCGCCACCTCTGACTTGAGCGTCGATTTTTGTGATGCTCGTCAGGGGGGCGGAGCCTATGGAAAAACGCCAGCAACGCGG
CCTTTTTACGGTTCCTGGCCTTTTGCTGGCCTTTTGCTCACATGTTCTTTCCTGCGTTATCCCCTGATTCTGTGGATAACCGTATT
ACCGCCTTTGAGTGAGCTGATACCGCTCGCCGCAGCCGAACGACCGAGCGCAGCGAGTCAGTGAGCGAGGAAGCGGAAGAG
CGCCTGATGCGGTATTTTCTCCTTACGCATCTGTGCGGTATTTCACACCGCATATATGGTGCACTCTCAGTACAATCTGCTCTGA
TGCCGCATAGTTAAGCCAGTATACACTCCGCTATCGCTACGTGACTGGGTCATGGCTGCGCCCCGACACCCGCCAACACCCGC
TGACGCGCCCTGACGGGCTTGTCTGCTCCCGGCATCCGCTTACAGACAAGCTGTGACCGTCTCCGGGAGCTGCATGTGTCAG
AGGTTTTCACCGTCATCACCGAAACGCGCGAGGCAGCTGCGGTAAAGCTCATCAGCGTGGTCGTGAAGCGATTCACAGATGTC
TGCCTGTTCATCCGCGTCCAGCTCGTTGAGTTTCTCCAGAAGCGTTAATGTCTGGCTTCTGATAAAGCGGGCCATGTTAAGGGC
GGTTTTTTCCTGTTTGGTCACTGATGCCTCCGTGTAAGGGGGATTTCTGTTCATGGGGGTAATGATACCGATGAAACGAGAGAG
GATGCTCACGATACGGGTTACTGATGATGAACATGCCCGGTTACTGGAACGTTGTGAGGGTAAACAACTGGCGGTATGGATGC
GGCGGGACCAGAGAAAAATCACTCAGGGTCAATGCCAGCGCTTCGTTAATACAGATGTAGGTGTTCCACAGGGTAGCCAGCAG
CATCCTGCGATGCAGATCCGGAACATAATGGTGCAGGGCGCTGACTTCCGCGTTTCCAGACTTTACGAAACACGGAAACCGAA
GACCATTCATGTTGTTGCTCAGGTCGCAGACGTTTTGCAGCAGCAGTCGCTTCACGTTCGCTCGCGTATCGGTGATTCATTCTG
CTAACCAGTAAGGCAACCCCGCCAGCCTAGCCGGGTCCTCAACGACAGGAGCACGATCATGCGCACCCGTGGGGCCGCCATG
CCGGCGATAATGGCCTGCTTCTCGCCGAAACGTTTGGTGGCGGGACCAGTGACGAAGGCTTGAGCGAGGGCGTGCAAGATTC
CGAATACCGCAAGCGACAGGCCGATCATCGTCGCGCTCCAGCGAAAGCGGTCCTCGCCGAAAATGACCCAGAGCGCTGCCGG
CACCTGTCCTACGAGTTGCATGATAAAGAAGACAGTCATAAGTGCGGCGACGATAGTCATGCCCCGCGCCCACCGGAAGGAG
CTGACTGGGTTGAAGGCTCTCAAGGGCATCGGTCGAGATCCCGGTGCCTAATGAGTGAGCTAACTTACATTAATTGCGTTGCG
CTCACTGCCCGCTTTCCAGTCGGGAAACCTGTCGTGCCAGCTGCATTAATGAATCGGCCAACGCGCGGGGAGAGGCGGTTTG
CGTATTGGGCGCCAGGGTGGTTTTTCTTTTCACCAGTGAGACGGGCAACAGCTGATTGCCCTTCACCGCCTGGCCCTGAGAGA
GTTGCAGCAAGCGGTCCACGCTGGTTTGCCCCAGCAGGCGAAAATCCTGTTTGATGGTGGTTAACGGCGGGATATAACATGAG
CTGTCTTCGGTATCGTCGTATCCCACTACCGAGATGTCCGCACCAACGCGCAGCCCGGACTCGGTAATGGCGCGCATTGCGC
CCAGCGCCATCTGATCGTTGGCAACCAGCATCGCAGTGGGAACGATGCCCTCATTCAGCATTTGCATGGTTTGTTGAAAACCG
GACATGGCACTCCAGTCGCCTTCCCGTTCCGCTATCGGCTGAATTTGATTGCGAGTGAGATATTTATGCCAGCCAGCCAGACG
CAGACGCGCCGAGACAGAACTTAATGGGCCCGCTAACAGCGCGATTTGCTGGTGACCCAATGCGACCAGATGCTCCACGCCC
AGTCGCGTACCGTCTTCATGGGAGAAAATAATACTGTTGATGGGTGTCTGGTCAGAGACATCAAGAAATAACGCCGGAACATTA
GTGCAGGCAGCTTCCACAGCAATGGCATCCTGGTCATCCAGCGGATAGTTAATGATCAGCCCACTGACGCGTTGCGCGAGAAG
ATTGTGCACCGCCGCTTTACAGGCTTCGACGCCGCTTCGTTCTACCATCGACACCACCACGCTGGCACCCAGTTGATCGGCGC
GAGATTTAATCGCCGCGACAATTTGCGACGGCGCGTGCAGGGCCAGACTGGAGGTGGCAACGCCAATCAGCAACGACTGTTT
GCCCGCCAGTTGTTGTGCCACGCGGTTGGGAATGTAATTCAGCTCCGCCATCGCCGCTTCCACTTTTTCCCGCGTTTTCGCAG
AAACGTGGCTGGCCTGGTTCACCACGCGGGAAACGGTCTGATAAGAGACACCGGCATACTCTGCGACATCGTATAACGTTACT
GGTTTCACATTCACCACCCTGAATTGACTCTCTTCCGGGCGCTATCATGCCATACCGCGAAAGGTTTTGCGCCATTCGATGGTG
TCCGGGATCTCGACGCTCTCCCTTATGCGACTCCTGCATTAGGAAGCAGCCCAGTAGTAGGTTGAGGCCGTTGAGCACCGCCG
CCGCAAGGAATGGTGCATGCAAGGAGATGGCGCCCAACAGTCCCCCGGCCACGGGGCCTGCCACCATACCCACGCCGAAAC
AAGCGCTCATGAGCCCGAAGTGGCGAGCCCGATCTTCCCCATCGGTGATGTCGGCGATATAGGCGCCAGCAACCGCACCTGT
GGCGCCGGTGATGCCGGCCACGATGCGTCCGGCGTAGAGGATCGAGATCGATCTCGATCCCGCGAAATTAATACGACTCACT
ATAGGGGAATTGTGAGCGGATAACAATTCCCCTCTAGAAATAATTTTGTTTAACTTTAAGAAGGAGATATACCATGGGCCATCAT
CATCATCATCATATGCAGAAGCAACGTACGACCAGCCAATGGCGCGAACTGGATGCCGCCCATCACCTGCATCCGTTCACCGA
TACCGCATCGCTGAACCAGGCGGGCGCGCGCGTGATGACGCGCGGAGAGGGCGTCTACCTGTGGGATTCGGAAGGCAACAA
GATCATCGACGGCATGGCCGGACTGTGGTGCGTGAACGTCGGCTACGGCCGCAAGGACTTTGCCGAAGCGGCGCGCCGGCA
GATGGAAGAGCTGCCGTTCTACAACACCTTCTTCAAGACCACCCATCCGGCGGTGGTCGAGCTGTCCAGCCTGCTGGCTGAAG
TGACGCCGGCCGGTTTCGACCGCGTGTTCTATACCAATTCCGGTTCCGAATCGGTGGACACCATGATCCGCATGGTGCGCCGC
TACTGGGACGTGCAGGGCAAGCCGGAGAAGAAGACGCTGATCGGCCGCTGGAACGGCTATCACGGCTCCACCATCGGCGGC
GCCAGCCTGGGCGGCATGAAGTACATGCACGAGCAGGGCGACTTGCCGATTCCGGGCATGGCCCACATCGAGCAGCCTTGGT
GGTACAAGCACGGCAAGGACATGACGCCGGACGAGTTCGGCGTGGTGGCCGCGCGCTGGCTGGAAGAGAAGATTCTGGAAA

TCGGCGCCGACAAGGTGGCCGCCTTCGTCGGCGAACCCATCCAGGGCGCCGGCGGCGTGATCGTCCCGCCGGCCACCTACT
GGCCGGAAATCGAGCGCATTTGCCGCAAGTACGACGTGCTGCTGGTGGCCGACGAAGTGATCTGCGGCTTCGGGCGTACCG
GCGAATGGTTCGGCCATCAGCATTTCGGCTTCCAGCCCGACCTGTTCACCGCCGCCAAGGGCCTGTCCTCCGGCTATCTGCC
GATAGGCGCGGTCTTTGTCGGCAAGCGCGTGGCCGAAGGCCTGATCGCCGGCGGCGACTTCAACCACGGCTTCACCTACTCC
GGCCACCCGGTCTGCGCCGCCGTCGCCCACGCCAACGTGGCGGCGCTGCGCGACGAGGGCATCGTCCAGCGCGTCAAGGA
CGACATCGGCCCGTACATGCAAAAGCGCTGGCGTGAAACCTTCAGCCGTTTCGAGCATGTGGACGACGTGCGCGGCGTCGGC
ATGGTGCAGGCGTTCACCCTGGTGAAGAACAAGGCGAAGCGCGAGCTGTTCCCCGATTTCGGCGAGATCGGCACGCTGTGCC
GCGACATCTTCTTCCGCAACAACCTGATCATGCGGGCATGCGGCGACCACATCGTGTCGGCGCCGCCGCTGGTGATGACGCG
GGCGGAAGTGGACGAGATGCTGGCGGTGGCGGAACGCTGTCTGGAGGAATTCGAGCAGACGCTGAAGGCGCGCGGGCTGG
CTTAGCTCGAGCACCACCACCACCACCACTGAGATCCGGCTGCTAACAAAGCCCGAAAGGAAGCTGAGTTGGCTGCTGCCACC
GCTGAGCAATAACTAGCATAACCCCTTGGGGCCTCTAAACGGGTCTTGAGGGGTTTTTTGCTGAAAGGAGGAACTATATCCGGA
T

Amino acid sequence of *Cv*2025-His6:

MGHHHHHHMQKQRTTSQWRELDAAHHLHPFTDTASLNQAGARVMTRGEGVYLWDSEGNKIIDGMAGLWCVNVGYGRKDFAEAA
RRQMEELPFYNTFFKTTHPAVVELSSLLAEVTPAGFDRVFYTNSGSESVDTMIRMVRRYWDVQGKPEKKTLIGRWNGYHGSTIGGA
SLGGMKYMHEQGDLPIPGMAHIEQPWWYKHGKDMTPDEFGVVAARWLEEKILEIGADKVAAFVGEPIQGAGGVIVPPATYWPEIERI
CRKYDVLLVADEVICGFGRTGEWFGHQHFGFQPDLFTAAKGLSSGYLPIGAVFVGKRVAEGLIAGGDFNHGFTYSGHPVCAAVAHA
NVAALRDEGIVQRVKDDIGPYMQKRWRETFSRFEHVDDVRGVGMVQAFTLVKNKAKRELFPDFGEIGTLCRDIFFRNNLIMRACGDH
IVSAPPLVMTRAEVDEMLAVAERCLEEFEQTLKARGLA

Gene sequence of amine transaminase from *Bacillus megaterium* (*Bm*TA) in pET21a:

TGGCGAATGGGACGCGCCCTGTAGCGGCGCATTAAGCGCGGCGGGTGTGGTGGTTACGCGCAGCGTGACCGCTACACTTGC
CAGCGCCCTAGCGCCCGCTCCTTTCGCTTTCTTCCCTTCCTTTCTCGCCACGTTCGCCGGCTTTCCCCGTCAAGCTCTAAATCG
GGGGCTCCCTTTAGGGTTCCGATTTAGTGCTTTACGGCACCTCGACCCCAAAAAACTTGATTAGGGTGATGGTTC
ACGTAGTGGGCCATCGCCCTGATAGACGGTTTTTCGCCCTTTGACGTTGGAGTCCACGTTCTTTAATAGTGGACTCTTGTTCCA
AACTGGAACAACACTCAACCCTATCTCGGTCTATTCTTTTGATTTATAAGGGATTTTGCCGATTTCGGCCTATTGGTTAAAAAATG
AGCTGATTTAACAAAAATTTAACGCGAATTTTAACAAAATATTAACGTTTACAATTTCAGGTGGCACTTTTCGGGGAAATGTGCGC
GGAACCCCTATTTGTTTATTTTTCTAAATACATTCAAATATGTATCCGCTCATGAGACAATAACCCTGATAAATGCTTCAATAATAT
TGAAAAAGGAAGAGTATGAGTATTCAACATTTCCGTGTCGCCCTTATTCCCTTTTTTGCGGCATTTTGCCTTCCTGTTTTTGCTCA
CCCAGAAACGCTGGTGAAAGTAAAAGATGCTGAAGATCAGTTGGGTGCACGAGTGGGTTACATCGAACTGGATCTCAACAGCG
GTAAGATCCTTGAGAGTTTTCGCCCCGAAGAACGTTTTCCAATGATGAGCACTTTTAAAGTTCTGCTATGTGGCGCGGTATTATC
CCGTATTGACGCCGGGCAAGAGCAACTCGGTCGCCGCATACACTATTCTCAGAATGACTTGGTTGAGTACTCACCAGTCACAG
AAAAGCATCTTACGGATGGCATGACAGTAAGAGAATTATGCAGTGCTGCCATAACCATGAGTGATAACACTGCGGCCAACTTAC
TTCTGACAACGATCGGAGGACCGAAGGAGCTAACCGCTTTTTTGCACAACATGGGGGATCATGTAACTCGCCTTGATCGTTGG
GAACCGGAGCTGAATGAAGCCATACCAAACGACGAGCGTGACACCACGATGCCTGCAGCAATGGCAACAACGTTGCGCAAACT
ATTAACTGGCGAACTACTTACTCTAGCTTCCCGGCAACAATTAATAGACTGGATGGAGGCGGATAAAGTTGCAGGACCACTTCT
GCGCTCGGCCCTTCCGGCTGGCTGGTTTATTGCTGATAAATCTGGAGCCGGTGAGCGTGGGTCTCGCGGTATCATTGCAGCAC
TGGGGCCAGATGGTAAGCCCTCCCGTATCGTAGTTATCTACACGACGGGGAGTCAGGCAACTATGGATGAACGAAATAGACAG
ATCGCTGAGATAGGTGCCTCACTGATTAAGCATTGGTAACTGTCAGACCAAGTTTACTCATATATACTTTAGATTGATTTAAAACT
TCATTTTTAATTTAAAAGGATCTAGGTGAAGATCCTTTTTGATAATCTCATGACCAAAATCCCTTAACGTGAGTTTTCGTTCCACT
GAGCGTCAGACCCCGTAGAAAAGATCAAAGGATCTTCTTGAGATCCTTTTTTTCTGCGCGTAATCTGCTGCTTGCAAACAAAAAA
ACCACCGCTACCAGCGGTGGTTTGTTTGCCGGATCAAGAGCTACCAACTCTTTTTCCGAAGGTAACTGGCTTCAGCAGAGCGC
AGATACCAAATACTGTCCTTCTAGTGTAGCCGTAGTTAGGCCACCACTTCAAGAACTCTGTAGCACCGCCTACATACCTCGCTC
TGCTAATCCTGTTACCAGTGGCTGCTGCCAGTGGCGATAAGTCGTGTCTTACCGGGTTGGACTCAAGACGATAGTTACCGGATA
AGGCGCAGCGGTCGGGCTGAACGGGGGGTTCGTGCACACAGCCCAGCTTGGAGCGAACGACCTACACCGAACTGAGATACC
TACAGCGTGAGCTATGAGAAAGCGCCACGCTTCCCGAAGGGAGAAAGGCGGACAGGTATCCGGTAAGCGGCAGGGTCGGAA
CAGGAGAGCGCACGAGGGAGCTTCCAGGGGGAAACGCCTGGTATCTTTATAGTCCTGTCGGGTTTCGCCACCTCTGACTTGAG
CGTCGATTTTTGTGATGCTCGTCAGGGGGGCGGAGCCTATGGAAAAACGCCAGCAACGCGGCCTTTTTACGGTTCCTGGCCTT
TTGCTGGCCTTTTGCTCACATGTTCTTTCCTGCGTTATCCCCTGATTCTGTGGATAACCGTATTACCGCCTTTGAGTGAGCTGAT
ACCGCTCGCCGCAGCCGAACGACCGAGCGCAGCGAGTCAGTGAGCGAGGAAGCGGAAGAGCGCCTGATGCGGTATTTTCTC
CTTACGCATCTGTGCGGTATTTCACACCGCATATATGGTGCACTCTCAGTACAATCTGCTCTGATGCCGCATAGTTAAGCCAGTA
TACACTCCGCTATCGCTACGTGACTGGGTCATGGCTGCGCCCCGACACCCGCCAACACCCGCTGACGCGCCCTGACGGGCTT
GTCTGCTCCCGGCATCCGCTTACAGACAAGCTGTGACCGTCTCCGGGAGCTGCATGTGTCAGAGGTTTTCACCGTCATCACCG
AAACGCGCGAGGCAGCTGCGGTAAAGCTCATCAGCGTGGTCGTGAAGCGATTCACAGATGTCTGCCTGTTCATCCGCGTCCAG
CTCGTTGAGTTTCTCCAGAAGCGTTAATGTCTGGCTTCTGATAAAGCGGGCCATGTTAAGGGCGGTTTTTTCCTGTTTGGTCACT
GATGCCTCCGTGTAAGGGGGATTTCTGTTCATGGGGGTAATGATACCGATGAAACGAGAGAGGATGCTCACGATACGGGTTAC
TGATGATGAACATGCCCGGTTACTGGAACGTTGTGAGGGTAAACAACTGGCGGTATGGATGCGGCGGGACCAGAGAAAAATCA
CTCAGGGTCAATGCCAGCGCTTCGTTAATACAGATGTAGGTGTTCCACAGGGTAGCCAGCAGCATCCTGCGATGCAGATCCGG
AACATAATGGTGCAGGGCGCTGACTTCCGCGTTTCCAGACTTTACGAAACACGGAAACCGAAGACCATTCATGTTGTTGCTCAG
GTCGCAGACGTTTTGCAGCAGCAGTCGCTTCACGTTCGCTCGCGTATCGGTGATTCATTCTGCTAACCAGTAAGGCAACCCCG
CCAGCCTAGCCGGGTCCTCAACGACAGGAGCACGATCATGCGCACCCGTGGGGCCGCCATGCCGGCGATAATGGCCTGCTTC
TCGCCGAAACGTTTGGTGGCGGGACCAGTGACGAAGGCTTGAGCGAGGGCGTGCAAGATTCCGAATACCGCAAGCGACAGGC
CGATCATCGTCGCGCTCCAGCGAAAGCGGTCCTCGCCGAAAATGACCCAGAGCGCTGCCGGCACCTGTCCTACGAGTTGCAT
GATAAAGAAGACAGTCATAAGTGCGGCGACGATAGTCATGCCCCGCGCCCACCGGAAGGAGCTGACTGGGTTGAAGGCTCTC
AAGGGCATCGGTCGAGATCCCGGTGCCTAATGAGTGAGCTAACTTACATTAATTGCGTTGCGCTCACTGCCCGCTTTCCAGTC
GGGAAACCTGTCGTGCCAGCTGCATTAATGAATCGGCCAACGCGCGGGGAGAGGCGGTTTGCGTATTGGGCGCCAGGGTGGT
TTTTCTTTTCACCAGTGAGACGGGCAACAGCTGATTGCCCTTCACCGCCTGGCCCTGAGAGAGTTGCAGCAAGCGGTCCACGC
TGGTTTGCCCCAGCAGGCGAAAATCCTGTTTGATGGTGGTTAACGGCGGGATATAACATGAGCTGTCTTCGGTATCGTCGTATC

CCACTACCGAGATATCCGCACCAACGCGCAGCCCGGACTCGGTAATGGCGCGCATTGCGCCCAGCGCCATCTGATCGTTGGC
AACCAGCATCGCAGTGGGAACGATGCCCTCATTCAGCATTTGCATGGTTTGTTGAAAACCGGACATGGCACTCCAGTCGCCTTC
CCGTTCCGCTATCGGCTGAATTTGATTGCGAGTGAGATATTTATGCCAGCCAGCCAGACGCAGACGCGCCGAGACAGAACTTA
ATGGGCCCGCTAACAGCGCGATTTGCTGGTGACCCAATGCGACCAGATGCTCCACGCCCAGTCGCGTACCGTCTTCATGGGA
GAAAATAATACTGTTGATGGGTGTCTGGTCAGAGACATCAAGAAATAACGCCGGAACATTAGTGCAGGCAGCTTCCACAGCAAT
GGCATCCTGGTCATCCAGCGGATAGTTAATGATCAGCCCACTGACGCGTTGCGCGAGAAGATTGTGCACCGCCGCTTTACAGG
CTTCGACGCCGCTTCGTTCTACCATCGACACCACCACGCTGGCACCCAGTTGATCGGCGCGAGATTTAATCGCCGCGACAATT
TGCGACGGCGCGTGCAGGGCCAGACTGGAGGTGGCAACGCCAATCAGCAACGACTGTTTGCCCGCCAGTTGTTGTGCCACGC
GGTTGGGAATGTAATTCAGCTCCGCCATCGCCGCTTCCACTTTTTCCCGCGTTTTCGCAGAAACGTGGCTGGCCTGGTTCACCA
CGCGGGAAACGGTCTGATAAGAGACACCGGCATACTCTGCGACATCGTATAACGTTACTGGTTTCACATTCACCACCCTGAATT
GACTCTCTTCCGGGCGCTATCATGCCATACCGCGAAAGGTTTTGCGCCATTCGATGGTGTCCGGGATCTCGACGCTCTCCCTT
ATGCGACTCCTGCATTAGGAAGCAGCCCAGTAGTAGGTTGAGGCCGTTGAGCACCGCCGCCGCAAGGAATGGTGCATGCAAG
GAGATGGCGCCCAACAGTCCCCCGGCCACGGGGCCTGCCACCATACCCACGCCGAAACAAGCGCTCATGAGCCCGAAGTGG
CGAGCCCGATCTTCCCCATCGGTGATGTCGGCGATATAGGCGCCAGCAACCGCACCTGTGGCGCCGGTGATGCCGGCCACGA
TGCGTCCGGCGTAGAGGATCGAGATCTCGATCCCGCGAAATTAATACGACTCACTATAGGGGAATTGTGAGCGGATAACAATT
CCCCTCTAGAAATAATTTTGTTTAACTTTAAGAAGGAGATATACATATGGCTAGCAGAGGATCGCATCACCATCACCATCACGGC
GCCAGCCTGACCGTGCAGAAAATTAATTGGGAACAGGTGAAAGAATGGGATCGCAAATATCTGATGCGTACCTTTAGCACCCA
GAATGAATATCAGCCGGTTCCGATTGAAAGCACCGAAGGCGATTATCTGATTATGCCGGATGGCACCCGTCTGCTGGATTTTTT
TAATCAGCTGTATTGCGTTAATCTGGGCCAGAAAAACCAGAAAGTGAACGCAGCAATTAAAGAAGCACTGGATCGTTACGGTTT
TGTGTGGGATACCTATGCCACCGATTATAAAGCAAAAGCCGCAAAAATTATTATTGAAGATATTCTGGGCGATGAAGATTGGCCT
GGTAAAGTTCGTTTTGTTAGCACCGGTAGCGAAGCAGTTGAAACCGCACTGAATATTGCACGTCTGTATACCAATCGTCCGCTG
GTTGTTACCCGTGAACATGATTATCATGGTTGGACCGGTGGTGCAGCAACCGTTACCCGTCTGCGTAGCTATCGTAGCGGTCT
GGTTGGTGAAAATAGCGAAAGCTTTAGCGCACAGATTCCGGGTAGCAGCTATAATAGCGCAGTTCTGATGGCACCGAGCCCGA
ATATGTTTCAGGATTCCGATGGTAATCTGCTGAAAGATGAAAATGGTGAACTGCTGTCCGTTAAATATACCCGTCGCATGATTGA
AAATTATGGTCCGGAACAGGTTGCAGCAGTTATTACCGAAGTTAGCCAGGGTGCAGGTAGCGCAATGCCTCCGTATGAATATAT
TCCGCAGATTCGTAAAATGACCAAAGAACTGGGTGTTCTGTGGATTAATGATGAAGTGCTGACCGGTTTTGGTCGTACCGGTAA
ATGGTTTGGCTATCAGCATTATGGTGTTCAGCCGGATATTATTACCATGGGTAAAGGTCTGAGCAGCAGCAGCCTGCCTGCAGG
TGCAGTTCTGGTTAGCAAAGAAATCGCAGCCTTTATGGATAAACATCGTTGGGAAAGCGTTAGCACCTATGCAGGTCATCCGGT
TGCAATGGCAGCAGTTTGTGCAAATCTGGAAGTGATGATGGAAGAAAATTTTGTGGAACAGGCCAAAGATAGCGGTGAATATAT
CCGTAGCAAACTGGAACTGCTGCAGGAAAAACATAAAAGCATTGGCAATTTTGATGGTTATGGCCTGCTGTGGATTGTTGATATT
GTGAATGCCAAAACCAAAACCCCGTATGTTAAACTGGATCGCAATTTTACCCATGGCATGAATCCGAATCAGATTCCGACCCAG
ATTATCATGAAAAAAGCCCTGGAAAAAGGTGTTCTGATTGGTGGTGTTATGCCGAATACCATGCGTATTGGTGCAAGCCTGAAT
GTTAGCCGTGGCGATATTGATAAAGCAATGGATGCACTGGATTATGCCCTGGATTATCTGGAAAGCGGTGAATGGCAGTAACTC
GAGCACCACCACCACCACCACTGAGATCCGGCTGCTAACAAAGCCCGAAAGGAAGCTGAGTTGGCTGCTGCCACCGCTGAGC
AATAACTAGCATAACCCCTTGGGGCCTCTAAACGGGTCTTGAGGGGTTTTTTGCTGAAAGGAGGAACTATATCCGGAT

Amino acid sequence of *Bm*TA-His6:

MASRGSHHHHHHGASLTVQKINWEQVKEWDRKYLMRTFSTQNEYQPVPIESTEGDYLIMPDGTRLLDFFNQLYCVNLGQKNQKVN
AAIKEALDRYGFVWDTYATDYKAKAAKIIIEDILGDEDWPGKVRFVSTGSEAVETALNIARLYTNRPLVVTREHDYHGWTGGAATVTRL
RSYRSGLVGENSESFSAQIPGSSYNSAVLMAPSPNMFQDSDGNLLKDENGELLSVKYTRRMIENYGPEQVAAVITEVSQGAGSAMP
PYEYIPQIRKMTKELGVLWINDEVLTGFGRTGKWFGYQHYGVQPDIITMGKGLSSSSLPAGAVLVSKEIAAFMDKHRWESVSTYAGH
PVAMAAVCANLEVMMEENFVEQAKDSGEYIRSKLELLQEKHKSIGNFDGYGLLWIVDIVNAKTKTPYVKLDRNFTHGMNPNQIPTQIIM
KKALEKGVLIGGVMPNTMRIGASLNVSRGDIDKAMDALDYALDYLESGEWQ

Gene sequence of pyruvate decarboxylase variant from *Acetobacter pasteurianus* (*Ap*PDC E469G) in pET22b:

AACCGCACCTGTGGCGCCGGTGATGCCGGCCACGATGCGTCCGGCGTAGAGGATCGAGATCTCGATCCCGCGAAATTAATAC
GACTCACTATAGGGGAATTGTGAGCGGATAACAATTCCCCTCTAGAAATAATTTTGTTTAACTTTAAGAAGGAGATATACATATGA
CCTATACTGTTGGCATGTATCTTGCAGAACGCCTTGTACAGATCGGGCTGAAGCATCACTTCGCCGTGGCGGGCGACTACAAT
CTCGTTCTTCTGGATCAGTTGCTCCTCAACAAGGACATGAAACAGATCTATTGCTGCAATGAGTTGAACTGTGGCTTCAGCGCG
GAAGGCTACGCCCGTTCTAACGGGGCTGCGGCAGCGGTTGTCACCTTCAGCGTTGGCGCCATTTCCGCCATGAACGCCCTCG
GCGGCGCCTATGCCGAAAACCTGCCGGTTATCCTGATTTCCGGCGCGCCCAACAGCAATGATCAGGGCACAGGTCATATCCTG
CATCACACAATCGGCAAGACGGATTACAGCTACCAGCTTGAAATGGCCCGTCAGGTCACCTGTGCCGCCGAAAGCATTACCGA
CGCTCACTCCGCCCCGGCCAAGATTGACCACGTCATTCGCACGGCGCTGCGCGAGCGTAAGCCGGCCTATCTGGACATCGCG
TGCAACATTGCCTCCGAGCCCTGCGTGCGGCCTGGCCCTGTCAGCAGCCTGCTGTCCGAGCCTGAAATCGACCACACGAGCC
TGAAGGCCGCAGTGGACGCCACGGTTGCCTTGCTGGAAAAATCGGCCAGCCCCGTCATGCTGCTGGGCAGCAAGCTGCGGG
CCGCCAACGCACTGGCCGCAACCGAAACGCTGGCAGACAAGCTGCAATGCGCGGTGACCATCATGGCGGCCGCGAAAGGCT
TTTTCCCCGAAGACCACGCGGGTTTCCGCGGCCTGTACTGGGGCGAAGTCTCGAACCCCGGCGTGCAGGAACTGGTGGAGAC
CTCCGACGCACTGCTGTGCATCGCCCCCGTATTCAACGACTATTCAACAGTCGGCTGGTCGGCATGGCCCAAGGGCCCCAATG
TGATTCTGGCTGAGCCCGACCGCGTAACGGTCGATGGCCGCGCCTATGACGGCTTTACCCTGCGCGCCTTCCTGCAGGCTCT
GGCGGAAAAAGCCCCCGCGCGCCCGGCCTCCGCACAGAAAAGCAGCGTCCCGACGTGCTCGCTCACCGCGACATCCGATGA
AGCCGGTCTGACGAATGACGAAATCGTCCGTCATATCAACGCCCTGCTGACATCAAACACGACGCTGGTGGCAGAAACCGGCG
ATTCTGGTTCAATGCCATGCGCATGACCCTGCCGCGCGGTGCGCGCGTGGAACTGGAAATGCAGTGGGGCCATATCGGCTGG
TCCGTGCCCTCCGCCTTCGGCAATGCCATGGGCTCGCAGGACCGCCAGCATGTGGTGATGGTAGGCGATGGCTCCTTCCAGC
TTACCGCGCAGGAAGTGGCTCAGATGGTGCGCTACGAACTGCCCGTCATTATCTTTCTGATCAACAACCGTGGCTATGTCATTG
GCATCGCCATTCATGACGGCCCGTACAACTATATCAAGAACTGGGATTACGCCGGCCTGATGGAAGTCTTCAACGCCGGAGAA
GGCCATGGACTTGGCCTGAAAGCCACCACCCCGAAGGAACTGACAGAAGCCATCGCCAGGGCAAAAGCCAATACCCGCGGCC
CGACGCTGATCGAATGCCAGATCGACCGCACGGACTGCACGGATATGCTGGTTCAATGGGGCCGCAAGGTTGCCTCAACCAA
CGCGCGCAAGACCACTCTGGCCCTCGAGCACCACCACCACCACCACTGAGATCCGGCTGCTAACAAAGCCCGAAAGGAAGCT
GAGTTGGCTGCTGCCACCGCTGAGCAATAACTAGCATAACCCCTTGGGGCCTCTAAACGGGTCTTGAGGGGTTTTTTGCTGAA
AGGAGGAACTATATCCGGATTGGCGAATGGGACGCGCCCTGTAGCGGCGCATTAAGCGCGGCGGGTGTGGTGGTTACGCGC
AGCGTGACCGCTACACTTGCCAGCGCCCTAGCGCCCGCTCCTTTCGCTTTCTTCCCTTCCTTTCTCGCCACGTTCGCCGGCTTT
CCCCGTCAAGCTCTAAATCGGGGGCTCCCTTTAGGGTTCCGATTTAGTGCTTTACGGCACCTCGACCCCAAAAAACTTGATTAG
GGTGATGGTTCACGTAGTGGGCCATCGCCCTGATAGACGGTTTTTCGCCCTTTGACGTTGGAGTCCACGTTCTTTAATAGTGGA

CTCTTGTTCCAAACTGGAACAACACTCAACCCTATCTCGGTCTATTCTTTTGATTTATAAGGGATTTTGCCGATTTCGGCCTATTG
GTTAAAAAATGAGCTGATTTAACAAAAATTTAACGCGAATTTTAACAAAATATTAACGTTTACAATTTCAGGTGGCACTTTTCGGG
GAAATGTGCGCGGAACCCCTATTTGTTTATTTTTCTAAATACATTCAAATATGTATCCGCTCATGAGACAATAACCCTGATAAATG
CTTCAATAATATTGAAAAAGGAAGAGTATGAGTATTCAACATTTCCGTGTCGCCCTTATTCCCTTTTTTGCGGCATTTTGCCTTCC
TGTTTTTGCTCACCCAGAAACGCTGGTGAAAGTAAAAGATGCTGAAGATCAGTTGGGTGCACGAGTGGGTTACATCGAACTGGA
TCTCAACAGCGGTAAGATCCTTGAGAGTTTTCGCCCCGAAGAACGTTTTCCAATGATGAGCACTTTTAAAGTTCTGCTATGTGGC
GCGGTATTATCCCGTATTGACGCCGGGCAAGAGCAACTCGGTCGCCGCATACACTATTCTCAGAATGACTTGGTTGAGTACTCA
CCAGTCACAGAAAAGCATCTTACGGATGGCATGACAGTAAGAGAATTATGCAGTGCTGCCATAACCATGAGTGATAACACTGCG
GCCAACTTACTTCTGACAACGATCGGAGGACCGAAGGAGCTAACCGCTTTTTTGCACAACATGGGGGATCATGTAACTCGCCTT
GATCGTTGGGAACCGGAGCTGAATGAAGCCATACCAAACGACGAGCGTGACACCACGATGCCTGCAGCAATGGCAACAACGTT
GCGCAAACTATTAACTGGCGAACTACTTACTCTAGCTTCCCGGCAACAATTAATAGACTGGATGGAGGCGGATAAAGTTGCAGG
ACCACTTCTGCGCTCGGCCCTTCCGGCTGGCTGGTTTATTGCTGATAAATCTGGAGCCGGTGAGCGTGGGTCTCGCGGTATCA
TTGCAGCACTGGGGCCAGATGGTAAGCCCTCCCGTATCGTAGTTATCTACACGACGGGGAGTCAGGCAACTATGGATGAACGA
AATAGACAGATCGCTGAGATAGGTGCCTCACTGATTAAGCATTGGTAACTGTCAGACCAAGTTTACTCATATATACTTTAGATTG
ATTTAAAACTTCATTTTTAATTTAAAAGGATCTAGGTGAAGATCCTTTTTGATAATCTCATGACCAAAATCCCTTAACGTGAGTTTT
CGTTCCACTGAGCGTCAGACCCCGTAGAAAAGATCAAAGGATCTTCTTGAGATCCTTTTTTTCTGCGCGTAATCTGCTGCTTGCA
AACAAAAAAACCACCGCTACCAGCGGTGGTTTGTTTGCCGGATCAAGAGCTACCAACTCTTTTTCCGAAGGTAACTGGCTTCAG
CAGAGCGCAGATACCAAATACTGTCCTTCTAGTGTAGCCGTAGTTAGGCCACCACTTCAAGAACTCTGTAGCACCGCCTACATA
CCTCGCTCTGCTAATCCTGTTACCAGTGGCTGCTGCCAGTGGCGATAAGTCGTGTCTTACCGGGTTGGACTCAAGACGATAGTT
ACCGGATAAGGCGCAGCGGTCGGGCTGAACGGGGGGTTCGTGCACACAGCCCAGCTTGGAGCGAACGACCTACACCGAACT
GAGATACCTACAGCGTGAGCTATGAGAAAGCGCCACGCTTCCCGAAGGGAGAAAGGCGGACAGGTATCCGGTAAGCGGCAGG
GTCGGAACAGGAGAGCGCACGAGGGAGCTTCCAGGGGGAAACGCCTGGTATCTTTATAGTCCTGTCGGGTTTCGCCACCTCT
GACTTGAGCGTCGATTTTTGTGATGCTCGTCAGGGGGGCGGAGCCTATGGAAAAACGCCAGCAACGCGGCCTTTTTACGGTTC
CTGGCCTTTTGCTGGCCTTTTGCTCACATGTTCTTTCCTGCGTTATCCCCTGATTCTGTGGATAACCGTATTACCGCCTTTGAGT
GAGCTGATACCGCTCGCCGCAGCCGAACGACCGAGCGCAGCGAGTCAGTGAGCGAGGAAGCGGAAGAGCGCCTGATGCGGT
ATTTTCTCCTTACGCATCTGTGCGGTATTTCACACCGCATATATGGTGCACTCTCAGTACAATCTGCTCTGATGCCGCATAGTTA
AGCCAGTATACACTCCGCTATCGCTACGTGACTGGGTCATGGCTGCGCCCCGACACCCGCCAACACCCGCTGACGCGCCCTG
ACGGGCTTGTCTGCTCCCGGCATCCGCTTACAGACAAGCTGTGACCGTCTCCGGGAGCTGCATGTGTCAGAGGTTTTCACCGT
CATCACCGAAACGCGCGAGGCAGCTGCGGTAAAGCTCATCAGCGTGGTCGTGAAGCGATTCACAGATGTCTGCCTGTTCATCC
GCGTCCAGCTCGTTGAGTTTCTCCAGAAGCGTTAATGTCTGGCTTCTGATAAAGCGGGCCATGTTAAGGGCGGTTTTTTCCTGT
TTGGTCACTGATGCCTCCGTGTAAGGGGGATTTCTGTTCATGGGGGTAATGATACCGATGAAACGAGAGAGGATGCTCACGAT
ACGGGTTACTGATGATGAACATGCCCGGTTACTGGAACGTTGTGAGGGTAAACAACTGGCGGTATGGATGCGGCGGGACCAG
AGAAAAATCACTCAGGGTCAATGCCAGCGCTTCGTTAATACAGATGTAGGTGTTCCACAGGGTAGCCAGCAGCATCCTGCGAT
GCAGATCCGGAACATAATGGTGCAGGGCGCTGACTTCCGCGTTTCCAGACTTTACGAAACACGGAAACCGAAGACCATTCATG
TTGTTGCTCAGGTCGCAGACGTTTTGCAGCAGCAGTCGCTTCACGTTCGCTCGCGTATCGGTGATTCATTCTGCTAACCAGTAA
GGCAACCCCGCCAGCCTAGCCGGGTCCTCAACGACAGGAGCACGATCATGCGCACCCGTGGGGCCGCCATGCCGGCGATAA
TGGCCTGCTTCTCGCCGAAACGTTTGGTGGCGGGACCAGTGACGAAGGCTTGAGCGAGGGCGTGCAAGATTCCGAATACCGC
AAGCGACAGGCCGATCATCGTCGCGCTCCAGCGAAAGCGGTCCTCGCCGAAAATGACCCAGAGCGCTGCCGGCACCTGTCCT
ACGAGTTGCATGATAAAGAAGACAGTCATAAGTGCGGCGACGATAGTCATGCCCCGCGCCCACCGGAAGGAGCTGACTGGGT
TGAAGGCTCTCAAGGGCATCGGTCGAGATCCCGGTGCCTAATGAGTGAGCTAACTTACATTAATTGCGTTGCGCTCACTGCCC
GCTTTCCAGTCGGGAAACCTGTCGTGCCAGCTGCATTAATGAATCGGCCAACGCGCGGGGAGAGGCGGTTTGCGTATTGGGC
GCCAGGGTGGTTTTTCTTTTCACCAGTGAGACGGGCAACAGCTGATTGCCCTTCACCGCCTGGCCCTGAGAGAGTTGCAGCAA
GCGGTCCACGCTGGTTTGCCCCAGCAGGCGAAAATCCTGTTTGATGGTGGTTAACGGCGGGATATAACATGAGCTGTCTTCGG
TATCGTCGTATCCCACTACCGAGATATCCGCACCAACGCGCAGCCCGGACTCGGTAATGGCGCGCATTGCGCCCAGCGCCAT
CTGATCGTTGGCAACCAGCATCGCAGTGGGAACGATGCCCTCATTCAGCATTTGCATGGTTTGTTGAAAACCGGACATGGCACT
CCAGTCGCCTTCCCGTTCCGCTATCGGCTGAATTTGATTGCGAGTGAGATATTTATGCCAGCCAGCCAGACGCAGACGCGCCG
AGACAGAACTTAATGGGCCCGCTAACAGCGCGATTTGCTGGTGACCCAATGCGACCAGATGCTCCACGCCCAGTCGCGTACC
GTCTTCATGGGAGAAAATAATACTGTTGATGGGTGTCTGGTCAGAGACATCAAGAAATAACGCCGGAACATTAGTGCAGGCAGC
TTCCACAGCAATGGCATCCTGGTCATCCAGCGGATAGTTAATGATCAGCCCACTGACGCGTTGCGCGAGAAGATTGTGCACCG
CCGCTTTACAGGCTTCGACGCCGCTTCGTTCTACCATCGACACCACCACGCTGGCACCCAGTTGATCGGCGCGAGATTTAATC
GCCGCGACAATTTGCGACGGCGCGTGCAGGGCCAGACTGGAGGTGGCAACGCCAATCAGCAACGACTGTTTGCCCGCCAGTT
GTTGTGCCACGCGGTTGGGAATGTAATTCAGCTCCGCCATCGCCGCTTCCACTTTTTCCCGCGTTTTCGCAGAAACGTGGCTG
GCCTGGTTCACCACGCGGGAAACGGTCTGATAAGAGACACCGGCATACTCTGCGACATCGTATAACGTTACTGGTTTCACATTC
ACCACCCTGAATTGACTCTCTTCCGGGCGCTATCATGCCATACCGCGAAAGGTTTTGCGCCATTCGATGGTGTCCGGGATCTC
GACGCTCTCCCTTATGCGACTCCTGCATTAGGAAGCAGCCCAGTAGTAGGTTGAGGCCGTTGAGCACCGCCGCCGCAAGGAA
TGGTGCATGCAAGGAGATGGCGCCCAACAGTCCCCCGGCCACGGGGCCTGCCACCATACCCACGCCGAAACAAGCGCTCATG
AGCCCGAAGTGGCGAGCCCGATCTTCCCCATCGGTGATGTCGGCGATATAGGCGCCAGC

Amino acid sequence of *Ap*PDC E469G-His6:

MTYTVGMYLAERLVQIGLKHHFAVAGDYNLVLLDQLLLNKDMKQIYCCNELNCGFSAEGYARSNGAAAAVVTFSVGAISAMNALGGA
YAENLPVILISGAPNSNDQGTGHILHHTIGKTDYSYQLEMARQVTCAAESITDAHSAPAKIDHVIRTALRERKPAYLDIACNIASEPCVRP
GPVSSLLSEPEIDHTSLKAAVDATVALLEKSASPVMLLGSKLRAANALAATETLADKLQCAVTIMAAAKGFFPEDHAGFRGLYWGEVS
NPGVQELVETSDALLCIAPVFNDYSTVGWSAWPKGPNVILAEPDRVTVDGRAYDGFTLRAFLQALAEKAPARPASAQKSSVPTCSLT
ATSDEAGLTNDEIVRHINALLTSNTTLVAETGDSWFNAMRMTLPRGARVELEMQWGHIGWSVPSAFGNAMGSQDRQHVVMVGDGS
FQLTAQEVAQMVRYELPVIIFLINNRGYVIGIAIHDGPYNYIKNWDYAGLMEVFNAGEGHGLGLKATTPKELTEAIARAKANTRGPTLIE
CQIDRTDCTDMLVQWGRKVASTNARKTTLALEHHHHHH

Gene sequence of pyruvate decarboxylase variant from *Acetobacter pasteurianus* (*Ap*PDC var) in pET22b:

AACCGCACCTGTGGCGCCGGTGATGCCGGCCACGATGCGTCCGGCGTAGAGGATCGAGATCTCGATCCCGCGAAATTAATAC
GACTCACTATAGGGGAATTGTGAGCGGATAACAATTCCCCTCTAGAAATAATTTTGTTTAACTTTAAGAAGGAGATATACATATGA
CCTATACTGTTGGCATGTATCTTGCAGAACGCCTTGTACAGATCGGGCTGAAGCATCACTTCGCCGTGGCGGGCGACTACAAT
CTCGTTCTTCTGGATCAGTTGCTCCTCAACAAGGACATGAAACAGATCTATTGCTGCAATGAGTTGAACTGTGGCTTCAGCGCG
GAAGGCTACGCCCGTTCTAACGGGGCTGCGGCAGCGGTTGTCACCTTCAGCGTTGGCGCCATTTCCGCCATGAACGCCCTCG
GCGGCGCCTATGCCGAAAACCTGCCGGTTATCCTGATTTCCGGCGCGCCCAACAGCAATGATCAGGGCACAGGTCATATCCTG
CATCACACAATCGGCAAGACGGATTACAGCTACCAGCTTGAAATGGCCCGTCAGGTCACCTGTGCCGCCGAAAGCATTACCGA
CGCTCACTCCGCCCCGGCCAAGATTGACCACGTCATTCGCACGGCGCTGCGCGAGCGTAAGCCGGCCTATCTGGACATCGCG
TGCAACATTGCCTCCGAGCCCTGCGTGCGGCCTGGCCCTGTCAGCAGCCTGCTGTCCGAGCCTGAAATCGACCACACGAGCC
TGAAGGCCGCAGTGGACGCCACGGTTGCCTTGCTGGAAAAATCGGCCAGCCCCGTCATGCTGCTGGGCAGCAAGCTGCGGG
CCGCCAACGCACTGGCCGCAACCGAAACGCTGGCAGACAAGCTGCAATGCGCGGTGACCATCATGGCGGCCGCGAAAGGCT
TTTTCCCCGAAGACCACGCGGGTTTCCGCGGCCTGTACTGGGGCGAAGTCTCGAACCCCGGCGTGCAGGAACTGGTGGAGAC
CTCCGACGCACTGCTGTGCATCGCCCCCGTATTCAACGACTATTCAACAGTCGGCTGGTCGGCATGGCCCAAGGGCCCCAATG
TGATTCTGGCTGAGCCCGACCGCGTAACGGTCGATGGCCGCGCCTATGACGGCTTTACCCTGCGCGCCTTCCTGCAGGCTCT
GGCGGAAAAAGCCCCCGCGCGCCCGGCCTCCGCACAGAAAAGCAGCGTCCCGACGTGCTCGCTCACCGCGACATCCGATGA
AGCCGGTCTGACGAATGACGAAATCGTCCGTCATATCAACGCCCTGCTGACATCAAACACGACGCTGGTGGCAGAAACCGGCG
ATTCATGGTTCAATGCCATGCGCATGACCCTGCCGCGCGGTGCGCGCGTGGAACTGGAAATGCAGTGGGGCCATATCGGCTG
GTCCGTGCCCTCCGCCTTCGGCAATGCCATGGGCTCGCAGGACCGCCAGCATGTGGTGATGGTAGGCGATGGCTCCTTCCAG
CTTACCGCGCAGGAAGTGGCTCAGATGGTGCGCTACGAACTGCCCGTCATTATCTTTCTGATCAACAACCGTGGCTATGTCATT
CAAATCGCCATTCATGACGGCCCGTACAACTATATCAAGAACTGGGATTACGCCGGCCTGATGGAAGTCTTCAACGCCGGAGA
AGGCCATGGACTTGGCCTGAAAGCCACCACCCCGAAGGAACTGACAGAAGCCATCGCCAGGGCAAAAGCCAATACCCGCGGC
CCGACGCTGATCGAATGCCAGATCGACCGCACGGACTGCACGGATATGCTGGTTCAATGGGGCCGCAAGGTTGCCTCAACCA
ACGCGCGCAAGACCACTCTGGCCCTCGAGCACCACCACCACCACCACTGAGATCCGGCTGCTAACAAAGCCCGAAAGGAAGC
TGAGTTGGCTGCTGCCACCGCTGAGCAATAACTAGCATAACCCCTTGGGGCCTCTAAACGGGTCTTGAGGGGTTTTTTGCTGA
AAGGAGGAACTATATCCGGATTGGCGAATGGGACGCGCCCTGTAGCGGCGCATTAAGCGCGGCGGGTGTGGTGGTTACGCG
CAGCGTGACCGCTACACTTGCCAGCGCCCTAGCGCCCGCTCCTTTCGCTTTCTTCCCTTCCTTTCTCGCCACGTTCGCCGGCT
TTCCCCGTCAAGCTCTAAATCGGGGGCTCCCTTTAGGGTTCCGATTTAGTGCTTTACGGCACCTCGACCCCAAAAAACTTGATT
AGGGTGATGGTTCACGTAGTGGGCCATCGCCCTGATAGACGGTTTTTCGCCCTTTGACGTTGGAGTCCACGTTCTTTAATAGTG
GACTCTTGTTCCAAACTGGAACAACACTCAACCCTATCTCGGTCTATTCTTTTGATTTATAAGGGATTTTGCCGATTTCGGCCTAT
TGGTTAAAAAATGAGCTGATTTAACAAAAATTTAACGCGAATTTTAACAAAATATTAACGTTTACAATTTCAGGTGGCACTTTTCG
GGGAAATGTGCGCGGAACCCCTATTTGTTTATTTTTCTAAATACATTCAAATATGTATCCGCTCATGAGACAATAACCCTGATAAA
TGCTTCAATAATATTGAAAAAGGAAGAGTATGAGTATTCAACATTTCCGTGTCGCCCTTATTCCCTTTTTTGCGGCATTTTGCCTT
CCTGTTTTTGCTCACCCAGAAACGCTGGTGAAAGTAAAAGATGCTGAAGATCAGTTGGGTGCACGAGTGGGTTACATCGAACTG
GATCTCAACAGCGGTAAGATCCTTGAGAGTTTTCGCCCCGAAGAACGTTTTCCAATGATGAGCACTTTTAAAGTTCTGCTATGTG
GCGCGGTATTATCCCGTATTGACGCCGGGCAAGAGCAACTCGGTCGCCGCATACACTATTCTCAGAATGACTTGGTTGAGTAC
TCACCAGTCACAGAAAAGCATCTTACGGATGGCATGACAGTAAGAGAATTATGCAGTGCTGCCATAACCATGAGTGATAACACT
GCGGCCAACTTACTTCTGACAACGATCGGAGGACCGAAGGAGCTAACCGCTTTTTTGCACAACATGGGGGATCATGTAACTCG
CCTTGATCGTTGGGAACCGGAGCTGAATGAAGCCATACCAAACGACGAGCGTGACACCACGATGCCTGCAGCAATGGCAACAA
CGTTGCGCAAACTATTAACTGGCGAACTACTTACTCTAGCTTCCCGGCAACAATTAATAGACTGGATGGAGGCGGATAAAGTTG
CAGGACCACTTCTGCGCTCGGCCCTTCCGGCTGGCTGGTTTATTGCTGATAAATCTGGAGCCGGTGAGCGTGGGTCTCGCGG
TATCATTGCAGCACTGGGGCCAGATGGTAAGCCCTCCCGTATCGTAGTTATCTACACGACGGGGAGTCAGGCAACTATGGATG
AACGAAATAGACAGATCGCTGAGATAGGTGCCTCACTGATTAAGCATTGGTAACTGTCAGACCAAGTTTACTCATATATACTTTA
GATTGATTTAAAACTTCATTTTTAATTTAAAAGGATCTAGGTGAAGATCCTTTTTGATAATCTCATGACCAAAATCCCTTAACGTGA
GTTTTCGTTCCACTGAGCGTCAGACCCCGTAGAAAAGATCAAAGGATCTTCTTGAGATCCTTTTTTTCTGCGCGTAATCTGCTGC
TTGCAAACAAAAAAACCACCGCTACCAGCGGTGGTTTGTTTGCCGGATCAAGAGCTACCAACTCTTTTTCCGAAGGTAACTGGC
TTCAGCAGAGCGCAGATACCAAATACTGTCCTTCTAGTGTAGCCGTAGTTAGGCCACCACTTCAAGAACTCTGTAGCACCGCCT
ACATACCTCGCTCTGCTAATCCTGTTACCAGTGGCTGCTGCCAGTGGCGATAAGTCGTGTCTTACCGGGTTGGACTCAAGACG
ATAGTTACCGGATAAGGCGCAGCGGTCGGGCTGAACGGGGGGTTCGTGCACACAGCCCAGCTTGGAGCGAACGACCTACACC
GAACTGAGATACCTACAGCGTGAGCTATGAGAAAGCGCCACGCTTCCCGAAGGGAGAAAGGCGGACAGGTATCCGGTAAGCG
GCAGGGTCGGAACAGGAGAGCGCACGAGGGAGCTTCCAGGGGGAAACGCCTGGTATCTTTATAGTCCTGTCGGGTTTCGCCA
CCTCTGACTTGAGCGTCGATTTTTGTGATGCTCGTCAGGGGGGCGGAGCCTATGGAAAAACGCCAGCAACGCGGCCTTTTTAC
GGTTCCTGGCCTTTTGCTGGCCTTTTGCTCACATGTTCTTTCCTGCGTTATCCCCTGATTCTGTGGATAACCGTATTACCGCCTT
TGAGTGAGCTGATACCGCTCGCCGCAGCCGAACGACCGAGCGCAGCGAGTCAGTGAGCGAGGAAGCGGAAGAGCGCCTGAT
GCGGTATTTTCTCCTTACGCATCTGTGCGGTATTTCACACCGCATATATGGTGCACTCTCAGTACAATCTGCTCTGATGCCGCAT
AGTTAAGCCAGTATACACTCCGCTATCGCTACGTGACTGGGTCATGGCTGCGCCCCGACACCCGCCAACACCCGCTGACGCG
CCCTGACGGGCTTGTCTGCTCCCGGCATCCGCTTACAGACAAGCTGTGACCGTCTCCGGGAGCTGCATGTGTCAGAGGTTTTC
ACCGTCATCACCGAAACGCGCGAGGCAGCTGCGGTAAAGCTCATCAGCGTGGTCGTGAAGCGATTCACAGATGTCTGCCTGTT
CATCCGCGTCCAGCTCGTTGAGTTTCTCCAGAAGCGTTAATGTCTGGCTTCTGATAAAGCGGGCCATGTTAAGGGCGGTTTTTT
CCTGTTTGGTCACTGATGCCTCCGTGTAAGGGGGATTTCTGTTCATGGGGGTAATGATACCGATGAAACGAGAGAGGATGCTC
ACGATACGGGTTACTGATGATGAACATGCCCGGTTACTGGAACGTTGTGAGGGTAAACAACTGGCGGTATGGATGCGGCGGGA
CCAGAGAAAAATCACTCAGGGTCAATGCCAGCGCTTCGTTAATACAGATGTAGGTGTTCCACAGGGTAGCCAGCAGCATCCTG
CGATGCAGATCCGGAACATAATGGTGCAGGGCGCTGACTTCCGCGTTTCCAGACTTTACGAAACACGGAAACCGAAGACCATT
CATGTTGTTGCTCAGGTCGCAGACGTTTTGCAGCAGCAGTCGCTTCACGTTCGCTCGCGTATCGGTGATTCATTCTGCTAACCA
GTAAGGCAACCCCGCCAGCCTAGCCGGGTCCTCAACGACAGGAGCACGATCATGCGCACCCGTGGGGCCGCCATGCCGGCG
ATAATGGCCTGCTTCTCGCCGAAACGTTTGGTGGCGGGACCAGTGACGAAGGCTTGAGCGAGGGCGTGCAAGATTCCGAATA
CCGCAAGCGACAGGCCGATCATCGTCGCGCTCCAGCGAAAGCGGTCCTCGCCGAAAATGACCCAGAGCGCTGCCGGCACCT
GTCCTACGAGTTGCATGATAAAGAAGACAGTCATAAGTGCGGCGACGATAGTCATGCCCCGCGCCCACCGGAAGGAGCTGACT
GGGTTGAAGGCTCTCAAGGGCATCGGTCGAGATCCCGGTGCCTAATGAGTGAGCTAACTTACATTAATTGCGTTGCGCTCACT
GCCCGCTTTCCAGTCGGGAAACCTGTCGTGCCAGCTGCATTAATGAATCGGCCAACGCGCGGGGAGAGGCGGTTTGCGTATT
GGGCGCCAGGGTGGTTTTTCTTTTCACCAGTGAGACGGGCAACAGCTGATTGCCCTTCACCGCCTGGCCCTGAGAGAGTTGCA
GCAAGCGGTCCACGCTGGTTTGCCCCAGCAGGCGAAAATCCTGTTTGATGGTGGTTAACGGCGGGATATAACATGAGCTGTCT
TCGGTATCGTCGTATCCCACTACCGAGATATCCGCACCAACGCGCAGCCCGGACTCGGTAATGGCGCGCATTGCGCCCAGCG
CCATCTGATCGTTGGCAACCAGCATCGCAGTGGGAACGATGCCCTCATTCAGCATTTGCATGGTTTGTTGAAAACCGGACATGG
CACTCCAGTCGCCTTCCCGTTCCGCTATCGGCTGAATTTGATTGCGAGTGAGATATTTATGCCAGCCAGCCAGACGCAGACGC

GCCGAGACAGAACTTAATGGGCCCGCTAACAGCGCGATTTGCTGGTGACCCAATGCGACCAGATGCTCCACGCCCAGTCGCG
TACCGTCTTCATGGGAGAAAATAATACTGTTGATGGGTGTCTGGTCAGAGACATCAAGAAATAACGCCGGAACATTAGTGCAGG
CAGCTTCCACAGCAATGGCATCCTGGTCATCCAGCGGATAGTTAATGATCAGCCCACTGACGCGTTGCGCGAGAAGATTGTGC
ACCGCCGCTTTACAGGCTTCGACGCCGCTTCGTTCTACCATCGACACCACCACGCTGGCACCCAGTTGATCGGCGCGAGATTT
AATCGCCGCGACAATTTGCGACGGCGCGTGCAGGGCCAGACTGGAGGTGGCAACGCCAATCAGCAACGACTGTTTGCCCGCC
AGTTGTTGTGCCACGCGGTTGGGAATGTAATTCAGCTCCGCCATCGCCGCTTCCACTTTTTCCCGCGTTTTCGCAGAAACGTGG
CTGGCCTGGTTCACCACGCGGGAAACGGTCTGATAAGAGACACCGGCATACTCTGCGACATCGTATAACGTTACTGGTTTCAC
ATTCACCACCCTGAATTGACTCTCTTCCGGGCGCTATCATGCCATACCGCGAAAGGTTTTGCGCCATTCGATGGTGTCCGGGAT
CTCGACGCTCTCCCTTATGCGACTCCTGCATTAGGAAGCAGCCCAGTAGTAGGTTGAGGCCGTTGAGCACCGCCGCCGCAAG
GAATGGTGCATGCAAGGAGATGGCGCCCAACAGTCCCCCGGCCACGGGGCCTGCCACCATACCCACGCCGAAACAAGCGCT
CATGAGCCCGAAGTGGCGAGCCCGATCTTCCCCATCGGTGATGTCGGCGATATAGGCGCCAGC

Amino acid sequence of *Ap*PDC var-His6:

MTYTVGMYLAERLVQIGLKHHFAVAGDYNLVLLDQLLLNKDMKQIYCCNELNCGFSAEGYARSNGAAAAVVTFSVGAISAMNALGGA
YAENLPVILISGAPNSNDQGTGHILHHTIGKTDYSYQLEMARQVTCAAESITDAHSAPAKIDHVIRTALRERKPAYLDIACNIASEPCVRP
GPVSSLLSEPEIDHTSLKAAVDATVALLEKSASPVMLLGSKLRAANALAATETLADKLQCAVTIMAAAKGFFPEDHAGFRGLYWGEVS
NPGVQELVETSDALLCIAPVFNDYSTVGWSAWPKGPNVILAEPDRVTVDGRAYDGFTLRAFLQALAEKAPARPASAQKSSVPTCSLT
ATSDEAGLTNDEIVRHINALLTSNTTLVAETGDSWFNAMRMTLPRGARVELEMQWGHIGWSVPSAFGNAMGSQDRQHVVMVGDGS
FQLTAQEVAQMVRYELPVIIFLINNRGYVIQIAIHDGPYNYIKNWDYAGLMEVFNAGEGHGLGLKATTPKELTEAIARAKANTRGPTLIE
CQIDRTDCTDMLVQWGRKVASTNARKTTLALEHHHHHH

Gene sequence of the branched-chain keto acid decarboxylase from *Lactococcus lactis* (*Ll*KdcA) in pET28:

ATCCGGATATAGTTCCTCCTTTCAGCAAAAAACCCCTCAAGACCCGTTTAGAGGCCCCAAGGGGTTATGCTAGTTATTGCTCAG
CGGTGGCAGCAGCCAACTCAGCTTCCTTTCGGGCTTTGTTAGCAGCCGGATCTCAGTGGTGGTGGTGGTGGTGCTCGAGTGC
GGCCGCAAGCTTGTCGACGGAGCTCGAATTCTTATTTATTTTGCTCAGCAAATAATTTACCCATTTTTTTCAGTAATTTTGGCGCA
TCTTCTTTTTCCAAAACTAGTTCTATCCAATACATTCTATTGACATCTGCTTGGGCTTCTTTCATGACAGACACAAATTCATTCTCT
GTTCTAACAATTTTTGATACTACACGATCTTCTGTTGCTCCAAATGTTTCTGGTAATTTCGAGTAATTCCACATTGGAATGTCGTT
ATAACTTTGAGTAGGTCCGTGGATTTCTCTTTCAACTGTATAACCATCATTATTTATGATAAAACAAATTGGATTGAGTTTTTCTCT
GATTGATAGTCCTAATTCTTGTACGGTAAGTTGAAGTGAACCATCACCAATAAATAAAAGGTGTCTGCTCTCTTTATCCGCAATTT
GGCTTCCTAAAGCCGCTGGAAAAGTATATCCAATAGAACCCCATAAAGGTTGTCCAATAAAACGACTATTTGATTTTAAGAAAAT
TGTTGAAGCTCCAAAAAATGAGGTTCCTTGTTCAGCAACGATTGTTTCATTGCTTTGAGTCAAACTTTCAACTGCCTGCCATAGA
CGGTCTTGTGATAAGGGAGCACTTGATGGAATAAATTCTTCATATTGCTTATCAATATATTGTCCTTCATATTCTATTCCTTTTAAT
TCTGATAAAGAAGAAACCACTGCTCTAAAATCAAAATCTTCTACCACTTTATTGAAAATTATTCCTTCATCTATGTTTAGTGAAATC
ATTTTATTTTCATCTAAATGATGTGTGAATGCACCTGTTGAGGAGTCCGTAAGCTTCACTCCAAGCATTAGGATAAAGTCTGCGG
ACTCCACAAAATTTTTAAGACTGATTTCTGAAAGTTTCCCGTTATATATTCCTAAAAATGAGGGCAAAGATTCATCAACAGCACTT
TTACCAAAATTTAGTGTCGTAATCGGTAGTTTTGTTTCTGAAACAAACTGAGTTACCGTTTTTTCTAAACCAAAACTAATTACTTCG
TGTCCTGCAATCACTACTGGTTTTTGGGCATTTTTCAAACTTTCTTCAATCTTACTCAAAATCACTTGTTCAGTTGTATTTGTTGTA
GAGCTTTCTTTTTCTAAAGATAATGCAGGCTTCTCTGCTTTTGCTGCAGCAACATCGACTGGTAAGTTAATATAGACTGGTTTTCT
TTCTTTTAGTAATTGAGAAAGTACTCGGTCAATTTCATATGTGGCATTTTCTGCTGTCAGTAAAGTCCGCGCTGCTGTAACAGGT
TCATGCATCTTCATAAAGTGTTTAAAATCACCATCTGCTAGTGTATGATGGACAAATTTTCCGTCATTTTGTACTTTTGAAGTTGG
TGAACCAACAATTTCTACTACTGGTAAATTTTCGGCATAACTTCCTGCCAGTCCATTGATCGCACTCAATTCGCCGACTCCAAAT
GTGGTGAGAAATGCGGCAGCTTTTTTAGTACGAGCATAACCATCAGCCATATAAGAAGCATTTAATTCATTAGCATTTCCAATCC
ATTTCATATCTTCGCGTGAAATAATTTGATCTAAAAATTGTAAGTTATAGTCACCAGGAACTCCAAAAATTTCTTCAATTCCCAACT
CGTGTAATCGGTCTAACAGGTAATCTCCTACTGTATACATGCTAGCCATATGGCTGCCGCGCGGCACCAGGCCGCTGCTGTGA
TGATGATGATGATGGCTGCTGCCCATGGTATATCTCCTTCTTAAAGTTAAACAAAATTATTTCTAGAGGGGAATTGTTATCCGCT
CACAATTCCCCTATAGTGAGTCGTATTAATTTCGCGGGATCGAGATCTCGATCCTCTACGCCGGACGCATCGTGGCCGGCATCA
CCGGCGCCACAGGTGCGGTTGCTGGCGCCTATATCGCCGACATCACCGATGGGGAAGATCGGGCTCGCCACTTCGGGCTCAT
GAGCGCTTGTTTCGGCGTGGGTATGGTGGCAGGCCCCGTGGCCGGGGGACTGTTGGGCGCCATCTCCTTGCATGCACCATTC
CTTGCGGCGGCGGTGCTCAACGGCCTCAACCTACTACTGGGCTGCTTCCTAATGCAGGAGTCGCATAAGGGAGAGCGTCGAG
ATCCCGGACACCATCGAATGGCGCAAAACCTTTCGCGGTATGGCATGATAGCGCCCGGAAGAGAGTCAATTCAGGGTGGTGAA
TGTGAAACCAGTAACGTTATACGATGTCGCAGAGTATGCCGGTGTCTCTTATCAGACCGTTTCCCGCGTGGTGAACCAGGCCA
GCCACGTTTCTGCGAAAACGCGGGAAAAAGTGGAAGCGGCGATGGCGGAGCTGAATTACATTCCCAACCGCGTGGCACAACA
ACTGGCGGGCAAACAGTCGTTGCTGATTGGCGTTGCCACCTCCAGTCTGGCCCTGCACGCGCCGTCGCAAATTGTCGCGGCG
ATTAAATCTCGCGCCGATCAACTGGGTGCCAGCGTGGTGGTGTCGATGGTAGAACGAAGCGGCGTCGAAGCCTGTAAAGCGG
CGGTGCACAATCTTCTCGCGCAACGCGTCAGTGGGCTGATCATTAACTATCCGCTGGATGACCAGGATGCCATTGCTGTGGAA
GCTGCCTGCACTAATGTTCCGGCGTTATTTCTTGATGTCTCTGACCAGACACCCATCAACAGTATTATTTTCTCCCATGAAGACG
GTACGCGACTGGGCGTGGAGCATCTGGTCGCATTGGGTCACCAGCAAATCGCGCTGTTAGCGGGCCCATTAAGTTCTGTCTCG
GCGCGTCTGCGTCTGGCTGGCTGGCATAAATATCTCACTCGCAATCAAATTCAGCCGATAGCGGAACGGGAAGGCGACTGGA
GTGCCATGTCCGGTTTTCAACAAACCATGCAAATGCTGAATGAGGGCATCGTTCCCACTGCGATGCTGGTTGCCAACGATCAGA
TGGCGCTGGGCGCAATGCGCGCCATTACCGAGTCCGGGCTGCGCGTTGGTGCGGATATCTCGGTAGTGGGATACGACGATAC
CGAAGACAGCTCATGTTATATCCCGCCGTTAACCACCATCAAACAGGATTTTCGCCTGCTGGGGCAAACCAGCGTGGACCGCT
TGCTGCAACTCTCTCAGGGCCAGGCGGTGAAGGGCAATCAGCTGTTGCCCGTCTCACTGGTGAAAAGAAAAACCACCCTGGC
GCCCAATACGCAAACCGCCTCTCCCCGCGCGTTGGCCGATTCATTAATGCAGCTGGCACGACAGGTTTCCCGACTGGAAAGCG
GGCAGTGAGCGCAACGCAATTAATGTAAGTTAGCTCACTCATTAGGCACCGGGATCTCGACCGATGCCCTTGAGAGCCTTCAA
CCCAGTCAGCTCCTTCCGGTGGGCGCGGGGCATGACTATCGTCGCCGCACTTATGACTGTCTTCTTTATCATGCAACTCGTAG
GACAGGTGCCGGCAGCGCTCTGGGTCATTTTCGGCGAGGACCGCTTTCGCTGGAGCGCGACGATGATCGGCCTGTCGCTTGC
GGTATTCGGAATCTTGCACGCCCTCGCTCAAGCCTTCGTCACTGGTCCCGCCACCAAACGTTTCGGCGAGAAGCAGGCCATTA
TCGCCGGCATGGCGGCCCCACGGGTGCGCATGATCGTGCTCCTGTCGTTGAGGACCCGGCTAGGCTGGCGGGGTTGCCTTA

CTGGTTAGCAGAATGAATCACCGATACGCGAGCGAACGTGAAGCGACTGCTGCTGCAAAACGTCTGCGACCTGAGCAACAACA
TGAATGGTCTTCGGTTTCCGTGTTTCGTAAAGTCTGGAAACGCGGAAGTCAGCGCCCTGCACCATTATGTTCCGGATCTGCATC
GCAGGATGCTGCTGGCTACCCTGTGGAACACCTACATCTGTATTAACGAAGCGCTGGCATTGACCCTGAGTGATTTTTCTCTGG
TCCCGCCGCATCCATACCGCCAGTTGTTTACCCTCACAACGTTCCAGTAACCGGGCATGTTCATCATCAGTAACCCGTATCGTG
AGCATCCTCTCTCGTTTCATCGGTATCATTACCCCCATGAACAGAAATCCCCCTTACACGGAGGCATCAGTGACCAAACAGGAA
AAAACCGCCCTTAACATGGCCCGCTTTATCAGAAGCCAGACATTAACGCTTCTGGAGAAACTCAACGAGCTGGACGCGGATGA
ACAGGCAGACATCTGTGAATCGCTTCACGACCACGCTGATGAGCTTTACCGCAGCTGCCTCGCGCGTTTCGGTGATGACGGTG
AAAACCTCTGACACATGCAGCTCCCGGAGACGGTCACAGCTTGTCTGTAAGCGGATGCCGGGAGCAGACAAGCCCGTCAGGG
CGCGTCAGCGGGTGTTGGCGGGTGTCGGGGCGCAGCCATGACCCAGTCACGTAGCGATAGCGGAGTGTATACTGGCTTAACT
ATGCGGCATCAGAGCAGATTGTACTGAGAGTGCACCATATATGCGGTGTGAAATACCGCACAGATGCGTAAGGAGAAAATACC
GCATCAGGCGCTCTTCCGCTTCCTCGCTCACTGACTCGCTGCGCTCGGTCGTTCGGCTGCGGCGAGCGGTATCAGCTCACTC
AAAGGCGGTAATACGGTTATCCACAGAATCAGGGGATAACGCAGGAAAGAACATGTGAGCAAAAGGCCAGCAAAAGGCCAGGA
ACCGTAAAAAGGCCGCGTTGCTGGCGTTTTTCCATAGGCTCCGCCCCCCTGACGAGCATCACAAAAATCGACGCTCAAGTCAG
AGGTGGCGAAACCCGACAGGACTATAAAGATACCAGGCGTTTCCCCCTGGAAGCTCCCTCGTGCGCTCTCCTGTTCCGACCCT
GCCGCTTACCGGATACCTGTCCGCCTTTCTCCCTTCGGGAAGCGTGGCGCTTTCTCATAGCTCACGCTGTAGGTATCTCAGTTC
GGTGTAGGTCGTTCGCTCCAAGCTGGGCTGTGTGCACGAACCCCCCGTTCAGCCCGACCGCTGCGCCTTATCCGGTAACTATC
GTCTTGAGTCCAACCCGGTAAGACACGACTTATCGCCACTGGCAGCAGCCACTGGTAACAGGATTAGCAGAGCGAGGTATGTA
GGCGGTGCTACAGAGTTCTTGAAGTGGTGGCCTAACTACGGCTACACTAGAAGGACAGTATTTGGTATCTGCGCTCTGCTGAA
GCCAGTTACCTTCGGAAAAAGAGTTGGTAGCTCTTGATCCGGCAAACAAACCACCGCTGGTAGCGGTGGTTTTTTTGTTTGCAA
GCAGCAGATTACGCGCAGAAAAAAAGGATCTCAAGAAGATCCTTTGATCTTTTCTACGGGGTCTGACGCTCAGTGGAACGAAAA
CTCACGTTAAGGGATTTTGGTCATGAACAATAAAACTGTCTGCTTACATAAACAGTAATACAAGGGGTGTTATGAGCCATATTCA
ACGGGAAACGTCTTGCTCTAGGCCGCGATTAAATTCCAACATGGATGCTGATTTATATGGGTATAAATGGGCTCGCGATAATGT
CGGGCAATCAGGTGCGACAATCTATCGATTGTATGGGAAGCCCGATGCGCCAGAGTTGTTTCTGAAACATGGCAAAGGTAGCG
TTGCCAATGATGTTACAGATGAGATGGTCAGACTAAACTGGCTGACGGAATTTATGCCTCTTCCGACCATCAAGCATTTTATCCG
TACTCCTGATGATGCATGGTTACTCACCACTGCGATCCCCGGGAAAACAGCATTCCAGGTATTAGAAGAATATCCTGATTCAGG
TGAAAATATTGTTGATGCGCTGGCAGTGTTCCTGCGCCGGTTGCATTCGATTCCTGTTTGTAATTGTCCTTTTAACAGCGATCGC
GTATTTCGTCTCGCTCAGGCGCAATCACGAATGAATAACGGTTTGGTTGATGCGAGTGATTTTGATGACGAGCGTAATGGCTGG
CCTGTTGAACAAGTCTGGAAAGAAATGCATAAACTTTTGCCATTCTCACCGGATTCAGTCGTCACTCATGGTGATTTCTCACTTG
ATAACCTTATTTTTGACGAGGGGAAATTAATAGGTTGTATTGATGTTGGACGAGTCGGAATCGCAGACCGATACCAGGATCTTG
CCATCCTATGGAACTGCCTCGGTGAGTTTTCTCCTTCATTACAGAAACGGCTTTTTCAAAAATATGGTATTGATAATCCTGATATG
AATAAATTGCAGTTTCATTTGATGCTCGATGAGTTTTTCTAAGAATTAATTCATGAGCGGATACATATTTGAATGTATTTAGAAAAA
TAAACAAATAGGGGTTCCGCGCACATTTCCCCGAAAAGTGCCACCTGAAATTGTAAACGTTAATATTTTGTTAAAATTCGCGTTA
AATTTTTGTTAAATCAGCTCATTTTTTAACCAATAGGCCGAAATCGGCAAAATCCCTTATAAATCAAAAGAATAGACCGAGATAGG
GTTGAGTGTTGTTCCAGTTTGGAACAAGAGTCCACTATTAAAGAACGTGGACTCCAACGTCAAAGGGCGAAAAACCGTCTATCA
GGGCGATGGCCCACTACGTGAACCATCACCCTAATCAAGTTTTTTGGGGTCGAGGTGCCGTAAAGCACTAAATCGGAACCCTA
AAGGGAGCCCCCGATTTAGAGCTTGACGGGGAAAGCCGGCGAACGTGGCGAGAAAGGAAGGGAAGAAAGCGAAAGGAGCGG
GCGCTAGGGCGCTGGCAAGTGTAGCGGTCACGCTGCGCGTAACCACCACACCCGCCGCGCTTAATGCGCCGCTACAGGGCG
CGTCCCATTCGCCA

Amino acid sequence of *Ll*KdcA-His6:

MGSSHHHHHHSSGLVPRGSHMASMYTVGDYLLDRLHELGIEEIFGVPGDYNLQFLDQIISREDMKWIGNANELNASYMADGYARTK
KAAAFLTTFGVGELSAINGLAGSYAENLPVVEIVGSPTSKVQNDGKFVHHTLADGDFKHFMKMHEPVTAARTLLTAENATYEIDRVLS
QLLKERKPVYINLPVDVAAAKAEKPALSLEKESSTTNTTEQVILSKIEESLKNAQKPVVIAGHEVISFGLEKTVTQFVSETKLPITTLNFGK
SAVDESLPSFLGIYNGKLSEISLKNFVESADFILMLGVKLTDSSTGAFTHHLDENKMISLNIDEGIIFNKVVEDFDFRAVVSSLSELKGIEY
EGQYIDKQYEEFIPSSAPLSQDRLWQAVESLTQSNETIVAEQGTSFFGASTIFLKSNSRFIGQPLWGSIGYTFPAALGSQIADKESRHL
LFIGDGSLQLTVQELGLSIREKLNPICFIINNDGYTVEREIHGPTQSYNDIPMWNYSKLPETFGATEDRVVSKIVRTENEFVSVMKEAQA
DVNRMYWIELVLEKEDAPKLLKKMGKLFAEQNK

Gene sequence of amine transaminase from *Arthrobacter sp.* KNK 168 (*As*TA) in pET21a:

TGGCGAATGGGACGCGCCCTGTAGCGGCGCATTAAGCGCGGCGGGTGTGGTGGTTACGCGCAGCGTGACCGCTACACTTGC
CAGCGCCCTAGCGCCCGCTCCTTTCGCTTTCTTCCCTTCCTTTCTCGCCACGTTCGCCGGCTTTCCCCGTCAAGCTCTAAATCG
GGGGCTCCCTTTAGGGTTCCGATTTAGTGCTTTACGGCACCTCGACCCCAAAAAACTTGATTAGGGTGATGGTTCACGTAGTGG
GCCATCGCCCTGATAGACGGTTTTTCGCCCTTTGACGTTGGAGTCCACGTTCTTTAATAGTGGACTCTTGTTCCAAACTGGAAC
AACACTCAACCCTATCTCGGTCTATTCTTTTGATTTATAAGGGATTTTGCCGATTTCGGCCTATTGGTTAAAAAATGAGCTGATTT
AACAAAAATTTAACGCGAATTTTAACAAAATATTAACGTTTACAATTTCAGGTGGCACTTTTCGGGGAAATGTGCGCGGAACCCC
TATTTGTTTATTTTTCTAAATACATTCAAATATGTATCCGCTCATGAGACAATAACCCTGATAAATGCTTCAATAATATTGAAAAAG
GAAGAGTATGAGTATTCAACATTTCCGTGTCGCCCTTATTCCCTTTTTTGCGGCATTTTGCCTTCCTGTTTTTGCTCACCCAGAAA
CGCTGGTGAAAGTAAAAGATGCTGAAGATCAGTTGGGTGCACGAGTGGGTTACATCGAACTGGATCTCAACAGCGGTAAGATC
CTTGAGAGTTTTCGCCCCGAAGAACGTTTTCCAATGATGAGCACTTTTAAAGTTCTGCTATGTGGCGCGGTATTATCCCGTATTG
ACGCCGGGCAAGAGCAACTCGGTCGCCGCATACACTATTCTCAGAATGACTTGGTTGAGTACTCACCAGTCACAGAAAAGCAT
CTTACGGATGGCATGACAGTAAGAGAATTATGCAGTGCTGCCATAACCATGAGTGATAACACTGCGGCCAACTTACTTCTGACA
ACGATCGGAGGACCGAAGGAGCTAACCGCTTTTTTGCACAACATGGGGGATCATGTAACTCGCCTTGATCGTTGGGAACCGGA
GCTGAATGAAGCCATACCAAACGACGAGCGTGACACCACGATGCCTGCAGCAATGGCAACAACGTTGCGCAAACTATTAACTG
GCGAACTACTTACTCTAGCTTCCCGGCAACAATTAATAGACTGGATGGAGGCGGATAAAGTTGCAGGACCACTTCTGCGCTCG
GCCCTTCCGGCTGGCTGGTTTATTGCTGATAAATCTGGAGCCGGTGAGCGTGGGTCTCGCGGTATCATTGCAGCACTGGGGC
CAGATGGTAAGCCCTCCCGTATCGTAGTTATCTACACGACGGGGAGTCAGGCAACTATGGATGAACGAAATAGACAGATCGCT
GAGATAGGTGCCTCACTGATTAAGCATTGGTAACTGTCAGACCAAGTTTACTCATATATACTTTAGATTGATTTAAAACTTCATTT
TTAATTTAAAAGGATCTAGGTGAAGATCCTTTTTGATAATCTCATGACCAAAATCCCTTAACGTGAGTTTTCGTTCCACTGAGCGT
CAGACCCCGTAGAAAAGATCAAAGGATCTTCTTGAGATCCTTTTTTTCTGCGCGTAATCTGCTGCTTGCAAACAAAAAAACCACC
GCTACCAGCGGTGGTTTGTTTGCCGGATCAAGAGCTACCAACTCTTTTTCCGAAGGTAACTGGCTTCAGCAGAGCGCAGATAC
CAAATACTGTCCTTCTAGTGTAGCCGTAGTTAGGCCACCACTTCAAGAACTCTGTAGCACCGCCTACATACCTCGCTCTGCTAAT
CCTGTTACCAGTGGCTGCTGCCAGTGGCGATAAGTCGTGTCTTACCGGGTTGGACTCAAGACGATAGTTACCGGATAAGGCGC
AGCGGTCGGGCTGAACGGGGGGTTCGTGCACACAGCCCAGCTTGGAGCGAACGACCTACACCGAACTGAGATACCTACAGCG
TGAGCTATGAGAAAGCGCCACGCTTCCCGAAGGGAGAAAGGCGGACAGGTATCCGGTAAGCGGCAGGGTCGGAACAGGAGA

GCGCACGAGGGAGCTTCCAGGGGGAAACGCCTGGTATCTTTATAGTCCTGTCGGGTTTCGCCACCTCTGACTTGAGCGTCGAT
TTTTGTGATGCTCGTCAGGGGGGCGGAGCCTATGGAAAAACGCCAGCAACGCGGCCTTTTTACGGTTCCTGGCCTTTTGCTGG
CCTTTTGCTCACATGTTCTTTCCTGCGTTATCCCCTGATTCTGTGGATAACCGTATTACCGCCTTTGAGTGAGCTGATACCGCTC
GCCGCAGCCGAACGACCGAGCGCAGCGAGTCAGTGAGCGAGGAAGCGGAAGAGCGCCTGATGCGGTATTTTCTCCTTACGCA
TCTGTGCGGTATTTCACACCGCATATATGGTGCACTCTCAGTACAATCTGCTCTGATGCCGCATAGTTAAGCCAGTATACACTCC
GCTATCGCTACGTGACTGGGTCATGGCTGCGCCCCGACACCCGCCAACACCCGCTGACGCGCCCTGACGGGCTTGTCTGCTC
CCGGCATCCGCTTACAGACAAGCTGTGACCGTCTCCGGGAGCTGCATGTGTCAGAGGTTTTCACCGTCATCACCGAAACGCGC
GAGGCAGCTGCGGTAAAGCTCATCAGCGTGGTCGTGAAGCGATTCACAGATGTCTGCCTGTTCATCCGCGTCCAGCTCGTTGA
GTTTCTCCAGAAGCGTTAATGTCTGGCTTCTGATAAAGCGGGCCATGTTAAGGGCGGTTTTTTCCTGTTTGGTCACTGATGCCT
CCGTGTAAGGGGGATTTCTGTTCATGGGGGTAATGATACCGATGAAACGAGAGAGGATGCTCACGATACGGGTTACTGATGAT
GAACATGCCCGGTTACTGGAACGTTGTGAGGGTAAACAACTGGCGGTATGGATGCGGCGGGACCAGAGAAAAATCACTCAGG
GTCAATGCCAGCGCTTCGTTAATACAGATGTAGGTGTTCCACAGGGTAGCCAGCAGCATCCTGCGATGCAGATCCGGAACATA
ATGGTGCAGGGCGCTGACTTCCGCGTTTCCAGACTTTACGAAACACGGAAACCGAAGACCATTCATGTTGTTGCTCAGGTCGC
AGACGTTTTGCAGCAGCAGTCGCTTCACGTTCGCTCGCGTATCGGTGATTCATTCTGCTAACCAGTAAGGCAACCCCGCCAGC
CTAGCCGGGTCCTCAACGACAGGAGCACGATCATGCGCACCCGTGGGGCCGCCATGCCGGCGATAATGGCCTGCTTCTCGCC
GAAACGTTTGGTGGCGGGACCAGTGACGAAGGCTTGAGCGAGGGCGTGCAAGATTCCGAATACCGCAAGCGACAGGCCGATC
ATCGTCGCGCTCCAGCGAAAGCGGTCCTCGCCGAAAATGACCCAGAGCGCTGCCGGCACCTGTCCTACGAGTTGCATGATAA
AGAAGACAGTCATAAGTGCGGCGACGATAGTCATGCCCCGCGCCCACCGGAAGGAGCTGACTGGGTTGAAGGCTCTCAAGGG
CATCGGTCGAGATCCCGGTGCCTAATGAGTGAGCTAACTTACATTAATTGCGTTGCGCTCACTGCCCGCTTTCCAGTCGGGAAA
CCTGTCGTGCCAGCTGCATTAATGAATCGGCCAACGCGCGGGGAGAGGCGGTTTGCGTATTGGGCGCCAGGGTGGTTTTTCT
TTTCACCAGTGAGACGGGCAACAGCTGATTGCCCTTCACCGCCTGGCCCTGAGAGAGTTGCAGCAAGCGGTCCACGCTGGTTT
GCCCCAGCAGGCGAAAATCCTGTTTGATGGTGGTTAACGGCGGGATATAACATGAGCTGTCTTCGGTATCGTCGTATCCCACTA
CCGAGATATCCGCACCAACGCGCAGCCCGGACTCGGTAATGGCGCGCATTGCGCCCAGCGCCATCTGATCGTTGGCAACCAG
CATCGCAGTGGGAACGATGCCCTCATTCAGCATTTGCATGGTTTGTTGAAAACCGGACATGGCACTCCAGTCGCCTTCCCGTTC
CGCTATCGGCTGAATTTGATTGCGAGTGAGATATTTATGCCAGCCAGCCAGACGCAGACGCGCCGAGACAGAACTTAATGGGC
CCGCTAACAGCGCGATTTGCTGGTGACCCAATGCGACCAGATGCTCCACGCCCAGTCGCGTACCGTCTTCATGGGAGAAAATA
ATACTGTTGATGGGTGTCTGGTCAGAGACATCAAGAAATAACGCCGGAACATTAGTGCAGGCAGCTTCCACAGCAATGGCATC
CTGGTCATCCAGCGGATAGTTAATGATCAGCCCACTGACGCGTTGCGCGAGAAGATTGTGCACCGCCGCTTTACAGGCTTCGA
CGCCGCTTCGTTCTACCATCGACACCACCACGCTGGCACCCAGTTGATCGGCGCGAGATTTAATCGCCGCGACAATTTGCGAC
GGCGCGTGCAGGGCCAGACTGGAGGTGGCAACGCCAATCAGCAACGACTGTTTGCCCGCCAGTTGTTGTGCCACGCGGTTGG
GAATGTAATTCAGCTCCGCCATCGCCGCTTCCACTTTTTCCCGCGTTTTCGCAGAAACGTGGCTGGCCTGGTTCACCACGCGG
GAAACGGTCTGATAAGAGACACCGGCATACTCTGCGACATCGTATAACGTTACTGGTTTCACATTCACCACCCTGAATTGACTC
TCTTCCGGGCGCTATCATGCCATACCGCGAAAGGTTTTGCGCCATTCGATGGTGTCCGGGATCTCGACGCTCTCCCTTATGCG
ACTCCTGCATTAGGAAGCAGCCCAGTAGTAGGTTGAGGCCGTTGAGCACCGCCGCCGCAAGGAATGGTGCATGCAAGGAGAT
GGCGCCCAACAGTCCCCCGGCCACGGGGCCTGCCACCATACCCACGCCGAAACAAGCGCTCATGAGCCCGAAGTGGCGAGC
CCGATCTTCCCCATCGGTGATGTCGGCGATATAGGCGCCAGCAACCGCACCTGTGGCGCCGGTGATGCCGGCCACGATGCGT
CCGGCGTAGAGGATCGAGATCTCGATCCCGCGAAATTAATACGACTCACTATAGGGGAATTGTGAGCGGATAACAATTCCCCT
CTAGAAATAATTTTGTTTAACTTTAAGAAGGAGATATACAT**ATGACCAGCGAAATTGTTTATACCCATGATACCGGTCTGGATTAT**
ATCACCTATAGCGATTATGAACTGGATCCGGCAAATCCGCTGGCAGGCGGTGCAGCATGGATTGAAGGTGCATTTGTTCCGCC
TAGCGAAGCACGTATTAGCATTTTTGATCAGGGCTATCTGCATAGTGATGTTACCTATACCGTGTTTCATGTGTGGAATGGTAAT
GCATTTCGCCTGGATGATCATATTGAACGTCTGTTTAGCAATGCAGAAAGCATGCGTATTATTCCGCCTCTGACCCAGGATGAA
GTTAAAGAAATTGCACTGGAACTGGTTGCAAAAACCGAACTGCGTGAAGCATTTGTTAGCGTTAGCATTACCCGTGGTTATAGC
AGCACACCGGGTGAACGTGATATTACCAAACATCGTCCGCAGGTTTATATGTATGCAGTTCCGTATCAGTGGATTGTTCCGTTT
GATCGTATTCGTGATGGTGTTCATGCAATGGTTGCACAGAGCGTTCGTCGTACACCGCGTAGCAGCATTGATCCGCAGGTTAAA
AATTTTCAGTGGGGTGATCTGATTCGTGCAGTTCAAGAAACCCATGATCGTGGTTTTGAAGCACCGCTGCTGCTGGATGGTGAT
GGTCTGCTGGCCGAAGGTAGCGGTTTTAATGTTGTTGTGATTAAAGATGGTGTGGTTCGTAGTCCGGGTCGTGCAGCACTGCC
TGGTATTACCCGTAAAACCGTTCTGGAAATTGCAGAAAGCCTGGGTCATGAAGCAATTCTGGCAGATATTACCCTGGCAGAACT
GCTGGATGCAGATGAAGTTCTGGGTTGTACCACCGCAGGCGGTGTTTGGCCGTTTGTTAGCGTGGATGGTAATCCGATTTCAG
ATGGTGTTCCGGGTCCGATTACCCAGAGCATTATTCGTCGTTATTGGGAACTGAATGTTGAAAGCAGCAGCCTGCTGACACCG
GTTCAGTATGCACTCGAGCACCACCACCACCACCACTGAGATCCGGCTGCTAACAAAGCCCGAAAGGAAGCTGAGTTGGCTGC
TGCCACCGCTGAGCAATAACTAGCATAACCCCTTGGGGCCTCTAAACGGGTCTTGAGGGGTTTTTTGCTGAAAGGAGGAACTAT
ATCCGGAT

Amino acid sequence of *As*TA-His6:

MTSEIVYTHDTGLDYITYSDYELDPANPLAGGAAWIEGAFVPPSEARISIFDQGYLHSDVTYTVFHVWNGNAFRLDDHIERLFSNAESM
RIIPPLTQDEVKEIALELVAKTELREAFVSVSITRGYSSTPGERDITKHRPQVYMYAVPYQWIVPFDRIRDGVHAMVAQSVRRTPRSSID
PQVKNFQWGDLIRAVQETHDRGFEAPLLLDGDGLLAEGSGFNVVVIKDGVVRSPGRAALPGITRKTVLEIAESLGHEAILADITLAELLD
ADEVLGCTTAGGVWPFVSVDGNPISDGVPGPITQSIIRRYWELNVESSSLLTPVQYALEHHHHHH

Curriculum Vitae

Personal data

Name:	Laura Katharina Grabowski
E-Mail:	Laura.grabowski@rwth-aachen.de
Date of birth:	24 June 1994 in Rheine, Germany

Education

11/2019 - 12/2022	Doctoral studies at RWTH Aachen University
04/2017 - 09/2019	Master of Science at RWTH Aachen University Major: Molecular and Applied Biotechnology – Biochemical engineering/ Industrial Biotechnology
10/2013 - 02/2017	Bachelor of Science at RWTH Aachen University Major: Molecular and Applied Biotechnology
2004 - 2013	Abitur with bilingual qualification at Kopernikus-Gymnasium Rheine

Professional experience

11/2019 - 12/2022	Doctoral researcher at the Institute of Bio- and Geosciences (IBG-1), Forschungszentrum Jülich
09/2018 - 12/2018	Research internship at the Joint BioEnergy Institute, Emeryville, CA, USA
04/2018	Research internship in multi-step biocatalysis at the Institute of Bio- and Geosciences (IBG-1), Forschungszentrum Jülich
10/2017 - 12/2017	Research internship at the Chair of Biochemical Engineering (AVT.BioVT), RWTH Aachen University
07/2016 - 09/2017	Graduate Research Assistant at the Institute of Molecular Biotechnology, RWTH Aachen University

Scholarships and Awards

06/2022	Molecular Science & Engineering RWTH Conference Support
12/2020	DECHEMA Student Award
11/2020	Springorium Commemorative Coin
09/2018 - 12/2018	DAAD Scholarship (ACalNet Grant)
10/2017 - 08/2018	Evonik AG Germany Scholarship *via* RWTH Education Fund
04/2017 - 09/2017	Clariant Germany Scholarship *via* RWTH Education Fund